Facultat de Física
Departament de Física Teòrica
Programa de Doctorado en Física

ELECTROWEAK BREAKING AND NEUTRINO MASS

Ph.D. THESIS

Submitted by:
Cesar Manuel Bonilla Diaz

Supervised by:
Jose Wagner Furtado Valle

Mayo, 2017

Dr. Jose Wagner Furtado Valle, Profesor de Investigación del Consejo Superior de Investigaciones Científicas, adscrito al Instituto de Física Corpuscular - Departamento de Física Teórica, Universidad de Valencia,

CERTIFICA:

> Que la presente Memoria *Electroweak Breaking and Neutrino Mass* ha sido realizada bajo mi dirección en el Departamento de Física Teórica de la Universidad de Valencia por Cesar Manuel Bonilla Diaz como Tesis para obtener el grado de Doctor en Física.

Y para que así conste en cumplimiento con la legislación vigente, presenta ante el Departamento de Física Teórica, la referida memoria, firmando el presente certificado.

En Valencia, a 29 de mayo de 2017

Fdo: Dr. Jose Wagner Furtado Valle

A Silvana

AGRADECIMIENTOS

Antes que nada agradezco a mis asesor de tesis, Prof. Jose W.F. Valle, por su guía y por trasmitir esa gran pasión que tiene por la física. Además, por su disposición para discutir cualquier tema, a cualquier hora y desde cualquier lugar.

Me gustaría agradecer a los miembros del grupo Astroparticles and High Energy Physics (AHEP). Sobre todo a Mariam, Martin y Sergio, por toda la ayuda proporcionada durante el doctorado, sobre todo en los temas más importantes para el desarrollo de la actividad científica (como la burocracia).

Me siento especialmente agradecido con las personas con las que tuve la fortuna de colaborar: Dorota, Eduardo, Ernest, Fefo, Jorge, Jose, Lorenzo, Manuel, Maria, Miguel, Neda, Rahul, Renato, Stefano, Tanmoy, Toby y Werner. Por todo lo que aprendí de ellos, su paciencia, el tiempo invertido y el interés mostrado en la realización de los proyectos conjuntos.

Durante la etapa doctoral tuve la oportunidad de realizar algunas estancias de investigación. Por lo tanto, quisiera agradecer a:

- Werner Porod, por recibirme y al Institut für Theoretische Physik und Astrophyik, en Würzburg (Alemania) por la hospitalidad.
- Jorge C. Romao, por recibirme y al Centro de Física Teórica de Partículas (CFTP), Instituto Superior Técnico en Lisboa (Portugal), por la hospitalidad.
- Omar Miranda, por recibirme y al CINVESTAV en México por su hopitalidad.

Finalmente, agradezco el apoyo económico de los proyectos: FPA2011-2297, FPA2014-58183-P, Multidark CSD2009-00064, SEV-2014-0398 (MINECO) and PROMETEOII/ 2014/084 (GVA). A la beca FPI y el apoyo parcial de CONACYT (MX).

CONTENTS

PUBLICATIONS

The outcome of my research during the PhD has been the publication of twelve articles. This thesis is based on the results obtained in the published papers, $A1 - A7$ below. These articles are faithfully reproduced in the second part of this document in order to support the discussion presented in the first part.

List of articles included in this thesis:

$A1$ **"Relating quarks and leptons with the T_7 flavour group"**. C. Bonilla, S. Morisi, E. Peinado, J.W.F. Valle. Phys.Lett.B742 (2015) 99-106.

$A2$ **"Neutrino mass and invisible Higgs decays at the LHC"**. C. Bonilla, J.C. Romao, J.W.F. Valle Phys.Rev.D91 (2015) no.11, 113015.

$A3$ **"Consistency of the triplet seesaw model revisited"**. C. Bonilla, R. Fonseca, J.W.F. Valle. Phys.Rev.D92 (2015) no.7, 075028.

$A4$ **"Electroweak Breaking and Neutrino Mass: Invisible Higgs Decays at the LHC (Type II Seesaw)"**. C. Bonilla, J.C. Romao, J.W.F. Valle. New J.Phys.18 (2016) no.3, 033033.

$A5$ **"Vacuum stability with spontaneous violation of lepton number"**. C. Bonilla, R. Fonseca, J.W.F. Valle. Phys.Lett.B756 (2016) 345-349.

$A6$ **"Naturally light neutrinos in Diracon model"**. C. Bonilla, J.W.F. Valle, Phys.Lett.B762 (2016) 162-165.

*A*7 **"Two-loop Dirac neutrino mass and WIMP dark matter"**. C. Bonilla, E. Ma, E. Peinado, J.W.F. Valle. Phys.Lett.B762 (2016) 214-218.

Other articles completed during the PHD but not included in this work:

*A*8 **"Dirac neutrinos from flavor symmetry"**. A. Aranda, C. Bonilla, S. Morisi, E. Peinado, J.W.F. Valle. Phys.Rev.D89 (2014) no.3, 033001.

*A*9 **"IDMS: Inert Dark Matter Model with a complex singlet"**. C. Bonilla, D. Sokolowska, N. Darvishi, J.L. Diaz-Cruz, M. Krawczyk. J.Phys.G43 (2016) no.6, 065001.

*A*10 **"A flavor physics scenario for the 750 GeV diphoton anomaly"**. C. Bonilla, M. Nebot, R. Srivastava, J.W.F. Valle. Phys.Rev.D93 (2016) no.7, 073009.

*A*11 **"Perspectives for Detecting Lepton Flavour Violation in Left-Right Symmetric Models"** C. Bonilla, M.E. Krauss, T. Opferkuch, W. Porod. JHEP 1703 (2017) 027.

*A*12 **"$U(1)_{B_3-3\mu}$ gauge symmetry as the simplest description of $b \to s$ anomalies"** C. Bonilla, T. Modak, R. Srivastava, J.W.F Valle. Submitted for publication to Phys.Lett.B.

Part I

General introduction and summary of results

INTRODUCTION

The experimental observation of neutrino oscillations (which implies that neutrinos are not massless) is one of the main reasons to think that there should be physics Beyond the Standard Model. In the Standard Model (SM) neutrinos masses are not generated after electroweak symmetry breaking as for the other particles. In particular, one of the most appealing questions is to figure out what is the mechanism chosen by nature to generate neutrino masses.

Another important experimental result comes from the Large Hadron Collider (LHC) which in 2012 announced the discovery of a Higgs-like particle with a mass of 125 GeV. One of the main goals of the LHC in the upcoming years is to fully determine the properties of this boson, i.e. its decay channels. On the other hand, it is expected that the LHC in the near future can probe the existence of new physics.

Neutrino mass generation is quite interesting mainly because it urges the existence of new physics, namely new degrees of freedom, which can potentially be discovered in collider experiments such as the LHC. These new particles can naturally explain: dark matter (DM), which represents about 80% of the matter of the universe; the matter-antimatter asymmetry of the universe; or even some other issues that the SM faces. In fact, it is possible to establish a connection between neutrino mass and the Higgs properties. This happens because the new particles, needed to generate neutrino masses, tend to affect the Higgs decay channels and hence these effects could also be measured by the LHC. The connection between neutrino physics and dark matter comes from symmetry reasons. It happens that the fields involved in the neutrino mass generation mechanism may carry a non-trivial charge under an additional symmetry which also stabilizes the DM candidate of the theory. In this thesis

we mainly focus on studying the connection between the neutrino properties and the phenomenology in the scalar sector. We also provide some hints on the flavor problem as well as the connection between the neutrino mass generation and dark matter.

This thesis consists of two parts and is organized as follows: The first part contains three chapters and a brief summary of the research work carried out during the PhD. The first two chapters are mainly introductory. In the third chapter we summarize the results of research articles on which this work is based. The second part contains the detailed discussion of the published papers that we have briefly summarized in the first part.

In Chapter 1 we make a brief review of the Standard Model. We start by showing its particle content in and how these particles get mass through the Brout-Englert-Higgs mechanism. In the next chapter, we discuss some problems that the SM cannot explain, for instance, neutrino masses. Then, we discuss some open questions in the neutrino sector, which makes neutrino physics a very interesting field. Besides, we make a brief list of the experiments devoted to study some of the neutrino properties. We show the current results of some of these experiments and their future perspectives. In this chapter we also show some of the most popular approaches to explain neutrino masses. We prove that, independently of the scheme, neutrino mass generation demands the existence of new physics. In Chapter 3 we show the results of some articles that came out as part of the research activity during the PhD. In the first two sections we describe the connection between the neutrino mass generation and the Higgs sector. On the one hand, we focus on the vacuum stability of the scalar potential, which provide important constraints on the parameter space and also to the mass spectrum of the scalars involved in the neutrino mass generation mechanism. After that, we also show how the Higgs properties may be affected by the presence of the new degrees of freedom added to the SM. In particular, we demonstrate that, there is a "new" (invisible) Higgs decay channel when neutrinos get mass after spontaneous breaking of lepton number. This is a consequence of the existence of a physical Nambu-Goldstone boson in the theory. In this chapter we also display the results obtained in a flavor model characterized by having a mass relation between down-type quarks and charged leptons. Later on, we present a model that can naturally explain the small neutrino masses in the case when neutrinos are Dirac fermions. To conclude the chapter we provide the results of a model which provides a possible connection between Dirac nature of neutrino and dark matter stability. We complete the first part of the thesis giving some conclusions.

The second part of this thesis comprises the research papers that discuss the following issues:

1) The impact of neutrino mass generation in the scalar sector.
   Articles:
   - *Vacuum stability with spontaneous violation of lepton number.*
   - *Consistency of the triplet seesaw model revisited.*
   - *Neutrino mass and invisible Higgs decays at the LHC.*
   - *Electroweak Breaking and Neutrino Mass: Invisible Higgs Decays at the LHC (Type II Seesaw).*

2) The flavor problem.
   Article:
   - *Relating quarks and leptons with the T_7 flavour group.*

3) The neutrino nature.
   Article:
   - *Naturally light neutrinos in Diracon model.*

4) The connection between Dirac neutrinos and dark matter.
   Article:
   - *Two-loop Dirac neutrino mass and WIMP dark matter.*

CHAPTER 1

THE STANDARD MODEL OF PARTICLE PHYSICS

The Standard Model (SM) is a renormalizable [1] Yang-Mills theory based on the gauge symmetry group $SU(3)_C \otimes SU(2)_L \otimes U(1)_Y$, where the subscript C is for color, L for left-handed and Y for hypercharge. The group $SU(3)_C$ describes strong interactions while the $SU(2)_L \times U(1)_Y$ group explains electroweak interactions. Essentially, the subscript L in the weak $SU(2)$ group is to remind us that it only acts on left-handed fermions, ψ_L. A fermion field with subindex R, i.e. a right-handed fermion ψ_R, transforms trivially under $SU(2)_L$ and is therefore blind to weak interactions. In the SM all particles, fermions and bosons, get mass after electroweak symmetry breaking (EWSB), through the Brout-Englert-Higgs (BEH) mechanism [2–4]. However, the SM contains only left-handed neutrinos ν_L and as a result they do not get mass after EWSB. The $SU(3)_C \otimes SU(2)_L \otimes U(1)_Y$invariant Lagrangian that describes all Standard Model interactions is written as [5–11],

$$\begin{aligned}\mathcal{L}_{SM} = &-\frac{1}{4}G^A_{\mu\nu}G^{A\,\mu\nu} - \frac{1}{4}W^a_{\mu\nu}W^{a\,\mu\nu} - \frac{1}{4}B_{\mu\nu}B^{\mu\nu} + \left(i\bar{\Psi}\gamma^\mu D_\mu \Psi + \text{h.c.}\right) \\ &+ \left(Y^d_{ij}\bar{\Psi}_{L_i}\Psi^d_{R_j}\Phi + \text{h.c.}\right) + \left(Y^u_{ij}\bar{\Psi}_{L_i}\Psi^u_{R_j}\tilde{\Phi} + \text{h.c.}\right) + |D_\mu\Phi|^2 - V(\Phi),\end{aligned} \tag{1.1}$$

where we have used the Einstein summation convention, $G^A_{\mu\nu}$ (with $A = 1, ..., 8$) are the gauge field strengths associated with $SU(3)_C$ (gluons), $W^a_{\mu\nu}$ (with $a = 1, 2, 3$) are related to $SU(2)_L$ and $B_{\mu\nu}$ is the gauge field strength in $U(1)_Y$. The first line in equation (1.1) describes gauge boson interactions, in particular, the fourth term, $i\bar{\Psi}\gamma^\mu D_\mu\Psi$ where $\Psi = (L_L, Q_L, e_R, d_R, u_R)$ are the SM fermions, contains the interactions between gauge bosons and fermions. The Yukawa terms in equation (1.1) provide the interactions between fermions and the

SU(2) scalar doublet Φ, where $\tilde{\Phi} = i\sigma^2\Phi^*$. The interactions between gauge boson and Φ are given in the kinetic term $|D_\mu\Phi|^2$ where D_μ is the covariant derivative defined in equation (1.7). The term $V(\Phi)$ is the scalar potential. In what follows we give some of the properties of the particle content in the SM, equation (1.1).

Building blocks of nature

In the SM there are only spin-1/2 fermions (leptons and quarks) and bosons with integer spin-1 which are the mediators of the interactions. In addition, there is a scalar boson with spin-0, responsible for the mass generation within the SM. The fermion content is formed by three electrically charged leptons (e, μ, τ), three left-handed neutrinos (ν_e, ν_μ, ν_τ) and six quarks (each one has three colors): three up-type (u, c, t) and three down-type (d, s, b). We can write the SM fermion fields in $SU(2)$ notation as follows,

$$\text{Leptons}: \quad L_{L_i}: \quad \begin{pmatrix} \nu_{eL} \\ e_L \end{pmatrix}, \quad \begin{pmatrix} \nu_{\mu L} \\ \mu_L \end{pmatrix}, \quad \begin{pmatrix} \nu_{\tau L} \\ \tau_L \end{pmatrix} \tag{1.2}$$

and

$$\text{Quarks}: \quad Q_{L_i}: \quad \begin{pmatrix} u_L \\ d_L \end{pmatrix}, \quad \begin{pmatrix} c_L \\ s_L \end{pmatrix}, \quad \begin{pmatrix} t_L \\ b_L \end{pmatrix}, \tag{1.3}$$

where $i = 1, 2, 3$ denotes a family index and there are three colors for each quark in (1.3). On the other hand, the right-handed components: (e_R, μ_R, τ_R), (u_R, c_R, t_R) and (d_R, s_R, b_R) transform as singlet under $SU(2)$. In Table 1.1 we summarize the fermion content in the SM and the charge assignments under the gauge group $SU(3)_C \otimes SU(2)_L \otimes U(1)_Y$.

	$SU(3)_C$	$SU(2)_L$	$U(1)_Y$
Q_{Li}	**3**	**2**	+1/6
L_{Li}	**1**	**2**	-1/2
u_{Ri}	**3**	**1**	+2/3
d_{Ri}	**3**	**1**	-1/3
e_{Ri}	**1**	**1**	-1

Table 1.1: Fermion content in the SM and the charge assignments under the gauge group $SU(3)_C \otimes SU(2)_L \otimes U(1)_Y$.

On the other hand, after EWSB, there are three massive gauge bosons, $W^\pm_\mu$ and Z^0_μ, that mediate the weak interactions, the massless photon A_μ that

mediates electromagnetic interactions and eight gluons G_μ^A which are massless and mediate strong interactions.

1.1 Electroweak symmetry breaking

As we already mentioned, all particles (bosons and fermions) in the SM get their mass after the breaking of the electroweak group $SU(2)_L \times U(1)_Y$ through the BEH mechanism [2–4]. Therefore, in this section we make a quick review on how this mechanism works within the SM.

The electroweak breaking happens when the scalar field $\Phi = \Phi(x)$ charged under $SU(2)_L \times U(1)_Y$ symmetry in equation (1.1) gets its vacuum expectation value (vev), usually denoted as $\langle\Phi\rangle$.

$$SU(2)_L \times U(1)_Y \xrightarrow{\langle\Phi\rangle} U(1)_{EM} \tag{1.4}$$

Then, let $\Phi = \Phi(x)$ be a $SU(2)$ doublet with complex entries written as

$$\Phi(x) = \frac{1}{\sqrt{2}} \begin{pmatrix} \phi_1(x) \\ \phi_2(x) \end{pmatrix}, \tag{1.5}$$

where $\phi_i(x)$ are complex fields, $\phi_i(x) \in \mathbb{C}$. The renormalizable and gauge invariant scalar Lagrangian is given by

$$\mathcal{L}_\Phi = (D_\mu \Phi)^\dagger D^\mu \Phi - \underbrace{\left(\mu^2 |\Phi|^2 + \lambda |\Phi^\dagger \Phi|^2\right)}_{V(\Phi)}, \tag{1.6}$$

where $V(\Phi)$ is the scalar potential, μ is a dimensionful (mass) parameter while λ is a dimensionless one. D_μ is defined as the covariant derivative,

$$D_\mu \equiv \partial_\mu + i\frac{g_1}{2} B_\mu + i\frac{g_2}{2} \sigma^a W_\mu^a \quad (a = 1, 2, 3), \tag{1.7}$$

where g_1 and g_2 are the coupling constants of the $U(1)_Y$ and $SU(2)_L$ symmetries, respectively. $B_\mu = B_\mu(x)$ is the gauge field associated with the $U(1)_Y$ group, σ^a are the (Pauli matrices) generators of the $SU(2)_L$ group,

$$\sigma^1 = \begin{pmatrix} 0 & 1 \\ 1 & 0 \end{pmatrix}, \quad \sigma^2 = \begin{pmatrix} 0 & -i \\ i & 0 \end{pmatrix} \quad \text{and} \quad \sigma^3 = \begin{pmatrix} 1 & 0 \\ 0 & -1 \end{pmatrix} \tag{1.8}$$

and W_μ^a are three gauge bosons associated with this group. Given that Φ is a $SU(3)$ singlet, D_μ only contains the $SU(2)$ and $U(1)$ generators. The

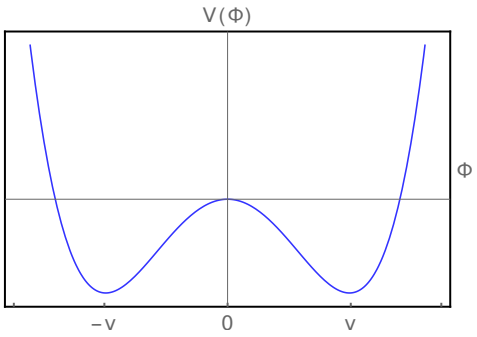

Figure 1.1: Scalar potential with degenerate minima at $v = \pm\sqrt{-\frac{\mu^2}{2\lambda}}$.

covariant derivative acting on the scalar doublet transforms as follows under gauge transformations,

$$(D'_\mu \Phi') \longrightarrow U(x) D_\mu \Phi, \tag{1.9}$$

just like the scalar doublet

$$\Phi' \longrightarrow U(x)\Phi, \tag{1.10}$$

where $U(x)$ is an element of the gauge group $SU(2)_L \times U(1)_Y$. Then, one can easily see that $\mathcal{L}_\Phi$ is invariant under the gauge transformations, equation (1.9). Looking at the scalar potential in equation (1.6),

$$V(|\Phi|) = \mu^2 |\Phi|^2 + \lambda |\Phi^\dagger \Phi|^2, \tag{1.11}$$

one finds that it has stationary points at $|\Phi|^2 = 0$ and $|\Phi|^2 = \pm\frac{\mu^2}{2\lambda}$. We are interested in a potential that is bounded from below (BFB) in order to have a ground state. This requirement tells us that $\lambda > 0$ and then we are left with the following possible configurations, either ($\mu^2 > 0$ & $\lambda > 0$) or ($\mu^2 < 0$ & $\lambda > 0$). Recall that the minimum of the potential is referred to as the minimum energy that the system can access, the vacuum, then the scalar field should take a value at either $\langle\Phi\rangle = 0$ or $\langle\Phi\rangle \equiv v = \pm\sqrt{-\frac{\mu^2}{2\lambda}}$. However, the symmetry remains unbroken when the field has a null value. As a consequence one gets ($\mu^2 < 0$ & $\lambda > 0$) and $v = \pm\sqrt{-\frac{\mu^2}{2\lambda}}$, as shown in Figure (1.1). From that figure it is possible to realize that there are two degenerate minima and, in particular, that because Φ has four (degrees of freedom) real-components the minimum is actually located in a hypersphere formed by the vevs of the real fields, which can be expressed as

$$\langle\Phi\rangle^2 = \langle\Re(\phi_1)\rangle^2 + \langle\Im(\phi_1)\rangle^2 + \langle\Re(\phi_2)\rangle^2 + \langle\Im(\phi_2)\rangle^2, \tag{1.12}$$

where $v = \langle\Phi\rangle = \pm\sqrt{-\frac{\mu^2}{2\lambda}}$. In principle, one can choose a particular direction to break the symmetry, say $\langle\Re(\phi_1)\rangle = \langle\Im(\phi_1)\rangle = \langle\Im(\phi_2)\rangle = 0$ and $\langle\Re(\phi_2)\rangle = v$, then the $SU(2)$ scalar doublet can be shifted as follows,

$$\Phi(x) = \frac{1}{\sqrt{2}}\begin{pmatrix} \phi_1(x) \\ \phi_2(x) \end{pmatrix} + \begin{pmatrix} 0 \\ v \end{pmatrix}. \tag{1.13}$$

Then, inserting equation (1.13) in (1.11), one gets a mass term for $\Re(\phi_2)$, namely the real field $\Re(\phi_2)$ gets mass after the symmetry breaking. The other real components of the complex scalar doublet remain massless, the so-called Nambu-Goldstone bosons, $G^{\pm} \equiv \phi_1$ and $G^0 \equiv \Im(\phi_2)$. According to the Goldstone's theorem [12,13] there is one for each broken generator of the symmetry. In fact, these three degrees of freedom are said to be *eaten up* by the gauge bosons and hence they get mass after the symmetry breaking (see below).

By choosing a gauge we can rewrite the $SU(2)$ scalar doublet as follows,

$$\Phi = e^{i\frac{\sigma^a}{2}\chi^a(x)}\varphi(x), \tag{1.14}$$

where

$$\varphi(x) = \frac{1}{\sqrt{2}}\begin{pmatrix} 0 \\ \sqrt{2}v + h(x) \end{pmatrix},$$

the coefficients χ^a as well as $h(x)$ are real fields and v vacuum expectation value of φ. Here h turns out to be a massive spin-0 particle. On the other hand, the operator $e^{i\frac{\sigma^a}{2}\chi^a(x)}$ is an element of the group of gauge transformations in $SU(2)$, so what we did is to fix a gauge transformation, where the one we have chosen is known as the *unitary gauge*. Then if we substitute equation (1.14) in equation (1.11) one gets the terms,

$$V' \supset m_h^2 h^2 + \frac{m_h^2}{\sqrt{2}v}h^3 + \frac{\lambda}{4}h^4,$$

where m_h represents the mass of the h particle, the so-called Higgs boson [2], which turns out to be the recently discoverd ~ 125 GeV scalar resonance by the ATLAS [14] and the CMS [15] collaborations at the LHC, see Figure 1.2, that is $m_h \simeq 125$ GeV.

The symmetry breaking, namely when the scalar field Φ gets a vev, also affects the kinetic part in the scalar Lagrangian, equation (1.6). Hence, using equation (1.14) we find that this term is given by

$$\mathcal{L}_K = (D_\mu\Phi)^\dagger D^\mu\Phi = (D_\mu\varphi)^\dagger D^\mu\varphi, \tag{1.15}$$

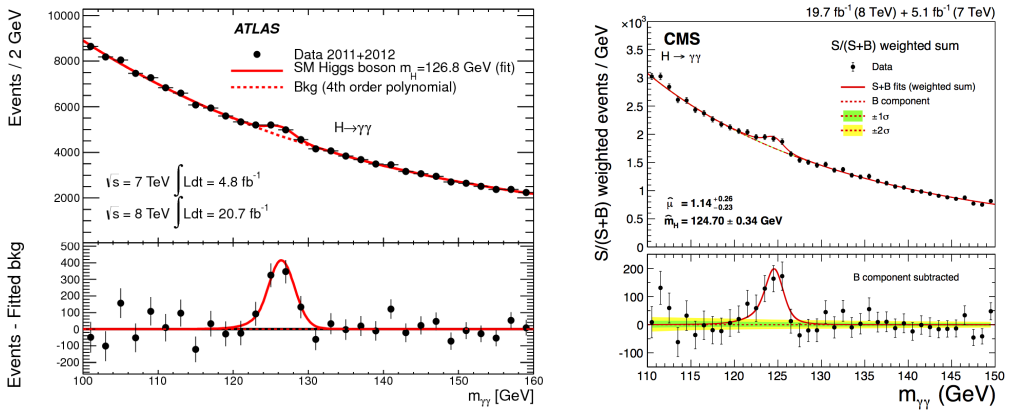

Figure 1.2: Higgs decaying into two photons (with the invariant mass $m_{\gamma\gamma} \simeq 125$ GeV) reported by the ATLAS [14] (left) and the CMS [15] collaborations (right).

where

$$D_\mu \varphi = \begin{pmatrix} \frac{g_2}{2} W_\mu^+ \left[\sqrt{2}v + h(x)\right] \\ \frac{1}{\sqrt{2}} \left[\partial_\mu + \frac{i}{2}(g_1 B_\mu - g_2 W_\mu^3)\right] \left[\sqrt{2}v + h(x)\right] \end{pmatrix}, \tag{1.16}$$

with $W_\mu^\pm \equiv \frac{1}{\sqrt{2}} \left(W_\mu^1 \mp i W_\mu^2\right)$. As a result, $\mathcal{L}_K$ is given by

$$\begin{aligned} (D^\mu \varphi)^\dagger D_\mu \varphi = {} & \frac{g_2^2 v^2}{2} W^{+\mu} W_\mu^- + \frac{v^2}{2} \left\{ g_1^2 B^\mu B_\mu + g_2^2 W^{3\mu} W_\mu^3 - 2 g_1 g_2 B^\mu W_\mu^3 \right\} \\ & + \frac{1}{4} \left(g_1^2 B^\mu B_\mu + g_2^2 W^{3\mu} W_\mu^3 - 2 g_1 g_2 B^\mu W_\mu^3 \right) (2\sqrt{2} v h + h^2) \\ & + \frac{g_2^2}{4} W^{+\mu} W_\mu^- (2\sqrt{2} v h + h^2) + \frac{1}{2} \partial^\mu h \partial_\mu h. \end{aligned} \tag{1.17}$$

From this equation one can easily recognize the kinetic term for the real field $h(x)$, a mass term for the vector $W_\mu^\pm$ and the interactions between the scalar and the vector fields. In addition, the expression inside the braces $\{...\}$ contain the mass terms for B_μ and W_μ^3 and a mixing term. Therefore, one has to rotate the fields to a basis in which the mass matrix for these vectors is diagonal, that is, to map the fields from the electroweak basis to the physical (mass) basis. The mass matrix for B_μ and W_μ^3 is given by

$$M_{BW}^2 = \frac{v^2}{2} \begin{pmatrix} g_1^2 & -g_1 g_2 \\ -g_1 g_2 & g_2^2 \end{pmatrix}, \tag{1.18}$$

which can be diagonalized with a unitary matrix U_{BW} as follows

$$\bar{M}_{BW}^2 = U_{BW} M_{BW}^2 U_{BW}^\dagger = \frac{v^2}{2} \mathrm{diag}\left(0, \left(g_1^2 + g_2^2\right)\right), \tag{1.19}$$

where $\bar{M}_{BW}$ is a diagonal matrix and the rotation matrix turns out to be

$$U_{BW} = \frac{1}{\sqrt{g_1^2 + g_2^2}} \begin{pmatrix} g_2 & g_1 \\ -g_1 & g_2 \end{pmatrix}. \tag{1.20}$$

Then, using the last equation we can rotate the fields (B_μ, W_μ^3) to the mass basis,

$$\begin{pmatrix} A_\mu \\ Z_\mu \end{pmatrix} = \frac{1}{\sqrt{g_1^2 + g_2^2}} \begin{pmatrix} g_2 & g_1 \\ -g_1 & g_2 \end{pmatrix} \begin{pmatrix} B_\mu \\ W_\mu^3 \end{pmatrix} \tag{1.21}$$

and hence the equation (1.17) becomes,

$$\begin{aligned} (D^\mu\varphi)^\dagger D_\mu\varphi = \frac{1}{2}\partial^\mu h \partial_\mu h + \frac{g_2^2 v^2}{2} W^{+\mu} W_\mu^- + \frac{v^2}{2}(g_1^2 + g_2^2) Z_\mu Z^\mu \\ + \frac{1}{4} Z_\mu Z^\mu (2\sqrt{2} v h + h^2) + \frac{g_2^2}{4} W^{+\mu} W_\mu^- (2\sqrt{2} v h + h^2). \end{aligned} \tag{1.22}$$

Notice that now the kinetic term corresponds to three massive vector fields, $W^\pm$ and Z_μ, their interactions with the scalar field and a massless gauge field,

$$A_\mu = \frac{1}{\sqrt{g_1^2 + g_1^2}} \left(g_2 B_\mu + g_1 W_\mu^3 \right). \tag{1.23}$$

Then, the gauge boson masses are,

$$m_W = \frac{1}{\sqrt{2}} g_2 v, \quad m_Z = \frac{v}{\sqrt{2}} \sqrt{g_1^2 + g_2^2}, \quad \text{and} \quad m_A = 0. \tag{1.24}$$

It is possible to parametrize the rotation matrix U_{BW} in terms of one single angle as follows

$$U_{BW} = \begin{pmatrix} \cos\theta_W & \sin\theta_W \\ -\sin\theta_W & \cos\theta_W \end{pmatrix}, \tag{1.25}$$

where $\cos\theta_W = g_2/\sqrt{g_1^2 + g_2^2}$ and θ_W is the electroweak (Weinberg) angle, which is related to the gauge couplings via $e = g_1 \cos\theta_W = g_2 \sin\theta_W$. In addition, the gauge boson masses are related by the Weinberg angle in the following way,

$$m_W = \cos\theta_W m_Z, \tag{1.26}$$

where $m_W = 80.385 \pm 0.015$ GeV and $m_Z = 91.1876 \pm 0.0021$ GeV [16, 17]. The measured masses of the gauge bosons imply (at tree-level) $\sin^2\theta_W = 1 - m_W^2/m_Z^2 \approx 0.223$. This relation gets slightly modified because of radiative corrections. Figure 1.3 depicts the results of the global fit for the SM parameters by [16] in the $(\sin^2\theta_W, m_W)$-plane (taking into account two-loop radiative corrections) which agrees nicely with the SM prediction.

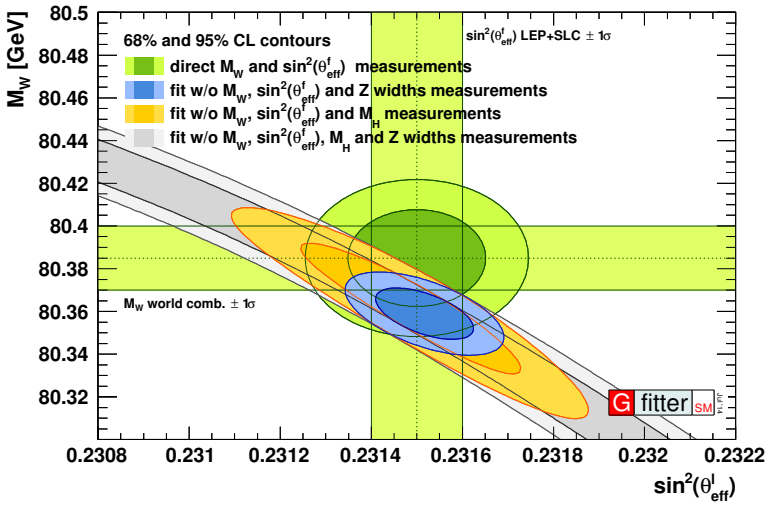

Figure 1.3: W boson mass versus sine square of the electroweak angle. Figure taken from [16], which shows the results of the global fit on the SM parameters. This fit takes into account corrections at two-loop level of the decay widths of Z^0_μ.

Using these quantities one can also define the so-called ρ-parameter, which turns out to be,

$$\rho \equiv \frac{m_W^2}{\cos^2\theta_W m_Z^2} = 1, \quad \text{in the SM.} \tag{1.27}$$

On the other hand, the vacuum expectation value of the scalar doublet has been determined from the decay rate $\mu^- \to e^-\nu_\mu\bar{\nu}_e$ and is found to be [17]

$$v = (\sqrt{2}G_F)^{-1/2} \approx 246\,\text{GeV}. \tag{1.28}$$

where $G_F = 1.1663787(6) \times 10^{-5}\text{GeV}^{-2}$ is the Fermi constant.

Finally, we check that the theory is actually $U(1)_{EM}$ invariant after symmetry breaking. To that end, we rotate the covariant derivative to the mass basis and obtain

$$\begin{aligned} D_\mu = \mathbb{I}\partial_\mu + i\frac{g_2}{\cos\theta_W} Z_\mu \left(\sin^2\theta_W Q - T^3\right) + ieA_\mu Q \\ + \frac{ig_2}{\sqrt{2}} W_\mu^+ T^+ + \frac{ig_2}{\sqrt{2}} W_\mu^- T^-, \end{aligned} \tag{1.29}$$

where the parameter e, in front of the massless gauge boson (the photon) A_μ, is the fermionic electric charge, $T^i = \sigma^i/2$ and $T^\pm = \frac{1}{2}(\sigma^1 \pm \sigma^2)$ are nothing else but the ladder operators known from quantum mechanics. $Y = \mathbb{I}/2$ is the

hypercharge operator, while Q is defined as the electric charge operator, i. e. $Q \equiv Y + T^3$. One can then show that the vacuum is invariant under electric charge transformations as follows,

$$Q\langle\Phi\rangle = Y\langle\Phi\rangle + T^3\langle\Phi\rangle = \begin{pmatrix} 0 \\ v/2 \end{pmatrix} + \begin{pmatrix} 0 \\ -v/2 \end{pmatrix} = 0, \tag{1.30}$$

and we say that the SM is invariant under the $U(1)_{EM}$ symmetry after electroweak symmetry breaking, as suggested in equation (1.4).

1.2 Yukawa sector

As we already mentioned, the scalar doublet Φ allows to write the following fermion-scalar couplings (namely, the Yukawa interactions),

$$\mathcal{L}_Y = \sum_{i,j=1}^{3} \left(Y^{\ell}_{ij} \bar{L}_{L_i} e_{R_j} \Phi + Y^{d}_{ij} \bar{Q}_{L_i} d_{R_j} \Phi + Y^{u}_{ij} \bar{Q}_{L_i} u_{R_j} \tilde{\Phi} + \text{h.c.} \right), \tag{1.31}$$

where we have used $SU(2)$ notation in equations (1.2) and (1.3) and $\tilde{\Phi} = i\sigma^2\Phi^*$. All the terms in equation (1.31) are renormalizable, Lorentz and gauge invariant. The subscripts $(i, j) = 1, 2, 3$ denote family indices and Y^a ($a = \ell, d, u$), in general, are complex matrices with *a priori* arbitrary elements. In the unitary gauge, the Yukawa Lagrangian becomes,

$$\begin{aligned} \mathcal{L}_Y &= \frac{1}{\sqrt{2}} \sum_{i,j=1}^{3} \left[Y^{\ell}_{ij} \bar{\ell}_{L_i} e_{R_j} \left(\sqrt{2}v + h(x) \right) + Y^{d}_{ij} \bar{d}_{L_i} d_{R_j} \left(\sqrt{2}v + h(x) \right) + \text{h.c.} \right] \\ &- \frac{1}{\sqrt{2}} \sum_{i,j=1}^{3} \left[Y^{u}_{ij} \bar{u}_{L_i} u_{R_j} \left(\sqrt{2}v + h(x) \right) + \text{h.c.} \right], \end{aligned} \tag{1.32}$$

where $\ell_L = (e_L, \mu_L, \tau_L)$, $e_R = (e_R, \mu_R, \tau_R)$, $u_{L,R} = (u_{L,R}, c_{L,R}, t_{L,R})$ and $d_{L,R} = (d_{L,R}, s_{L,R}, b_{L,R})$. One can see in equation (1.32) the appearance of fermion mass terms after EWSB which are defined by the product between the Yukawa matrices and the vev $\langle\Phi\rangle = v$ as follows

$$M^a \equiv vY^a \quad \text{with} \quad a = \ell, u, d. \tag{1.33}$$

These mass matrices are non-diagonal in the electroweak basis. Therefore, since any complex matrix can be diagonalized through a bi-unitary transformation, we rotate equation (1.33) from the weak to the basis in which the mass matrix is diagonal (the mass basis) in the following way,

$$\hat{M}^a = (U^a)^\dagger M^a V^a, \tag{1.34}$$

where $\hat{M}$ is a diagonal matrix. The unitary matrix U^a (V^a) rotates left(right)-handed fermionic states,

$$\psi'_{L_i} = U^a_{ij}\psi_{L_j} \tag{1.35}$$

and

$$\psi'_{Ri} = V^a_{ij}\psi_{Rj}, \tag{1.36}$$

where ψ'_{L_i,R_i} has been used to denote any left(right)-handed SM fermion in the mass basis and $(i,j=1,2,3)$ is the family index. Then, using equation (1.35) and (1.36) one finds that equation (1.32) in the physical basis is given by,

$$\begin{aligned}\mathcal{L}_Y &= \frac{1}{\sqrt{2}}\left[\bar{\ell'}_{La}\left(U^\ell_{ia}\right)^\dagger Y^\ell_{ij}V^\ell_{jb}e'_{Rb}\left(\sqrt{2}v+h(x)\right)\right] \\ &+ \frac{1}{\sqrt{2}}\left[\bar{d'}_{La}\left(U^d_{ia}\right)^\dagger Y^d_{ij}V^d_{jb}d'_{Rb}\left(\sqrt{2}v+h(x)\right)\right] \\ &- \frac{1}{\sqrt{2}}\left[\bar{u'}_{La}\left(U^u_{ia}\right)^\dagger Y^u_{ij}V^u_{jb}u'_{Rb}\left(\sqrt{2}v+h(x)\right)\right] + \text{h.c.}.\end{aligned} \tag{1.37}$$

It is worth mentioning that since the fermion mass matrices are proportional to the Yukawa ones, equation (1.33), they are diagonalized by the same unitary matrices U^a and V^a. Then, one can rewrite equation (1.37) as,

$$\begin{aligned}\mathcal{L}_Y &= \left[\bar{\ell'}_{La}(\hat{M}^\ell)_{ab}e'_{Rb} + \bar{d'}_{La}(\hat{M}^d)_{ab}d'_{Rb} - \bar{u'}_{La}(\hat{M}^u)_{ab}u'_{Rb}\right]\delta_{ab} \\ &+ \frac{1}{v\sqrt{2}}\left[\bar{\ell'}_{La}(\hat{M}^\ell)_{ab}e'_{Rb}h(x) + \bar{d'}_{La}(\hat{M}^d)_{ab}d'_{Rb}h(x)\right. \\ &- \left.\bar{u'}_{La}(\hat{M}^u)_{ab}u'_{Rb}h(x)\right]\delta_{ab}.\end{aligned} \tag{1.38}$$

From the last equation one can easily see that there is no mass term for neutrinos. However, given the discovery of neutrino oscillations [18–22] we know that they have (small) mass, roughly, six orders magnitude smaller than the electron mass [23], see Figure 1.4. This fact leads us to think that the SM is not a complete theory. On the other hand, in equation (1.38), one can notice, since $M^a = vY^a$, that there is no explanation within the SM for the mass hierarchy shown by fermions, Figure 1.4.

1.3 Charged and neutral currents

The last part to be analyzed from the SM Lagrangian, equation (1.1), are the interactions between fermions and gauge bosons A_μ, $W^\pm$ and Z_μ, which basically are encoded in the following term,

$$i\bar{\Psi}\not{D}\Psi \quad \text{with} \quad \Psi = (L_{L_i}, Q_{L_i}, e_{R_i}, d_{R_i}, u_{R_i}) \tag{1.39}$$

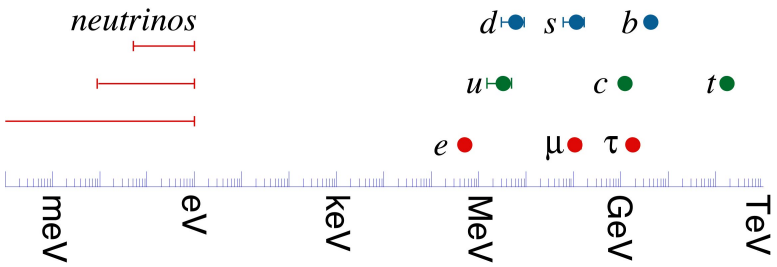

Figure 1.4: Fermion mass distribution. Figure taken from [24].

where $\not{D} \equiv \gamma^\mu D_\mu$. Then, this term in the SM takes the following form

$$\begin{aligned} i\bar{\Psi}\not{D}\Psi = {} & i\bar{\ell}_{L_i}\not{\partial}\ell_{L_i} + i\bar{e}_{R_i}\not{\partial}e_{R_i} + i\bar{u}_{L_i}\not{\partial}u_{L_i} + i\bar{u}_{R_i}\not{\partial}u_{R_i} + \bar{d}_{L_i}\not{\partial}d_{L_i} + i\bar{d}_{R_i}\not{\partial}d_{R_i} \\ & - \frac{g_2}{\sqrt{2}}W^+_\mu J^{+\mu} - \frac{g_2}{\sqrt{2}}W^-_\mu J^{-\mu} - g_2 Z_\mu J^{0\mu} - eA_\mu J^{EM\mu}, \end{aligned} \tag{1.40}$$

where $J^\pm$, J^0 are the weak charged and neutral currents respectively, while J^{EM} represents the electromagnetic interactions. The weak currents are given by,

$$J^{+\mu} = \bar{\nu}_{L_i}\gamma^\mu \ell_{jL} + \bar{d}_{L_i}\gamma^\mu u_{jL}, \qquad J^{-\mu} = \bar{\ell}_{L_i}\gamma^\mu \nu_{L_i} + \bar{u}_{L_i}\gamma^\mu d_{L_i}, \tag{1.41}$$

and

$$\begin{aligned} c_W^2 J^{0\mu} = {} & \bar{u}_L\gamma^\mu\left(\frac{2}{3}s_W^2 - \frac{1}{2}\right)u_L + \bar{d}_L\gamma^\mu\left(-\frac{1}{3}s_W^2 + \frac{1}{2}\right)d_L \\ & + \bar{\nu}_L\gamma^\mu\left(-\frac{1}{2}\right)\nu_L + \bar{\ell}_L\gamma^\mu\left(-s_W^2 + \frac{1}{2}\right)\ell_L \\ & + \bar{u}_R\gamma^\mu\left(\frac{2}{3}s_W^2\right)u_R - \bar{d}_R\gamma^\mu\left(\frac{1}{3}s_W^2\right)d_R - \bar{\ell}_R\gamma^\mu s_W^2\ell_R. \end{aligned} \tag{1.42}$$

where we have defined $s_W \equiv \sin\theta_W$ and $c_W \equiv \cos\theta_W$. On the other hand, the electromagnetic current turns out to be

$$J^{EM\mu} = -\bar{\ell}_i\gamma^\mu\ell_i + \frac{2}{3}\bar{u}_i\gamma^\mu u_i - \frac{1}{3}\bar{d}_i\gamma^\mu d_i. \tag{1.43}$$

Now, we proceed to rotate the fermion fields to the mass basis. Then, using equations (1.35) and (1.36), and taking, for instance, the second term from J^- in equation (1.41), one finds

$$\gamma^\mu\bar{u}_{L_i}d_{L_i} \longrightarrow \gamma^\mu\bar{u'}_{L_i}(U^{u\,\dagger})_{ik}U^d_{kj}d'_{jL}, \tag{1.44}$$

where the product of the unitary matrices that rotate left-handed up- and down-type quarks defined as the *Cabbibo-Kobayashi-Maskawa* (CKM) matrix as follows [25, 26],

$$V_{CKM} \equiv (U^u)^\dagger U^d. \tag{1.45}$$

The values of the CKM entries are not predicted by the SM, however they have been measured experimentally [17],

$$|V_{\rm CKM}^{\rm exp}| = \begin{pmatrix} 0.97434^{+0.00011}_{-0.00012} & 0.22506 \pm 0.00050 & 0.00357 \pm 0.00015 \\ 0.22492 \pm 0.00050 & 0.97351 \pm 0.00013 & 0.0411 \pm 0.0013 \\ 0.00875^{+0.00032}_{-0.00033} & 0.0403 \pm 0.0013 & 0.99915 \pm 0.00005 \end{pmatrix}, \tag{1.46}$$

and the Jarlskog invariant is $J = \mathrm{Im}\,[V_{us}V_{cb}V_{ub}^*V_{cs}^*] = (3.04^{+0.21}_{-0.20}) \times 10^{-5}$, which contains the information about CP violation in the quark sector.

From the term $\bar{\ell}_{L_i}\gamma^\mu\nu_{L_i}$ in equation (1.41) we can define a CKM-like matrix for the lepton sector. Then, the lepton mixing matrix is given by [1]

$$U_{\rm lep} \equiv (U^\ell)^\dagger U^\nu, \tag{1.47}$$

where U^ℓ is a unitary matrix that rotates left-handed charged leptons, while U^ν is the one that rotates left-handed (active) neutrinos. For an extended discussion see section 2.1 where the values of $U_{\rm lep}$ are given.

The determination of the values and the explanation of the pattern shown by the fermion mixing matrix is still an open problem in theoretical physics. In particular, we would like to understand why the lepton mixing matrix $U_{\rm lep}$ is so different from V_{CKM}.

Finally, one should mention that in the SM there are no flavor changing neutral currents (FCNC) at tree-level mediated neither by the Z_μ boson nor the photon A_μ nor even by the Higgs, because of the Glashow-Iliopoulos-Maiani (GIM) mechanism [27]. In fact, the flavor changing processes occur via the interactions between fermions and $W^\pm$ bosons, which are very well measured and suppressed. However, these interactions are quite relevant in SM extensions given that they might put important restrictions to the parameter space.

1.4 Higgs Properties

After the Higgs-like scalar discovery there are two important goals to be achieved in near future by the LHC: on the one hand is, hopefully, to find new

[1] This matrix is also known as the Pontecorvo-Maki-Nakagawa-Sakata (PMNS).

physics. Although, so far, there is no sign of new resonances in proton-proton collisions at $\sqrt{s} = 13$ TeV, the LHC now is putting experimental constraints to popular SM extensions, for instance, SUSY models [28, 29], theories with extra-dimensions [30, 31], composite models [32], etc. On the other hand, an important task of collider experiments is to determine the Higgs properties, i.e. its decay channels.

In Table 1.2 we show the current experimental status of Higgs decays, where the signal strength is defined as follows,

$$\mu_f \equiv \frac{\sigma^{\rm Exp}(pp \to h)}{\sigma^{\rm SM}(pp \to h)} \frac{{\rm BR}^{\rm Exp}(h \to f)}{{\rm BR}^{\rm SM}(h \to f)}, \tag{1.48}$$

where σ is the cross section for Higgs production, ${\rm BR}(h \to f)$ is the Higgs branching ratio into the final state f. The superscripts Exp and SM stand for Experimental rate and Standard Model rate, respectively.

	Signal Strength μ	
Channel	ATLAS	CMS
$h \to \gamma\gamma$	$1.14^{+0.27}_{-0.25}$	$1.11^{+0.25}_{-0.23}$
$h \to WW$	$1.22^{+0.23}_{-0.21}$	$0.90^{+0.23}_{-0.21}$
$h \to ZZ$	$1.52^{+0.40}_{-0.34}$	$1.04^{+0.32}_{-0.26}$
$h \to \tau\tau$	$1.41^{+0.40}_{-0.36}$	$0.88^{+0.30}_{-0.28}$
$h \to bb$	$0.62^{+0.37}_{-0.37}$	$0.81^{+0.45}_{-0.43}$

Table 1.2: Current experimental results on the Higgs decays by ATLAS and CMS, [33].

Even though the current experimental data is quite compatible with the SM prediction there are some Higgs decay channels that are sensitive to new physics. For instance, the one-loop decays $h \to \gamma\gamma$ and $h \to Z\gamma$ might be affected by the the existence of new charged particles. Particularly, the signal strength $\mu_{\gamma\gamma}$ can put constraints on the mass of the charged scalar bosons predicted by scenarios with, for example, either more replicas of Higgs-like particles [34] or an additional $SU(2)$ scalar triplet [35]. The latter case has additional constraints from precision physics given that the scalar triplet has a tree-level contribution to the ρ-parameter, equation (1.27).

In addition to the "visible" decay channels in Table 1.2 there also exists upper limits on the Higgs decays that result in events with missing energy, namely the "invisible" Higgs decays ($h \to \text{Inv}$), where the current limits reported by the ATLAS and CMS collaborations are, respectively,

$$\text{BR}(h \to \text{Inv}) < \begin{cases} 0.23 & [36] \\ 0.24 & [37] \end{cases} \quad \text{at } 95\% \text{ C.L.}$$

These (loose) bounds leave some room for the existence of scalar bosons lighter than the Higgs, namely $m_\sigma < m_h/2$ where σ is the new light scalar boson. In fact, σ can be either a dark matter (DM) candidate [38] or even be a physical Nambu-Goldstone boson [39].

Stability of the electroweak vacuum

As we have described in section 1.1, the quartic coupling λ in equation (1.11) determines the stability of the vacuum, namely if $\lambda < 0$ the potential is unbounded from below and hence unstable. Since, we know experimentally the vev $v = 246$ GeV and $m_h = \sqrt{2\lambda}v \simeq 125$ GeV, it is possible to derive the exact value of the quartic coupling at the electroweak scale, i.e. $\lambda_{\text{EW}} \equiv \lambda(\Lambda_{\text{EW}}) \simeq 0.13$.

One can take the approximation $V(|\Phi|) \sim \lambda_\Lambda |\Phi|^4$ where λ_Λ is the running coupling at some large scale $\Lambda \equiv |\Phi|$. The Yukawa interactions provide a negative contribution to the evolution of the equations, preventing λ to hit a Landau pole at high energies. Indeed, in the SM the main contribution to the running comes from the top Yukawa which is of the order $\mathcal{O}(1)$ and sends the Higgs self-coupling to negative values at very large scales (but few orders of magnitude before the Planck scale) and, as a result, the SM vacuum is not stable. In other words, the SM vacuum turns out to be unstable for the measured values of the top and Higgs masses [40–42].

In Figure 1.5, the evolution of λ in the SM is shown. One can see that at a scale $\sim 10^{10}$ TeV the Higgs self-coupling becomes negative which implies that there is a global minimum at large $|\Phi|$ deeper than the electroweak vacuum.

One can wonder if the instability of the SM potential at large energies represents a problem or how that behavior could be controlled. Actually, the electroweak vacuum is metastable, which implies that its average lifetime is greater than the age of the universe [43]. On the other hand, the electroweak vacuum is very sensitive to new physics, like for instance, the existence of additional scalar bosons can help to keep the Higgs self-interaction positive up

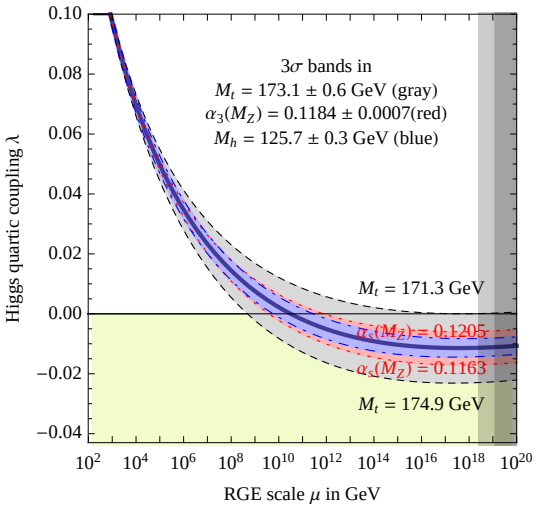

Figure 1.5: Running of the Higgs self-coupling λ. Figure taken from [41].

to the Planck scale and therefore make the vacuum stable [44, 45]. Basically, this reinforces the idea that the SM should be extended. This will be discussed in Chapter 3.

CHAPTER 2

WHY TO GO BEYOND THE SM?

The SM successfully explains three of the four known forces. However, there are three observational results that SM description cannot elucidate, these are:

- The (small) neutrino masses,
- Dark matter (DM), which represents about 80% of matter of the universe,
- The baryon asymmetry of the universe (BAU).

Therefore, one can immediately conclude that there should be some new physics to account for these issues and that the SM is not a complete theory of nature. In this regard there are many other conceptual questions that the SM cannot answer like, for instance,

- Why are there three families of quarks and leptons?
- How to explain the hierarchy of fermion masses and their mixing?
- The hierarchy between the electroweak and the Planck scale,
- Inflation,
- The cosmological constant,
- The strong CP-problem.

Over the last decades people have proposed many different SM extensions to explain one or more of these issues. The most popular descriptions like supersymmetry, Grand Unification Theories (GUT) and extra-dimensions, predict the existence of a huge (or even infinite) number of new particles. The

main accelerator experiment that might prove these ideas is the LHC, but, unfortunately, current experimental reports show no signs of new phenomena at the electroweak-TeV scale.

From the list of the various problems that we have mentioned, the origin of neutrino masses is one of the most appealing and challenging. In particular, because we do not have any experimental hint about the mechanism chosen by nature to generate the mass of these elusive particles. Despite this, it is phenomenologically interesting because the neutrino mass generation mechanism might (naturally) provide a simple explanation to some other issues faced by the SM. For instance, it is possible to build consistent models to account for neutrino mass generation, why there are three generations of quarks and leptons, the fermion mass spectrum and mixing oscillation patterns, this is known as the "flavor problem". These models usually add discrete global symmetries [46] to the SM and although there are many models in the literature that deal with these issues (namely, to explain the mass spectrum and reproduce the mixing angles in the quark and lepton sector), it is interesting to pin down particular signatures of each one in order to test them [47, 48].

There are still many unknowns in the neutrino sector but what makes it quite interesting to be taken as **the window to new physics** is that there are ongoing and future experiments (apart from the LHC) that might provide more information on the neutrino properties and then test the ideas (to be) developed in this area.

In what follows we will discuss the problems in the neutrino sector and provide a list of experiments that hopefully will give a clue of new physics.

2.1 The (ν) window to new physics

Neutrino physics has become a very active field, both experimentally and theoretically, since the experimental confirmation (by reactor and accelerator experiments) that neutrinos change flavour along their flight path, namely they oscillate, and therefore are massive particles. In addition, the LEP experiment [49] has determined (from the Z^0 decays) that there are only three active neutrino species, which in the electroweak basis turn out to be $\nu_\alpha \equiv (\nu_e, \nu_\mu, \nu_\tau)$. Therefore, the neutrino flavor and mass basis are related as follows,

$$\nu_\alpha = \sum_{j=1}^{3} [U^*_{\rm lep}]_{\alpha j} \nu_j, \tag{2.1}$$

where $U_{\rm lep}$ is the leptonic mixing matrix in equation (1.47), whose coefficients also determine the oscillations amplitudes, and (ν_1, ν_2, ν_3) are the neutrino mass eigenstates. The leptonic mixing matrix in standard parametrisation is given by

$$U_{\rm lep} = \begin{pmatrix} c_{12}c_{13} & c_{13}s_{12} & s_{13}e^{i\delta_{CP}} \\ -c_{23}s_{12} - c_{12}s_{13}s_{23}e^{i\delta_{CP}} & c_{23}c_{12} - s_{12}s_{13}s_{23}e^{i\delta_{CP}} & c_{13}s_{23} \\ s_{23}s_{12} - c_{12}c_{23}s_{13}e^{i\delta_{CP}} & -c_{12}s_{23} - c_{23}s_{12}s_{13}e^{i\delta_{CP}} & c_{13}c_{23} \end{pmatrix} K \,,$$

where $c_{ij} = \cos\theta_{ij}, s_{ij} = \sin\theta_{ij}$, δ_{CP} corresponds to the Dirac CP-violating phase and K is a complex diagonal matrix which contains two Majorana phases [63], which are present if neutrinos turn out to be their own antiparticles (namely, they are Majorana particles).

In Table 2.1 we show (the best fit values and the 1σ intervals) the results from global fits of neutrino oscillation parameters [23].

Parameter	Best Fit $\pm 1\sigma$ NH	IH
$\sin^2\theta_{13}$	0.0234 ± 0.002	0.0240 ± 0.0019
$\sin^2\theta_{12}$	0.323 ± 0.016	0.323 ± 0.016
$\sin^2\theta_{23}$	$0.567^{+0.032}_{-0.128}$	$0.573^{+0.025}_{-0.043}$
$\Delta m^2_{21}\,[10^{-5}\mathrm{eV}^2]$	$7.60^{+0.19}_{-0.18}$	$7.60^{+0.19}_{-0.18}$
$\lvert\Delta m^2_{31}\rvert\,[10^{-3}\mathrm{eV}^2]$	$2.48^{+0.05}_{-0.07}$	$2.38^{+0.05}_{-0.06}$
δ_{CP}/π	$1.34^{+0.64}_{-0.38}$	$1.48^{+0.34}_{-0.32}$

Table 2.1: Results of global fit on the neutrino oscillation parameters by [23]

Even with all these accumulated information there are still some experimental and theoretical challenges in the neutrino sector. For instance, it is yet to be determined:

i) the absolute value of neutrino masses;

ii) what is the neutrino nature (Majorana or Dirac);

iii) the neutrino mass hierarchy (namely, if it is normal $m_{\nu_1} < m_{\nu_2} < m_{\nu_3}$ or inverted $m_{\nu_3} < m_{\nu_1} < m_{\nu_2}$);

iv) the value of the CP violating phases in the lepton sector.

One of the experiments that would provide some hint of one of these issues is the Karlsruhe Tritium Neutrino (KATRIN) experiment [50], which expects to probe the absolute neutrino mass scale with a sensitivity of $\lesssim 0.2$ eV by studying the β decay of tritium ($^3_1\mathrm{H} \rightarrow {}^3_2\mathrm{He} + e^- + \bar{\nu}_e$). KATRIN started operation last year and is scheduled to collect measurements this year (2017).

There are some other experiments devoted to measure neutrinoless double beta decay $0\nu\beta\beta$. This is important since it could confirm that neutrinos are Majorana particles and give some clue about the mass hierarchy. Over the last year, the KamLAND-Zen experiment [51] released the results on $\nu 0\beta\beta$ by studying ($^{136}\mathrm{Xe} \rightarrow {}^{136}\mathrm{Ba} + 2e^-$). No such signal has been observed, which sets the limit on the half-life for this decay at $T > 1.1 \times 10^{26}$ years. The neutrinoless double beta decay is characterized by the following effective Majorana mass,

$$\langle m_{\beta\beta} \rangle = \left| \sum_{i=1}^{3} [U_{\mathrm{lep}}]^2_{ei} m_{\nu_i} \right| , \tag{2.2}$$

where U_{lep} is the leptonic mixing matrix. Figure 2.1 shows the results (blue strip in the plot) of the KamLAND-Zen experiment. The lower limit of the effective Majorana mass also depends on the uncertanty of the nuclear matrix element calculation.

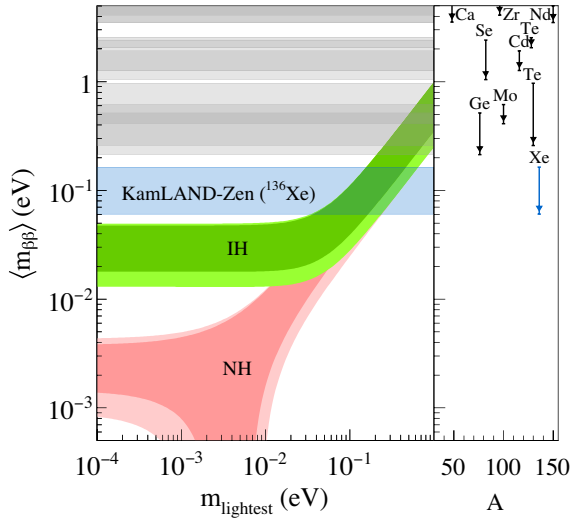

Figure 2.1: KamLAND-Zen results on $\nu 0\beta\beta$ searches. Figure taken from [51].

This plot is obtained by rewriting the effective mass, equation (2.2), in terms of the neutrino mass splittings and the (yet unknown), lightest neutrino

mass. One can see that the KamLAND-Zen experiment almost reaches the inverted hierarchy case (green region in the plot), while the normal hierarchy scenario (red region in the plot) is out of experimental reach at the moment.

Similarly, the Planck collaboration [52] (based on the Planck satellite observations of the cosmic microwave background) has put limits on the scale of the light neutrino masses (i.e. $\sum_{i=1}^{3} |m_{\nu_i}| < 0.23$ eV) and other parameters such as the number of light neutrinos $N_{\text{eff}} = 3.046$. Basically, the Planck results strongly disfavor the possibility of having neutrinos with degenerate mass spectrum.

Regarding the Dirac CP-phase in the lepton sector, the T2K experiment [53] reported a value for a phase close to $3\pi/2$. This comes from a tension between reactor and accelerator neutrino experiments. Therefore, the main goal of other experiments like DUNE [54, 55] is to measure the leptonic CP-violating phase.

On top of the open problems listed above, the origin of neutrino masses (namely the mechanism chosen by nature to generate their masses) represents one of the biggest mysteries in particle physics and an enormous experimental challenge.

2.2 Neutrino mass generation

Majorana neutrino mass

In the Standard Model, due to the gauge symmetry group, there is no way to write a renormalizable mass term for neutrinos, like for the other fermions. Instead, Majorana neutrino masses can be generated at the non-renormalizable level, for instance, through the dimension-five Weinberg operator [56] [1],

$$\mathcal{O}_5 \propto \frac{1}{\Lambda} LL\Phi\Phi, \tag{2.3}$$

where Λ is some unknown large new physics scale, $L = (\nu_L, e_L)^T$ and Φ is the $SU(2)$ scalar doublet. Notice that this operator breaks lepton number by two units, assuming that the lepton doublet transforms as $[L]_L = 1$ under the global $U(1)_L$ symmetry [2] accidentally conserved in the SM.

[1] Higher order operators that violate lepton number by two units, $\Delta L = 2$, e.g. $LLHH(H^\dagger H)^n$, can also give rise to Majorana neutrino masses [57, 58].

[2] Here the transformation of a field X under the global $U(1)_L$ symmetry is given by $[X]_L = n$, where n is lepton number assignment.

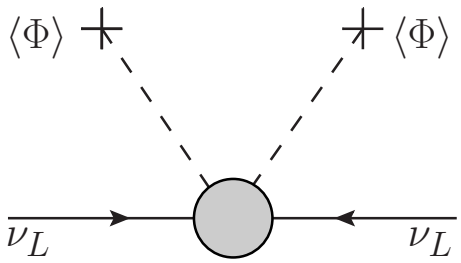

Figure 2.2: Generation of the Majorana neutrino mass through the effective dimension-five Weinberg operator.

Figure 2.2 depicts the Majorana neutrino mass generation through the dimension-five operator after electroweak symmetry breaking. Then,

$$m_\nu \propto \frac{\langle \Phi \rangle^2}{\Lambda}. \tag{2.4}$$

In general, the effective vertex involves new particles mediating the generation of the Majorana neutrino mass at either the tree- or the (n)loop-level. Typically the energy scale Λ is related to the mass(es) of the messenger particle(s) and then to neutrino mass suppression, as shown in equation (2.4). The most popular idea to generate the dimension-five Weinberg operator, equation (2.3), and hence account for the small neutrino masses is by the so-called seesaw mechanism [59–66]. Basically, at tree-level there are only three variants:

- Type I seesaw, in this case the SM is extended by adding right-handed (RH) neutrinos, which are singlets under the $SU(2)_L$ symmetry;
- Type II seesaw, here a $SU(2)$ scalar triplet Δ which carries lepton number charge is added to the SM;
- Type III seesaw, in this scheme fermion triplet Σ mediators are required.

In what follows we will only describe the first two possibilities.

TYPE-I SEESAW MECHANISM

For the type-I seesaw scenario, as we already mentioned, one introduces RH-neutrinos to the theory and then the Lagrangian for the neutrino sector is given by [63],

$$\mathcal{L}_Y \supset Y^{(I)} \bar{L} \nu_R \tilde{\Phi} + M_R \nu_R \nu_R + \text{h.c.} \tag{2.5}$$

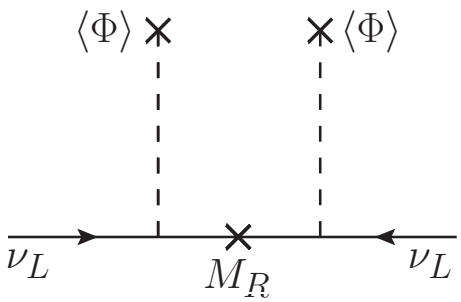

Figure 2.3: Neutrino mass generation through Type-I seesaw mechanism.

where M_R is the effective Majorana mass for RH-neutrinos. The diagram of the mass generation mechanism is shown in Figure 2.3.

After EWSB the neutrino mass matrix turns out to be,

$$M_\nu = \begin{pmatrix} 0 & M_D \\ M_D^T & M_R \end{pmatrix}, \tag{2.6}$$

where $M_D = \frac{1}{\sqrt{2}} Y^{(I)} v$. In the limit $M_R \gg M_D$ the light neutrino masses are given by,

$$m_\nu^{(I)} = -M_D M_R^{-1} M_D^T. \tag{2.7}$$

Notice that if the neutrino Yukawa $Y^{(I)}$ is of the order $\lesssim \mathcal{O}(1)$ then $M_R \sim 10^{16}$ GeV (naturally matching the GUT scale and then quite close to the Planck scale $\Lambda_{\text{Planck}} \sim 10^{19}$ GeV) in order to account for $m_\nu^{\text{light}} \sim 0.05$ eV. If the new physics scale turns out to be $\Lambda = M_R \sim \Lambda_{\text{GUT}}$, this leads to the suppression of lepton flavor violating processes and there is no hope that RH-neutrinos could be produced in collider experiments like the LHC, whose maximum operational energy is 14 TeV. On the other hand, if the Yukawa coupling $Y^{(I)} \ll 1$, then the RH-neutrino mass can be of the order of GeV, $M_R \sim \mathcal{O}(\text{GeV})$. As a consequence, these sterile particles will also contribute to $\Delta L = 2$ processes like neutrinoless double beta decay [67] or LFV processes such as $\mu \to e\gamma$ and that could give a possible way to test their existence [68].

TYPE-II SEESAW MECHANISM

In the type-II seesaw mechanism the additional $SU(2)$ scalar triplet with hypercharge $Y = 1$, is given by

$$\Delta = \begin{pmatrix} \frac{\Delta^+}{\sqrt{2}} & \Delta^{++} \\ \Delta^0 & -\frac{\Delta^+}{\sqrt{2}} \end{pmatrix}. \tag{2.8}$$

In this case, the scalar sector is given by

$$V = V(\Phi) + V(\Delta, \Phi) + \mu \left[\Phi^T (i\sigma^2) \Delta^\dagger \Phi + \text{h.c.}\right] \tag{2.9}$$

where μ is a dimensionful parameter, $V(\Phi)$ is the SM scalar potential and $V(\Delta, \Phi)$ contains Δ self- and $\Delta - \Phi$ quartic interactions. In order to generate neutrino masses $[\Delta]_L = -2$ and hence the neutrino Yukawa Lagrangian is given by [63],

$$\mathcal{L}_Y \supset Y^{(II)} L^T (i\sigma^2) \Delta L + \text{h.c.} \tag{2.10}$$

Then, after electroweak symmetry breaking the neutrino mass matrix turns out to be

$$m_\nu^{(II)} = Y^{(II)} \langle \Delta \rangle, \tag{2.11}$$

where the triplet vev [3] satisfies the following relation,

$$\langle \Delta \rangle = \mu \frac{\langle \Phi \rangle^2}{M_\Delta^2}. \tag{2.12}$$

The diagram of the neutrino mass generation mechanism is depicted in Figure 2.4.

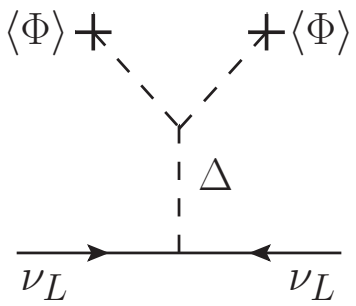

Figure 2.4: Neutrino mass generation through Type-II seesaw mechanism.

We can see from equations (3.10) that $\langle \Delta \rangle \sim m_\nu^{(II)} \sim$ eV for $Y^{(II)} \sim \mathcal{O}(1)$ which puts a stronger constraint on the triplet vev than the one coming from the ρ parameter.

In addition, this scenario predics the existence of several scalars particles: two CP-even Higgs bosons (h and H), one CP-odd Higgs boson (A), a singly charged Higgs boson ($H^\pm$) and a doubly-charged Higgs boson ($\Delta^{\pm\pm}$). One can notice from equation (2.12) that the smallness of the vev $\langle \Delta \rangle$ and hence the smallness of the neutrino mass can be regulated by the dimensionful parameter

[3] The $SU(2)$ triplet vev contributes to the ρ parameter, equation (1.27), and it is constrained to be less than a few GeV.

μ and, as result, this scheme allows these new scalars to be within the energy range of the LHC searches [69–72]. The charged particles are particularly interesting because they are characterized by having very clean decay channels (i.e. lepton number violating decays) [73, 74] as well as by contributing to the one-loop decay channels of the Higgs boson, e.g. $h \to \gamma\gamma$ [35, 75].

There are many other approaches to account for neutrino masses [76]. In relation to some low energy scale the most popular ideas are the inverse seesaw [77] and the linear seesaw [78–80]. These schemes are the so-called low-scale seesaws [81] because the small neutrino mass is not related to the heaviness of the mediators but to some free dimensionful parameter μ which is "naturally" small [4]. On the other hand, another possible explanation for tiny neutrino masses can be that they are generated at the n-loop level [82–84]. For radiative seesaw models usually a new symmetry G_X is introduced to forbid neutrino masses at lower orders, bringing, for instance, the possibility to provide a DM candidate which is connected to the neutrino mass generation and whose stability is related to the new symmetry [85, 86].

We already mentioned that it is possible to explain the mass spectrum and reproduce the mixing angles in the quark and lepton sector by adding a symmetry G_F (the so-called flavor symmetry) that relates all fermion families in certain a fashion [46, 48]. Then, one could also ask, how neutrino mass generation is related to the other SM issues (Vacuum Stability, DM, BAU, Inflation, Strong CP-problem,...)? This question can be partially answered [85, 87–95] but a full picture (theory) is still lacking.

Dirac neutrino mass

Another interesting puzzle in the neutrino sector is the one related to the neutrino nature (namely, if they are Dirac or Majorana particles). We already gave a short review about the generation of Majorana neutrino masses. However, nothing prevents neutrinos to be Dirac particles. In this case, right-handed neutrinos ν_R are required to be added to the SM. In addition, a new symmetry G_D should be present in order to forbid Majorana terms at any order. Then, assuming the absence of Majorana terms, the Yukawa Lagrangian turns out to be

$$\mathcal{L}_Y \supset Y^D \bar{L} \nu_R \tilde{\Phi}, \tag{2.13}$$

[4] In the limit $\mu \to 0$ lepton number symmetry is recovered and this is what is called the 't Hooft's naturalness principle.

and after EWSB the neutrino mass matrix is given by,

$$m_\nu^{\text{Dirac}} = Y^D v. \tag{2.14}$$

In Figure 2.5 is depicted the mass generation for a Dirac neutrino. It is easy to see that for this particular case to explain the small neutrino mass the Yukawas should be very small and as a consequence some potential phenomenological implications are erased.

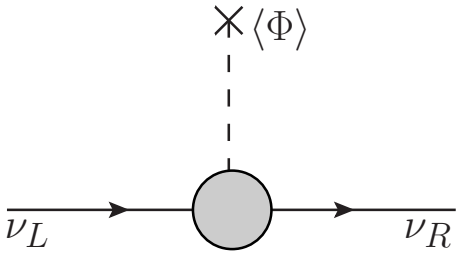

Figure 2.5: Effective Dirac neutrino mass diagram.

However one could also generate the effective vertex in Figure 2.5 and small Dirac neutrino masses through the introduction of new mediators at either the tree- or the (n)loop-level similar to the seesaw mechanisms for Majorana neutrinos [96, 97].

The most salient prediction of Dirac neutrinos is the absence of neutrinoless double beta decay. Although connections to the flavor problem have also been explored in this context [96, 98]. Here, it is also possible to find connections between the generation of Dirac neutrinos and other SM issues [99, 100] but this option is not as widely studied as the Majorana case.

CHAPTER **3**

NEUTRINO MASS GENERATION AND NEW PHYSICS

In this chapter we summarize the main results on the implications of neutrino mass generation.

3.1 The Impact on the Vacuum Stability

Neutrino masses à la Higgs

In section 1.4 we have discussed the stability of the electroweak vacuum suggests that there should be some new physics (particles) somewhere, at least, to account for neutrino mass generation, dark matter and the baryon asymmetry of the universe. In particular the neutrino sector urges the existence of new degrees of freedom which may well affect the vacuum stability [44].

We had discussed that there exist many variants of the seesaw mechanism. Here we put our attention on a variant of the inverse seesaw mechanism [77] (see [81] for a recent review) where the neutrino mass is generated after the spontaneous breaking of lepton number [101]. In this scheme the new particles added to the SM are[1]: a right-handed neutrino ν_R (with lepton number $[\nu_R]_L = 1$), a left-handed singlet S (with $[S]_L = 1$) and a $SU(2)$ scalar singlet σ (with $[\sigma]_L = -2$). Then the Yukawa Lagrangian, invariant under the SM gauge symmetry as well as the global $U(1)_L$ symmetry, for the neutrino sector is given by,

[1]For simplicity we are considering the one family case. However the discussion can be easily extended to three families.

$$-\mathcal{L}_\nu = Y_\nu H \nu_R^c L + M \nu_R^c S + Y_S S S \sigma + \text{h.c.} \tag{3.1}$$

On the other hand, the scalar potential turns out to be [39] ,

$$V(\sigma, H) = \mu_1^2 |\sigma|^2 + \mu_2^2 H^\dagger H + \lambda_1 |\sigma|^4 + \lambda_2 \left(H^\dagger H\right)^2 + \lambda_{12} \left(H^\dagger H\right) |\sigma|^2 . \tag{3.2}$$

Here the $SU(2)$ scalar doublet is denoted by H and its vacuum expectation value is given by $\langle H^0 \rangle = v_H$. One can notice from equations (3.1) and (3.2) that the role of the complex scalar singlet σ is to break lepton number after it develops a vev $\langle \sigma \rangle = v_\sigma$. Then, after EWSB the neutrino mass is,

$$m_\nu = Y_S \langle \sigma \rangle \left(\frac{Y_\nu \langle H^0 \rangle}{M} \right)^2 . \tag{3.3}$$

After spontaneous symmetry breaking, there are three physical scalars: two CP-even (H_1, H_2) and one CP-odd. One of the CP-even states should have a mass of 125 GeV (say for instance H_1) while the mass of the other one is free. The CP-odd scalar remains massless, the so-called Majoron, $J \propto \Im(\sigma)$.

In order to guarantee the vacuum stability of the scalar potential, equation (3.2), we use one-loop renormalization group equations in this model (given in the appendix of Chapter 4) and require that the following boundedness conditions,

$$\lambda_1 > 0, \quad \lambda_2 > 0 \quad \text{and} \quad -\lambda_{12}^2 + 4\lambda_1\lambda_2 > 0, \tag{3.4}$$

are fulfilled from the electroweak scale up to the Planck scale.

In Figure 3.1, we show the doublet-singlet mixing angle α versus m_{H_2}, where the region in green leads to a potential bounded from below, the orange one represents that the potential hits a Landau pole at some energy scale and the red one are the values which give an unstable potential. In this case the lepton number breaking scale v_σ is at the TeV scale, $Y_\nu \sim \mathcal{O}(1)$ and hence the tiny neutrino mass is related to the smallness of the dimensionless parameter Y_S.

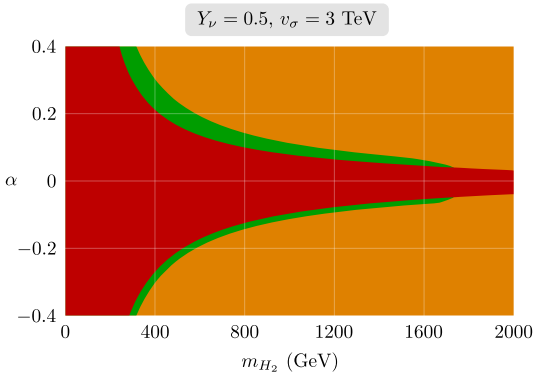

Figure 3.1: Doublet-singlet mixing angle α versus m_{H_2}. See text for color description.

Another interesting possible configuration to account for the neutrino masses is to have $v_\sigma \sim$ TeV, $Y_S \sim \mathcal{O}(1)$ and $Y_\nu << 1$. The results for this case are shown in Figure 3.2. As before, the green color is used to display the region where the scalar potential is stable, the red one is for an unstable potential and the orange one is for the non-perturbative region (where one, or more, dimensionless parameter(s) is/are $> \sqrt{4\pi}$).

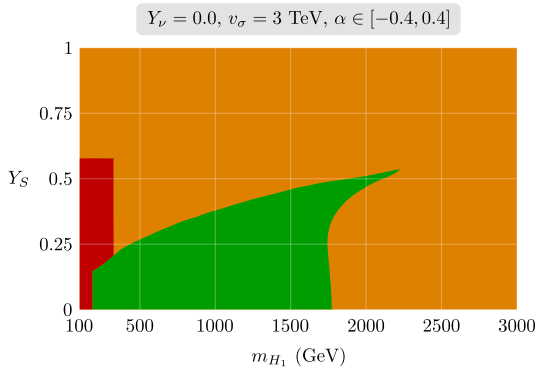

Figure 3.2: The stability and perturbativity regions for non-zero $Y_S > 0$ and very small Y_ν; the color code is as in Figure 3.1.

From these outcomes one can conclude that the vacuum stability can be achieved in these class of models with the new degrees of freedom needed to generate neutrino masses at low scale. This conclusion was not clear a priori, since the neutrino Yukawas are of the order $\mathcal{O}(1)$ and they tend to drive the scalar self-couplings to negative values [102, 103] as the top Yukawa does.

Other interesting features of this approach are the following:

- There is a physical Nambu-Goldstone boson J associated with the lepton number breaking which might be related to the invisible Higgs decays [39] (see section 3.2);

- The neutrino mass generation can be achieved at the TeV scale and hence the new physics effects could be within the reach of the LHC searches.

Revisiting the Type-II seesaw mechanism

In section 2.2 we described the type-II seesaw mechanism and from the previous discussion we have seen that vacuum stability as well as the boundedness conditions can provide constraints in the parameter space.

The full scalar potential for the type-II seesaw is given by,

$$\begin{aligned} V\left(H,\Delta\right) &= -\mu_H^2 H^\dagger H + \mu_\Delta^2 \mathrm{Tr}\left(\Delta^\dagger\Delta\right) + \left[\frac{m_{H\Delta}}{2} H^T\left(i\sigma^2\right)\Delta^\dagger H + \mathrm{h.c.}\right] \\ &+ \frac{1}{2}\lambda_H\left(H^\dagger H\right)^2 + \lambda_{H\Delta}\mathrm{Tr}\left(\Delta^\dagger\Delta\right)\left(H^\dagger H\right) + \lambda'_{H\Delta} H^\dagger\Delta\Delta^\dagger H \\ &+ \frac{\lambda_\Delta}{2}\left[\mathrm{Tr}\left(\Delta^\dagger\Delta\right)\right]^2 + \frac{\lambda'_\Delta}{2}\mathrm{Tr}\left(\Delta^\dagger\Delta\Delta^\dagger\Delta\right), \end{aligned} \tag{3.5}$$

where H is the $SU(2)$ scalar doublet and Δ is the $SU(2)$ scalar triplet in equation (2.8). In this case, the boundedness conditions turn out to be,

$$\begin{gathered} \lambda_H,\ \lambda_\Delta + \lambda'_\Delta,\ \lambda_\Delta + \frac{1}{2}\lambda'_\Delta > 0 \\ \lambda_{H\Delta} + \sqrt{\lambda_H\left(\lambda_\Delta + \lambda'_\Delta\right)},\ \lambda_{H\Delta} + \lambda'_{H\Delta} + \sqrt{\lambda_H\left(\lambda_\Delta + \lambda'_\Delta\right)} > 0 \\ \text{and} \\ \left[\lambda'_\Delta\sqrt{\lambda_H} \leq \left|\lambda'_{H\Delta}\right|\sqrt{\lambda_\Delta + \lambda'_\Delta}\right. \\ \left.\text{or}\ \ 2\lambda_{H\Delta} + \lambda'_{H\Delta} + \sqrt{\left(2\lambda_H\lambda'_\Delta - {\lambda'_{H\Delta}}^2\right)\left(2\frac{\lambda_\Delta}{\lambda'_\Delta} + 1\right)} > 0\right]. \end{gathered} \tag{3.6}$$

The parameter space restrictions are obtained by imposing the boundedness conditions of equation (3.6) and considering the renormalization group evolution of the triplet seesaw model [2]. In addition, we demanded that all quartic couplings remain small (i.e. $|\lambda_i| < \sqrt{4\pi}$) up to m_{Planck}. Then, in this case, the vacuum stability requirement also constraints the mass splittings of the triplet components as shown in Figure 3.3. This plot is obtained by using the mass relation (sum rule) between the charged particles given by,

$$m^2_{H^{\pm\pm}} - m^2_{H^\pm} \simeq -\frac{\lambda'_{H\Delta}}{2}v_H^2$$

where $\lambda'_{H\Delta}$ (fulfilling the above requirements) is bounded to be in the range $\sim \pm|0.85|$. In addition, the experimental bound ($m_{H^{\pm\pm}} \lesssim 400$ GeV [3]) comes from direct searches of $H^{\pm\pm}$ decaying into like-sign leptons at the LHC [104, 105].

[2] Here we used the one-loop renormalization group equations given in Chapter 5.

[3] This bound is a good approximation assuming that the branching ratio of $H^{\pm\pm}$ decay into either $e^\pm e^\pm$, $e^\pm\mu^\pm$ or $\mu^\pm\mu^\pm$ is 100%.

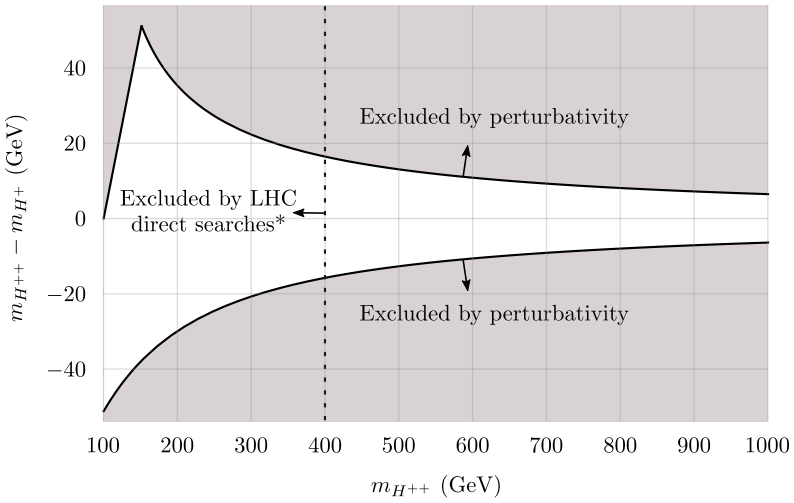

Figure 3.3: $m_{H^{++}} - m_{H^+}$ versus $m_{H^{++}}$. The exclusion region (in gray) is defined by the points that violate the perturbativity condition at some scale before m_{Planck}.

One can notice here, or from the previous section, that the vacuum stability requirement puts important constraints on the parameter space, however it does not rule out the model, particularly for these well-motivated scenarios that can account for the small neutrino masses.

This scheme can also have a dynamical completion, namely that the dimensionful parameter $m_{H\Delta}$ is generated after the spontaneous breaking of lepton number $m_{H\Delta} \propto \langle\sigma\rangle$ [101]. As a consequence, a physical Nambu-Goldstone boson (J) is present in the theory and hence the decay channel $H \to JJ$ opens up, namely the invisible Higgs boson decay [39, 106, 107].

3.2 Modifications of the Higgs Properties

In what follows we discuss the invisible decays of the Higgs which open up due to the presence of a physical Nambu-Goldstone boson, the Majoron J.

Invisible Higgs Decays

In section 3.1 we described the inverse seesaw mechanism [77] where the scalar sector contains a $SU(2)$ scalar doublet H and the singlet σ, responsible for the lepton number breaking. After electroweak symmetry breaking there are three physical states: two massive CP-even (H_1, H_2) and one massless CP-odd, J. Therefore, there exist an invisible decay channel for both CP-even scalars, that is,

$$H_i \to JJ. \tag{3.7}$$

One interesting possibility is the existence of a light scalar (i.e. $m_{H_i} < 125$ GeV), whose dominant decay channel is the invisible one. This is not yet excluded by current LHC data nor by the LEP experiment [108]. Instead, LEP-II data can be translated as a constraint on the mixing angle between the doublet and the singlet scalars, where $H_1 = \cos\alpha\,\Re(\sigma) + \sin\alpha\,\Re(H^0)$ and $H_2 = -\sin\alpha\,\Re(\sigma) + \cos\alpha\,\Re(H^0)$. In Figure 3.4 the LEP results are shown, assuming that $m_{H_1} < m_{H_2} = 125$ GeV. The blue region is the region excluded by LEP results. The red, cyan and magenta regions correspond to $BR(H_2 \to JJ) < (75\%, 50\%, 25\%)$ respectively. Notice that in the plot there is a jump when $H_2 \to 2H_1$ is kinematically allowed (i.e. $m_{H_1} < m_{H_2}/2$) and hence $H_2 \to 2H_1 \to 4J$.

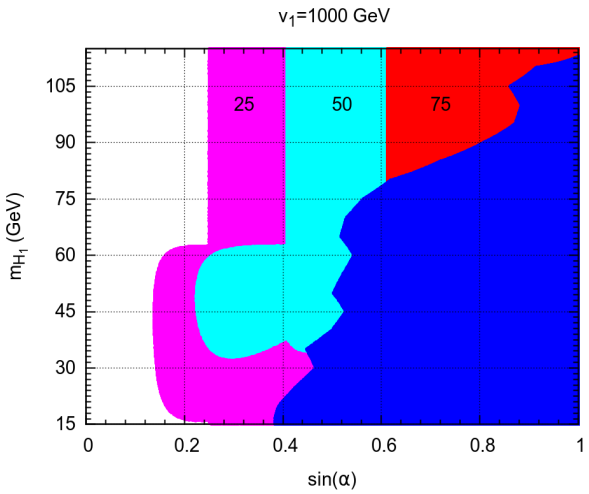

Figure 3.4: m_{H_1} versus $\sin\alpha$ in the model for a lepton number breaking scale at 1000 GeV.

From the LHC results on the *visible* Higgs decays, listed in Table 1.2, one can see that the signal strengths μ_f are compatible within a 20% deviation from the SM prediction , i.e. $\mu_f = 1.0 \pm 0.2$. Therefore, one can combine the LEP and LHC constraints in the $(m_{H_1}, \sin\alpha)$-plane as shown in Figure 3.5. In the plot, the blue region is the LEP exclusion region, the red one corresponds to LHC exclusion region (namely $\mu_f \notin 1.0 \pm 0.2$) and the green one are the values that satisfy all the experimental constraints. One can see from the plot that $\sin\alpha \lesssim 0.2$, implying that a large doublet-singlet mixing is rule out by current data.

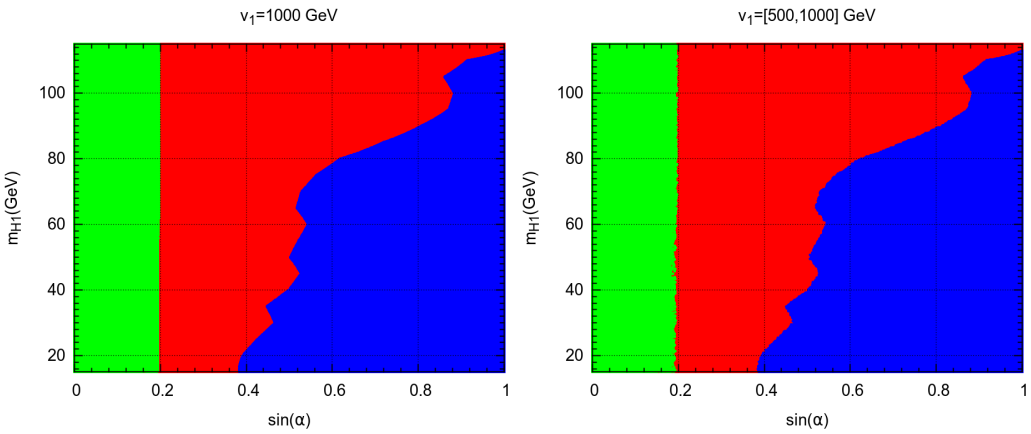

Figure 3.5: m_{H_1} versus $\sin\alpha$ in the model for lepton number breaking scale $v_1 = 1000$ GeV (left panel) and $v_1 \in [500, 1000]$ GeV (right panel). See text for the color description.

In Figure 3.6 we show the correlation between the signal strengths μ_{ZZ} and $\mu_{\gamma\gamma}$ along with the LEP and the LHC constraints as described before. From the plot we can conclude that within the model current data implies that the signal strengths should be in the range $0.8 \lesssim \mu_{ZZ} \lesssim 1$ and $0.8 \lesssim \mu_{\gamma\gamma} \lesssim 1$. A detailed discussion is given in Chapter 6.

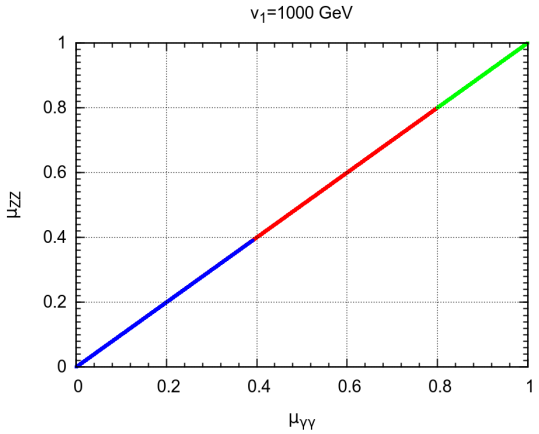

Figure 3.6: Correlation between μ_{ZZ} and $\mu_{\gamma\gamma}$. The color code is as in Figure 3.5.

More Non-Standard Higgs Decays

The Higgs sector has a much richer phenomenology when the dynamical completion of the Type-II seesaw is realized[4]. This is because, apart from the invisible Higgs decays ($H_i \to JJ$), there are other non-standard (one-loop) Higgs decays (namely $H_i \to \gamma\gamma$ and $H_i \to Z\gamma$) due to the presence of the charged scalars. In this case, there are nine physical states and two possible configurations of interest as shown in Figure 3.7.

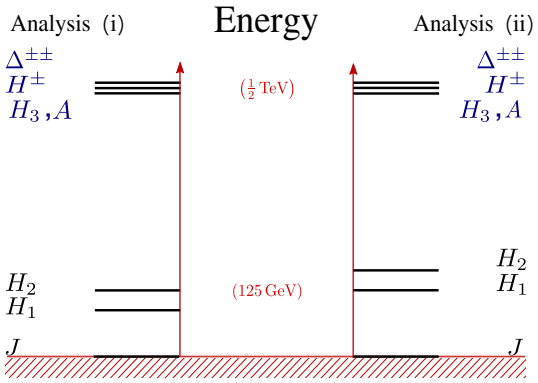

Figure 3.7: Higgs boson mass spectrum in Type-II seesaw with spontaneous breaking of lepton number. Analysis (i) considers: $m_{H_1} < m_{H_2} = 125$ GeV. Analysis (ii) assumes: $m_{H_1} = 125$ GeV $< m_{H_2}$. In both we took $m_{H_3} \sim m_A \sim m_{H^+} \sim m_{\Delta^{++}} \sim 0.5$ TeV.

These alternatives are well motivated from the available experimental data:

[4]The details of the model are given in Chapter 7.

- First, from the LEP data [108] we know that the existence of a light CP-even boson is still possible, see Figure 3.4.
- Second, from the LHC searches of the $\Delta^{\pm\pm}$ boson [104, 105], we have that $m_{\Delta^{\pm\pm}} \gtrsim 400$ GeV.

Then, in Analysis (i) we consider: $m_{H_1} < m_{H_2} = 125$ GeV, while the members of the triplet $m_{H_3} \sim m_A \sim m_{H^+} \sim m_{\Delta^{++}} \sim 1/2$ TeV. Here the triplet vev is defined as $\langle \Delta^0 \rangle \equiv v_3 = 10^{-5}$ GeV and the lepton number breaking scale (the singlet's vev) is varied in the range $v_1 = [100, 2500]$ GeV. Figure 3.8 shows the correlation between the signal strengths $(\mu_{\gamma\gamma}, \mu_{ZZ})$ and the branching fraction $H_2 \to$ Inv. As before, the blue region is the LEP exclusion region, the red one are the values lying outside the region $\mu_f = [0.8, 1.2]$ and the green one defines the region that fulfills LEP and LHC experimental constraints. One can observe that in our analysis BR$(H_2 \to \text{Inv}) < 0.20$, which is a tighter constraint than the current limits reported by the ATLAS and the CMS collaborations,

$$BR(h \to \text{Inv}) < \begin{cases} 0.23 & [36] \\ 0.24 & [37] \end{cases} \quad \text{at } 95\% \text{ C.L.}$$

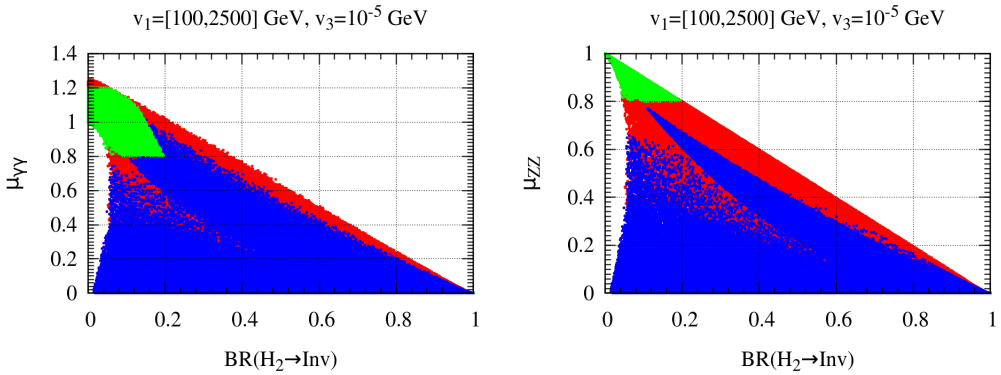

Figure 3.8: Analysis (i). The signal strength $\mu_{\gamma\gamma}$ versus BR$(H_2 \to \text{Inv})$, left panel. The signal strength μ_{ZZ} versus BR$(H_2 \to \text{Inv})$, right panel. The color code is as in Figure 3.5.

In Analysis (ii) we consider: $m_{H_1} = 125$ GeV $< m_{H_2}$, while the members of the triplet $m_{H_3} \sim m_A \sim m_{H^+} \sim m_{\Delta^{++}} \sim 1/2$ TeV, $v_3 = 10^{-5}$ GeV and $v_1 = [100, 2500]$ GeV. Some results for this Higgs boson mass spectrum are shown in Figure 3.9. Here the LEP constraint does not apply. Then, the green region is the allowed region by the LHC, namely $\mu_f = [0.8, 1.2]$, while the red one is excluded. The correlation between the signal strengths $(\mu_{\gamma\gamma}, \mu_{ZZ})$ and the invisible Higgs decay suggests that in this case as well, BR$(H_1 \to \text{Inv}) < 0.20$ as in Analysis (i).

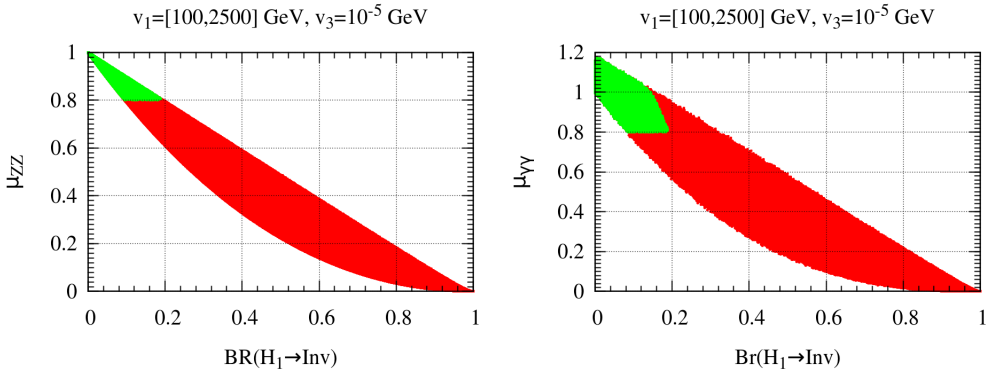

Figure 3.9: Analysis (ii). The signal strength μ_{ZZ} versus $\mathrm{Br}(H_1 \to \mathrm{Inv})$, left panel. The signal strength $\mu_{\gamma\gamma}$ versus $\mathrm{Br}(H_1 \to \mathrm{Inv})$. See text for color code definition.

In this brief summary we have shown the impact of neutrino mass generation on the scalar sector. The full model as well as the neutrino mass generation mechanism are described in Chapter 7.

3.3 Constraining the neutrino mass with flavor symmetries

We have mentioned that one of most interesting problems from the theoretical perspective resides in trying to elucidate why the neutrino oscillation parameters, Table 2.1, are so different from the ones that characterize the quark sector, equation (1.46).

One idea that has been widely studied to tackle this problem is to invoke additional global discrete symmetries G_F that relate the fermion families, the so-called *flavor symmetries* [46]. The advantage of this approach is that these symmetries also provide certain structure to the Yukawa matrices and hence it is possible to get correlations between the oscillation parameters and the observables, for instance the neutrino masses [48].

The possible predictions that one can obtain in models with flavor symmetries G_F are:

- neutrino mass sum rules [47, 109];
- neutrino mixing sum rules [110].

Another interesting prediction of flavor symmetries are the charged fermion *mass relations* [111–113], which relates down-type quarks and charged lepton

mass as,

$$\frac{m_b}{\sqrt{m_d m_s}} = \frac{m_\tau}{\sqrt{m_e m_\mu}}. \tag{3.8}$$

This relation is obtained from the flavor structure in the Yukawa sector, assuming certain hierarchy among the parameters. The equation (3.8) can be naturally generated by flavor groups with three-dimensional irreducible representations such as: A_4, T', $T_n \cong Z_n \rtimes Z_3$ (with $n = 7, 13, 19, 31, 43, 49$). Such groups are discussed in [46].

In a scenario where T_7 is the flavor symmetry and the neutrino mass generation is through the Type-I seesaw mechanism, one can also predict a lower bound for the lightest neutrino mass[5]. This is similar to the results that one obtains with the neutrino mass sum rules [47, 109], which suggests that there could be a flavor symmetry behind it.

In Figure 3.10 the correlation between effective neutrino mass parameter $|m_{ee}|$ (which characterizes $0\nu\beta\beta$) and the lightest neutrino mass is shown. The purple region is the prediction for normal hierarchy while the magenta one is for the inverted case. The vertical dot-dashed line represents the bound coming from cosmological observations (that is, the combination of CMB and BAO data [114]) and the dotted line is the future sensitivity of KATRIN [50].

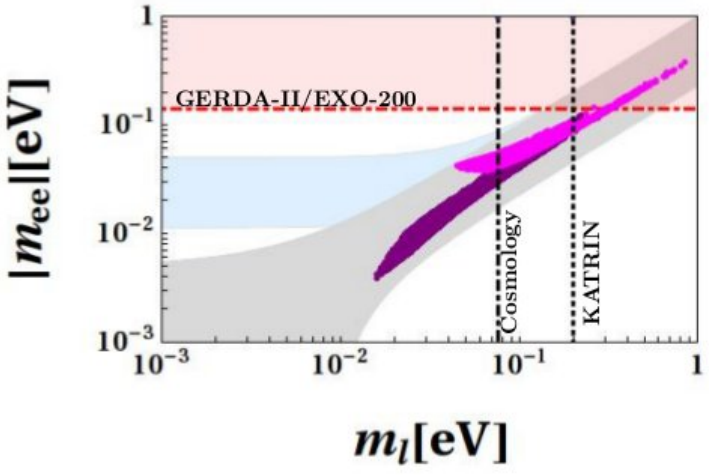

Figure 3.10: Effective neutrino mass parameter $|m_{ee}|$ (which characterizes $0\nu\beta\beta$) and the lightest neutrino mass.

[5] The details of the model and results are given in Chapter 8.

3.4 Naturally Small Dirac Neutrinos

There are several experiments devoted to measure neutrinoless double beta decay, whose confirmation according to the "Black Box theorem" [115] would confirm that neutrinos are indeed Majorana particles. However, so far, there is no experimental evidence preventing neutrinos to be Dirac particles. In fact, for instance, the non-observation of $\nu 0\beta\beta$ might suggest that neutrinos could be Dirac.

In general, there are two ingredients that one has to add to the SM in order to have Dirac neutrinos,

1) right-handed particles ν_R, see Figure 2.5, and

2) an additional symmetry G_D that forbids Majorana terms.

With this information one can ask, what is the matter content required for the seesaw mechanisms in this case? [96, 116]. For the Dirac Type-II seesaw mechanism, instead of adding a $SU(2)$ scalar triplet, another (neutrinophilic) $SU(2)$ scalar doublet is required. Figure 3.11 shows the diagram to generate naturally small Dirac neutrino masses. Here H is the SM scalar doublet, Φ is a neutrinophilic scalar doublet and σ is a scalar singlet added for the dynamical completion. In order to accomplish this mechanism leptons are charged under a global $G_D \equiv \mathbb{Z}_5 \times \mathbb{Z}_3$, while H is blind under G_D. The scalars Φ and σ are charged only under the $\mathbb{Z}_5 \in G_D$ symmetry. For a complete description of the charge assignments see Table 9.1 in Chapter 9. These simple requirements/assignments forbids all Majorana terms. The tree-level Dirac terms $\bar{L}\nu_R\tilde{H}$ and $\bar{L}\ell_R\tilde{\Phi}$ are forbidden by $\mathbb{Z}_3$ and $\mathbb{Z}_5$, respectively. Given that all scalars are blind under $\mathbb{Z}_3$, this symmetry remains unbroken after EWSB.

In this particular model, there is an accidental global $U(1)$ symmetry. Therefore, after spontaneous breaking, a physical Nambu-Goldstone boson appears, the *Diracon* denoted by $\mathcal{D}$ and the small vacuum expectation value of $\langle\Phi\rangle = v_\Phi$ is induced by the vevs $\langle\sigma\rangle = v_\sigma$ and $\langle H\rangle = v_H$, as shown in Figure 3.11.

In this case, since Φ is a doublet, its vev has no constraint from the ρ-parameter. However, the coupling of σ to charged leptons could lead to excessive stellar cooling through the Compton–like process $\gamma + e \to e\mathcal{D}$ [117]. Taking this into account it is possible to provide a bound on v_Φ. This bound is shown in Figure 3.12.

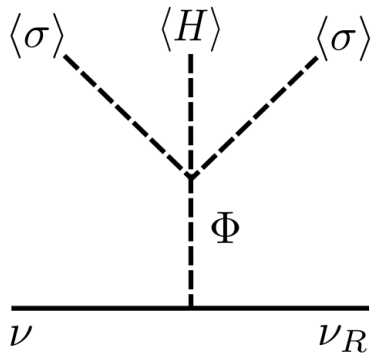

Figure 3.11: Neutrino mass generation in Dirac type-II seesaw mechanism.

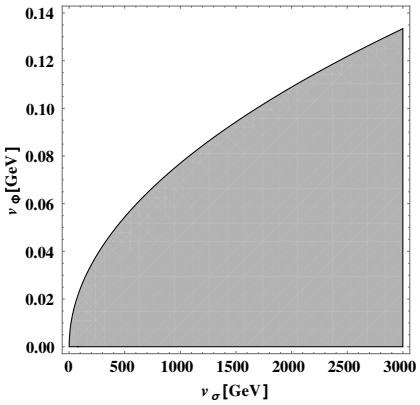

Figure 3.12: Bound on v_Φ coming from stellar energy loss limits. The shaded region represents the allowed region.

One can also wonder if the symmetry G_D could be related to some flavor symmetry, i.e. $G_D = G_F$. Indeed this connection is possible and only few flavor symmetry groups will do the job of G_D [98].

Even though it was not mentioned, Dirac neutrinos suggest the existence of a residual symmetry in the broken phase that forbids Majorana mass terms at all orders. For the Dirac Type-II seesaw scheme this symmetry turns out to be $\mathbb{Z}_3$, which implies that in the broken phase the residual symmetry is $U(1)_{EM} \times \mathbb{Z}_3$.

3.5 The link to Dark Matter Stability

It is interesting to note that the residual symmetry that forbids the "unwanted" Majorana mass terms at all orders can be also connected to the symmetry that

stabilizes the dark matter candidate [100, 118]. Therefore, the Dirac nature of neutrinos might be linked to the dark matter stability.

In Figure 3.13 we show the diagram to generate Dirac neutrino mass at the two loop level. Here there are two $SU(2)_L$ doublets, H and η and three complex singlets, σ, χ and ξ; ν^c is the right-handed neutrino and N and S are fermions singlets. In this case the global symmetry is $G_D \equiv U(1)_D \times \mathbb{Z}_3^{DM} \times \mathbb{Z}_3$, where $\mathbb{Z}_3$ forbids tree-level Dirac terms. The charge assignments of the model are given in Table 10.1 in Chapter 10.The physical Nambu-Goldstone boson $\mathcal{D} = \Im(\sigma)$ is also present in this model because of the breaking of the global $U(1)_D$ symmetry. The important point is that the scalars $X = (\eta, \chi, \xi)$ carry a $\mathbb{Z}_3^{DM}$ charge. However, given that none of the X scalars develop a vev the $\mathbb{Z}_3^{DM}$ symmetry remains unbroken after spontaneous symmetry breaking. Therefore, the dark matter candidate which will be the lightest among the neutral components of η, χ or ξ, can be stabilized by the Z_3^{DM} symmetry [119, 120].

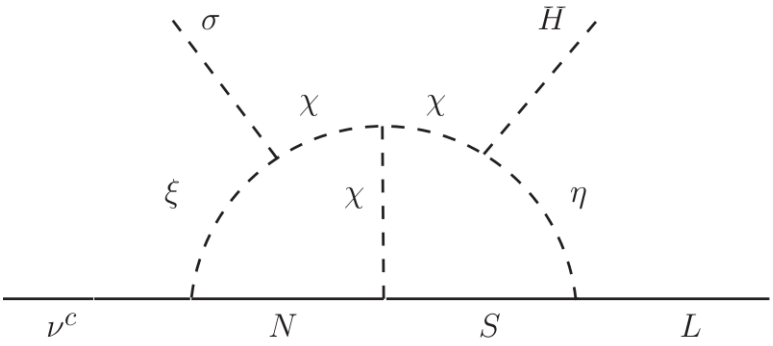

Figure 3.13: Dirac neutrino mass at two-loop level.

If one assumes that the dark matter candidate in $X = (\eta, \chi, \xi)$ is mainly singlet, then its detection is given by the Higgs portal interaction, namely λ_{HX}. Figure 3.14 shows the exclusion regions in the (m_X,λ_{HX})-plane. The LUX results [121] on dark matter searches correspond to the purple line while the bound given by PandaX [122] match to the dot-dashed blue line. The red region defines the constraint coming from the invisible Higgs decays. One notices that there are different shades of red corresponding to different contributions of the decay $H \to \mathcal{D}\mathcal{D}$ to the branching fraction $H \to$ Inv.

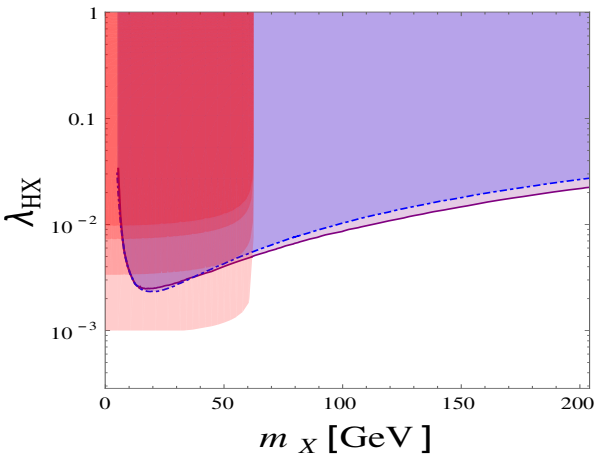

Figure 3.14: Exclusion regions in the (m_X,λ_{HX})-plane. See text for color code definition.

CONCLUSIONS

In this thesis we have explored the connection between neutrino properties and new physics. In particular, we focused on the study of neutrino mass generation which requires the existence of new degrees of freedom. As a result, neutrino physics turns out to be the natural path to new phenomena and is a very interesting field on its own.

We first discussed the impact of neutrino mass generation in the scalar sector. In order to do that, we studied the vacuum stability in schemes that explain neutrino masses at low-scale, i.e. close to the electroweak scale. This kind of analysis was done for two distinct cases: 1) in the inverse seesaw scheme where both the Yukawa and the scalar sector are extended with respect to the SM; and, 2) in the type II seesaw scheme, where only a new $SU(2)$ scalar triplet is added to the standard description of electroweak phenomena. From our study we found that in both scenarios the vacuum stability is possible in contrast to what happens in the SM. However, it turns out that the vacuum stability puts stringent constraints on the parameter space of our models. For instance, in the type-II seesaw, this requirement demands a compressed Higgs spectrum. We also studied the connection of these schemes and the Higgs properties. Specifically, we went through the variants of the seesaw mechanisms in which neutrino masses are generated after the spontaneous breaking of lepton number (an Abelian continuous symmetry). The breaking of this symmetry gives rise to the existence of a physical Nambu-Goldstone boson, the Majoron (J), and hence to the invisible Higgs decays ($h \to JJ$). From our results, which take into account the existing experimental constraints coming from the collider experiments (LEP and LHC), we found that the branching ratio $BR(h \to \text{Invisible})$ should be less than 20% within the scenarios we have explored. This can be established from the correlations we found between the

visible and the *invisible* Higgs decay channels.

This thesis also contains our results on the study of the flavor problem, namely, what explains the masses and mixings in the fermion sector? In this case, we presented a model that predicts a mass relation between down-type quarks and charged leptons and that consistently explains the mass spectrum as well as mixing parameters in both the quark and the lepton sectors. In this scenario we found correlations between the atmospheric angle and the absolute value of neutrino masses. We also provided a lower bound for the lightest neutrino mass (for both normal and inverted hierarchy) stemming from the results on neutrinoless double beta decay.

We also explored the possibility that neutrinos are Dirac particles. We gave a consistent framework that naturally explains the small neutrino masses. In fact, the scenario we have built is characterized by the presence of an additional symmetry $U(1)_D$ that forbids Majorana mass terms at all orders. We found that the symmetry that guarantees the Diracness of neutrinos can be the one that stabilizes the dark matter candidate of the theory. Such a possibility was explored in a scheme where neutrino masses are generated at the 2-loop level. The most relevant and interesting result comes when the neutrino masses are generated after the spontaneous breaking of the $U(1)_D$ symmetry, because this predicts the existence of a physical Nambu-Goldstone boson, the Diracon ($\mathcal{D}$), which might be related to the invisible Higgs decays.

RESUMEN

En este trabajo de tesis hemos analizado algunas de las posibles conexiones entre la generación de la masa de los neutrinos y la nueva física. Para ello, como preámbulo, en el primer capítulo hemos hecho un repaso del Modelo Estándar (SM) de la física de partículas, siendo ésta la descripción más precisa que tenemos de las las interacciones fuertes, débiles y electromagnéticas. Sin embargo, existen algunas interrogantes a las que el SM no ofrece respuesta, por ejemplo, ¿Por qué hay tres familias de quarks y leptones?, ¿Cuál es la explicación a la jerarquía de las masas de los fermiones y a sus ángulos de mezcla?, ¿Cómo explicar la jerarquía entre la escala electrodébil y la escala de Planck?, etc. Sin embargo, los problemas más importantes a los que el SM no ofrece una explicación son,

1) la masa de los neutrinos,

2) la materia oscura (DM),

3) la asimetría entre la materia bariónica y anti-bariónica en el universo (BAU).

Dicho esto, resulta evidente la necesidad de ir más allá de la descripción estándar de la naturaleza, es decir, más allá del Modelo Estándar. Por lo tanto, esta tesis toma la física de neutrinos como el camino para resolver algunos de los problemas que, por construcción, el SM no ofrece una explicación. Por esta razón se han estudiado algunos de los mecanismos de generación de masa de los neutrinos y sus implicaciones.

La física de neutrinos se ha transformado en un campo muy activo, tanto desde el punto de vista experimental como del teórico, desde la confirmación experimental de que los neutrinos cambian de sabor a lo largo de su viaje. Es

decir, que los neutrinos oscilan y por lo tanto son partículas masivas. Además, experimentos como LEP [49] han establecido (a partir de los decaimientos del bosón Z^0) que solamente hay tres especies de neutrinos activos, los cuales en la base electrodébil resultan ser, $\nu_\alpha \equiv (\nu_e, \nu_\mu, \nu_\tau)$. Por otro lado, de los ajustes globales de los parámetros de oscilación, los ángulos de mezcla y las diferencias cuadradas de las masas entre los neutrinos están muy bien determinados [23].

Sin embargo, aun con toda la información que se tiene acerca de los los neutrinos y sus propiedades, existen algunos desafíos experimentales y teóricos. Por ejemplo, todavía no se ha podido determinar:

i) el valor absoluto de la masa de los neutrinos;

ii) ¿cuál es la naturaleza de los neutrinos (si son partículas de Majorana o de Dirac)?;

iii) la jerarquía de la masa de los neutrinos (es decir, si es normal $m_{\nu_1} < m_{\nu_2} < m_{\nu_3}$ o invertida $m_{\nu_3} < m_{\nu_1} < m_{\nu_2}$);

iv) el valor de la fase de violación CP en el sector leptónico.

Uno de los experimentos que podrían proporcionar alguna pista de algunas de estas incógnitas es el experimento KATRIN [50], el cual espera examinar hasta la escala absoluta de la masa de los neutrinos $\lesssim 0.2$ eV mediante el estudio del decaimiento β del tritium (${}^3_1\mathrm{H} \to {}^3_2\mathrm{He} + e^- + \bar{\nu}_e$).

Otros experimentos están dedicados a medir el decaimiento doble beta sin neutrinos $0\nu\beta\beta$. La importancia de este tipos de experimentos está en que, en el caso de observar $0\nu\beta\beta$, confirmaría que los neutrinos son partículas de Majorana y a su vez proporcionaría algún indicio sobre la jerarquía de las masas. El año pasado el experimento the KamLAND-Zen [51] anunció sus resultados sobre $0\nu\beta\beta$ del estudio del proceso (${}^{136}\mathrm{Xe} \to {}^{136}\mathrm{Ba} + 2e^-$), pero ninguna señal ha sido observada. Lo único que obtuvimos de dicho experimentos es el límite más estricto para el decaimiento doble beta sin neutrinos, cuyas cotas están cerca de alcanzar la región característica donde la jerarquía de las masas es invertida, es decir $m_{\nu_3} < m_{\nu_1} < m_{\nu_2}$. Esta información está plasmada en la Figura 2.1. Del mismo modo, la colaboración de Planck [52] (a partir de observaciones cosmológicas) ha puesto límites en la escala de la masa de los neutrinos. Por ejemplo, los reportes que combinan datos de microondas cósmicas de fondo (CMB) y oscilaciones acústicas de bariones (BAO) resulta en la cota $\sum_{i=1}^{3} |m_{\nu_i}| < 0.23$ eV. Este resultado desfavorecería fuertemente la posibilidad de que los neutrinos tengan un espectro de masa degenerado.

Aunque esta cota puede ser relajada.

Respecto a la fase de violación CP en el sector leptónico, el experimento T2K [53] ha reportado un valor de la fase de Dirac cercana al valor $3\pi/2$. Dicho resultado proviene de cierta tensión que hay entre los experimentos de reactor y los de aceleradores. Por lo tanto, el principal objetivo de otros experimentos como DUNE [54, 55] es el de medir la fase de violación de CP.

Estos experimentos ponen de manifiesto el gran interés de la comunidad experimental en determinar algunas de las propiedades de los neutrinos. Desde el punto de vista teórico, el problema más interesante y que representa uno de los misterios más grandes de la física de partículas es el que respecta al origen de la masa de los neutrinos, el cual experimentalmente también resulta ser un gran reto.

Además en el capítulo 2 hemos descrito en qué consiste y cuáles son los ingredientes necesarios para generar la masa de los neutrinos por medio de los mecanismos de *seesaw*. Una vez que sabemos cómo generar la masa de los neutrinos, inmediatamente, nos damos cuenta de que el hecho de que los neutrinos sean partículas con una masa tan pequeña, del orden $\lesssim \mathcal{O}(0.1)$ eV, es necesario la existencia de nueva física. En particular, se requiere que existan nuevos grados de libertad o partículas, las cuales actúan como mediadores entre la escala de la nueva física y la escala electrodébil, 246 GeV.

El hecho que la masa de los neutrinos sea tan pequeña, comparada con el resto de las partículas de Modelo Estándar, puede deberse a que las nuevas partículas sean muy masivas, es decir: $m_\nu \propto 1/M'$ donde M' es usada para denotar la masa de las nuevas partículas. Si es el caso, la masa de los mediadores puede ser tan grande como la escala de gran unificación, o sea $M' \lesssim 10^{16}$ GeV, por lo cual probar su existencia resulta imposible para los experimentos actuales. La otra posibilidad de explicar la pequeñez de la masa de los neutrinos es que los parámetros de interacción necesarios para generar su masa sean extremadamente pequeños. Por ejemplo, $m_\nu \propto \alpha \ll 1$ donde el parámetro α puede tener dimensiones de masa o ser adimensional. De esta manera resulta que la masa de los mediadores podría estar a una escala cercana a la escala del rompimiento de la simetría electrodébil.

Sin embargo, en el caso que los parámetros pequeños sean aquellos de las interacciones de Yukawa ($\alpha = Y^\nu \ll 1$), los posibles procesos donde se podría observar el impacto de dichos mediadores tienden a ser muy pequeños. Esta situación ocurre con los procesos de violación de sabor leptónico que involucran

a los leptones cargados como $\mu \to e\gamma$. Por lo tanto, la posibilidad más interesante reside en los escenarios donde el parámetro "naturalmente" pequeño se encuentra en el sector escalar. A dichos mecanismos los conocemos como mecanismos seesaw de energía baja [81]. Los cuales se caracterizan no sólo de tener una predicción para los procesos de violación de sabor leptónico sino también en que experimentos tales como el LHC podrían producir las nuevas partículas (ligeras) involucradas en la generación de la masa de los neutrinos.

Las características que hemos mencionado nos ayudan a hacer distinción entre la variedad de mecanismos de seesaw que existen [76]. A nivel árbol existen solo tres tipos de seesaw: [59–66]:

- Seesaw tipo I, en este caso el SM se extiende añadiendo neutrinos derechos (RH), los cuales son singletes bajo la simetría $SU(2)_L$;
- Seesaw tipo II, aquí el mediador es un escalar Δ que transforma como triplete bajo la simetría $SU(2)$ y tiene número leptónico;
- Seesaw tipo III, en este escenario se requiere la presencia de tripletes fermiónicos Σ.

Esta clasificación es válida en el caso que los neutrinos sean partículas de Majorana. Sin embargo, no existe evidencia experimental que prohiba que los neutrinos sean partículas de Dirac. En este caso no sólo es necesario la introducción de nuevas partículas al SM si no también la existencia de una simetría G_D que no permita la aparición de términos de Majorana a ningún orden.

La predicción más relevante de los neutrinos de Dirac es la ausencia del decaimiento doble beta sin neutrinos. Sin embargo otro tipo te conexiones y predicciones son posibles. Por ejemplo, la simetría G_D podría estar relacionada a un grupo de simetría de sabor [96, 98], de tal modo que es posible explicar porqué existen tres generaciones de leptones y de quarks, sus masas y los valores de los parámetros de mezcla en ambos sectores.

Resultados

Después de hacer un repaso por los problemas en Modelo Estándar, la generación de la masa de los neutrinos y las interrogantes que existen en sector de los neutrinos presentamos los resultados originales de la investigación realizada durante el doctorado. El resumen de dichos resultados están condensados en

el capítulo 3 de este trabajo de tesis.

Como ya hemos mencionado el trabajo de investigación ha sido enfocado en estudiar las conexiones entre la generación de la masa de los neutrinos y búsqueda de nueva física a la escala electrodébil. Después de revisar la generación de la masa de los neutrinos notamos la necesidad de que haya nueva física (partículas). Del mismo modo que es necesario para explicar DM y BAU. Esto resulta interesante ya que la existencia de nuevos grados de libertad podría ser probada en experimentos de colisionador como el LHC. Sin embargo, también podrían afectar la estabilidad del vacío.

Ha sido mostrado, por ejemplo en la referencia [44], que la estabilidad del vacío es muy sensible a la presencia de nueva física. Por lo tanto, partiendo de éste hecho, hemos estudiado el impacto que tienen las nuevas partículas necesarias para generar la masa de los neutrinos. Para este fin, nos hemos concentrado en mecanismos seesaw de energía baja, que como hemos mencionado son caracterizados en tener mediadores ligeros. El primero de los casos estudiados (en la sección 3.1) es el mecanismo de seesaw invertido [77], donde la masa de los neutrinos es generada después del rompimiento espontáneo de, la simetría global $U(1)_L$, número leptónico [101]. En este escenario las nuevas partículas añadidas al SM son un neutrino derecho ν_R (con número leptónico $[\nu_R]_L = 1$), un singlete izquierdo S (con $[S]_L = 1$) y un escalar σ singlete del grupo $SU(2)$ (con carga $[\sigma]_L = -2$). Dicho escalar es el responsable de romper la simetría $U(1)_L$ después de adquirir un valor de expectación del vacío (vev) $\langle\sigma\rangle$. Entonces en este caso, después del rompimiento espontáneo de la simetría, la masa de los neutrinos está dada por la siguiente expresión,

$$m_\nu = Y_S \langle\sigma\rangle \left(\frac{Y_\nu \langle H^0\rangle}{M}\right)^2 . \tag{3.9}$$

donde Y_ν e Y_S son parámetros adimensionales en el Lagrangiano de Yukawa, $\langle H^0\rangle$ es el vev del doblete H del SM y M es la masa de Dirac en el término $M\nu_R^c S$. Además, después del rompimiento de la de la simetría electrodébil, existen dos escalares CP-par (H_1, H_2) y un escalar CP-impar físico sin masa J, el Majoron, asociado a la rotura de la simetría global $U(1)_L$.

Del estudio realizado en este contexto encontramos que el caso más interesante es donde la pequeñez de la masa de los neutrinos sea consecuencia de que alguno de los Yukawas (en la ecuación anterior) es pequeño y el otro de orden $\mathcal{O}(1)$. Principalmente porque los Yukawas de orden $\mathcal{O}(1)$ tienden a llevar el acoplo de auto-interacción del Higgs a valores negativos [102, 103] como es el caso del Yukawa del quark top. También fue posible proporcionar cotas del

espacio de parámetros y la masa de uno de los escalares CP-par. La masa del otro escalar está fijada por los resultados experimentales, es decir, uno de los escalares debe tener una masa de 125 GeV.

Una de las implicaciones interesantes de este escenario es, por ejemplo, la presencia del boson de Nambu-Goldstone J asociado al rompimiento del número leptónico podría estar relacionado a los decaimientos invisibles del Higgs ($H_i \to JJ$) [39]. Para esto es necesario que el vev $\langle\sigma\rangle$ sea del orden de TeV y por lo tanto los efectos de la nueva física podrían estar dentro del alcance de las búsquedas de experimentos tales como el LHC.

Otro escenario donde estudiamos la estabilidad del vacío fue para el mecanismo de seesaw tipo II, también en la sección 3.1. Como ya hemos mencionado, en este caso, además del escalar H que transforma como doblete bajo la simetría $SU(2)$, para generar la masa de los neutrinos, es necesario añadir al SM un triplete escalar Δ que tiene número leptónico $[\Delta]_L = -2$ e hipercarga $Y = 1$. Después del rompimiento espontáneo de la simetría electrodébil, la masa de los neutrinos está dada por,

$$m_\nu^{(II)} = Y^{(II)}\langle\Delta\rangle, \tag{3.10}$$

donde $Y^{(II)}$ es el Yukawa de los neutrinos y $\langle\Delta\rangle = \mu\frac{\langle H^0\rangle^2}{M_\Delta^2}$ es el vev del triplete. Por otro lado, en la teoría hay siete escalares físicos: dos CP-par, uno CP-impar, dos con carga simple $H^\pm$ y dos con carga doble $\Delta^{\pm\pm}$.

Aunque el estudio de la estabilidad del vacío en este contexto ya existía en la literatura, encontramos que las condiciones de acotamiento por abajo (BFB) del potencial no eran las correctas. Lo cual nos llevo a rehacer el análisis y encontramos que las diferencias eran significativas con los resultados ya conocidos.

En este esquema encontramos que el requerir que el vacío sea estable pone restricciones importantes en el espacio de parámetros y en particular en el espectro de masas de los escalares físicos. En este escenario existe un término con dimensión de masa μ en el potencial escalar que rompe número leptónico explícitamente, necesario para la generación de la masa de los neutrinos. Lo interesante es que es posible generar el término μ dinámicamente como en el caso del seesaw invertido que discutimos anteriormente, es decir, que μ es generado después del rompimiento espontáneo de la simetría $U(1)_L$, o bien $\mu \propto \langle\sigma\rangle$ [101]. Como resultado, el bosón físico de Nambu-Goldstone (J) está presente en la teoría y por lo tanto el canal de decaimiento invisible del Higgs se abre, es decir $H_i \to JJ$ [39,106,107]. Además, en este escenario también los

canales de decaimiento visibles del Higgs se ven modificados debido a la presencia de los escalares cargados. Por ejemplo, los canales de decaimiento con 1-loop $h \to \gamma\gamma$ y $h \to Z\gamma$. Entonces, resulta interesante llevar a cabo el estudio de las propiedades del Higgs, es decir sus decaimientos, en los mecanismos de seesaw descritos tomando en cuenta los resultados obtenidos del análisis de la estabilidad del vacío.

En la sección 3.2 hemos descrito los resultados obtenidos sobre la fenomenología en el sector de Higgs en contextos donde la masa de los neutrinos es generada después del rompimiento espontáneo del número leptónico [77], los cuales, como hemos visto, están caracterizados por la presencia del bosón físico de Nambu-Goldstone J y, por lo tanto, del decaimiento invisible del Higgs. En primer lugar, mostramos los resultados en el caso que la masa de los neutrinos es generada a través del seesaw invertido. Como ya hemos visto antes, el sector escalar está compuesto por H y σ, que transforman como doblete y singlete de $SU(2)$ respectivamente. La rotura del número leptónico es llevada a cabo a través del vev del singlete $\langle\sigma\rangle$. Después del rompimiento espontáneo de la simetría electrodébil esta teoría contiene tres escalares físicos: dos CP-par masivos (H_1, H_2) y uno CP-impar sin masa, J. Por lo tanto, ambos escalares CP-par decaen invisiblemente de la siguiente manera,

$$H_i \to JJ. \tag{3.11}$$

En este caso hemos analizado la posibilidad de que exista un escalar más ligero que el descubierto recientemente por el LHC, es decir, $m_{H_1} < m_{H_2} = 125$ GeV. Para nuestro estudio, además de la restricciones teóricas como BFC, hemos implementado, por un lado, los resultados del experimento LEP [108] los cuales proporcionan constricciones para la mezcla entre el doblete y el singlete y la masa del escalar ligero, como se muestra en la Figura 3.4. Por otro lado, se implementaron los resultados obtenidos por las colaboraciones ATLAS y CMS del LHC sobre los canales de decaimiento del Higgs [33], los cuales están resumidos en la Tabla 1.2. Dichos resultados están expresados en términos de la fuerza de la señal, definida por μ_f en la ecuación (1.48) como el cociente de la tasa de decaimiento del Higgs en cierto estado final f medida por el experimento y la predicción del SM. Es fácil ver que la fuerza de la señal para cada estado final es compatible con desviaciones de hasta un 20% con respecto de la predicción del SM, es decir $0.8 < \mu_f < 1.2$.

Una vez hechas estas consideraciones hemos encontrado las regiones del espacio de parámetros permitidas de la teoría. A partir de nuestros resultados hemos concluido que la posibilidad de tener un escalar menor masa al de 125 GeV no está excluida. Dicho escalar se caracterizaría por decaer mayori-

tariamente a través de su canal invisible, o bien $H_1 \to JJ$. En el caso del escalar tipo Higgs con masa de 125 GeV hemos encontrado que su tasa de decaimiento invisible debe ser menor al 20%, o sea, BR($H_2 \to$ Invisible) < 0.20. Este resultado es más restrictivo que las cotas reportadas por los experimentos ATLAS [36] y CMS [37] para este canal de decaimiento del Higgs.

Un análisis similar al anterior fue realizado en el contexto donde la masa de los neutrinos es generada a través del mecanismo de seesaw tipo II. Para que los decaimientos invisibles del Higgs estén presentes en dicho escenario hemos considerado el caso donde la rotura de número leptónico ocurre dinámicamente. Es por ello que además del triplete escalar Δ se añade a la teoría un singlete complejo σ con número leptónico $[\sigma]_L = 2$. Entonces, después del rompimiento espontáneo de la simetría electrodébil obtenemos que los escalares físicos son nueve: tres CP-par (H_1, H_2, H_3); dos CP-impar: uno masivo A y uno sin masa J; dos con carga simple $H^\pm$ y dos con carga doble $\Delta^{\pm\pm}$ Por lo cual el sector de Higgs tiene una fenomenología más rica, ya que además del los decaimientos invisibles del Higgs ($H_i \to JJ$), existen otros decaimientos no-estándares del Higgs a 1-loop (es decir $H_i \to \gamma\gamma$ y $H_i \to Z\gamma$) debido a la presencia de los escalares cargados.

Las configuraciones del espectro de masa de los escalares estudiadas fueron:

i) $m_{H_1} < m_{H_2} = 125$ GeV $< m_{H_3}$ y $m_{H_3} \sim m_A \sim m_{H^+} \sim m_{\Delta^{++}}$,

ii) $m_{H_1} = 125$ GeV $< m_{H_2} < m_{H_3}$ y $m_{H_3} \sim m_A \sim m_{H^+} \sim m_{\Delta^{++}}$.

Para la configuración i) fueron implementados los resultados de LEP [108] como lo hicimos para el análisis del mecanismo de seesaw invertido. En ambos casos se consideró para los decaimientos del Higgs que la fuerza de la señal está en el rango $0.8 < \mu_f < 1.2$ como lo sugieren los resultados del LHC [33]. Además, se tomó en cuenta la cota $m_{\Delta^{++}} \gtrsim 400$ GeV, proveniente de las búsquedas directas del bosón Δ^{++} (bajo la suposición de que la tasa de decaimiento de $\Delta^{\pm\pm}$ a $e^\pm e^\pm$, $e^\pm \mu^\pm$ o $\mu^\pm \mu^\pm$ es del 100%.) [104, 105].

Habiendo tomado en cuenta las restricciones experimentales mencionadas, en nuestro estudio hemos encontrando ciertas correlaciones entre los canales de decaimiento visibles (por ejemplo, $\mu_{\gamma\gamma}$ y μ_{ZZ}) y los decaimientos invisibles del Higgs. Esto se muestra en las Figuras 3.8 y 3.9. Además, para ambas configuraciones i) y ii) hemos concluido que la tasa del decaimiento del Higgs a Majarones (invisibles) debe ser menor que el 20%, es decir, BR($H_2 \to$ Invisible) < 0.20 en el caso i) y BR($H_1 \to$ Invisible) < 0.20 para el caso ii).

En la sección 3.3 mostramos los resultados que hemos obtenido de nuestro estudio relacionado a la física de neutrinos y el problema del sabor. Este problema básicamente consiste en explicar, ¿por qué los parámetros de oscilación de los neutrinos, Tabla 2.1, son tan distintos a los que caracterizan el sector de quarks, equation (1.46)?. Una de las ideas que ha sido ampliamente estudiada para atacar este problema consiste en invocar la existencia de una simetrías discretas globales G_F que relacionan las familias de fermiones, las cuales son conocidas como *simetrías de sabor* [46]. La ventaja de este enfoque es que las simetrías de sabor también proporcionan cierta estructura a las matrices de Yukawa y por lo tanto es posible obtener correlaciones entre los parámetros de oscilación y las observables, como por ejemplo la masa de los neutrinos [48].

Entre las posibles predicciones que uno puede obtener en modelos con simetrías de sabor G_F están:

- las reglas de suma de las masas de los neutrinos [47, 109];
- las reglas de suma de las mezclas de los neutrinos [110].

Otra predicción interesante de las simetría de sabor es las *relaciones de masa* de los fermiones cargados [111–113]. Hasta el momento solo conocemos una regla de suma que relaciona la masa quarks tipo down con los la masa de los leptones cargados, la cual está dada por la siguiente relación:

$$\frac{m_b}{\sqrt{m_d m_s}} = \frac{m_\tau}{\sqrt{m_e m_\mu}}. \tag{3.12}$$

Entonces, de nuestro trabajo realizado en esta dirección, encontramos que la estructura de las matrices de Yukawa que generan la relación de masa antes mencionada es generada naturalmente por los siguiente grupos: A_4, T', $T_n \cong Z_n \rtimes Z_3$ (donde $n = 7, 13, 19, 31, 43, 49$) [46]. Dichos grupos comparten la característica de contener representaciones irreducibles de tres dimensiones.

Posteriormente, construimos un modelo consistente con el grupo T_7 como simetría de sabor, donde la masa de los neutrinos es generada a través del mecanismo de seesaw tipo I. De los resultados obtenidos encontramos que en éste modelo, además de la posibilidad de explicar los ángulos de mezcla en el sector leptónico y de los quarks, posee correlaciones entre el ángulo atmosférico, θ_{23}, y la suma de la masa de los neutrinos. Estos resultados fueron mostrados tanto para el caso en el que la masa de los neutrinos posee jerarquía normal como para cuando la jerarquía es invertida. Por otro lado, de nuestros resultados se predice una cota para la masa del neutrino más ligero, para ambas jerarquías. Esto es muy similar a lo que se obtiene con las reglas

de suma de la masa de los neutrinos [47, 109]. Este resultado es mostrado en la Figura 3.10 a través de la correlación del parámetro de masa de Majorana efectivo $|m_{ee}|$ (el cual caracteriza $0\nu\beta\beta$) y la masa del neutrino más ligero.

En la sección 3.4 son presentados los resultados obtenidos del estudio de la generación de la masa de los neutrinos en el caso de que estos sean partículas de Dirac. Básicamente, se describe un modelo que explica de manera natural la pequeñez de la masa de los neutrinos en éste caso, el cual resulta ser mecanismo análogo al mecanismo de seesaw tipo II para neutrinos de Majorana. La posibilidad de que los neutrinos sean fermiones de Dirac podría ser excluida si el decaimiento doble beta sin neutrinos es medido, dado que de acuerdo con el "Teorema Black Box" [115] esto confirmaría que los neutrinos son fermiones de Majorana. Sin embargo, hasta el momento, no existe evidencia experimental que prohiba que los neutrinos sean partículas de Dirac.

En el modelo que hemos construido determinamos cuáles son los ingredientes necesarios para generar la masa de los neutrinos de Dirac a través de un mecanismo de seesaw tipo II. Los cuales son,

1) Un campo escalar Φ_ν que transforma como doblete de $SU(2)$ y solamente se acopla a los neutrinos;

2) La presencia de neutrinos derechos ν_R en la teoría;

3) Una simetría adicional G_D que prohiba los términos de Majorana.

En la teoría descrita hemos considerado que la simetría adicional es una simetría Abeliana global, es decir $G_D = U(1)_D$. Donde esta simetría es rota espontáneamente cuando un singlete σ, que transforma de manera no trivial bajo la simetría $U(1)_D$, adquiere vev, $\langle\sigma\rangle$. En este escenario $\langle\sigma\rangle$ induce el vev del escalar Φ_ν, el cual resulta ser pequeño, lo que a su vez también explicaría la pequeñez de la masa de los neutrinos de manera natural. Debido a que la simetría $U(1)_D$ se rompe espontáneamente, se predice la existencia de un bosón de Nambu-Goldstone físico al cual hemos bautizado como *Diracon* y es denotado con la letra $\mathcal{D}$.

Uno de los resultados interesantes al estudiar la posibilidad de que los neutrinos sean fermiones de Dirac es que esto sugiere también la existencia de una simetría residual la cual prohiba que términos de Majorana sean generados a cualquier orden. En el caso del mecanismo de seesaw tipo II para neutrinos de Dirac la simetría residual resulta ser el grupo discreto Abeliano $\mathbb{Z}_3$, lo que implica que la simetría residual después del rompimiento espontáneo de

la simetría electrodébil es $U(1)_{EM} \times \mathbb{Z}_3$. Esta información nos llevó a preguntarnos si la simetría que garantiza que los neutrinos sean fermiones de Dirac podría estar relacionada con la simetría que estabiliza la materia oscura, en este caso $\mathbb{Z}_3$ [119, 120].

En la sección 3.5 mostramos un modelo que hemos construido con las características mencionadas. En dicho esquema la masa de los neutrinos es generada a 2-loops, lo cual explicaría su pequeñez. Por otro lado, la simetría que garantiza que los neutrinos sean partículas de Dirac resulta ser la misma que estabiliza la materia oscura.

Conclusiones

En esta tesis hemos explorado la conexión entre las propiedades de los neutrinos y la nueva física. En particular, nos concentramos en el estudio de la generación de la masa de los neutrinos, la cual requiere la existencia de nuevos grados de libertad. Como resultado, la física de neutrinos resulta ser el camino natural a nuevos fenómenos y, por si mismo, un campo muy interesante.

Primero discutimos cuál es el impacto de la generación de la masa de los neutrinos en el sector escalar. Para ello, hemos estudiado la estabilidad del vacío en esquemas que explican la masa de los neutrinos a baja energía, es decir, a energía cercanas a la electrodébil. Éste análisis fue hecho para dos casos distintos: 1) en el esquema del seesaw invertido, donde tanto el sector de Yukawa como el escalar son extendidos con respecto al SM; y, 2) en el esquema de seesaw tipo II, donde solamente es añadido un triplete escalar $SU(2)$ a la descripción estándar de los fenómenos electrodébiles. A partir de nuestro estudio hemos encontrado que en ambos escenarios la estabilidad del vacío es posible a diferencia de lo que ocurre en el SM. Sin embargo, resulta que, al requerir que el vacío sea estable surgen restricciones importantes en el espacio de parámetros. Por ejemplo, esto constriñe el espectro de masas de las nuevas partículas necesarias para generar la masa de los neutrinos. Por otro lado, hemos estudiado la conexión entre estos escenarios y las propiedades del Higgs. Especialmente, las variantes de los mecanismos de seesaw en donde la masa de los neutrinos es generada después del rompimiento espontáneo del número leptónico (una simetría continua Abeliana). El rompimiento de dicha simetría da lugar a la existencia de un bosón de Nambu-Goldstone, el Majoron (J), y por lo tanto también a los decaimientos invisibles del Higgs ($h \to JJ$). A partir de nuestros resultados, los cuales toman en cuenta las cotas experimentales provenientes de los experimentos de colisionador (LEP y LHC), hemos encontrado que la

tasa de decaimiento $BR(h \rightarrow \text{Invisibles})$ debe ser menor que el 20% dentro de los escenarios explorados. Esto se puede deducir de las correlaciones que encontramos entre los canales de decaimiento *visibles* e *invisible* del Higgs.

Esta tesis también contiene nuestros resultados del estudio del problema del sabor, es decir, ¿cómo explicar las masas y las mezclas en el sector fermiónico?. En este caso, presentamos un modelo que predice una relación de masa entre los quarks tipo down y los leptones cargados, el cual también explica los parámetros de mezcla tanto en el sector de quarks como en el leptónico. En este escenario hemos encontrado correlaciones entre el ángulo atmosférico y el valor absoluto de la masa de los neutrinos. Además, hemos proporcionado una cota inferior para la masa del neutrino más ligero (tanto para la jerarquía normal como la invertida) proveniente de los resultados sobre el decaimiento doble beta sin neutrinos.

También hemos explorado la posibilidad de que los neutrinos sean partículas de Dirac. Para ello, hemos construido un esquema consistente que explica la pequeñez de la masa de los neutrinos. De hecho, nuestro escenario se caracteriza por la presencia de una simetría adicional $U(1)_D$ que prohibe los términos de Majorana a todos los órdenes. Hemos encontrado que la simetría que garantiza que los neutrinos sean fermiones de Dirac puede ser la misma que estabiliza al candidato a materia oscura en la teoría. Esta posibilidad fue explorada en un esquema en donde la masa de los neutrinos es generada a 2-loops. El resultado más relevante e interesante viene cuando la masa de los neutrinos es generada después del rompimiento espontáneo de la simetría $U(1)_D$, porque esto predice la existencia de un boson físico de Nambu-Goldstone, el Diracon ($\mathcal{D}$), el cual podría estar relacionado a los decaimientos invisibles del Higgs.

BIBLIOGRAPHY

[1] G. 't Hooft and M. Veltman, *Regularization and Renormalization of Gauge Fields*, Nucl.Phys. **B44** (1972) 189–213.

[2] P. W. Higgs, *Broken symmetries, massless particles and gauge fields*, Phys.Lett. **12** (1964) 132–133.

[3] F. Englert and R. Brout, *Broken Symmetry and the Mass of Gauge Vector Mesons*, Phys.Rev.Lett. **13** (1964) 321–323.

[4] G. Guralnik, C. Hagen and T. Kibble, *Global Conservation Laws and Massless Particles*, Phys.Rev.Lett. **13** (1964) 585–587.

[5] S. Glashow, *Partial Symmetries of Weak Interactions*, Nucl.Phys. **22** (1961) 579–588.

[6] S. Weinberg, *A Model of Leptons*, Phys.Rev.Lett. **19** (1967) 1264–1266.

[7] A. Salam, *Weak and Electromagnetic Interactions*, Conf.Proc. **C680519** (1968) 367–377.

[8] M. Gell-Mann, *Quarks*, Acta Phys.Austriaca Suppl. **9** (1972) 733–761.

[9] D. J. Gross and F. Wilczek, *Ultraviolet Behavior of Nonabelian Gauge Theories*, Phys.Rev.Lett. **30** (1973) 1343–1346.

[10] H. D. Politzer, *Reliable Perturbative Results for Strong Interactions?*, Phys.Rev.Lett. **30** (1973) 1346–1349.

[11] S. Weinberg, *Nonabelian Gauge Theories of the Strong Interactions*, Phys.Rev.Lett. **31** (1973) 494–497.

[12] J. Goldstone, *Field Theories with Superconductor Solutions*, Nuovo Cim. **19** (1961) 154–164.

[13] J. Goldstone, A. Salam and S. Weinberg, *Broken Symmetries*, Phys.Rev. **127** (1962) 965–970.

[14] G. Aad et al. (ATLAS Collaboration), *Observation of a new particle in the search for the Standard Model Higgs boson with the ATLAS detector at the LHC*, Phys.Lett. **B716** (2012) 1–29, arXiv:1207.7214 [hep-ex].

[15] S. Chatrchyan et al. (CMS), *Observation of a new boson at a mass of 125 GeV with the CMS experiment at the LHC*, Phys. Lett. **B716** (2012) 30–61, arXiv:1207.7235 [hep-ex].

[16] M. Baak et al. (Gfitter Group), *The global electroweak fit at NNLO and prospects for the LHC and ILC*, Eur. Phys. J. **C74** (2014) 3046, arXiv:1407.3792 [hep-ph].

[17] C. Patrignani et al. (Particle Data Group), *Review of Particle Physics*, Chin. Phys. **C40** (2016) 10 100001.

[18] Y. Fukuda et al. (Super-Kamiokande), *Evidence for oscillation of atmospheric neutrinos*, Phys. Rev. Lett. **81** (1998) 1562–1567, arXiv:hep-ex/9807003 [hep-ex].

[19] S. Fukuda et al. (Super-Kamiokande), *Determination of solar neutrino oscillation parameters using 1496 days of Super-Kamiokande I data*, Phys. Lett. **B539** (2002) 179–187, arXiv:hep-ex/0205075 [hep-ex].

[20] Q. Ahmad et al. (SNO Collaboration), *Direct evidence for neutrino flavor transformation from neutral current interactions in the Sudbury Neutrino Observatory*, Phys.Rev.Lett. **89** (2002) 011301, arXiv:nucl-ex/0204008 [nucl-ex].

[21] K. Eguchi et al. (KamLAND Collaboration), *First results from KamLAND: Evidence for reactor anti-neutrino disappearance*, Phys.Rev.Lett. **90** (2003) 021802, arXiv:hep-ex/0212021 [hep-ex].

[22] Y. Ashie et al. (Super-Kamiokande), *Evidence for an oscillatory signature in atmospheric neutrino oscillation*, Phys. Rev. Lett. **93** (2004) 101801, arXiv:hep-ex/0404034 [hep-ex].

[23] D. Forero, M. Tortola and J. Valle, *Neutrino oscillations refitted*, Phys.Rev. **D90** (2014) 9 093006, arXiv:1405.7540 [hep-ph].

[24] Ethan, *The second most abundant particles in the universe are undetectable!*, URL http://scienceblogs.com/startswithabang/2013/07/17/.

[25] N. Cabibbo, *Unitary symmetry and leptonic decays*, Phys. Rev. Lett. **10** (1963) 531–533.

[26] M. Kobayashi and T. Maskawa, *Cp-violation in the renormalizable theory of weak interaction*, Progress of Theoretical Physics **49** (1973) 2 652.

[27] S. L. Glashow, J. Iliopoulos and L. Maiani, *Weak Interactions with Lepton-Hadron Symmetry*, Phys. Rev. **D2** (1970) 1285–1292.

[28] T. A. collaboration (ATLAS), *Search for supersymmetry in final states with two same-sign or three leptons and jets using 36 fb^{-1} of $\sqrt{s} = 13$ TeV pp collision data with the ATLAS detector* (2017).

[29] C. Collaboration (CMS), *Search for supersymmetry using hadronic top quark tagging in 13 TeV pp collisions* (2017).

[30] M. Aaboud et al. (ATLAS), *Search for TeV-scale gravity signatures in high-mass final states with leptons and jets with the ATLAS detector at $\sqrt{s} = 13$ TeV*, Phys. Lett. **B760** (2016) 520–537, arXiv:1606.02265 [hep-ex].

[31] C. Collaboration (CMS), *Search for dark matter, invisible Higgs boson decays, and large extra dimensions in the $\ell\ell + E_{\mathrm{T}}^{\mathrm{miss}}$ final state using 2016 data* (2017).

[32] L. Longo, A. Favareto and C. Galloni (ATLAS, CMS), *Search for signatures with top, bottom, tau and exotics*, PoS **PP@LHC2016** (2016) 006.

[33] G. Aad et al. (ATLAS, CMS), *Measurements of the Higgs boson production and decay rates and constraints on its couplings from a combined ATLAS and CMS analysis of the LHC pp collision data at $\sqrt{s} = 7$ and 8 TeV*, JHEP **08** (2016) 045, arXiv:1606.02266 [hep-ex].

[34] G. C. Branco et al., *Theory and phenomenology of two-Higgs-doublet models*, Phys. Rept. **516** (2012) 1–102, arXiv:1106.0034 [hep-ph].

[35] A. G. Akeroyd and S. Moretti, *Enhancement of H to gamma gamma from doubly charged scalars in the Higgs Triplet Model*, Phys. Rev. **D86** (2012) 035015, arXiv:1206.0535 [hep-ph].

[36] G. Aad et al. (ATLAS), *Constraints on new phenomena via Higgs boson couplings and invisible decays with the ATLAS detector*, JHEP **11** (2015) 206, arXiv:1509.00672 [hep-ex].

[37] V. Khachatryan et al. (CMS), *Searches for invisible decays of the Higgs boson in pp collisions at sqrt(s) = 7, 8, and 13 TeV*, JHEP **02** (2017) 135, arXiv:1610.09218 [hep-ex].

[38] C. Bonilla et al., *IDMS: Inert Dark Matter Model with a complex singlet*, J. Phys. **G43** (2016) 6 065001, arXiv:1412.8730 [hep-ph].

[39] A. S. Joshipura and J. Valle, *Invisible Higgs decays and neutrino physics*, Nucl.Phys. **B397** (1993) 105–122.

[40] S. Alekhin, A. Djouadi and S. Moch, *The top quark and Higgs boson masses and the stability of the electroweak vacuum*, Phys.Lett. **B716** (2012) 214–219, arXiv:1207.0980 [hep-ph].

[41] G. Degrassi et al., *Higgs mass and vacuum stability in the Standard Model at NNLO*, JHEP **08** (2012) 098, arXiv:1205.6497 [hep-ph].

[42] V. Branchina, E. Messina and A. Platania, *Top mass determination, Higgs inflation, and vacuum stability*, JHEP **09** (2014) 182, arXiv:1407.4112 [hep-ph].

[43] V. Branchina, E. Messina and M. Sher, *Lifetime of the electroweak vacuum and sensitivity to Planck scale physics*, Phys. Rev. **D91** (2015) 013003, arXiv:1408.5302 [hep-ph].

[44] V. Branchina and E. Messina, *Stability, Higgs Boson Mass and New Physics*, Phys. Rev. Lett. **111** (2013) 241801, arXiv:1307.5193 [hep-ph].

[45] R. Costa, A. P. Morais, M. O. P. Sampaio and R. Santos, *Two-loop stability of a complex singlet extended Standard Model*, Phys. Rev. **D92** (2015) 2 025024, arXiv:1411.4048 [hep-ph].

[46] H. Ishimori et al., *Non-Abelian Discrete Symmetries in Particle Physics*, Prog.Theor.Phys.Suppl. **183** (2010) 1–163, arXiv:1003.3552 [hep-th].

[47] S. F. King, A. Merle and A. J. Stuart, *The Power of Neutrino Mass Sum Rules for Neutrinoless Double Beta Decay Experiments*, JHEP **1312** (2013) 005, arXiv:1307.2901 [hep-ph].

[48] S. F. King et al., *Neutrino Mass and Mixing: from Theory to Experiment*, New J.Phys. **16** (2014) 045018, arXiv:1402.4271 [hep-ph].

[49] S. Schael et al. (SLD Electroweak Group, DELPHI, ALEPH, SLD, SLD Heavy Flavour Group, OPAL, LEP Electroweak Working Group, L3), *Precision electroweak measurements on the Z resonance*, Phys. Rept. **427** (2006) 257–454, arXiv:hep-ex/0509008 [hep-ex].

[50] L. Bornschein (KATRIN Collaboration), *KATRIN: Direct measurement of neutrino masses in the sub-Ev region*, eConf **C030626** (2003) FRAP14, arXiv:hep-ex/0309007 [hep-ex].

[51] A. Gando et al. (KamLAND-Zen), *Search for Majorana Neutrinos near the Inverted Mass Hierarchy Region with KamLAND-Zen*, Phys. Rev. Lett. **117** (2016) 8 082503, [Addendum: Phys. Rev. Lett.117,no.10,109903(2016)], arXiv:1605.02889 [hep-ex].

[52] P. A. R. Ade et al. (Planck), *Planck 2015 results. XIII. Cosmological parameters*, Astron. Astrophys. **594** (2016) A13, arXiv:1502.01589 [astro-ph.CO].

[53] K. Abe et al. (T2K), *Neutrino oscillation physics potential of the T2K experiment*, PTEP **2015** (2015) 4 043C01, arXiv:1409.7469 [hep-ex].

[54] R. Acciarri et al. (DUNE), *Long-Baseline Neutrino Facility (LBNF) and Deep Underground Neutrino Experiment (DUNE)* (2015), arXiv:1512.06148 [physics.ins-det].

[55] S. S. Chatterjee, P. Pasquini and J. W. F. Valle, *Probing atmospheric mixing and leptonic CP violation in current and future long baseline oscillation experiments* (2017), arXiv:1702.03160 [hep-ph].

[56] S. Weinberg, *Baryon and Lepton Nonconserving Processes*, Phys.Rev.Lett. **43** (1979) 1566–1570.

[57] A. de Gouvea and J. Jenkins, *A Survey of Lepton Number Violation Via Effective Operators*, Phys. Rev. **D77** (2008) 013008, arXiv:0708.1344 [hep-ph].

[58] F. Bonnet, D. Hernandez, T. Ota and W. Winter, *Neutrino masses from higher than d=5 effective operators*, JHEP **0910** (2009) 076, arXiv:0907.3143 [hep-ph].

[59] P. Minkowski, $\mu \to e\gamma$ *at a Rate of One Out of 1-Billion Muon Decays?*, Phys.Lett. **B67** (1977) 421.

[60] T. Yanagida, *HORIZONTAL SYMMETRY AND MASSES OF NEUTRINOS*, Conf.Proc. **C7902131** (1979) 95–99.

[61] R. N. Mohapatra and G. Senjanovic, *Neutrino Mass and Spontaneous Parity Violation*, Phys.Rev.Lett. **44** (1980) 912.

[62] M. Magg and C. Wetterich, *Neutrino Mass Problem and Gauge Hierarchy*, Phys.Lett. **B94** (1980) 61.

[63] J. Schechter and J. Valle, *Neutrino Masses in SU(2) x U(1) Theories*, Phys.Rev. **D22** (1980) 2227.

[64] T. Cheng and L.-F. Li, *Neutrino Masses, Mixings and Oscillations in SU(2) x U(1) Models of Electroweak Interactions*, Phys.Rev. **D22** (1980) 2860.

[65] C. Wetterich, *Neutrino Masses and the Scale of B-L Violation*, Nucl.Phys. **B187** (1981) 343.

[66] R. Foot, H. Lew, X. He and G. C. Joshi, *Seesaw Neutrino Masses Induced by a Triplet of Leptons*, Z.Phys. **C44** (1989) 441.

[67] F. F. Deppisch, M. Hirsch and H. Pas, *Neutrinoless Double Beta Decay and Physics Beyond the Standard Model*, J. Phys. **G39** (2012) 124007, arXiv:1208.0727 [hep-ph].

[68] F. J. Escrihuela et al., *Constraining right-handed neutrinos*, Nucl. Part. Phys. Proc. **273-275** (2016) 1909–1914, arXiv:1505.01097 [hep-ph].

[69] J. Garayoa and T. Schwetz, *Neutrino mass hierarchy and Majorana CP phases within the Higgs triplet model at the LHC*, JHEP **03** (2008) 009, arXiv:0712.1453 [hep-ph].

[70] P. Fileviez Perez et al., *Testing a Neutrino Mass Generation Mechanism at the LHC*, Phys. Rev. **D78** (2008) 071301, arXiv:0803.3450 [hep-ph].

[71] P. Fileviez Perez et al., *Neutrino Masses and the CERN LHC: Testing Type II Seesaw*, Phys.Rev. **D78** (2008) 015018, arXiv:0805.3536 [hep-ph].

[72] M. Aoki, S. Kanemura and K. Yagyu, *Testing the Higgs triplet model with the mass difference at the LHC*, Phys. Rev. **D85** (2012) 055007, arXiv:1110.4625 [hep-ph].

[73] F. del Águila and M. Chala, *LHC bounds on Lepton Number Violation mediated by doubly and singly-charged scalars*, JHEP **03** (2014) 027, arXiv:1311.1510 [hep-ph].

[74] S. Kanemura, M. Kikuchi, K. Yagyu and H. Yokoya, *Bounds on the mass of doubly-charged Higgs bosons in the same-sign diboson decay scenario*, Phys. Rev. **D90** (2014) 11 115018, arXiv:1407.6547 [hep-ph].

[75] P. S. Bhupal Dev, D. K. Ghosh, N. Okada and I. Saha, *125 GeV Higgs Boson and the Type-II Seesaw Model*, JHEP **03** (2013) 150, [Erratum: JHEP05,049(2013)], arXiv:1301.3453 [hep-ph].

[76] E. Ma, *Pathways to naturally small neutrino masses*, Phys.Rev.Lett. **81** (1998) 1171–1174, arXiv:hep-ph/9805219 [hep-ph].

[77] R. Mohapatra and J. Valle, *Neutrino Mass and Baryon Number Nonconservation in Superstring Models*, Phys.Rev. **D34** (1986) 1642.

[78] E. K. Akhmedov, M. Lindner, E. Schnapka and J. Valle, *Left-right symmetry breaking in NJL approach*, Phys.Lett. **B368** (1996) 270–280, arXiv:hep-ph/9507275 [hep-ph].

[79] E. K. Akhmedov, M. Lindner, E. Schnapka and J. Valle, *Dynamical left-right symmetry breaking*, Phys.Rev. **D53** (1996) 2752–2780, arXiv:hep-ph/9509255 [hep-ph].

[80] M. Malinsky, J. Romao and J. Valle, *Novel supersymmetric SO(10) seesaw mechanism*, Phys.Rev.Lett. **95** (2005) 161801, arXiv:hep-ph/0506296 [hep-ph].

[81] S. M. Boucenna, S. Morisi and J. W. F. Valle, *The low-scale approach to neutrino masses*, Adv. High Energy Phys. **2014** (2014) 831598, arXiv:1404.3751 [hep-ph].

[82] F. Bonnet, M. Hirsch, T. Ota and W. Winter, *Systematic study of the d=5 Weinberg operator at one-loop order*, JHEP **1207** (2012) 153, arXiv:1204.5862 [hep-ph].

[83] Y. Farzan, S. Pascoli and M. A. Schmidt, *Recipes and Ingredients for Neutrino Mass at Loop Level*, JHEP **1303** (2013) 107, arXiv:1208.2732 [hep-ph].

[84] D. Aristizabal Sierra, A. Degee, L. Dorame and M. Hirsch, *Systematic classification of two-loop realizations of the Weinberg operator*, JHEP **03** (2015) 040, arXiv:1411.7038 [hep-ph].

[85] E. Ma, *Verifiable radiative seesaw mechanism of neutrino mass and dark matter*, Phys. Rev. **D73** (2006) 077301, arXiv:hep-ph/0601225 [hep-ph].

[86] S. Fraser, E. Ma and O. Popov, *Scotogenic Inverse Seesaw Model of Neutrino Mass*, Phys. Lett. **B737** (2014) 280–282, arXiv:1408.4785 [hep-ph].

[87] J. Peltoniemi and J. Valle, *Massive neutrinos and electroweak baryogenesis*, Phys.Lett. **B304** (1993) 147–151, arXiv:hep-ph/9301231 [hep-ph].

[88] L. M. Krauss, S. Nasri and M. Trodden, *A Model for neutrino masses and dark matter*, Phys.Rev. **D67** (2003) 085002, arXiv:hep-ph/0210389 [hep-ph].

[89] S. Davidson, E. Nardi and Y. Nir, *Leptogenesis*, Phys.Rept. **466** (2008) 105–177, arXiv:0802.2962 [hep-ph].

[90] M. Hirsch, S. Morisi, E. Peinado and J. Valle, *Discrete dark matter*, Phys.Rev. **D82** (2010) 116003, arXiv:1007.0871 [hep-ph].

[91] F. F. Deppisch, J. Harz and M. Hirsch, *Falsifying Leptogenesis at the LHC* (2013), arXiv:1312.4447 [hep-ph].

[92] S. M. Boucenna, S. Morisi, Q. Shafi and J. W. F. Valle, *Inflation and majoron dark matter in the seesaw mechanism* (2014), arXiv:1404.3198 [hep-ph].

[93] A. Merle et al., *Consistency of WIMP Dark Matter as radiative neutrino mass messenger*, JHEP **07** (2016) 013, arXiv:1603.05685 [hep-ph].

[94] G. Ballesteros, J. Redondo, A. Ringwald and C. Tamarit, *Standard Model-Axion-Seesaw-Higgs Portal Inflation. Five problems of particle physics and cosmology solved in one stroke* (2016), arXiv:1610.01639 [hep-ph].

[95] G. Ballesteros, J. Redondo, A. Ringwald and C. Tamarit, *Unifying inflation with the axion, dark matter, baryogenesis and the seesaw mechanism*, Phys. Rev. Lett. **118** (2017) 7 071802, arXiv:1608.05414 [hep-ph].

[96] E. Ma and O. Popov, *Pathways to Naturally Small Dirac Neutrino Masses*, Phys. Lett. **B764** (2017) 142–144, arXiv:1609.02538 [hep-ph].

[97] W. Wang and Z.-L. Han, *Naturally Small Dirac Neutrino Mass with Intermediate $SU(2)_L$ Multiplet Fields* (2016), arXiv:1611.03240 [hep-ph].

[98] A. Aranda et al., *Dirac neutrinos from flavor symmetry*, Phys. Rev. **D89** (2014) 3 033001, arXiv:1307.3553 [hep-ph].

[99] K. Dick, M. Lindner, M. Ratz and D. Wright, *Leptogenesis with Dirac neutrinos*, Phys. Rev. Lett. **84** (2000) 4039–4042, arXiv:hep-ph/9907562 [hep-ph].

[100] Y. Farzan and E. Ma, *Dirac neutrino mass generation from dark matter*, Phys. Rev. **D86** (2012) 033007, arXiv:1204.4890 [hep-ph].

[101] J. Schechter and J. Valle, *Neutrino Decay and Spontaneous Violation of Lepton Number*, Phys.Rev. **D25** (1982) 774.

[102] J. Casas, V. Di Clemente, A. Ibarra and M. Quiros, *Massive neutrinos and the Higgs mass window*, Phys.Rev. **D62** (2000) 053005, arXiv:hep-ph/9904295 [hep-ph].

[103] L. Basso, S. Moretti and G. M. Pruna, *A Renormalisation Group Equation Study of the Scalar Sector of the Minimal B-L Extension of the Standard Model*, Phys. Rev. **D82** (2010) 055018, arXiv:1004.3039 [hep-ph].

[104] G. Aad et al. (ATLAS), *Search for doubly-charged Higgs bosons in like-sign dilepton final states at $\sqrt{s} = 7$ TeV with the ATLAS detector*, Eur. Phys. J. **C72** (2012) 2244, arXiv:1210.5070 [hep-ex].

[105] S. Chatrchyan et al. (CMS), *A search for a doubly-charged Higgs boson in pp collisions at $\sqrt{s} = 7$ TeV*, Eur. Phys. J. **C72** (2012) 2189, arXiv:1207.2666 [hep-ex].

[106] M. A. Diaz, M. A. Garcia-Jareno, D. A. Restrepo and J. W. F. Valle, *Neutrino mass and missing momentum Higgs boson signals*, Phys. Rev. **D58** (1998) 057702, arXiv:hep-ph/9712487 [hep-ph].

[107] M. A. Diaz, M. Garcia-Jareno, D. A. Restrepo and J. Valle, *Seesaw Majoron model of neutrino mass and novel signals in Higgs boson production at LEP*, Nucl.Phys. **B527** (1998) 44–60, arXiv:hep-ph/9803362 [hep-ph].

[108] J. Abdallah et al. (DELPHI Collaboration), *Searches for neutral higgs bosons in extended models*, Eur.Phys.J. **C38** (2004) 1–28, arXiv:hep-ex/0410017 [hep-ex].

[109] L. Dorame et al., *Constraining Neutrinoless Double Beta Decay*, Nucl.Phys. **B861** (2012) 259–270, arXiv:1111.5614 [hep-ph].

[110] S. King, *Predicting neutrino parameters from SO(3) family symmetry and quark-lepton unification*, JHEP **0508** (2005) 105, arXiv:hep-ph/0506297 [hep-ph].

[111] S. Morisi, E. Peinado, Y. Shimizu and J. W. F. Valle, *Relating quarks and leptons without grand-unification*, Phys. Rev. **D84** (2011) 036003, arXiv:1104.1633 [hep-ph].

[112] S. Morisi et al., *Quark-Lepton Mass Relation and CKM mixing in an A4 Extension of the Minimal Supersymmetric Standard Model*, Phys. Rev. **D88** (2013) 036001, arXiv:1303.4394 [hep-ph].

[113] S. F. King, S. Morisi, E. Peinado and J. W. F. Valle, *Quark-Lepton Mass Relation in a Realistic A_4 Extension of the Standard Model*, Phys. Lett. **B724** (2013) 68–72, arXiv:1301.7065 [hep-ph].

[114] P. Ade et al. (Planck Collaboration), *Planck 2013 results. XVI. Cosmological parameters*, Astron.Astrophys. (2014), arXiv:1303.5076 [astro-ph.CO].

[115] J. Schechter and J. Valle, *Neutrinoless Double beta Decay in SU(2) x U(1) Theories*, Phys.Rev. **D25** (1982) 2951.

[116] E. Ma and R. Srivastava, *Dirac or inverse seesaw neutrino masses with $B-L$ gauge symmetry and S_3 flavor symmetry*, Phys. Lett. **B741** (2015) 217–222, arXiv:1411.5042 [hep-ph].

[117] N. Viaux et al., *Neutrino and axion bounds from the globular cluster M5 (NGC 5904)*, Phys. Rev. Lett. **111** (2013) 231301, arXiv:1311.1669 [astro-ph.SR].

[118] S. Centelles Chuliá, E. Ma, R. Srivastava and J. W. F. Valle, *Dirac Neutrinos and Dark Matter Stability from Lepton Quarticity*, Phys. Lett. **B767** (2017) 209–213, arXiv:1606.04543 [hep-ph].

[119] G. Belanger, K. Kannike, A. Pukhov and M. Raidal, *Z_3 Scalar Singlet Dark Matter*, JCAP **1301** (2013) 022, arXiv:1211.1014 [hep-ph].

[120] G. Bélanger, K. Kannike, A. Pukhov and M. Raidal, *Minimal semi-annihilating $\mathbb{Z}_N$ scalar dark matter*, JCAP **1406** (2014) 021, arXiv:1403.4960 [hep-ph].

[121] D. S. Akerib et al. (LUX), *Results from a search for dark matter in the complete LUX exposure*, Phys. Rev. Lett. **118** (2017) 2 021303, arXiv:1608.07648 [astro-ph.CO].

[122] A. Tan et al. (PandaX-II), *Dark Matter Results from First 98.7 Days of Data from the PandaX-II Experiment*, Phys. Rev. Lett. **117** (2016) 12 121303, arXiv:1607.07400 [hep-ex].

Part II

Scientific Articles

CHAPTER **4**

VACUUM STABILITY WITH SPONTANEOUS VIOLATION OF LEPTON NUMBER

Authors: Cesar Bonilla, Renato M. Fonseca, Jose W.F. Valle.
Journal reference: Phys. Rev. D92 (2015) no.7, 075028.

Abstract

The vacuum of the Standard Model is known to be unstable for the measured values of the top and Higgs masses. Here we show how vacuum stability can be achieved naturally if lepton number is violated spontaneously at the TeV scale. More precise Higgs measurements in the next LHC run should provide a crucial test of our symmetry breaking scenario. In addition, these schemes typically lead to enhanced rates for processes involving lepton flavour violation.

4.1 Introduction

The vacuum of the Standard Model (SM) scalar potential is unstable since at high energies the Higgs effective quartic coupling is driven to negative values by the renormalization group flow [1, 2]. Nevertheless, the SM cannot be a complete theory of Nature for various reasons, one of which is that neutrinos need to be massive in order to account for neutrino oscillation results [3].[1]

With only the SM fields, neutrino masses can arise in a model-independent way from a dimension 5 effective operator $\kappa LLHH$ which gives rise to a $\kappa \langle H \rangle^2$ neutrino mass after electroweak symmetry breaking [5]. This same operator unavoidably provides a correction to the Higgs self-coupling λ below the scale of the mechanism of neutrino mass generation through the diagram in Fig. 8.1. Although tiny[2] and negative, it suggests that the mechanism responsible for generating neutrino masses and lepton number violation is potentially relevant for the Higgs stability problem. The quantitative effect of neutrino masses on the stability of the scalar potential will, however, be dependent on the ultraviolet completion of the model.

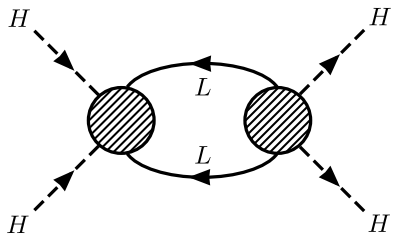

Figure 4.1: Contribution of Weinberg's effective operator to the Higgs quartic interaction.

After the historic Higgs boson discovery at CERN and the confirmation of the Brout-Englert-Higgs mechanism, it is natural to imagine that all symmetries in Nature are broken spontaneously by the vacuum expectation values of scalar fields. The charge neutrality of neutrinos suggests them to be Majorana fermions [6], and that the smallness of their mass is due to the feeble breaking of lepton number symmetry. Hence we need generalized electroweak breaking sectors leading to the double breaking of electroweak and lepton number symmetries.

In this letter we examine the vacuum stability issue within the simplest of such extended scenarios [3], showing how one can naturally obtain a fully

[1] Planck scale physics could also play a role [4].

[2] The contribution to λ is suppressed by a factor $(m_\nu / \langle H \rangle)^2 / (4\pi)^2$.

[3] Extended Higgs scenarios without connection to neutrino mass generation schemes have been extensively discussed, see for example, Ref. [7] and references therein.

consistent behavior of the scalar potential at all scales for lepton number broken spontaneously at the TeV scale. Note that within the simplest $SU(3)_C \otimes SU(2)_L \otimes U(1)_Y$ gauge structure lepton number is a global symmetry whose spontaneous breaking implies the existence of a physical Goldstone boson, generically called majoron and denoted J, which must be a gauge singlet [8,9] in order to comply with LEP restrictions [10]. Its existence brings in new invisible Higgs boson decays [11]

$$H \to JJ,$$

leading to potentially sizable rates for missing momentum signals at accelerators [12–14] including the current LHC [15]. Given the agreement of the ATLAS and CMS results with the SM scenario, one can place limits on the presence of such invisible Higgs decay channels. Current LHC data on Higgs boson physics still leaves room to be explored at the next run.

Absolute stability of the scalar potential is attainable as a result of the presence of the Majoron, which is part of a complex scalar singlet. Indeed, it is well known that generically the quartic coupling which controls the mixing between a scalar singlet and the Higgs doublet contributes positively to the value of the Higgs quartic coupling (which we shall call λ_2) at high energies [16–24] — see diagram A in figure 6.3. On the other hand, new fermions coupling to the Higgs field H, such as right-handed neutrinos [16,18,25], tend to destabilize λ_2 not only through the 1-loop effect depicted in diagram B_1 of figure 6.3, but also in what is effectively a two-loop effect (diagram B_2): through their Yukawa interaction with H, the new fermions soften the fall of the top Yukawa coupling at higher energies, which in turn contributes negatively to λ_2 [4]. The model we consider below is a low–scale version of the standard type I majoron seesaw mechanism, such as the inverse seesaw type [26,27]. We stress however that, even though our renormalization group equations (RGEs) are the same as those characterizing standard case, the values of the Dirac–type neutrino Yukawa couplings are typically much higher in our inverse seeaw scenario.

4.2 Electroweak breaking with spontaneous lepton number violation

The simplest scalar sector capable of driving the double breaking of electroweak and lepton number symmetry consists of the SM doublet H plus a complex

[4] Even though it does not happen in our case, one should keep in mind that fermions alone could in principle stabilize the Higgs potential by increasing the value of the gauge couplings at higher energies, which in turn have a positive effect on the Higgs quartic coupling.

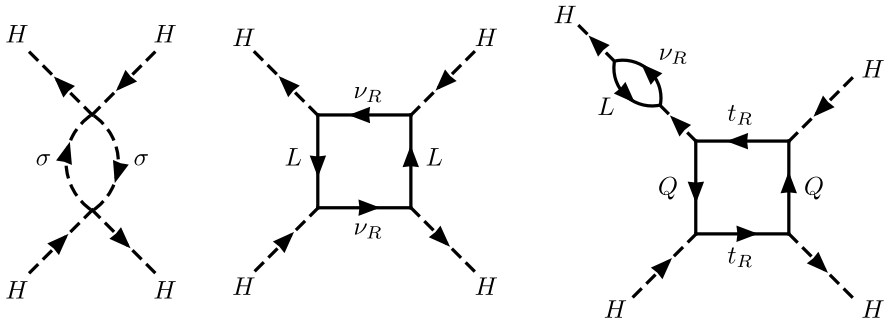

Figure 4.2: In models with a complex singlet scalar σ, such as majoron type-I seesaw schemes, the positive contribution to the RGE of the Higgs quartic coupling (diagram A) is accompanied by the destabilizing effect of right-handed neutrinos through the 1-loop diagram B_1 and also through the two-loop diagram B_2.

singlet σ, leading to the following Higgs potential [11]

$$V(\sigma, H) = \mu_1^2 |\sigma|^2 + \mu_2^2 H^\dagger H + \lambda_1 |\sigma|^4 + \lambda_2 \left(H^\dagger H\right)^2 + \lambda_{12} \left(H^\dagger H\right) |\sigma|^2 \,. \tag{4.1}$$

In addition to the $SU(3)_C \otimes SU(2)_L \otimes U(1)_Y$ gauge invariance, $V(\sigma, H)$ has a global U(1) symmetry which will be associated to lepton number within specific model realizations. The potential is bounded from below provided that λ_1, λ_2 and $\lambda_{12} + 2\sqrt{\lambda_1 \lambda_2}$ are positive; these are less constraining conditions than those required for the existence of a consistent electroweak and lepton number breaking vacuum where both H and σ adquire non-zero vacuum expectation values ($\equiv \frac{v_H}{\sqrt{2}}$ and $\frac{v_\sigma}{\sqrt{2}}$). For that to happen, λ_1, λ_2 and $4\lambda_1\lambda_2 - \lambda_{12}^2$ need to be all positive [5]. Three of the degrees of freedom in H are absorbed by the massive electroweak gauge bosons, as usual. On the other hand, the imaginary part of σ becomes the Nambu-Goldstone boson associated to the breaking of the global lepton number symmetry, therefore it remains massless. As for the real oscillating parts of H^0 and σ, these lead to two CP-even mass eigenstates H_1 and H_2, with a mixing angle α which can be constrained from LHC data [15, 28–30]. We take the lighter state H_1 to be the 125 GeV Higgs particle recently discovered by the CMS and ATLAS collaborations.

Using the renormalization group equations (given in the appendix) we evolved the three quartic couplings of the model imposing the vacuum sta-

[5] However, this last condition need not hold for arbitrarily large energy scales. Indeed, it is enough to consider $4\lambda_1\lambda_2 - \lambda_{12}^2 > 0$ for energies up to $\Lambda \approx \text{Max}\left(\sqrt{2\frac{|\mu_1^2|}{\lambda_{12}}}, \sqrt{\frac{|\mu_2^2|}{\lambda_2}}\right)$ — see [18, 23] for details.

bility conditions mentioned previously. Given that such equations rely on perturbation theory, the calculations were taken to be trustable only in those cases where the running couplings do not exceed $\sqrt{4\pi}$. [6]

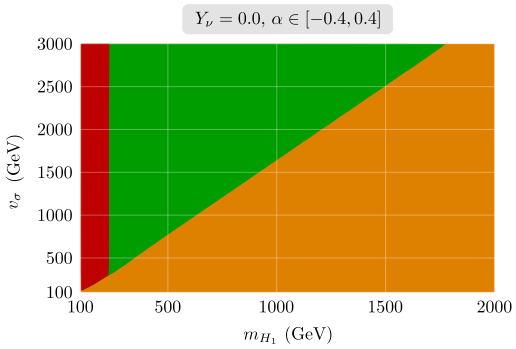

Figure 4.3: Values of m_{H_2} and v_σ leading to a potential bounded from below (in green on top), a Landau pole at some energy scale (in orange, next), or an unstable potential (in red, last).

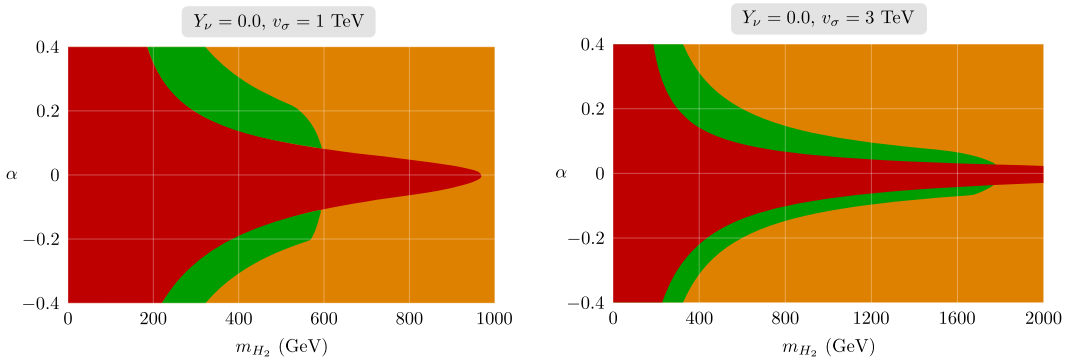

Figure 4.4: Values of m_{H_2} and α leading to a potential bounded from below (in green), a Landau pole at some energy scale (in orange), or an unstable potential (in red). Comparing top and bottom panels shows the effect of changing v_σ.

4.3 Neutrino mass generation

In order to assign to the U(1) symmetry present in Eq. (4.1) the role of lepton number we must couple the new scalar singlet to leptonic fields. This can be

[6] Since all the new particles present in the low-scale seesaw model under consideration have yet to be observed, leading order calculations suffice. For our plots we have used the values $\alpha_S \approx 0.1185$ and $y_t \approx 0.96$ at the m_Z scale — more precise values with higher order corrections can be found in [31]. Small changes to these input values (for example a change of 0.03 in the top Yukawa y_t) do not affect substancially our plots.

done in a variety of ways. Here we focus on low-scale generation of neutrino mass [32]. For definitiveness we choose to generate neutrino masses through the inverse seesaw mechanism [26] with spontaneous lepton number violation [27].

The fermion content of the Standard Model is augmented by right-handed neutrinos ν_R (with lepton number +1) and left-handed gauge singlets S (also with lepton number +1) such that the mass term $\nu_R^c S$ as well as the interactions $SS\sigma$ and $H\nu_R^c L$ are allowed if σ carries -2 units of lepton number:[7]

$$-\mathcal{L}_\nu = Y_\nu H \nu_R^c L + M \nu_R^c S + Y_S S S \sigma + \text{h.c.} \tag{4.2}$$

The effective neutrino mass, in the one family approximation, is given by the expression

$$m_\nu = Y_S \langle\sigma\rangle \left(\frac{Y_\nu \langle H^0\rangle}{M}\right)^2 , \tag{4.3}$$

which shows that the smallness of the neutrino masses can be attributed to a small (but natural) Y_S coupling, while still having Y_ν of order one and both $\langle\sigma\rangle$, M in the TeV range.

4.4 Interplay between neutrino mass and Higgs physics

In most cases, the stability of the potential is threatened by the violation of the condition $\lambda_2 > 0$, as in the Standard Model. Instability can be avoided with a large λ_{12}, which might, however, lead to an unacceptably large mixing angle α between the two CP-even Higgs mass eigenstates [22]. In such cases, one must rely instead on a heavy H_2 — see the green region in Figs. 4.3–4.5. Indeed, within the red regions therein, the potential becomes unbounded from below at some high energy scale, just like in the Standard Model. This happens for relatively small values of either α or m_{H_2}. As a result, a tight experimental bound on α can be used to place a lower limit on the mass of the heavier CP-even scalar. From Fig. 4.3 one can also see that the lepton breaking scale $v_\sigma \equiv \sqrt{2}\langle\sigma\rangle$ must not be too low, otherwise a big ratio $m_{H_2}/\langle\sigma\rangle$ will lead to the existence of a Landau pole in the running parameters of the model before the Planck scale is reached (shown in orange). This also accounts for the difference between the two plots in Fig. 4.4.

As far as the neutrino sector is concerned, since Y_S is taken to be small, this parameter has no direct impact on the potential's stability. However, it

[7] We ignore for simplicity the extra term $\nu_R^c \nu_R^c \sigma^*$ which is, in principle, also allowed.

should be noted that in order to obtain neutrino masses in the correct range, the values of both v_σ and Y_ν will depend on the one of Y_S. In principle then, Y_ν might be large, but not too large, as $|Y_\nu| \gtrsim 0.6$ leads to either unstable or non-perturbative dynamics. A non-zero Dirac neutrino Yukawa coupling has a destabilizing effect on the scalar potential which is visible in the recession of the green region to bigger values of α and m_{H_2}, when comparing the bottom plot in Fig. 4.4 and the one in Fig. 4.5.

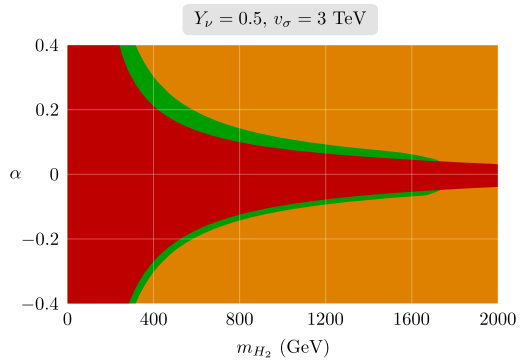

Figure 4.5: Same as in the bottom plot of Fig. 4.4, but with $Y_\nu \neq 0$.

Another interesting possibility is to have a negligible Y_ν and potentially sizeable Y_S. In this case, if we keep M of the order of the TeV, we find that the region of stability and perturbativity (shown in green in Fig. 4.6) depends significantly upon the parameter Y_S characterizing spontaneous lepton number violation and neutrino mass generation through $\langle\sigma\rangle$. To be more precise, as shown in Fig. 4.6 the allowed values for the mass of the heavy scalar boson (m_{H_2}) varies with this Yukawa coupling; for example, if m_{H_2} was to be found to be, say, ~ 2 TeV ($v_\sigma = 3$ TeV by assumption here), then one would conclude that either $Y_S \sim 0.5$ or the scalar sector must be strongly interacting.

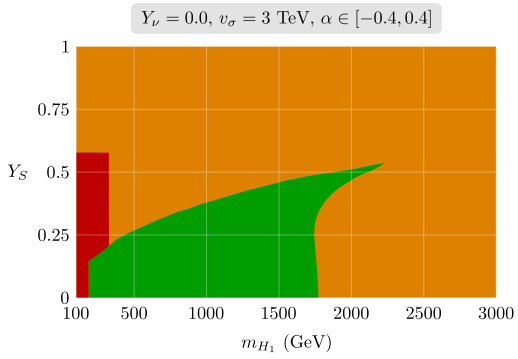

Figure 4.6: The region stability and perturbativity for the case of non-zero $Y_S > 0$ and very small Y_ν is displayed in green; the color ordering code is the same as in the scan in Fig. 4.3.

4.5 Conclusions

In conclusion, the Standard Model vacuum is unstable for the measured top and Higgs boson masses. However the theory is incomplete as it has no masses for neutrinos. We have therefore generalized its symmetry breaking potential in order to induce naturally small neutrino masses from the breaking of lepton number. We have examined the vacuum stability issue in schemes with spontaneous breaking of global lepton number at the TeV scale, showing how one can naturally obtain a consistent behavior of the scalar potential at all scales, avoiding the vacuum instability. Given that the new physics parameters of the theory are not known, it sufficed for us to adopt one-loop renormalization group equations. Since all new particles in the model lie at the TeV scale, they can be probed with current experiments, such as the LHC. Invisible decays of the two CP-even Higgs bosons, $H_i \to JJ$, were discussed in [15]. Improved sensitivity is expected from the 13 TeV run of the LHC. In addition, we expect enhanced rates for lepton flavour violating processes [33–35]. In summary, schemes such as the one explored in this letter may shed light on two important drawbacks of the Standard Model namely, the instability associated to its gauge symmetry breaking mechanism and the lack of neutrino mass.

Acknowledgments

We thank Sofiane Boucenna for discussions in the early phase of this project. This work was supported by MINECO grants FPA2014-58183-P, Multidark CSD2009-00064 and the PROMETEOII/2014/084 grant from Generalitat Valenciana.

4.A Appendix A

In this appendix we provide some details on the scalar sector of the model. The potential in equation (4.1) is controlled by 5 parameters (μ_1^2, μ_2^2, λ_1, λ_2, and λ_{12}) which one can translate into two vacuum expectation values ($v_\sigma = \sqrt{2}\,\langle \mathrm{Re}\,(\sigma)\rangle$ and $v_H = \sqrt{2}\,\langle \mathrm{Re}\,(H^0)\rangle$), two mass eigenvalues (m_{H_1} and m_{H_2})

and a mixing angle α:

$$\lambda_1 = \frac{m_{H_1}^2 \cos^2\alpha + m_{H_2}^2 \sin^2\alpha}{2v_\sigma^2}\,, \tag{4.4}$$

$$\lambda_2 = \frac{m_{H_1}^2 \sin^2\alpha + m_{H_2}^2 \cos^2\alpha}{2v_H^2}\,, \tag{4.5}$$

$$\lambda_{12} = \frac{\left(m_{H_1}^2 - m_{H_2}^2\right)\cos\alpha\sin\alpha}{v_\sigma v_H}\,, \tag{4.6}$$

$$-\mu_1^2 = \frac{v_H \cos\alpha\sin\alpha\left(m_{H_1}^2 - m_{H_2}^2\right) + m_{H_1}^2 v_\sigma \cos^2\alpha + m_{H_2}^2 v_\sigma \sin^2\alpha}{2v_\sigma}\,, \tag{4.7}$$

$$-\mu_2^2 = \frac{v_\sigma \cos\alpha\sin\alpha\left(m_{H_1}^2 - m_{H_2}^2\right) + m_{H_1}^2 v_H \sin^2\alpha + m_{H_2}^2 v_H \cos^2\alpha}{2v_H}\,, \tag{4.8}$$

with

$$\begin{pmatrix} H_1 \\ H_2 \end{pmatrix} \equiv \begin{pmatrix} \cos\alpha & \sin\alpha \\ -\sin\alpha & \cos\alpha \end{pmatrix} \begin{pmatrix} \sqrt{2}\mathrm{Re}\left(\sigma\right) \\ \sqrt{2}\mathrm{Re}\left(H^0\right) \end{pmatrix}\,. \tag{4.9}$$

On the other hand, it is well known that the Standard Model potential is controlled by just two parameters μ^2 and λ:

$$V_{SM}\left(H\right) = \mu^2\left(H^\dagger H\right) + \lambda\left(H^\dagger H\right)^2\,. \tag{4.10}$$

For a reasonably small mixing angle α, one can consider that the state H_1 is mostly made of the real part of the singlet, hence we may integrate out $\sqrt{2}\mathrm{Re}\left(\sigma\right)$. In this approximation, we note that

$$\lambda \approx \lambda_2 - \frac{\lambda_{12}^2}{4\lambda_1}\,, \tag{4.11}$$

$$\mu^2 \approx \mu_2^2 - \frac{\lambda_{12}}{2\lambda_1}\mu_1^2\,, \tag{4.12}$$

at the scale of decoupling, meaning in particular that there is a tree-level threshold correction between λ_2 and the Standard Model quartic coupling λ. For the results in this paper, we neglect altogether the small Standard Model range between the m_Z and m_{H_1} scale, starting instead with equations (4.4)–(4.8), which already include this threshold effect.

4.B Appendix B

For completeness, we write down here the renormalization group equations of the model parameters which are relevant for the study of the potential's

stability. We work with the 1-family approximation, ignoring the bottom and tau Yukawa couplings. These equations were obtained with the SARAH program [36] (see also [37]) and explicitly checked by us using the results in [38]; furthermore they are consistent with [18]. As usual, t stands for the natural logarithm of the energy scale.

$$(4\pi)^2\frac{dg_i}{dt} = b_i g_i^3 \text{ with } b_i = \left(\frac{41}{10}, -\frac{19}{6}, -7\right), \tag{4.13}$$

$$(4\pi)^2\frac{dY_t}{dt} = \left(-\frac{17}{20}g_1^2 - \frac{9}{4}g_2^2 - 8g_3^2 + \frac{9}{2}Y_t^2 + Y_\nu^2\right)Y_t, \tag{4.14}$$

$$(4\pi)^2\frac{dY_\nu}{dt} = \left(-\frac{9}{20}g_1^2 - \frac{9}{4}g_2^2 + 3Y_t^2 + \frac{5}{2}Y_\nu^2\right)Y_\nu, \tag{4.15}$$

$$(4\pi)^2\frac{dY_S}{dt} = 6Y_S^3, \tag{4.16}$$

$$(4\pi)^2\frac{d\lambda_1}{dt} = 20\lambda_1^2 + 2\lambda_{12}^2 + 8\lambda_1 Y_S^2 - 16Y_S^4, \tag{4.17}$$

$$\begin{aligned}(4\pi)^2\frac{d\lambda_2}{dt} &= \frac{27}{200}g_1^4 + \frac{9}{20}g_1^2 g_2^2 + \frac{9}{8}g_2^4 \\ &- \left(\frac{9}{5}g_1^2 + 9g_2^2\right)\lambda_2 + 24\lambda_2^2 + \lambda_{12}^2 \\ &+ \lambda_2\left(12Y_t^2 + 4Y_\nu^2\right) - \left(6Y_t^4 + 2Y_\nu^4\right),\end{aligned} \tag{4.18}$$

$$\begin{aligned}(4\pi)^2\frac{d\lambda_{12}}{dt} &= \left[-\left(\frac{9}{10}g_1^2 + \frac{9}{2}g_2^2\right) + 6Y_t^2 + 2Y_\nu^2\right. \\ &+ \left. 4Y_S^2 + 8\lambda_1 + 12\lambda_2 + 4\lambda_{12}\right]\lambda_{12}.\end{aligned} \tag{4.19}$$

BIBLIOGRAPHY

[1] S. Alekhin, A. Djouadi and S. Moch, *The top quark and Higgs boson masses and the stability of the electroweak vacuum*, Phys.Lett. **B716** (2012) 214–219, arXiv:1207.0980 [hep-ph].

[2] D. Buttazzo et al., *Investigating the near-criticality of the Higgs boson*, JHEP **1312** (2013) 089, arXiv:1307.3536 [hep-ph].

[3] D. Forero, M. Tortola and J. Valle, *Neutrino oscillations refitted*, Phys.Rev. **D90** (2014) 9 093006, arXiv:1405.7540 [hep-ph].

[4] V. Branchina and E. Messina, *Stability, Higgs Boson Mass and New Physics*, Phys. Rev. Lett. **111** (2013) 241801, arXiv:1307.5193 [hep-ph].

[5] S. Weinberg, *Baryon and Lepton Nonconserving Processes*, Phys.Rev.Lett. **43** (1979) 1566–1570.

[6] J. Schechter and J. Valle, *Neutrino Masses in SU(2) x U(1) Theories*, Phys.Rev. **D22** (1980) 2227.

[7] R. Costa, A. P. Morais, M. O. P. Sampaio and R. Santos, *Two-loop stability of a complex singlet extended Standard Model*, Phys. Rev. **D92** (2015) 2 025024, arXiv:1411.4048 [hep-ph].

[8] Y. Chikashige, R. N. Mohapatra and R. Peccei, *Are There Real Goldstone Bosons Associated with Broken Lepton Number?*, Phys.Lett. **B98** (1981) 265.

[9] J. Schechter and J. Valle, *Neutrino Decay and Spontaneous Violation of Lepton Number*, Phys.Rev. **D25** (1982) 774.

[10] K. Olive et al. (Particle Data Group), *Review of Particle Physics*, Chin.Phys. **C38** (2014) 090001.

[11] A. S. Joshipura and J. Valle, *Invisible Higgs decays and neutrino physics*, Nucl.Phys. **B397** (1993) 105–122.

[12] F. de Campos, O. J. P. Eboli, M. A. Garcia-Jareno and J. W. F. Valle, *R-parity violating signals for chargino production at LEP-2*, Nucl. Phys. **B546** (1999) 33–51, arXiv:hep-ph/9710545 [hep-ph].

[13] J. Abdallah et al. (DELPHI Collaboration), *Searches for neutral higgs bosons in extended models*, Eur.Phys.J. **C38** (2004) 1–28, arXiv:hep-ex/0410017 [hep-ex].

[14] J. Abdallah et al. (DELPHI), *Searches for invisibly decaying Higgs bosons with the DELPHI detector at LEP*, Eur. Phys. J. **C32** (2004) 475–492, arXiv:hep-ex/0401022 [hep-ex].

[15] C. Bonilla, J. W. F. Valle and J. C. Romao, *Neutrino mass and invisible Higgs decays at the LHC* (2015), arXiv:1502.01649 [hep-ph].

[16] J. Casas, V. Di Clemente, A. Ibarra and M. Quiros, *Massive neutrinos and the Higgs mass window*, Phys.Rev. **D62** (2000) 053005, arXiv:hep-ph/9904295 [hep-ph].

[17] J. Elias-Miro et al., *Higgs mass implications on the stability of the electroweak vacuum*, Phys. Lett. **B709** (2012) 222–228, arXiv:1112.3022 [hep-ph].

[18] J. Elias-Miro et al., *Stabilization of the Electroweak Vacuum by a Scalar Threshold Effect*, JHEP **1206** (2012) 031, arXiv:1203.0237 [hep-ph].

[19] L. Basso, S. Moretti and G. M. Pruna, *A Renormalisation Group Equation Study of the Scalar Sector of the Minimal B-L Extension of the Standard Model*, Phys. Rev. **D82** (2010) 055018, arXiv:1004.3039 [hep-ph].

[20] M. Gonderinger, Y. Li, H. Patel and M. J. Ramsey-Musolf, *Vacuum Stability, Perturbativity, and Scalar Singlet Dark Matter*, JHEP **01** (2010) 053, arXiv:0910.3167 [hep-ph].

[21] O. Lebedev, *On Stability of the Electroweak Vacuum and the Higgs Portal*, Eur.Phys.J. **C72** (2012) 2058, arXiv:1203.0156 [hep-ph].

[22] A. Falkowski, C. Gross and O. Lebedev, *A second Higgs from the Higgs portal*, JHEP **1505** (2015) 057, arXiv:1502.01361 [hep-ph].

[23] G. Ballesteros and C. Tamarit, *Higgs portal valleys, stability and inflation*, JHEP **09** (2015) 210, arXiv:1505.07476 [hep-ph].

[24] L. Delle Rose, C. Marzo and A. Urbano, *On the stability of the electroweak vacuum in the presence of low-scale seesaw models*, JHEP **12** (2015) 050, arXiv:1506.03360 [hep-ph].

[25] A. Salvio, *A Simple Motivated Completion of the Standard Model below the Planck Scale: Axions and Right-Handed Neutrinos*, Phys. Lett. **B743** (2015) 428–434, arXiv:1501.03781 [hep-ph].

[26] R. Mohapatra and J. Valle, *Neutrino Mass and Baryon Number Nonconservation in Superstring Models*, Phys.Rev. **D34** (1986) 1642.

[27] M. Gonzalez-Garcia and J. Valle, *Fast Decaying Neutrinos and Observable Flavor Violation in a New Class of Majoron Models*, Phys.Lett. **B216** (1989) 360.

[28] G. Aad et al. (ATLAS Collaboration), *Search for Invisible Decays of a Higgs Boson Produced in Association with a Z Boson in ATLAS*, Phys.Rev.Lett. **112** (2014) 201802, arXiv:1402.3244 [hep-ex].

[29] S. Chatrchyan et al. (CMS Collaboration), *Search for invisible decays of Higgs bosons in the vector boson fusion and associated ZH production modes*, Eur.Phys.J. **C74** (2014) 2980, arXiv:1404.1344 [hep-ex].

[30] *Search for invisible decays of Higgs bosons in the vector boson fusion production mode*, Technical Report CMS-PAS-HIG-14-038, CERN, Geneva (2015), URL https://cds.cern.ch/record/2007270.

[31] G. Degrassi et al., *Higgs mass and vacuum stability in the Standard Model at NNLO*, JHEP **08** (2012) 098, arXiv:1205.6497 [hep-ph].

[32] S. M. Boucenna, S. Morisi and J. W. F. Valle, *The low-scale approach to neutrino masses*, Adv. High Energy Phys. **2014** (2014) 831598, arXiv:1404.3751 [hep-ph].

[33] J. Bernabeu et al., *Lepton Flavor Nonconservation at High-Energies in a Superstring Inspired Standard Model*, Phys.Lett. **B187** (1987) 303.

[34] F. Deppisch and J. Valle, *Enhanced lepton flavor violation in the supersymmetric inverse seesaw model*, Phys.Rev. **D72** (2005) 036001, arXiv:hep-ph/0406040 [hep-ph].

[35] F. Deppisch, T. Kosmas and J. Valle, *Enhanced mu- - e- conversion in nuclei in the inverse seesaw model*, Nucl.Phys. **B752** (2006) 80–92, arXiv:hep-ph/0512360 [hep-ph].

[36] F. Staub, *Exploring new models in all detail with SARAH* (2015), arXiv:1503.04200 [hep-ph].

[37] F. Lyonnet, I. Schienbein, F. Staub and A. Wingerter, *PyR@TE: Renormalization Group Equations for General Gauge Theories*, Comput. Phys. Commun. **185** (2014) 1130–1152, arXiv:1309.7030 [hep-ph].

[38] M.-x. Luo, H.-w. Wang and Y. Xiao, *Two loop renormalization group equations in general gauge field theories*, Phys.Rev. **D67** (2003) 065019, arXiv:hep-ph/0211440 [hep-ph].

CHAPTER **5**

CONSISTENCY OF THE TRIPLET SEESAW MODEL REVISITED

Authors: Cesar Bonilla, Renato M. Fonseca, Jose W.F. Valle.
Journal reference: Phys. Rev. D92 (2015) no.7, 075028.

Abstract

Adding a scalar triplet to the Standard Model is one of the simplest ways of giving mass to neutrinos, providing at the same time a mechanism to stabilize the theory's vacuum. In this paper, we revisit these aspects of the type-II seesaw model pointing out that the bounded-from-below conditions for the scalar potential in use in the literature are not correct. We discuss some scenarios where the correction can be significant and sketch the typical scalar boson profile expected by consistency.

5.1 Introduction

More than ever, after the discovery of the Higgs boson, particle physicists are eager for new results that can shed light on the symmetry breaking puzzle. The tiny neutrino masses suggest that probably a different mass generation scheme associated to their charge neutrality is at work. Neutrino masses can be introduced in the Standard Model (SM) through the lepton number violating coupling of a scalar triplet Δ (hypercharge +1) with the left-handed leptons,

$$\frac{Y_{\Delta,ij}}{2} L_i^T C\,(i\tau_2)\,\Delta L_j + \text{h.c.} \tag{5.1}$$

and generate a neutrino mass matrix $Y_\Delta \langle \Delta^0 \rangle$ after electroweak symmetry breaking. Here $i\tau_2$ is the weak isospin conjugation matrix. The vacuum expectation value of the triplet is proportional to the strength $m_{H\Delta}$ of the coupling $HH\Delta$ which can be an arbitrarily small parameter since this is the only lepton number violating coupling in the model. This is arguably the most economical way of realizing Weinberg' s dimension five operator [3]. For simplicity here we focus upon the case of explicit lepton number violation [4] since the implementation of spontaneous lepton number violation [5] would require an extended scalar sector containing also a singlet. In this scheme one "explains" the smallness of neutrino masses with the smallness of $m_{H\Delta}$ — and hence the smallness of the "induced" vacuum expectation value (VEV) $v_\Delta \equiv \langle \Delta^0 \rangle$ — even with a light messenger scalar triplet Δ, potentially accessible at the next run of the LHC.

On the other hand, it is known that the Higgs quartic coupling in the SM is driven to negative values at high energies, before the Planck scale is reached [6, 7]. With the triplet scalar field, the situation changes as the new quartic scalar interactions between H and Δ are able to soften the decrease of the Higgs quartic coupling λ_H as the energy scale is increased [8–11]. The effect is qualitatively the same if the triplet is replaced by an $SU(2)_L$ singlet [12–16]. However, with the new triplet scalar, it is no longer enough to check that the Higgs quartic coupling stays positive, as the conditions for the potential to be bounded from below become more elaborate.

Regardless of the energy scale one may ask, under what conditions is the potential of the type-II seesaw model bounded from below? An attempt to write down for the first time these necessary and sufficient vacuum stability conditions taking into account all field directions has been made in [17]. However, as we point out in this paper, those conditions are too strong — they are sufficient but not necessary to ensure that a set of values for the quartic couplings corresponds to a stable vacuum. The structure of this paper is the following: after a brief review of the basic properties of the model (section

5.2) we derive the necessary and sufficient conditions for the potential to be bounded from below in section 5.3, discussing the difference with the conditions in use in the literature both from a theoretical point-of-view as well as a numerical one. In section 5.4 we apply these conditions to explore the region in parameter space of the type-II seesaw where the potential is stable up to some given scale. Finally, we present some conclusions in section 5.6. (Two appendices provide supplementary material.)

5.2 Basic properties of the type-II seesaw model

Here we consider the simplest neutrino mass generation scheme based on an effective seesaw mechanism with explicit lepton number violation described by the complex triplet, given as

$$\Delta \equiv \begin{pmatrix} \frac{\Delta^+}{\sqrt{2}} & \Delta^{++} \\ \Delta^0 & -\frac{\Delta^+}{\sqrt{2}} \end{pmatrix} . \tag{5.2}$$

The most general potential involving Δ and the Standard Model Higgs doublet $H = (H^+, H^0)^T$ has a total of eight parameters which we can take to be real:

$$\begin{aligned} V(H,\Delta) &= -\mu_H^2 H^\dagger H + \mu_\Delta^2 \mathrm{Tr}\left(\Delta^\dagger \Delta\right) + \left[\frac{m_{H\Delta}}{2} H^T (i\tau_2) \Delta^\dagger H + \mathrm{h.c.}\right] \\ &+ \frac{1}{2}\lambda_H \left(H^\dagger H\right)^2 + \lambda_{H\Delta} \mathrm{Tr}\left(\Delta^\dagger \Delta\right)\left(H^\dagger H\right) + \lambda'_{H\Delta} H^\dagger \Delta\Delta^\dagger H \\ &+ \frac{\lambda_\Delta}{2}\left[\mathrm{Tr}\left(\Delta^\dagger \Delta\right)\right]^2 + \frac{\lambda'_\Delta}{2}\mathrm{Tr}\left(\Delta^\dagger \Delta\Delta^\dagger \Delta\right) . \end{aligned} \tag{5.3}$$

The vacuum expectation value of the neutral component of the triplet, $v_\Delta \equiv \langle \Delta^0 \rangle$, must be significantly smaller than the one of the standard Higgs, $v_H \equiv \langle H^0 \rangle$, otherwise the ρ parameter will deviate too much from 1. Indeed,

$$\rho \approx 1 - 2\alpha^2 \tag{5.4}$$

with $\alpha \equiv v_\Delta / v_H$ so this ratio of VEVs can be at most of the percent order given the experimental constraints on ρ [18]. Furthermore, since neutrino masses are proportional to v_Δ, this VEV should indeed be very small. Under the approximation that $\alpha \ll 1$, the minimization solution of the potential requires that

$$\mu_H^2 \approx \lambda_H v_H^2 , \tag{5.5}$$

$$\mu_\Delta^2 \approx \left(\frac{\chi}{2} - \lambda_{H\Delta} - \lambda'_{H\Delta}\right) v_H^2 , \tag{5.6}$$

where

$$\chi \equiv m_{H\Delta}/v_\Delta. \tag{5.7}$$

Using these relations one can write the scalar boson mass eigenstates as shown in table 5.1.

Mass eigenstate ϕ	Mass squared m_ϕ^2	Composition
H^{++}	$v_H^2\left(\frac{\chi}{2}-\lambda'_{H\Delta}\right)$	Δ^{++}
G^+	0	$H^+ + \sqrt{2}\alpha\Delta^+$
H^+	$v_H^2\left(\frac{\chi}{2}-\frac{\lambda'_{H\Delta}}{2}\right)$	$\Delta^+ - \sqrt{2}\alpha H^+$
G^0	0	$H_I^0 + 2\alpha\Delta_I^0$
A^0	$\frac{1}{2}v_H^2\chi$	$\Delta_I^0 - 2\alpha H_I^0$
h^0	$2\lambda_H v_H^2$	$H_R^0 + 2\alpha\frac{\chi-2\lambda_{H\Delta}-2\lambda'_{H\Delta}}{\chi-4\lambda_H}\Delta_R^0$
H^0	$\frac{1}{2}v_H^2\chi$	$\Delta_R^0 - 2\alpha\frac{\chi-2\lambda_{H\Delta}-2\lambda'_{H\Delta}}{\chi-4\lambda_H}H_R^0$

Table 5.1: Scalar mass eigenstates in the type-II seesaw model. We have defined the dimensionless parameters $\alpha \equiv v_\Delta/v_H$ and $\chi \equiv m_{H\Delta}/v_\Delta$.

Note that if the doubly charged Higgs H^{++} is to be heavier than half a TeV or so, then $\chi \gtrsim 10$, making χ significantly larger than any of the quartic couplings λ_i which one expects to be, at most, of order 1. Moreover, one sees that for a suitable χ the would-be triplet Nambu-Goldstone boson state A^0 can be massive enough to have escaped detection at LEP.

5.3 When is the scalar potential bounded from below?

We now turn to the important issue of the stability of the VEV solution mentioned above. As long as all scalar masses are positive, the potential will not roll down classically to another minimum, but this still leaves open the possibility of a tunneling to a deeper minimum. In order for this not to happen, it is necessary (although not sufficient) that the potential does not fall to infinitely negative values in any VEV direction. In other words, we must ensure that V is bounded from below, which is equivalent to the requirement that the quartic part of the potential in equation (5.3), $V^{(4)}$, must be positive for all non-zero field values. In the following then, we shall derive the necessary and sufficient conditions for this to be true, correcting the result obtained in [17].

While there are ten real degrees of freedom (four in H plus six in Δ), V depends on them only through 4 quantities: $H^\dagger H$, $\mathrm{Tr}\left(\Delta^\dagger\Delta\right)$, $H^\dagger\Delta\Delta^\dagger H$ and

$\mathrm{Tr}\left(\Delta^\dagger\Delta\Delta^\dagger\Delta\right)$. In the following, we shall take $\mathrm{Tr}\left(\Delta^\dagger\Delta\right)$ to be non-zero.[1] We now define r, ζ and ξ as the following non-negative dimensionless quantities [17],

$$H^\dagger H \equiv r\mathrm{Tr}\left(\Delta^\dagger\Delta\right) , \tag{5.8}$$

$$\mathrm{Tr}\left(\Delta^\dagger\Delta\Delta^\dagger\Delta\right) \equiv \zeta\left[\mathrm{Tr}\left(\Delta^\dagger\Delta\right)\right]^2 , \tag{5.9}$$

$$H^\dagger\Delta\Delta^\dagger H \equiv \xi\mathrm{Tr}\left(\Delta^\dagger\Delta\right)\left(H^\dagger H\right) , \tag{5.10}$$

such that the quartic part of the potential reads

$$\frac{V^{(4)}}{\left[\mathrm{Tr}\left(\Delta^\dagger\Delta\right)\right]^2} = \frac{1}{2}\lambda_H r^2 + \lambda_{H\Delta} r + \lambda'_{H\Delta}\xi r + \frac{\lambda_\Delta}{2} + \frac{\lambda'_\Delta}{2}\zeta . \tag{5.11}$$

This expression must be positive for all allowed values of r, ζ and ξ. Consider first r: from equation (5.8) it is clear that r can take any non-negative value which means that, given the quadratic dependence of equation (5.11) on r that one must have

$$0 < \lambda_H , \tag{5.12}$$

$$0 < \lambda_\Delta + \lambda'_\Delta\zeta \equiv F_1(\zeta) , \tag{5.13}$$

$$0 < \lambda_{H\Delta} + \xi\lambda'_{H\Delta} + \sqrt{\lambda_H\left(\lambda_\Delta + \lambda'_\Delta\zeta\right)} \equiv F_2(\xi,\zeta) . \tag{5.14}$$

These conditions match those given in [17] with a different notation. However, what follows differs with [17] in a crucial way.

In order to obtain the necessary and sufficient conditions for the quartic couplings λ_i which yield a potential bounded from below, one needs to get rid of ζ and ξ from conditions (5.12)–(5.14). Note that these conditions must be respected for all ζ and ξ, so one needs to find what are the allowed values of (ξ,ζ) from the definition of these two quantities. We do not show the details here, but the reader can convince her/himself that ξ can take any value between 0 and 1 and ζ can be anywhere between 1/2 and 1, as noted in [17].

However, the crucial point is that this does not mean that (ξ,ζ) can be anywhere in the rectangle with vertices in $\left(0,\frac{1}{2}\right)$ and $(1,1)$. Indeed, from equations (5.9) and (5.10) it can be shown that the possible values of (ξ,ζ) correspond to

$$2\xi^2 - 2\xi + 1 \leq \zeta \leq 1 , \tag{5.15}$$

which defines the shaded region depicted in figure 8.1. Since the function $F_1(\zeta)$ defined in (5.13) is monotonic, the condition '$0 < F_1(\zeta)$ for all ζ' is equivalent

[1] If this is not the case, the quartic part of the potential is reduced to $\frac{1}{2}\lambda_H\left(H^\dagger H\right)^2$ in which case it is clear that one must have $\lambda_H > 0$.

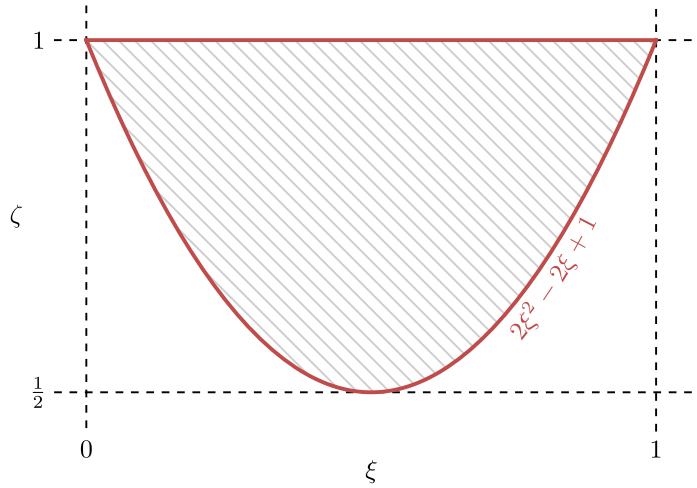

Figure 5.1: The shaded region is the allowed one for the parameters (ξ, ζ).

to '$0 < F_1\left(\frac{1}{2}\right)$ and $0 < F_1(1)$' which translates into the requirement

$$0 < \lambda_\Delta + \frac{1}{2}\lambda'_\Delta \text{ and } 0 < \lambda_\Delta + \lambda'_\Delta \,. \tag{5.16}$$

As for the condition in (5.14), note that '$0 < F_2(\xi, \zeta)$ for all ξ and ζ' is trivially the same as $0 < \min F_2(\xi, \zeta)$, so one is left with the job of finding the minimum of F_2. Furthermore, since this function is monotonic in both ξ and ζ, we know that its minimum occurs at the border of the shaded region in figure 8.1; to be more specific, this argument shows that the minimum of the function must occur somewhere along the line defined by $\zeta = 2\xi^2 - 2\xi + 1$, with $0 \leq \xi \leq 1$. Then we may take

$$\widehat{F}(\xi) \equiv F_2\left(\xi, 2\xi^2 - 2\xi + 1\right) \tag{5.17}$$

noticing that the sign of $\widehat{F}''(\xi)$ is constant — it is the same as the one of λ'_Δ. Therefore, one can always find a value ξ_0 where $\widehat{F}'(\xi_0) = 0$. Such a ξ_0 will be a minimum if $\widehat{F}''(\xi_0) > 0$ and, furthermore, one must also make sure that $0 \leq \xi_0 \leq 1$ (or equivalently that $\widehat{F}'(0) < 0$ and $\widehat{F}'(1) > 0$ since $\widehat{F}'$ is a monotonous function). This will be true if and only if $\lambda'_\Delta \sqrt{\lambda_H} > |\lambda'_{H\Delta}| \sqrt{\lambda_\Delta + \lambda'_\Delta}$, in which case

$$\widehat{F}(\xi_0) = \lambda_{H\Delta} + \frac{1}{2}\lambda'_{H\Delta} + \frac{1}{2}\sqrt{\left(2\lambda_H\lambda'_\Delta - {\lambda'_{H\Delta}}^2\right)\left(2\frac{\lambda_\Delta}{\lambda'_\Delta} + 1\right)} \,. \tag{5.18}$$

The remaining possibility is that the minimum of $\widehat{F}$ in the interval $\xi \in [0, 1]$ is at $\xi = 0$ or 1, from which we get the constraints that both $\widehat{F}(0) = \lambda_{H\Delta} +$

$\sqrt{\lambda_H\left(\lambda_\Delta+\lambda'_\Delta\right)}$ and $\widehat{F}\left(1\right)=\lambda_{H\Delta}+\lambda'_{H\Delta}+\sqrt{\lambda_H\left(\lambda_\Delta+\lambda'_\Delta\right)}$ should be positive quantities.

In summary, the potential will be bounded from below if and only if

$$\begin{gathered}\lambda_H,\,\lambda_\Delta+\lambda'_\Delta,\,\lambda_\Delta+\frac{1}{2}\lambda'_\Delta>0\\ \lambda_{H\Delta}+\sqrt{\lambda_H\left(\lambda_\Delta+\lambda'_\Delta\right)},\,\lambda_{H\Delta}+\lambda'_{H\Delta}+\sqrt{\lambda_H\left(\lambda_\Delta+\lambda'_\Delta\right)}>0\\ \text{and}\\ \left[\lambda'_\Delta\sqrt{\lambda_H}\leq\left|\lambda'_{H\Delta}\right|\sqrt{\lambda_\Delta+\lambda'_\Delta}\right.\\ \left.\text{or}\;\;2\lambda_{H\Delta}+\lambda'_{H\Delta}+\sqrt{\left(2\lambda_H\lambda'_\Delta-{\lambda'_{H\Delta}}^2\right)\left(2\frac{\lambda_\Delta}{\lambda'_\Delta}+1\right)}>0\right]\,.\end{gathered}\tag{5.19}$$

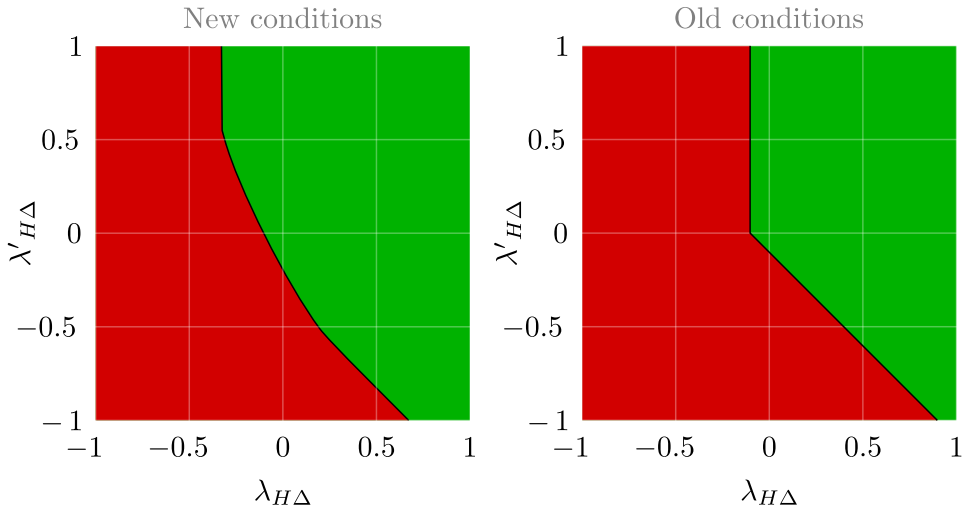

Figure 5.2: Regions of stability (green) and instability (red) of the potential for $\lambda_\Delta=-\frac{1}{3}$, $\lambda'_\Delta=\frac{3}{4}$ and $\lambda_H\approx\frac{1}{4}$. The two plots make it possible to compare the correct stability conditions as given in equation (5.20) (left) with the ones in use in the literature (right).

The condition in (5.19) should be compared with the one used up to now in the literature, where the last line of (5.19) is replaced by $F_2\left(0,\frac{1}{2}\right)$, $F_2\left(1,\frac{1}{2}\right)>0$, which translates into

$$\lambda_{H\Delta}+\sqrt{\lambda_H\left(\lambda_\Delta+\frac{1}{2}\lambda'_\Delta\right)},\,\lambda_{H\Delta}+\lambda'_{H\Delta}+\sqrt{\lambda_H\left(\lambda_\Delta+\frac{1}{2}\lambda'_\Delta\right)}>0\,.\tag{5.20}$$

From the discussion so far it should be clear that this condition is too strict: potentials V which obey it are necessarily bounded from below, but not all potentials which are bounded from below do obey it. Indeed, the constraint in (5.20) assumes that by varying the fields H and Δ the point (ξ, ζ) can be anywhere within the dashed rectangle in figure 8.1, when in reality only the shaded region is allowed, with two thirds of the area of the rectangle. Restricting to the 5-dimensional box region where $|\lambda_i| \leq 1$, a numerical scan indicates that close to 5% of the valid points are excluded by the constraint in (5.20), although in certain special scenarios, as in figure 5.2, this percentage can be significantly larger.

5.4 Regions of stability and perturbativity

Now that we have the correct stability conditions we consider the renormalization group evolution of the triplet seesaw model. Ignoring all Yukawa couplings except the one of the top, using [19–21] one finds the renormalization group equations of the model to be the following (see also [22, 23]):[2]

$$(4\pi)^2 \frac{dg_i}{dt} = b_i g_i^3 \text{ with } b_i = \left(\frac{47}{10}, -\frac{5}{2}, -7\right) , \tag{5.21}$$

$$\begin{aligned}(4\pi)^2 \frac{d\lambda_H}{dt} = {} & \frac{27}{100}g_1^4 + \frac{9}{10}g_1^2 g_2^2 + \frac{9}{4}g_2^4 - \left(\frac{9}{5}g_1^2 + 9g_2^2\right)\lambda_H + 12\lambda_H^2 + 6\lambda_{H\Delta}^2 \\ & + 6\lambda_{H\Delta}\lambda'_{H\Delta} + \frac{5}{2}{\lambda'_{H\Delta}}^2 + 12\lambda_H y_t^2 - 12y_t^4 ,\end{aligned} \tag{5.22}$$

$$\begin{aligned}(4\pi)^2 \frac{d\lambda_{H\Delta}}{dt} = {} & \frac{27}{25}g_1^4 - \frac{18}{5}g_1^2 g_2^2 + 6g_2^4 - \left(\frac{9}{2}g_1^2 + \frac{33}{2}g_2^2\right)\lambda_{H\Delta} + 6\lambda_H\lambda_{H\Delta} \\ & + 2\lambda_H\lambda'_{H\Delta} + 4\lambda_{H\Delta}^2 + 8\lambda_\Delta\lambda_{H\Delta} + 6\lambda'_\Delta\lambda_{H\Delta} + {\lambda'_{H\Delta}}^2 + 3\lambda_\Delta\lambda'_{H\Delta} \\ & + \lambda'_\Delta\lambda'_{H\Delta} + 6\lambda_{H\Delta}y_t^2 ,\end{aligned} \tag{5.23}$$

$$\begin{aligned}(4\pi)^2 \frac{d\lambda'_{H\Delta}}{dt} = {} & \frac{36}{5}g_1^2 g_2^2 - \left(\frac{9}{2}g_1^2 + \frac{33}{2}g_2^2\right)\lambda'_{H\Delta} + 2\lambda_H\lambda'_{H\Delta} + 8\lambda_{H\Delta}\lambda'_{H\Delta} \\ & + 4{\lambda'_{H\Delta}}^2 + 2\lambda_\Delta\lambda'_{H\Delta} + 4\lambda'_\Delta\lambda'_{H\Delta} + 6\lambda'_{H\Delta}y_t^2 ,\end{aligned} \tag{5.24}$$

[2] Using the dictionary in appendix A, it can be checked that these expressions match those in (3.2) of [10], the only difference being that in $(4\pi)^2 \frac{d\lambda_4}{dt}$, instead of a term $+\frac{9}{5}g'^2$, we get $+3g'^2$.

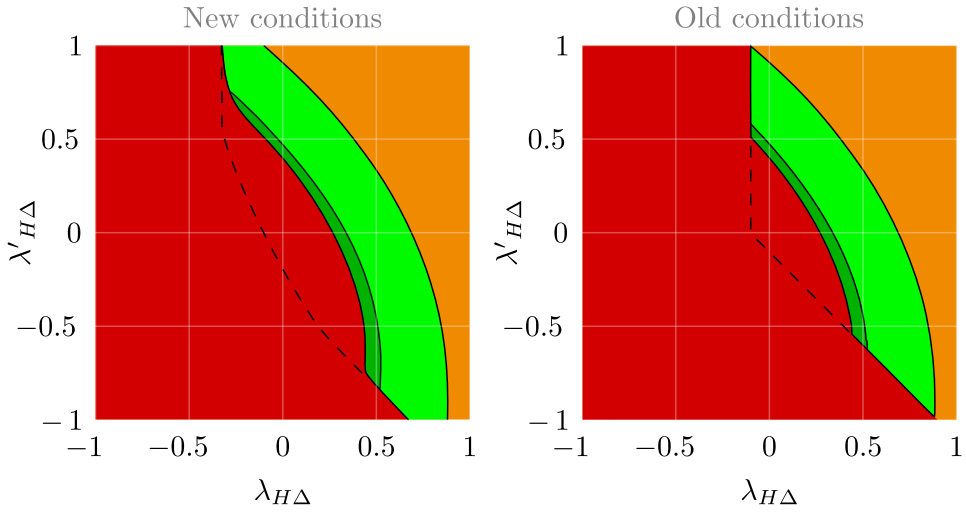

Figure 5.3: Regions of stability (dark green) and instability (red) considering the energy range going from the top mass all the way to the Planck mass. Those cases which (appear to) lead to a stable vacuum but involve non-perturbative dynamics because $|\lambda_i| > \sqrt{4\pi}$ for some quartic coupling λ_i are shown in orange. If one requires stability only up to 10^{12} GeV the stable region becomes bigger, as indicated by the light green region. The dashed lines indicate the border between the stable and unstable regions at low energies (see figure 5.2).

$$(4\pi)^2 \frac{d\lambda_\Delta}{dt} = \frac{108}{25} g_1^4 - \frac{72}{5} g_1^2 g_2^2 + 30 g_2^4 - \left(\frac{36}{5} g_1^2 + 24 g_2^2\right) \lambda_\Delta + 4\lambda_{H\Delta}^2 + 4\lambda_{H\Delta}\lambda'_{H\Delta} + 14\lambda_\Delta^2 + 12\lambda_\Delta\lambda'_\Delta + 3{\lambda'_\Delta}^2 , \tag{5.25}$$

$$(4\pi)^2 \frac{d\lambda'_\Delta}{dt} = \frac{144}{5} g_1^2 g_2^2 - 12 g_2^4 + 2{\lambda'_{H\Delta}}^2 - \left(\frac{36}{5} g_1^2 + 24 g_2^2\right) \lambda'_\Delta + 12\lambda_\Delta\lambda'_\Delta + 9{\lambda'_\Delta}^2 . \tag{5.26}$$

Using these equations and requiring stability of the scalar potential in the energy range going from the top mass all the way to the Planck mass one obtains the regions of quartic couplings indicated in green in figure 5.3. The right panel corresponds to the use of the stability conditions used in the literature, while the left panel refers to our new and less restrictive stability conditions. On the other hand the instability regions are indicated in red. Finally those cases which correspond to a stable vacuum but involve non-perturbative dynamics because $|\lambda_i| > \sqrt{4\pi}$ for some quartic coupling λ_i are indicated in orange. Notice also that the stable region becomes bigger if one imposes stability only up to some intermediate scale, chosen to be 10^{12} GeV, as indicated by the light green region in figure 5.3.

5.5 Phenomenological profile of the triplet seesaw Higgs sector

Since its original proposal there have been many phenomenological studies of the scalar sector of the triplet model, as it constitutes an essential ingredient of the type-II seesaw mechanism. For the benefit of the reader we present in figure 5.5 of Appendix B a schematic view of the scalar boson mass spectrum in the model given in table 5.1. One sees that, in addition to the SM Higgs boson found, one has heavy neutral (H^0,A^0), singly (H^+) and doubly charged (H^{++}) scalar bosons, whose mass is controlled by χ and with a small splitting which should not be bigger than indicated on figure 5.4 if the model is to remain perturbative all the way up to the Planck scale.

The doubly–charged state comes just from the triplet, while all other heavy states come mainly from the triplet, but with a small admixture with the Standard Model Higgs boson, controlled by the ratio of VEVs $\alpha \equiv v_\Delta/v_H$. Note that the state A^0 is identified with the would-be triplet Nambu-Goldstone boson associated to spontaneous lepton number violation which becomes massless as $v_\Delta \to 0$. All of these scalar states have a nearly common mass, with a small splitting, both indicated in figure 5.5. This follows from the consistency requirements such as perturbativity studied in the previous section and displayed in figure 5.4. Hence, altogether, once the lightest Higgs boson discovered at the LHC is accommodated, one can describe fairly well the scalar sector with just three parameters (α, $\lambda'_{H\Delta}$ and χ). This is in sharp contrast with other extended electroweak breaking potentials, such as those of supersymmetric models.

For example the singly and doubly–charged members of the triplet have been searched for at accelerators such as LEP as well as hadron colliders [1, 2, 24, 25]. If sufficiently light, say below 400 GeV or so, the H^{++} will be copiously produced at the LHC, which could enable interesting measurements of its branching ratios of the various leptonic decay channels [26], as well as the leading WW decay branch [27, 28]. The former are determined by the triplet Yukawa couplings. These determine also the pattern of lepton flavour violation decays. Given the small neutrino masses indicated by experiment [29–32] and our assumption that the scalars are in the TeV region, these Yukawa couplings are expected to be too small to cause detectable signals.

The near degeneracy of the heavy scalars implies that, once the constraints on the charged Higgs bosons are imposed, by choosing a suitably large χ, the neutral ones, including the would–be Majoron, will also have escaped detection at LEP. Moreover, the charged components in the Higgs triplet model provide a potential enhancement of the $H \to \gamma\gamma$ decay branching [10, 33, 34] ratio,

which can be probed at the LHC. Last but not least, the triplet introduces changes to the S, T, U oblique parameters.[3]

All of the above phenomena should be studied within parameter regions where the electroweak symmetry breaking is consistent and, as we saw in figure 5.3, consistency implies strong restrictions on quartic parameter values. Although the relevant restrictions apply mainly to the quartic scalar interactions, and in principle do not translate directly into stringent constraints upon the Higgs boson masses, one has an important restriction on the splitting between the masses of the heavy states, such as the singly and doubly charged scalar bosons, illustrated by the funnel region depicted in figure 5.4. Performing a dedicated phenomenological study of the scalar sector lies outside the scope of this paper but we hope to have given a helpful guideline.

One last word regarding the naturalness of the scalar potential in the presence of the cubic mass parameter. This follows from the principle that its removal would lead to a theory of enhanced symmetry, in which neutrinos would be massless and lepton number would be conserved. In any case, a dynamical completion of this theory in which the cubic term is replaced by a quartic one is possible and has in fact been suggested long ago [5]. This would imply the presence of a mainly singlet Nambu-Goldstone boson with implications for Higgs decays such as invisibly decaying Higgs bosons [35–37] whose detailed analysis is more general than the one recently given in reference [16] and lies outside the scope of the present paper.

5.6 Final remarks

In this paper, we have considered the consistency of the type-II seesaw model symmetry breaking. We included under consistency both the requirements of boundedness from below as well as perturbativity up to some scale. We found that the bounded-from-below conditions for the scalar potential in use in the literature are not correct. For definiteness and simplicity we focused on the case of explicit violation of lepton number. We discussed some scenarios where the correction we have found can be significant. Moreover we have sketched the typical scalar boson profile expected by consistency of the vacuum. Before closing we note that, the restrictions discussed in this paper do not depend on the hypercharge of the scalar triplet Δ, hence the same set of conditions also applies for any other model which extends the scalar sector of the Standard Model with an $SU(2)_L$ triplet.

[3] In practice these are expected to be small, just like the changes in the ρ parameter discussed previously.

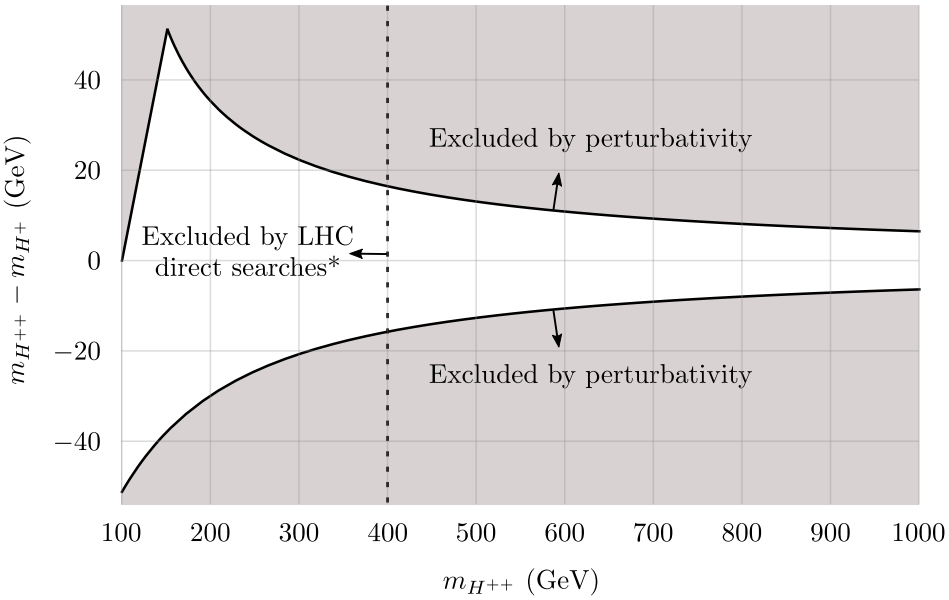

Figure 5.4: The coupling $\lambda'_{H\Delta}$ must be roughly between -0.85 and 0.85 if all quartic couplings are to remain small up to m_{Planck} ($|\lambda_i| < \sqrt{4\pi}$). This perturbativity requirement strongly constrains the mass splitting of the triplet components, particularly if one considers the LHC lower bound $m_{H^{++}} \sim 400$ GeV from direct searches of H^{++} decaying in to leptons [1, 2] (*assuming 100% branching fractions). This plot also assumes that $m_{H^+} > 100$ GeV.

Acknowledgments

This work supported by the Spanish grants FPA2014-58183-P, Multidark CSD2009-00064 and SEV-2014-0398 (MINECO), and PROMETEOII/2014/084 (Generalitat Valenciana).

5.A Appendix A: Conversion between different notations

Given that different notations are used in the literature to write down the different terms in the scalar potential of the model, we provide here table 5.2 to facilitate comparisons.

Source	μ_H^2	μ_Δ^2	$m_{H\Delta}$	λ_H	$\lambda_{H\Delta}$	$\lambda'_{H\Delta}$	λ_Δ	λ'_Δ
[17]	m_H^2	M_Δ^2	$\frac{1}{2}\mu$	$\frac{1}{2}\lambda$	λ_1	λ_4	$2\lambda_2$	$2\lambda_3$
[10]*	$-m^2$	M^2	$\sqrt{2}\mu$	$2\lambda_1$	$\lambda_4-\lambda_5$	$2\lambda_5$	$2\lambda_2+2\lambda_3$	$-2\lambda_3$
[22]*	$-m_\phi^2$	M_ξ^2	$-(\lambda_H M_\xi)^*$	$\frac{1}{2}\lambda$	$\lambda_\phi-\frac{1}{2}\lambda_T$	λ_T	$4\lambda_C+\frac{1}{2}\lambda_\xi$	$-4\lambda_C$
[11]*	$-m_\Phi^2$	M_Δ^2	$\sqrt{2}\Lambda_6$	λ	$\lambda_4+\lambda_5$	$-2\lambda_5$	$\lambda_1+\lambda_2$	$-\lambda_2$

Table 5.2: Translation between the notation used in this paper and the one used by other authors. Note that in the cases marked with an asterisk it is also necessary to flip the sign of the doubly charged component of the triplet.

5.B Appendix B: Representative triplet seesaw scalar mass spectrum

In order to grasp in a visual manner the scalar spectrum of the model (see table 5.1) as well as the effect on the degeneracy of the three new scalars of having $\lambda'_{H\Delta}$ constrained to be roughly between -0.85 and 0.85, we present here figure 5.5.

5.B Appendix B: Representative triplet seesaw scalar mass spectrum

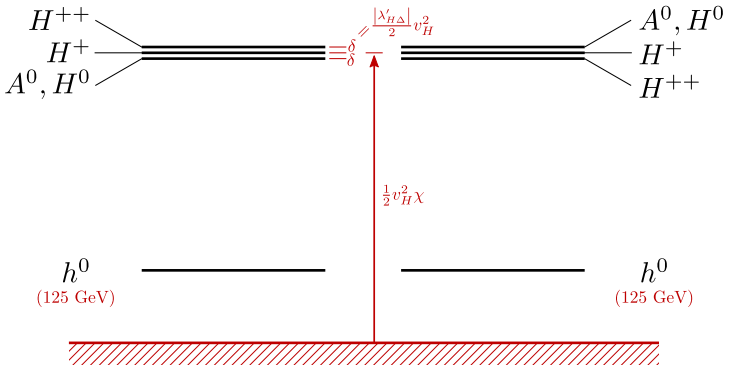

Figure 5.5: Schematic view of the scalar boson mass spectrum in the triplet seesaw model. The heavy scalars are nearly degenerate. The ordering of the heavy scalar masses depends on the sign of $\lambda'_{H\Delta}$ as shown in table 5.1. Recall that χ refers to the ratio $m_{H\Delta}/v_\Delta$.

BIBLIOGRAPHY

[1] G. Aad et al. (ATLAS), *Search for doubly-charged Higgs bosons in like-sign dilepton final states at $\sqrt{s} = 7$ TeV with the ATLAS detector*, Eur. Phys. J. **C72** (2012) 2244, arXiv:1210.5070 [hep-ex].

[2] S. Chatrchyan et al. (CMS), *A search for a doubly-charged Higgs boson in pp collisions at $\sqrt{s} = 7$ TeV*, Eur. Phys. J. **C72** (2012) 2189, arXiv:1207.2666 [hep-ex].

[3] S. Weinberg, *Varieties of Baryon and Lepton Nonconservation*, Phys. Rev. **D22** (1980) 1694.

[4] J. Schechter and J. Valle, *Neutrino Masses in SU(2) x U(1) Theories*, Phys.Rev. **D22** (1980) 2227.

[5] J. Schechter and J. Valle, *Neutrino Decay and Spontaneous Violation of Lepton Number*, Phys.Rev. **D25** (1982) 774.

[6] M. Sher, *Electroweak Higgs Potentials and Vacuum Stability*, Phys. Rept. **179** (1989) 273–418.

[7] S. Alekhin, A. Djouadi and S. Moch, *The top quark and Higgs boson masses and the stability of the electroweak vacuum*, Phys.Lett. **B716** (2012) 214–219, arXiv:1207.0980 [hep-ph].

[8] I. Gogoladze, N. Okada and Q. Shafi, *Higgs boson mass bounds in a type II seesaw model with triplet scalars*, Phys. Rev. **D78** (2008) 085005, arXiv:0802.3257 [hep-ph].

[9] W. Chao, M. Gonderinger and M. J. Ramsey-Musolf, *Higgs vacuum stability, neutrino mass, and dark matter*, Phys. Rev. **D86** (2012) 113017, arXiv:1210.0491 [hep-ph].

[10] E. J. Chun, H. M. Lee and P. Sharma, *Vacuum stability, perturbativity, EWPD and Higgs-to-diphoton rate in type II seesaw models*, JHEP **11** (2012) 106, arXiv:1209.1303 [hep-ph].

[11] P. S. Bhupal Dev, D. K. Ghosh, N. Okada and I. Saha, *125 GeV Higgs Boson and the Type-II Seesaw Model*, JHEP **03** (2013) 150, [Erratum: JHEP05,049(2013)], arXiv:1301.3453 [hep-ph].

[12] O. Lebedev, *On stability of the electroweak vacuum and the Higgs portal*, Eur. Phys. J. **C72** (2012) 2058, arXiv:1203.0156 [hep-ph].

[13] J. Elias-Miro et al., *Stabilization of the electroweak vacuum by a scalar threshold effect*, JHEP **06** (2012) 031, arXiv:1203.0237 [hep-ph].

[14] A. Falkowski, C. Gross and O. Lebedev, *A second Higgs from the Higgs portal*, JHEP **05** (2015) 057, arXiv:1502.01361 [hep-ph].

[15] R. Costa, A. P. Morais, M. O. P. Sampaio and R. Santos, *Two-loop stability of a complex singlet extended Standard Model*, Phys. Rev. **D92** (2015) 2 025024, arXiv:1411.4048 [hep-ph].

[16] C. Bonilla, R. M. Fonseca and J. W. F. Valle, *Vacuum stability with spontaneous violation of lepton number* (2015), arXiv:1506.04031 [hep-ph].

[17] A. Arhrib et al., *The Higgs potential in the type II seesaw model*, Phys.Rev. **D84** (2011) 095005, arXiv:1105.1925 [hep-ph].

[18] K. Olive et al. (Particle Data Group), *Review of Particle Physics*, Chin.Phys. **C38** (2014) 090001.

[19] M. E. Machacek and M. T. Vaughn, *Two loop renormalization group equations in a general quantum field theory. 1. Wave function renormalization*, Nucl. Phys. **B222** (1983) 83.

[20] M. E. Machacek and M. T. Vaughn, *Two loop renormalization group equations in a general quantum field theory. 2. Yukawa couplings*, Nucl. Phys. **B236** (1984) 221.

[21] M. E. Machacek and M. T. Vaughn, *Two loop renormalization group equations in a general quantum field theory. 3. Scalar quartic couplings*, Nucl. Phys. **B249** (1985) 70.

[22] W. Chao and H. Zhang, *One-loop renormalization group equations of the neutrino mass matrix in the triplet seesaw model*, Phys. Rev. **D75** (2007) 033003, arXiv:hep-ph/0611323 [hep-ph].

[23] M. A. Schmidt, *Renormalization group evolution in the type I+II seesaw model*, Phys. Rev. **D76** (2007) 073010, [Erratum: Phys. Rev.D85,099903(2012)], arXiv:0705.3841 [hep-ph].

[24] E. Accomando et al., *Workshop on CP Studies and Non-Standard Higgs Physics* (2006), arXiv:hep-ph/0608079 [hep-ph].

[25] A. G. Akeroyd and M. Aoki, *Single and pair production of doubly charged Higgs bosons at hadron colliders*, Phys. Rev. **D72** (2005) 035011, arXiv:hep-ph/0506176 [hep-ph].

[26] A. G. Akeroyd, M. Aoki and H. Sugiyama, *Probing Majorana Phases and Neutrino Mass Spectrum in the Higgs Triplet Model at the CERN LHC*, Phys. Rev. **D77** (2008) 075010, arXiv:0712.4019 [hep-ph].

[27] S. Kanemura, M. Kikuchi, H. Yokoya and K. Yagyu, *LHC Run-I constraint on the mass of doubly charged Higgs bosons in the same-sign diboson decay scenario*, PTEP **2015** (2015) 051B02, arXiv:1412.7603 [hep-ph].

[28] S. Kanemura, M. Kikuchi, K. Yagyu and H. Yokoya, *Bounds on the mass of doubly-charged Higgs bosons in the same-sign diboson decay scenario*, Phys. Rev. **D90** (2014) 11 115018, arXiv:1407.6547 [hep-ph].

[29] D. Forero, M. Tortola and J. Valle, *Neutrino oscillations refitted*, Phys.Rev. **D90** (2014) 9 093006, arXiv:1405.7540 [hep-ph].

[30] H. Nunokawa, S. J. Parke and J. W. Valle, *CP Violation and Neutrino Oscillations*, Prog.Part.Nucl.Phys. **60** (2008) 338–402, arXiv:0710.0554 [hep-ph].

[31] A. Barabash, *75 years of double beta decay: yesterday, today and tomorrow* (2011), arXiv:1101.4502 [nucl-ex].

[32] F. F. Deppisch, M. Hirsch and H. Pas, *Neutrinoless Double Beta Decay and Physics Beyond the Standard Model*, J. Phys. **G39** (2012) 124007, arXiv:1208.0727 [hep-ph].

[33] A. Arhrib et al., *Higgs boson decay into 2 photons in the type II Seesaw Model*, JHEP **04** (2012) 136, arXiv:1112.5453 [hep-ph].

[34] A. G. Akeroyd and S. Moretti, *Enhancement of H to gamma gamma from doubly charged scalars in the Higgs Triplet Model*, Phys. Rev. **D86** (2012) 035015, arXiv:1206.0535 [hep-ph].

[35] A. S. Joshipura and J. Valle, *Invisible Higgs decays and neutrino physics*, Nucl.Phys. **B397** (1993) 105–122.

[36] M. A. Diaz, M. A. Garcia-Jareno, D. A. Restrepo and J. W. F. Valle, *Neutrino mass and missing momentum Higgs boson signals*, Phys. Rev. **D58** (1998) 057702, arXiv:hep-ph/9712487 [hep-ph].

[37] M. A. Diaz, M. Garcia-Jareno, D. A. Restrepo and J. Valle, *Seesaw Majoron model of neutrino mass and novel signals in Higgs boson production at LEP*, Nucl.Phys. **B527** (1998) 44–60, arXiv:hep-ph/9803362 [hep-ph].

CHAPTER **6**

NEUTRINO MASS AND INVISIBLE HIGGS DECAYS AT THE LHC

Authors: Cesar Bonilla, Jorge C. Romao, Jose W.F. Valle.
Journal reference: Phys.Rev. D91 (2015) no.11, 113015.

Abstract

The discovery of the Higgs boson suggests that also neutrinos get their mass from spontaneous symmetry breaking. In the simplest ungauged lepton number scheme, the Standard Model (SM) Higgs has now two other partners: a massive CP-even, as well as the massless Nambu-Goldstone boson, called majoron. For weak-scale breaking of lepton number the invisible decays of the CP-even Higgs bosons to the majoron lead to potentially copious sources of events with large missing energy. Using LHC results we study how the constraints on invisible decays of the Higgs boson restrict the relevant parameters, substantially extending those previously derived from LEP and shedding light on spontaneous lepton number violation.

6.1 Introduction

The recently discovered Standard Model (SM) Higgs boson is most likely the first of a family. Indeed, after the historic Higgs discovery by the LHC experiments [2, 3] it is more than ever natural to imagine that the BEH mechanism [4–6] is also the one responsible for generating all masses in particle physics, including those of neutrinos [7] Extra Higgs scalars are also expected in order to account for the existing cosmological puzzles, such as dark matter and inflation, as well as to realize natural schemes of symmetry breaking, such as those based on supersymmetry.

Here we focus on neutrino masses. These are expected to arise from the exchange of some heavy messenger states which, depending on the underlying mechanism, need not be too heavy [8, 9]. If lepton number is broken through a $SU(3)_C \otimes SU(2)_L \otimes U(1)_Y$singlet vacuum expectation value [10, 11] there is a physical pseudoscalar Nambu-Goldstone boson — the majoron. All majoron couplings to SM particles are very small except, perhaps, those with the Higgs boson. As a result the CP even Higgs scalars have sizeable "invisible" decays, for example, [9, 12, 13]

$$h \to JJ, \tag{6.1}$$

where $J \equiv \sqrt{2}\,\mathrm{Im}\,\sigma$ denotes the associated pseudoscalar Goldstone boson — the majoron. The coexistence of such novel decays with the SM decay modes affects the Higgs mass bounds obtained [14–17], as well as provide new clues to the ongoing Higgs boson searches at the LHC.

Current LHC data suggest that the new particle discovered with a mass $m = 125$ GeV [2, 3] is indeed the long-awaited for Standard Model (SM) Higgs boson ($m_H = m$). This places restrictions on the extended Higgs sector providing neutrino masses, which we now analyse. We find that, despite the data accumulated so far at the LHC, the possibility of having an invisibly decaying Higgs boson is not too tightly constrained. Experimental searches have been mainly motivated by dark matter models where the Higgs might decay into the dark matter candidate, say χ, if its mass is $m_\chi < \frac{m_H}{2}$, such as supersymmetric models with R-parity conservation. However, invisible Higgs boson decays appear most naturally in low-scale models of neutrino mass generation. In these models neutrino masses arise from the spontaneous breaking of an additional $U(1)$ global symmetry associated to lepton number in the $SU(3)_C \otimes SU(2)_L \otimes U(1)_Y$theory. This symmetry is broken when a lepton-number-carrying scalar singlet σ gets a non-zero vacuum expectation value (vev), i.e. $\langle\sigma\rangle = v_1$.

There are many genuine low-scale neutrino mass scenarios of this type [8], such as inverse [18, 19] or linear [20–22] seesaw schemes. For simplicity, however, one may take the simplest $SU(3)_C \otimes SU(2)_L \otimes U(1)_Y$extension of neu-

trino mass generation, namely the type-I seesaw mechanism [23–27]. In this case in order to account for the small neutrino masses one must assume very small Dirac-type Yukawa couplings. The important consequence of spontaneous breaking of lepton number is the appearance of a physical Goldstone boson [10, 11], and the decays in Eq. (6.1). The scalar sector, in the simplest scenario, contains only one $SU(2)$ scalar doublet ϕ and a singlet σ, called 12-model in [11]. Hence there are three physical spin zero states, the two massive CP-even scalars H_1 and H_2 and one massless pseudo-scalar, the majoron J. Assuming the ordering $m_{H_1} < m_{H_2}$ the most interesting case is when $m_{H_2} = 125$ GeV. In this letter we focus on the possibility that the Higgs H_2 is the one reported by the LHC[1], i.e. $m_{H_2} = 125\,\text{GeV}$, and that in general the CP-even scalars can decay into majorons as follows,

$$H_i \to JJ \quad \text{and} \quad H_2 \to 2H_1 \to 4J \quad \left(\text{when} \quad m_{H_1} < \frac{m_{H_2}}{2}\right), \tag{6.2}$$

We note that there are strong constraints on invisible decays of a scalar with mass below $\sim 115\,\text{GeV}$ coming from the searches carried out by LEP [16]. In the next section we describe the main features of the symmetry breaking sector of the 12-model. We present our results in section III, and we discuss how the main features of this simplest model can also be present in other schemes with additional experimental signatures in section IV. We conclude in section V.

6.2 Symmetry breaking in the 12-model

The simplest way to model spontaneous lepton number violation contains, in addition to the usual SM Higgs doublet ϕ,

$$\phi = \begin{bmatrix} \phi^0 \\ \phi^- \end{bmatrix} \tag{6.3}$$

a complex lepton-number-carrying scalar singlet σ that acquires a non-zero vev $\langle\sigma\rangle$ that breaks the global $U(1)_L$ symmetry [10,11]. This scalar gives Majorana mass to right-handed neutrinos, while ϕ couples to SM fermions. This structure defines the simplest type-I seesaw scheme with spontaneous symmetry breaking. Many other scenarios sharing the same symmetry breaking sector can be envisaged though, for definiteness, we assume the simplest type-I seesaw.

[1]The latest results from LHC for the Higgs boson mass are 125.36 ± 0.37 GeV from ATLAS [28] and $125.02 + 0.26 - 0.27\,(\text{stat}) + 0.14 - 0.15\,(\text{syst})$ GeV from CMS [29].

6.2.1 The scalar potential

The scalar potential is given by [9, 12, 13]

$$V = \mu_1^2 \sigma^\dagger \sigma + \mu_2^2 \phi^\dagger \phi + \lambda_1 \left(\sigma^\dagger \sigma\right)^2 + \lambda_2 \left(\phi^\dagger \phi\right)^2 + \lambda_{12} \left(\sigma^\dagger \sigma\right) \left(\phi^\dagger \phi\right) \tag{6.4}$$

The singlet σ and the neutral component of the doublet ϕ acquire vacuum expectation values v_1 and v_2, respectively. Therefore we shift the fields as

$$\begin{aligned} \sigma =& \frac{v_1}{\sqrt{2}} + \frac{R_1 + i\, I_1}{\sqrt{2}} \\ \phi^0 =& \frac{v_2}{\sqrt{2}} + \frac{R_2 + i\, I_2}{\sqrt{2}} \end{aligned} \tag{6.5}$$

Solving the minimization equations we can obtain μ_1^2 and μ_2^2 as functions of the vevs, in the usual way,

$$\begin{aligned} \mu_1^2 =& -\lambda_1 v_1^2 - \frac{1}{2}\lambda_{12} v_2^2 \\ \mu_2^2 =& -\lambda_2 v_2^2 - \frac{1}{2}\lambda_{12} v_1^2 \end{aligned} \tag{6.6}$$

6.2.2 Neutral Higgs mass matrices

Evaluating the second derivatives of the scalar potential at the minimum one finds, in the basis (R_1, R_2) and (I_1, I_2), the CP-even and CP-odd mass matrices, M_R^2 and M_I^2 read

$$M_R^2 = \begin{bmatrix} 2\lambda_1 v_1^2 & \lambda_{12} v_1 v_2 \\ \lambda_{12} v_1 v_2 & 2\lambda_2 v_2^2 \end{bmatrix}, \quad M_I^2 = \begin{bmatrix} 0 & 0 \\ 0 & 0 \end{bmatrix} \tag{6.7}$$

As expected, the CP-odd mass matrix has two zero eigenvalues. One corresponds to the would-be Goldstone boson which becomes the longitudinal component of the Z boson after the BEH mechanism. The other is the physical Goldstone boson resulting from the breaking of the global symmetry, namely the majoron J. Hence we have,

$$J = I_1, \quad G^0 = I_2\ . \tag{6.8}$$

For the CP-even Higgs bosons we define the two mass eigenstates H_i through the rotation matrix O_R as,

$$\begin{bmatrix} H_1 \\ H_2 \end{bmatrix} = O_R \begin{bmatrix} R_1 \\ R_2 \end{bmatrix} \equiv \begin{bmatrix} \cos\alpha & \sin\alpha \\ -\sin\alpha & \cos\alpha \end{bmatrix} \begin{bmatrix} R_1 \\ R_2 \end{bmatrix}, \tag{6.9}$$

satisfying

$$O_R\, M_R^2\, O_R^T = \mathrm{diag}(m_{H_1}^2, m_{H_2}^2)\,. \tag{6.10}$$

One can use Eq. (6.10) and Eq. (7.6) in order to solve for the parameters $\lambda_1, \lambda_2, \lambda_{12}$ in terms of the two physical masses and the mixing angle α. We get

$$\begin{aligned}
\lambda_1 =& \frac{m_{H_1}^2 \cos^2\alpha + m_{H_2}^2 \sin^2\alpha}{2v_1^2}\,,\\
\lambda_2 =& \frac{m_{H_1}^2 \sin^2\alpha + m_{H_2}^2 \cos^2\alpha}{2v_2^2}\,,\\
\lambda_{12} =& \frac{\sin\alpha\cos\alpha\ (m_{H_1}^2 - m_{H_2}^2)}{v_1 v_2}\,.
\end{aligned} \tag{6.11}$$

6.2.3 Higgs couplings and decay widths

The couplings of the Higgs boson to Standard Model particles get modified according to the substitution rule

$$h \to \sin\alpha\, H_1 + \cos\alpha\, H_2\,. \tag{6.12}$$

In addition to these, there are two new important couplings coming from the extended Higgs sector, namely $H_2H_1H_1$ and H_iJJ. The former is given, with our conventions[2], by

$$\begin{aligned}
g_{H_2H_1H_1} &= 2v\Big[3\lambda_2 \cos\alpha \sin\alpha^2 - 3\lambda_1 \cos\alpha^2 \sin\alpha \cot\beta\\
&- \frac{\lambda_{12}}{8}\csc\beta(\sin(\alpha-\beta) - 3\sin(3\alpha+\beta))\Big]\,,
\end{aligned} \tag{6.13}$$

or in terms of the masses,

$$\begin{aligned}
g_{H_2H_1H_1} &= \frac{1}{2v_1v_2}(2m_{H_1}^2 + m_{H_2}^2)\sin 2\alpha\,(\sin\alpha v_1 - \cos\alpha v_2)\\
&= \frac{\tan\beta}{2v}(2m_{H_1}^2 + m_{H_2}^2)\sin 2\alpha\,(\cot\beta\sin\alpha - \cos\alpha)\,,
\end{aligned}$$

while the couplings H_iJJ are given by

$$g_{H_iJJ} = \frac{\tan\beta}{v}\, m_{H_i}^2\, O_{Ri1}\,, \tag{6.14}$$

where we have defined

$$v = v_2 = \frac{2m_W}{g}, \quad \tan\beta = \frac{v_2}{v_1}\,, \tag{6.15}$$

[2]Our Higgs trilinear self-coupling parameters are obtained after minimizing the Higgs potential. In order to get the Feynman rules we have to multiply by $-i$.

are responsible for the invisible Higgs decays. The decay widths to SM states are obtained from those of the SM with the help of the substitution rule in Eq. (6.12). On the other hand the new widths leading to the invisible Higgs boson decays are

$$H_2 \to H_1 H_1 \quad \text{and} \quad H_i \to JJ\,, \tag{6.16}$$

are given by

$$\Gamma\left(H_2 \to H_1 H_1\right) = \frac{g^2_{H_2 H_1 H_1}}{32\pi m_{H_2}} \left(1 - \frac{4m^2_{H_1}}{m^2_{H_2}}\right)^{1/2} \tag{6.17}$$

and

$$\Gamma(H_i \to JJ) = \frac{1}{32\pi} \frac{g^2_{H_i JJ}}{m_{H_i}}\,. \tag{6.18}$$

6.3 Results

We now discuss the constraints on invisibly decaying Higgs bosons which follow from searches performed at LEP as well as LHC. We focus on the case where the Higgs H_2 is the one reported by the LHC, i.e. $m_{H_2} = 125\,\text{GeV}$, while $m_{H_1} < m_{H_2}$. Both states may in principle have SM-like as well as invisible decays to majorons as given in Eq. (6.2).

6.3.1 Parameter sampling procedure

In order to cover the possibility of a Higgs boson with mass below 125 GeV, we generate points in parameter space taking $m_{H_2} = 125$ GeV and $15 < m_{H_1} < 115$ GeV. In our simple model, the only remaining parameters are the vev v_1 characterizing the spontaneous violation of lepton number and the mixing angle α, which we take as,

$$v_1 \in [500, 1500]\ \text{GeV}, \quad \alpha \in [0, \pi]\,. \tag{6.19}$$

However, as the results do not depend very much on the value of v_1 in that interval, we will use $v_1 = 1000$ GeV in most of the results presented.

6.3.2 Theoretical constraints

The points generated must fulfill several constraints. First come the consistency requirements for the scalar potential, namely that it must be bounded from below and that perturbative unitarity be respected. The unbounded from below constraint reads [30]

$$\lambda_1 > 0, \quad \lambda_2 > 0, \quad \lambda_{12} + 2\sqrt{\lambda_1 \lambda_2} > 0 \tag{6.20}$$

while for the unitarity we just take a simplified approach requiring that all couplings are less than $\sqrt{4\pi}$. Certainly this can be refined [31], though Eq. (6.20) is sufficient for our current purposes.

6.3.3 Constraints from invisible decay searches

The second type of constraints comes from the LEP collider. Searches for invisibly decaying Higgs bosons using the LEP-II data have been performed by the LEP collaborations. In our setup these constraints apply to the lightest Higgs boson, H_1. For the channel $e^+e^- \to ZH \to Zb\bar{b}$ the final state is expressed in terms of the SM HZ cross section through

$$\begin{aligned}\sigma_{hZ\to b\bar{b}Z} =& \sigma_{HZ}^{SM} \times R_{HZ} \times BR(H \to b\bar{b}) \\ =& \sigma_{HZ}^{SM} \times C^2_{Z(H\to b\bar{b})}\,,\end{aligned} \tag{6.21}$$

where R_{HZ} is the suppression factor related to the coupling of the Higgs boson to the gauge boson Z (i.e. $R_{hZ}^{SM} = 1$ and for the model we have $R_{H_1Z} = \sin^2\alpha$; note also that $C^2_{Z(H\to b\bar{b})}$ is independent of m_H). Here $BR(H \to b\bar{b})$ is the branching ratio of the channel $H \to b\bar{b}$ which in the model is modified with respect to the SM by the presence of the invisible Higgs boson decay into the Goldstone boson J associated to the breaking of the global $\mathrm{U(1)_L}$ symmetry.

As illustration we consider the results from the DELPHI collaboration, Ref. [16], where they give upper bounds for the coefficients $C^2_{Z(H\to b\bar{b})}$ corresponding to a lightest CP-even Higgs boson mass in the range from 15 GeV up to 100 GeV. From this one determines the regions of $m_{H_1} - \sin\alpha$ which are currently allowed by the LEP-II searches. The results are shown in Fig. 6.1. The region excluded by the LEP results corresponds to the blue regions in this figure. One sees that the LEP results do not exclude much of the parameter space for a light Higgs boson (below 115 GeV) as long as its coupling to the Z boson is reduced with respect to that of the SM. However, in this simple model, if we take into account the discovery at the LHC of a Higgs boson at 125 GeV the parameter space is further restricted. In fact, in this picture the heavier Higgs boson couples to the Z boson with a reduced strength $\cos\alpha$. The restriction on $\cos\alpha$ depends on the upper limit on the invisible decay of the Higgs boson. Here we consider three values, from 25% up to 75%, which is the current upper bound given by the ATLAS collaboration [32] for the branching ratio to invisible particle decay modes. This will be improved in next run of the LHC, but current results indicate that there is still room for such decays, as shown in Fig. 6.1. Note that the kink in the plot is associated to the decay in Eq. (6.17).

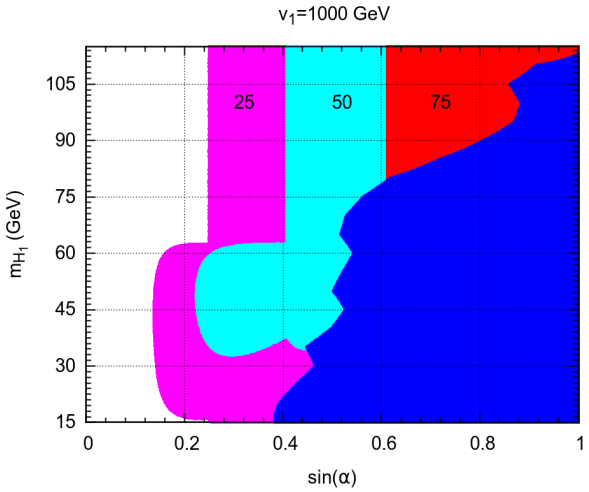

Figure 6.1: m_{H_1} versus $\sin\alpha$ in the model for $v_1 = 1000$ GeV. The blue region is the region excluded by LEP results. The red, cyan and magenta regions correspond to an invisible BR excluded at 75%, 50% and 25% respectively.

6.3.4 Constraints from visible decay searches

We just saw the implementation of the LHC upper limit on the invisible decay of the Higgs boson. However we must also enforce the limits coming from the other, well-measured, SM channels. These are normally expressed, for a SM final state f, in terms of the signal strength parameter,

$$\mu_f = \frac{\sigma^{\rm NP}(pp \to h)}{\sigma^{\rm SM}(pp \to h)} \frac{\Gamma^{\rm NP}[h \to f]}{\Gamma^{\rm SM}[h \to f]} \frac{\Gamma^{\rm SM}[h \to \text{all}]}{\Gamma^{\rm NP}[h \to \text{all}]}\,, \tag{6.22}$$

where σ is the cross section for Higgs production, $\Gamma[h \to f]$ is the decay width into the final state f, the labels NP and SM stand for New Physics and Standard Model respectively, and $\Gamma[h \to \text{all}]$ is the total width of the Higgs boson. These can be compared with those given by the experimental collaborations. We reproduce here the compilation performed in Ref. [1] for the most recent results of the ATLAS [33] and CMS [34] collaborations. One sees that the current limits, although compatible at $1-\sigma$, still have quite large errors.

Since the number of parameters is very small in our model, it suffices to take as a constraint the limits on μ_{VV} ($V = W, Z$) in order to illustrate the situation. Instead of taking each experiment individually, we just note that, in a qualitative sense, the LHC results indicate that $\mu_{VV} \sim 1$ to within 20%, that is,

$$0.8 \leq \mu_{VV} \leq 1.2 \tag{6.23}$$

channel	ATLAS	CMS
$\mu_{\gamma\gamma}$	1.17 ± 0.27	$1.14^{+0.26}_{-0.23}$
μ_{WW}	$1.00^{+0.32}_{-0.29}$	0.83 ± 0.21
μ_{ZZ}	$1.44^{+0.40}_{-0.35}$	1.00 ± 0.29
$\mu_{\tau^+\tau^-}$	$1.4^{+0.5}_{-0.4}$	0.91 ± 0.27
$\mu_{b\bar{b}}$	$0.2^{+0.7}_{-0.6}$	0.93 ± 0.49

Table 6.1: Current experimental results of ATLAS and CMS, taken from the compilation performed in Ref. [1].

The results are shown in Fig. 8.1. On the left panel we consider $v_1 = 1000$ GeV while on the right panel we let it vary in the range $v_1 \in [500, 1000]$ GeV. As before, the blue region is the LEP exclusion region, while the red region is

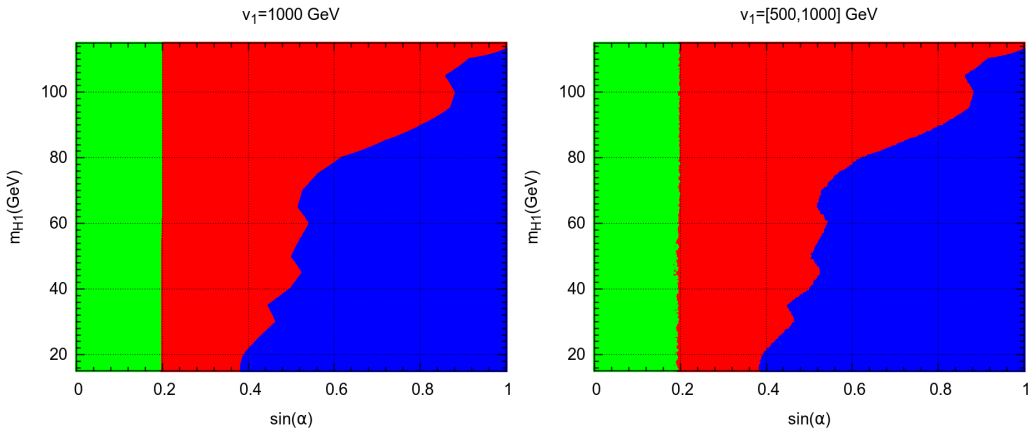

Figure 6.2: m_{H_1} versus $\sin\alpha$ in the model for $v_1 = 1000$ GeV (left panel) and $v_1 \in [500, 1000]$ GeV (right panel). The blue region is the region excluded by LEP results. The red corresponds to the points excluded by the LHC as discussed in the text and the points in green pass all constraints.

excluded by the LHC limit on μ_{VV}. The green region is the region still allowed by the current LHC data. If we compare the left panel of Fig. 8.1 with Fig. 6.1 that corresponds to the same value of v_1, we see that the limit imposed by μ_{VV} implies, in this model, an upper bound on the invisible Higgs decay of around 20%, therefore more stringent that the one presented by the ATLAS collaboration [32]. This is due to the fact that the number of independent parameters is very much reduced in this model, and the cut on μ_{VV} implies a cut on α. To show this, we plot in Fig. 6.3, μ_{ZZ} against BR($H_i \to$ Inv). The color code is as in Fig. 8.1. On the left panel we see that the invisible

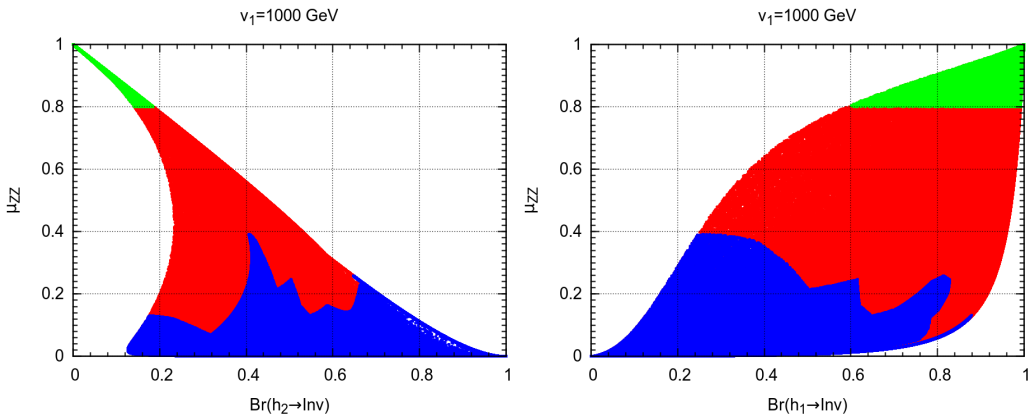

Figure 6.3: Left panel: μ_{VV} versus BR($H_2 \to$ Inv). Right panel: the same for BR($H_1 \to$ Inv). The color code is as in Fig. 8.1.

branching ratio of the 125 GeV Higgs boson, H_2 in our model, could be as large as one but this is ruled out by LEP. Furthermore the LHC limit on μ_{ZZ}, reduces the allowed space, and we obtain an upper bound on the invisible decay, for this simple model, of around 20% as we explained before. The corresponding plot for the lightest Higgs boson is shown on the right panel. We see that an invisible branching ratio of 100% is compatible with the LHC results for this model. The correlation between the invisible branching ratios of the two Higgs bosons is shown on the left panel of Fig. 6.4 with the same convention for the colors. Finally, on the right panel we plot m_{H_1} as function of BR($H_1 \to$ Inv), with the same conventions. We see a strong anti-correlation among these panels, due to the simplicity of the model.

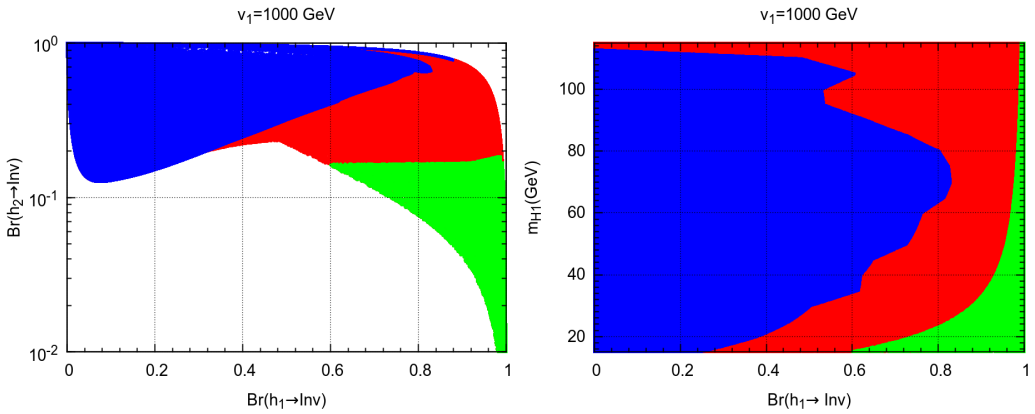

Figure 6.4: Left panel: BR($H_2 \to$ Inv) as a function of BR($H_1 \to$ Inv). Right panel: m_{H_1} as a function of BR($H_1 \to$ Inv). The color code is as in Fig. 8.1.

In order to better illustrate this anti-correlation we plot in Fig. 6.5, μ_{ZZ}

as a function of $\mu_{\gamma\gamma}$. The straight line reflects the fact the there is essentially

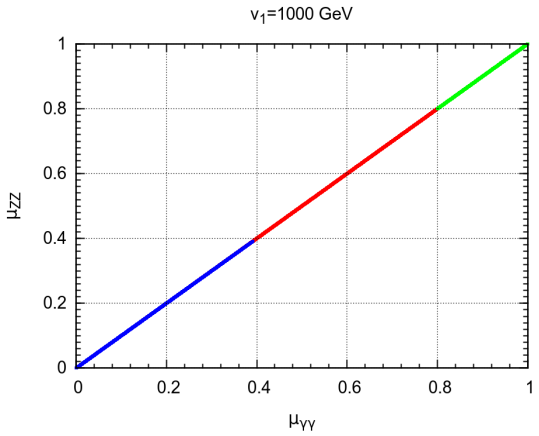

Figure 6.5: Correlation between μ_{ZZ} and $\mu_{\gamma\gamma}$. The color code is as in Fig. 8.1.

only one parameter left, the angle α, after we fix the two Higgs boson masses. We also notice that in the model, the μ_f for the channels where the final state f exists in the SM can only be less then one. This results from the reduced coupling of the SM-like Higgs boson.

More general models with a richer Higgs boson sector naturally emerge, for example, in neutrino mass schemes with more than one scalar doublet [9,13,35] or models with a doublet and triplet [36]. In this case, in addition to the scalars considered here there are also charged Higgs bosons. Similar features hold in models where the origin of neutrino mass is supersymmetric, due to spontaneous breaking of R-parity [37,38].

6.4 Discussion

In this paper we have given a simple "generic" example illustrating how the physics associated to the Higgs boson may get modified within extensions of the minimal $SU(3)_C \otimes SU(2)_L \otimes U(1)_Y$ theory with spontaneous lepton number violation at low-scale [7] [3]. So far we have considered the simplest scenario for spontaneous breaking of ungauged lepton number symmetry responsible for inducing the tiny neutrino masses. The latter involves the standard $SU(3)_C \otimes SU(2)_L \otimes U(1)_Y$ electroweak gauge structure, and hence gives rise to a physical Goldstone boson that provides an invisible Higgs decay channel. Such simple

[3] High-scale seesaw models may lead to sizeable lepton flavour violation rates coming from supersymmetric contributions [39]. However here we discard this possibility, since the sizeable invisible Higgs boson decay physics would be absent in that case.

scheme can be implemented in a variety of ways both at the tree level as well as within radiative schemes [8, 9].

Additional phenomenological signatures beyond the invisible Higgs decay channel in Eq. (6.1) include charged lepton flavour violation processes such as radiative muon and tau decays, e.g. $\mu \to e\gamma$, $\mu \to 3e$ as well as mu-e conversion in nuclei. The expected rates for such processes will depend on the details of the model considered. For this reason they have not been discussed explicitly in the present paper. For example $\mu \to e\gamma$ can be large in inverse seesaw schemes [40–42]. Likewise, mu-e conversion in nuclei is also enhanced [43]. Similar enhancement of lepton flavour violation processes exists for linear seesaw-type schemes [44]. Similar features arise within radiative models of neutrino mass generation, for example models of the Zee-Babu-type [45]. These models include also physical charged scalar bosons running in the neutrino mass loop, and their scalar potential is richer than we have considered above. Note that the charged scalar states present in such models also give a contribution to $H \to \gamma\gamma$ decays. Finally, there is a different class of charged lepton flavour violation processes involving majoron emission, for example $\mu \to eJ$. This possibility has been considered, for example, within supersymmetric models with spontaneous R parity violation [46–48].

6.5 Conclusions

Here we have considered the constraints implied by current data, including the Higgs discovery, on the extended electroweak symmetry breaking potential corresponding to the simplest neutrino mass schemes with spontaneous breaking of lepton number. There are two CP-even Higgs scalars that can decay to Standard Model states as well as invisibly to the majoron, the pseudoscalar Goldstone boson associated to lepton number violation. If lepton number symmetry breaks at the weak scale, the invisible modes can yield potentially large rates for missing energy events. Using current results from LEP and ATLAS/CMS at the LHC we have studied the constraints coming from SM searches as well as invisible decays, showing how, despite the large data sample, there is still room for improvement of invisible decay limits in the coming LHC run. Within our simple framework these limits provide a probe into the scale characterizing the violation of lepton number responsible for neutrino mass generation. Having set out the general strategy, other more complex symmetry breaking sectors may be analysed in a similar way such as, for example, those arising in models containing charged Higgs bosons.

Acknowledgments

Work supported by the Spanish grants FPA2011-22975 and Multidark CSD2009-00064 (MINECO), and PROMETEOII/2014/084 (Generalitat Valenciana). J.C.R. is also support in part by the Portuguese Fundação para a Ciência e Tecnologia (FCT) under contracts PEst-OE/FIS/UI0777/2013, CERN/FP/123580/2011 and EXPL/FIS-NUC/0460/2013.

BIBLIOGRAPHY

[1] D. Fontes, J. Romão and J. P. Silva, *$h \to Z\gamma$ in the complex two Higgs doublet model* (2014), arXiv:1408.2534 [hep-ph].

[2] G. Aad et al. (ATLAS Collaboration), *Observation of a new particle in the search for the Standard Model Higgs boson with the ATLAS detector at the LHC*, Phys.Lett. **B716** (2012) 1–29, arXiv:1207.7214 [hep-ex].

[3] S. Chatrchyan et al. (CMS Collaboration), *Observation of a new boson at a mass of 125 GeV with the CMS experiment at the LHC*, Phys.Lett. **B716** (2012) 30–61, arXiv:1207.7235 [hep-ex].

[4] F. Englert and R. Brout, *Broken Symmetry and the Mass of Gauge Vector Mesons*, Phys.Rev.Lett. **13** (1964) 321–323.

[5] P. W. Higgs, *Broken symmetries, massless particles and gauge fields*, Phys.Lett. **12** (1964) 132–133.

[6] P. W. Higgs, *Spontaneous Symmetry Breakdown without Massless Bosons*, Phys. Rev. **145** (1966) 1156–1163.

[7] J. W. Valle and J. C. Romao, *Neutrinos in high energy and astroparticle physics*, Wiley-VCH, Berlin, 1st edition edition (2015).

[8] S. M. Boucenna, S. Morisi and J. W. F. Valle, *The low-scale approach to neutrino masses*, Adv. High Energy Phys. **2014** (2014) 831598, arXiv:1404.3751 [hep-ph].

[9] A. S. Joshipura and J. Valle, *Invisible Higgs decays and neutrino physics*, Nucl.Phys. **B397** (1993) 105–122.

[10] Y. Chikashige, R. N. Mohapatra and R. Peccei, *Are There Real Goldstone Bosons Associated with Broken Lepton Number?*, Phys.Lett. **B98** (1981) 265.

[11] J. Schechter and J. Valle, *Neutrino Decay and Spontaneous Violation of Lepton Number*, Phys.Rev. **D25** (1982) 774.

[12] A. S. Joshipura and S. D. Rindani, *Majoron models and the Higgs search*, Phys.Rev.Lett. **69** (1992) 3269–3273.

[13] J. C. Romao, F. de Campos and J. W. F. Valle, *New Higgs signatures in supersymmetry with spontaneous broken R parity*, Phys. Lett. **B292** (1992) 329–336, arXiv:hep-ph/9207269 [hep-ph].

[14] F. De Campos, J. W. F. Valle, A. Lopez-Fernandez and J. C. Romao, *Updated limits on visibly and invisibly decaying Higgs bosons from LEP*, in *'94 electroweak interactions and unified theories. Proceedings, Leptonic Session of the 29th Rencontres de Moriond, Moriond Particle Physics Meeting, Meribel les Allues, France, March 12-19, 1994* (1994) pages 81–86, [,81(1994)], arXiv:hep-ph/9405382 [hep-ph], URL http://inspirehep.net/record/373630/files/arXiv:hep-ph_9405382.pdf.

[15] F. de Campos, O. J. P. Eboli, J. Rosiek and J. W. F. Valle, *Searching for invisibly decaying Higgs bosons at LEP-2*, Phys. Rev. **D55** (1997) 1316–1325, arXiv:hep-ph/9601269 [hep-ph].

[16] J. Abdallah et al. (DELPHI Collaboration), *Searches for neutral higgs bosons in extended models*, Eur.Phys.J. **C38** (2004) 1–28, arXiv:hep-ex/0410017 [hep-ex].

[17] J. Abdallah et al. (DELPHI), *Searches for invisibly decaying Higgs bosons with the DELPHI detector at LEP*, Eur. Phys. J. **C32** (2004) 475–492, arXiv:hep-ex/0401022 [hep-ex].

[18] R. Mohapatra and J. Valle, *Neutrino Mass and Baryon Number Nonconservation in Superstring Models*, Phys.Rev. **D34** (1986) 1642.

[19] M. Gonzalez-Garcia and J. Valle, *Fast Decaying Neutrinos and Observable Flavor Violation in a New Class of Majoron Models*, Phys.Lett. **B216** (1989) 360.

[20] E. K. Akhmedov, M. Lindner, E. Schnapka and J. Valle, *Left-right symmetry breaking in NJL approach*, Phys.Lett. **B368** (1996) 270–280, arXiv:hep-ph/9507275 [hep-ph].

[21] E. K. Akhmedov, M. Lindner, E. Schnapka and J. Valle, *Dynamical left-right symmetry breaking*, Phys.Rev. **D53** (1996) 2752–2780, arXiv:hep-ph/9509255 [hep-ph].

[22] M. Malinsky, J. Romao and J. Valle, *Novel supersymmetric SO(10) seesaw mechanism*, Phys.Rev.Lett. **95** (2005) 161801, arXiv:hep-ph/0506296 [hep-ph].

[23] M. Gell-Mann, P. Ramond and R. Slansky, *Complex Spinors and Unified Theories*, Conf.Proc. **C790927** (1979) 315–321, arXiv:1306.4669 [hep-th].

[24] T. Yanagida, *HORIZONTAL SYMMETRY AND MASSES OF NEUTRINOS*, Conf.Proc. **C7902131** (1979) 95–99.

[25] R. N. Mohapatra and G. Senjanovic, *Neutrino Mass and Spontaneous Parity Violation*, Phys.Rev.Lett. **44** (1980) 912.

[26] J. Schechter and J. Valle, *Neutrino Masses in SU(2) x U(1) Theories*, Phys.Rev. **D22** (1980) 2227.

[27] G. Lazarides, Q. Shafi and C. Wetterich, *Proton Lifetime and Fermion Masses in an SO(10) Model*, Nucl.Phys. **B181** (1981) 287–300.

[28] G. Aad et al. (ATLAS), *Measurement of the Higgs boson mass from the $H \to \gamma\gamma$ and $H \to ZZ^* \to 4\ell$ channels with the ATLAS detector using 25 fb^{-1} of pp collision data*, Phys.Rev. **D90** (2014) 5 052004, arXiv:1406.3827 [hep-ex].

[29] V. Khachatryan et al. (CMS), *Precise determination of the mass of the Higgs boson and tests of compatibility of its couplings with the standard model predictions using proton collisions at 7 and 8 TeV* (2014), arXiv:1412.8662 [hep-ex].

[30] K. Kannike, *Vacuum Stability Conditions From Copositivity Criteria*, Eur.Phys.J. **C72** (2012) 2093, arXiv:1205.3781 [hep-ph].

[31] A. Djouadi, *The Anatomy of electro-weak symmetry breaking. I: The Higgs boson in the standard model*, Phys. Rept. **457** (2008) 1–216, arXiv:hep-ph/0503172 [hep-ph].

[32] G. Aad et al. (ATLAS Collaboration), *Search for Invisible Decays of a Higgs Boson Produced in Association with a Z Boson in ATLAS*, Phys.Rev.Lett. **112** (2014) 201802, arXiv:1402.3244 [hep-ex].

[33] G. Aad et al. (ATLAS Collaboration), *Measurement of Higgs boson production in the diphoton decay channel in pp collisions at center-of-mass energies of 7 and 8 TeV with the ATLAS detector* (2014), arXiv:1408.7084 [hep-ex].

[34] V. Khachatryan et al. (CMS Collaboration), *Observation of the diphoton decay of the Higgs boson and measurement of its properties*, Eur.Phys.J. **C74** (2014) 10 3076, arXiv:1407.0558 [hep-ex].

[35] A. Lopez-Fernandez, J. Romao, F. de Campos and J. Valle, *Model independent Higgs boson mass limits at LEP*, Phys.Lett. **B312** (1993) 240–246, arXiv:hep-ph/9304255 [hep-ph].

[36] M. A. Diaz, M. Garcia-Jareno, D. A. Restrepo and J. Valle, *Seesaw Majoron model of neutrino mass and novel signals in Higgs boson production at LEP*, Nucl.Phys. **B527** (1998) 44–60, arXiv:hep-ph/9803362 [hep-ph].

[37] M. Hirsch, J. Romao, J. Valle and A. Villanova del Moral, *Invisible Higgs boson decays in spontaneously broken R-parity*, Phys.Rev. **D70** (2004) 073012, arXiv:hep-ph/0407269 [hep-ph].

[38] M. Hirsch, J. Romao, J. Valle and A. Villanova del Moral, *Production and decays of supersymmetric Higgs bosons in spontaneously broken R-parity*, Phys.Rev. **D73** (2006) 055007, arXiv:hep-ph/0512257 [hep-ph].

[39] S. Antusch, E. Arganda, M. J. Herrero and A. M. Teixeira, *Impact of theta(13) on lepton flavour violating processes within SUSY seesaw*, JHEP **11** (2006) 090, arXiv:hep-ph/0607263 [hep-ph].

[40] J. Bernabeu et al., *Lepton Flavor Nonconservation at High-Energies in a Superstring Inspired Standard Model*, Phys.Lett. **B187** (1987) 303.

[41] F. Deppisch and J. Valle, *Enhanced lepton flavor violation in the supersymmetric inverse seesaw model*, Phys.Rev. **D72** (2005) 036001, arXiv:hep-ph/0406040 [hep-ph].

[42] P. B. Dev and R. Mohapatra, *TeV Scale Inverse Seesaw in SO(10) and Leptonic Non-Unitarity Effects*, Phys.Rev. **D81** (2010) 013001, arXiv:0910.3924 [hep-ph].

[43] F. Deppisch, T. Kosmas and J. Valle, *Enhanced mu- - e- conversion in nuclei in the inverse seesaw model*, Nucl.Phys. **B752** (2006) 80–92, arXiv:hep-ph/0512360 [hep-ph].

[44] D. Forero, S. Morisi, M. Tortola and J. Valle, *Lepton flavor violation and non-unitary lepton mixing in low-scale type-I seesaw*, JHEP **1109** (2011) 142, arXiv:1107.6009 [hep-ph].

[45] D. Aristizabal Sierra and M. Hirsch, *Experimental tests for the Babu-Zee two-loop model of Majorana neutrino masses*, JHEP **0612** (2006) 052, arXiv:hep-ph/0609307 [hep-ph].

[46] A. Santamaria and J. W. F. Valle, *Supersymmetric Majoron Signatures and Solar Neutrino Oscillations*, Phys. Rev. Lett. **60** (1988) 397–400.

[47] J. C. Romao, N. Rius and J. W. F. Valle, *Supersymmetric signals in muon and τ decays*, Nucl. Phys. **B363** (1991) 369–384.

[48] M. Hirsch, A. Vicente, J. Meyer and W. Porod, *Majoron emission in muon and tau decays revisited*, Phys. Rev. D **79** (2009) 055023, URL http://link.aps.org/doi/10.1103/PhysRevD.79.055023.

CHAPTER **7**

ELECTROWEAK BREAKING AND NEUTRINO MASS: "INVISIBLE" HIGGS DECAYS AT THE LHC (TYPE II SEESAW)

Authors: Cesar Bonilla, Jorge C. Romao, Jose W.F. Valle.
Journal reference: New J.Phys. 18 (2016) no.3, 033033.

Abstract

Neutrino mass generation through the Higgs mechanism not only suggests the need to reconsider the physics of electroweak symmetry breaking from a new perspective, but also provides a new theoretically consistent and experimentally viable paradigm. We illustrate this by describing the main features of the electroweak symmetry breaking sector of the simplest type-II seesaw model with spontaneous breaking of lepton number. After reviewing the relevant "theoretical" and astrophysical restrictions on the Higgs sector, we perform an analysis of the sensitivities of Higgs boson searches at the ongoing ATLAS and CMS experiments at the LHC, including not only the new contributions to the decay channels present in the Standard Model (SM) but also genuinely non-SM Higgs boson decays, such as "invisible" Higgs boson decays to majorons. We find sensitivities that are likely to be reached at the upcoming Run of the experiments.

7.1 Introduction

The electroweak breaking sector is a fundamental ingredient of the Standard Model many of whose detailed properties remain open, even after the historic discovery of the Higgs boson [1, 2]. The electroweak breaking sector is subject to many restrictions following from direct experimental searches at colliders [3, 4], as well as global fits [5, 6] of precision observables [7–9]. Moreover, its properties are may also be restricted by theoretical consistency arguments, such as naturalness, perturbativity and stability [10]. The latter have long provided strong motivation for extensions of the Standard Model such as those based on the idea of supersymmetry.

Following the approach recently suggested in Refs. [11, 12] we propose to take seriously the hints from the neutrino mass generation scenario to the structure of the scalar sector. In particular, the most accepted scenario of neutrino mass generation associates the smallness of neutrino mass to their charge neutrality which suggests them to be of Majorana nature due to some, currently unknown, mechanism of lepton number violation . The latter requires an extension of the $SU(3)_C \otimes SU(2)_L \otimes U(1)_Y$ Higgs sector and hence the need to reconsider the physics of symmetry breaking from a new perspective. In broad terms this would provide an alternative to supersymmetry as paradigm of electroweak breaking. Amongst its other characteristic features is the presence of doubly charged scalar bosons, compressed mass spectra of heavy scalars dictated by stability and perturbativity and the presence of "invisible" decays of Higgs bosons to the Nambu-Goldstone boson associated to spontaneous lepton number violation and neutrino mass generation [13].

In this paper we study the invisible decays of the Higgs bosons in the context of a type-II seesaw majoron model [14] in which the neutrino mass is generated after spontaneous violation of lepton number at some low energy scale, $\Lambda_{\rm EW} \lesssim \Lambda \sim \mathcal{O}(\text{TeV})$ [15, 16] [1]. This scheme requires the presence of two lepton number–carrying scalar multiplets in the extended $SU(3)_C \otimes SU(2)_L \otimes U(1)_Y$ model, a singlet σ and a triplet Δ under SU(2) – this seesaw scheme was called "123"-seesaw model in [14] and here we take the "pure" version of this scheme, without right-handed neutrinos. The presence of the new scalars implies the existence of new contributions to "visible" SM Higgs decays, such as the $h \to \gamma\gamma$ decay channel, in addition to intrinsically new Higgs decay channels involving the emission of majorons, such as the "invisible" decays

[1] The idea of the Majoron was first proposed in [17] though in the framework of the Type I seesaw, not relevant for our current paper. On the other hand the triplet Majoron was suggested in [18] but has been ruled out since the first measurements of the invisible Z width by the LEP experiments. Regarding the idea of invisible Higgs decays was first given in Ref. [19], though the early scenarios have been ruled out.

of the CP-even scalar bosons. As a result, one can set upper limits on the invisible decay channel based on the available data which restrict the "visible" channels.

The plan of this paper is as follows. In the next section we describe the main features of the symmetry breaking sector of the "123" type II seesaw model. In section III we discuss the "theoretical" and astrophysical constraints relevant for the Higgs sector. Taking these into account, we study the sensitivities of Higgs boson searches at the LHC to Standard Model scalar boson decays in section IV. Section V addresses the non-SM Higgs decays of the model. Section VI summarizes our results and we conclude in section VII.

7.2 The type-II seesaw model

Our basic framework is the "123" seesaw scheme originally proposed in Ref. [14] whose Higgs sector contains, in addition to the $SU(3)_C \otimes SU(2)_L \otimes U(1)_Y$ scalar doublet Φ, two lepton-number-carrying scalars: a complex singlet σ and a triplet Δ. All these fields develop non-zero vacuum expectation values (vevs) leading to the breaking of the Standard Model (SM) gauge group as well as the global symmetry $U(1)_L$ associated to lepton number. The latter breaking accounts for generation of the small neutrino masses. Therefore, the scalar sector is given by

$$\Phi = \begin{bmatrix} \phi^0 \\ \phi^- \end{bmatrix} \quad \text{and} \quad \Delta = \begin{bmatrix} \Delta^0 & \frac{\Delta^+}{\sqrt{2}} \\ \frac{\Delta^+}{\sqrt{2}} & \Delta^{++} \end{bmatrix} \tag{7.1}$$

with $L = 0$ and $L = -2$, respectively, and the scalar field σ with lepton number $L = 2$. Below we will consider the required vev hierarchies in the model.

7.2.1 Yukawa Sector

Here we consider the simplest version of the seesaw scheme proposed in Ref. [14] in which no right-handed neutrinos are added, and only the $SU(3)_C \otimes SU(2)_L \otimes U(1)_Y$ electroweak breaking sector is extended so as to spontaneously break lepton number giving mass to neutrinos. Such "123" majoron–seesaw model is described by the $SU(3)_C \otimes SU(2)_L \otimes U(1)_Y \otimes \mathrm{U(1)_L}$ invariant Yukawa Lagrangian,

$$\mathcal{L}_Y = y^d_{ij} \overline{Q}_i u_{R_j} \Phi + y^u_{ij} \overline{Q}_i d_{R_j} \tilde{\Phi} + y^\ell_{ij} \overline{L_i} \ell_{R_j} \Phi + y^\nu_{ij} L_i^T C \Delta L_j + \mathrm{h.c.} \tag{7.2}$$

In this model the neutrino mass (see Fig. 7.1) is given by,

$$m_\nu = y^\nu \kappa v_1 \frac{v_2^2}{m_\Delta^2} \tag{7.3}$$

where v_1 and v_2 are the vevs of the singlet and the doublet, respectively. Here κ is a dimensionless parameter that describes the interaction amongst the three scalar fields (see below), and m_Δ is the mass of the scalar triplet Δ.

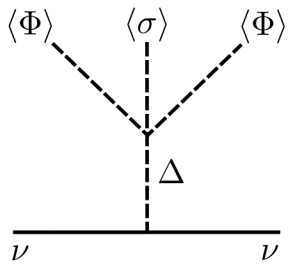

Figure 7.1: Diagram that generates non-zero neutrino mass in the model.

At this point we note that the smallness of neutrino mass i.e.

$$m_\nu \lesssim 1\ eV$$

may define interesting regions of the parameter space in any neutrino mass generation model where the new physics is expected to be hidden from direct observation. In particular, we are interested in spotting those regions accessible at collider searches such as the ongoing experiments at the LHC (see Ref. [20] and references therein).

In our pure type II seesaw model where lepton number is spontaneously violated at some low energy scale we have

$$m_\nu = y^\nu \langle \Delta \rangle$$

with the effective vev is given as $\langle \Delta \rangle = \mu \langle \Phi \rangle^2 / M_\Delta^2$ where Δ is the isotriplet lepton–number–carrying scalar. Here $\langle \Phi \rangle$ is fixed by the mass of the W boson and

$$\mu = \kappa v_1$$

is the dimensionful parameter responsible of lepton number violation, see eq. (7.3). Therefore if $y^\nu \sim \mathcal{O}(1)$ and the mass M_Δ lies at 1 TeV region then one has that $\langle \Delta \rangle \sim m_\nu$ and $\mu \sim 1$ eV. Note that one may consider two situations: $v_1 \gg \Lambda_{EW}$ (high-scale seesaw mechanism) in whose case the scalar singlet and the invisible decays of the Higgs are decoupled [15]; the second interesting case is when $\Lambda_{EW} \lesssim v_1 \lesssim$ few TeV (low-scale seesaw mechanism). In this case the parameter κ is the range $[10^{-14}, 10^{-16}]$ for $y^\nu \sim \mathcal{O}(1)$. In this case one has new physics at the TeV region including the "invisible" decays of the Higgs bosons.

Therefore, led by the smallness of the neutrino mass we can qualitatively determine that the analysis to be carried out is characterized by having a vev hierarchy

$$v_1 \gtrsim v_2 \gg v_3$$

and the smallness of the coupling κ, that is $\kappa \ll 1$.

7.2.2 The scalar potential

The scalar potential invariant under the $SU(3)_C \otimes SU(2)_L \otimes U(1)_Y \otimes$ U(1)$_{\rm L}$ symmetry is given by [15, 16] [2]

$$\begin{aligned} V &= \mu_1^2\sigma^*\sigma + \mu_2^2\Phi^\dagger\Phi + \mu_3^2 \mathrm{tr}(\Delta^\dagger\Delta) + \lambda_1(\Phi^\dagger\Phi)^2 + \lambda_2[\mathrm{tr}(\Delta^\dagger\Delta)]^2 \\ &+ \lambda_3\Phi^\dagger\Phi \mathrm{tr}(\Delta^\dagger\Delta) + \lambda_4 \mathrm{tr}(\Delta^\dagger\Delta\Delta^\dagger\Delta) + \lambda_5(\Phi^\dagger\Delta^\dagger\Delta\Phi) + \beta_1(\sigma^*\sigma)^2 \\ &+ \beta_2(\Phi^\dagger\Phi)(\sigma^*\sigma) + \beta_3 \mathrm{tr}(\Delta^\dagger\Delta)(\sigma^*\sigma) - \kappa(\Phi^T\Delta\Phi\sigma + \mathrm{h.c.}). \end{aligned} \tag{7.4}$$

As mentioned above the scalar fields σ, ϕ and Δ acquire non-zero vacuum expectation values, v_1, v_2 and v_3, respectively, so that, they can be shifted as follows,

$$\begin{aligned} \sigma &= \frac{v_1}{\sqrt{2}} + \frac{R_1 + iI_1}{\sqrt{2}}, \\ \phi^0 &= \frac{v_2}{\sqrt{2}} + \frac{R_2 + iI_2}{\sqrt{2}}, \\ \Delta^0 &= \frac{v_3}{\sqrt{2}} + \frac{R_3 + iI_3}{\sqrt{2}}. \end{aligned}$$

The minimization conditions of eq. (7.4) are given by,

$$\begin{aligned} \mu_1^2 &= \frac{-2\beta_1 v_1^3 - \beta_2 v_1 v_2^2 - \beta_3 v_1 v_3^2 + \kappa v_2^2 v_3}{2v_1}, \\ \mu_2^2 &= -\frac{1}{2}\left(2\lambda_1 v_2^2 + \beta_2 v_1^2 + (\lambda_3 + \lambda_5)v_3^2 - 2\kappa v_1 v_3\right), \\ \mu_3^2 &= \frac{-2(\lambda_2 + \lambda_4)v_3^3 - (\lambda_3 + \lambda_5)v_2^2 v_3 - \beta_3 v_1^2 v_3 + \kappa v_1 v_2^2}{2v_3}. \end{aligned} \tag{7.5}$$

and from these one can derive a vev seesaw relation of the type

$$v_1 v_3 \sim \kappa v_2^2 \ ,$$

where κ is the dimensionless coupling that generates the mass parameter associated to the cubic term in the scalar potential of the simplest triplet seesaw

[2] From now on we follow the notation and conventions used in Ref. [16].

scheme with explicit lepton number violation as proposed in [21] and recently revisited in [12].

Neutral Higgs bosons

One can now write the resulting squared mass matrix for the CP-even scalars in the weak basis (R_1, R_2, R_3) as follows,

$$M_R^2 = \begin{bmatrix} 2\beta_1 v_1^2 + \frac{1}{2}\kappa v_2^2 \frac{v_3}{v_1} & \beta_2 v_1 v_2 - \kappa v_2 v_3 & \beta_3 v_1 v_3 - \frac{1}{2}\kappa v_2^2 \\ \beta_2 v_1 v_2 - \kappa v_2 v_3 & 2\lambda_1 v_2^2 & (\lambda_3+\lambda_5) v_2 v_3 - \kappa v_1 v_2 \\ \beta_3 v_1 v_3 - \frac{1}{2}\kappa v_2^2 & (\lambda_3+\lambda_5) v_2 v_3 - \kappa v_1 v_2 & 2(\lambda_2+\lambda_4) v_3^2 + \frac{1}{2}\kappa v_2^2 \frac{v_1}{v_3} \end{bmatrix} \quad (7.6)$$

The matrix M_R^2 is diagonalized by an orthogonal matrix as follows, $\mathcal{O}_R M_R^2 \mathcal{O}_R^T = \text{diag}(m_{H_1}^2, m_{H_2}^2, m_{H_3}^2)$, where

$$\begin{pmatrix} H_1 \\ H_2 \\ H_3 \end{pmatrix} = \mathcal{O}_R \begin{pmatrix} R_1 \\ R_2 \\ R_3 \end{pmatrix}. \quad (7.7)$$

We use the standard parameterization $\mathcal{O}_R = R_{23} R_{13} R_{12}$ where

$$R_{12} = \begin{pmatrix} c_{12} & s_{12} & 0 \\ -s_{12} & c_{12} & 0 \\ 0 & 0 & 1 \end{pmatrix}, \quad R_{13} = \begin{pmatrix} c_{13} & 0 & s_{13} \\ 0 & 1 & 0 \\ -s_{13} & 0 & c_{13} \end{pmatrix}, \quad R_{23} = \begin{pmatrix} 1 & 0 & 0 \\ 0 & c_{23} & s_{23} \\ 0 & -s_{23} & c_{23} \end{pmatrix} \quad (7.8)$$

and $c_{ij} = \cos\alpha_{ij}, s_{ij} = \sin\alpha_{ij}$, so that the rotation matrix $\mathcal{O}_R$ is re-expressed in terms of the mixing angles in the following way:

$$\mathcal{O}_R = \begin{pmatrix} c_{12}c_{13} & c_{13}s_{12} & s_{13} \\ -c_{23}s_{12} - c_{12}s_{13}s_{23} & c_{23}c_{12} - s_{12}s_{13}s_{23} & c_{13}s_{23} \\ -c_{12}c_{23}s_{13} + s_{23}s_{12} & -c_{23}s_{12}s_{13} - c_{12}s_{23} & c_{13}c_{23} \end{pmatrix}. \quad (7.9)$$

On the other hand, the squared mass matrix for the CP-odd scalars in the weak basis (I_1, I_2, I_3) is given as,

$$M_I^2 = \kappa \begin{bmatrix} \frac{1}{2} v_2^2 \frac{v_3}{v_1} & v_2 v_3 & \frac{1}{2} v_2^2 \\ v_2 v_3 & 2 v_1 v_3 & v_1 v_2 \\ \frac{1}{2} v_2^2 & v_1 v_2 & \frac{1}{2} v_2^2 \frac{v_1}{v_3} \end{bmatrix}. \quad (7.10)$$

The matrix M_I^2 is diagonalized as, $\mathcal{O}_I M_I^2 \mathcal{O}_I^T = \text{diag}(0, 0, m_A^2)$, where the null masses correspond to the would-be Goldstone boson G^0 and the Majoron J, while the squared CP-odd mass is

$$m_A^2 = \kappa \left(\frac{v_2^2 v_1^2 + v_2^2 v_3^2 + 4 v_3^2 v_1^2}{2 v_3 v_1} \right). \quad (7.11)$$

The mass eigenstates are linked with the original ones by the following rotation,

$$\begin{pmatrix} A_1 \\ A_2 \\ A_3 \end{pmatrix} \equiv \begin{pmatrix} J \\ G^0 \\ A \end{pmatrix} = \mathcal{O}_I \begin{pmatrix} I_1 \\ I_2 \\ I_3 \end{pmatrix} \tag{7.12}$$

where the matrix $\mathcal{O}_I$ is given by,

$$O_I = \begin{bmatrix} cv_1V^2 & -2cv_2v_3^2 & -cv_2^2v_3 \\ 0 & v_2/V & -2v_3/V \\ bv_2/2v_1 & b & bv_2/2v_3 \end{bmatrix}, \tag{7.13}$$

with

$$V^2 = v_2^2 + 4v_3^2,$$
$$c^{-2} = v_1^2V^4 + 4v_2^2v_3^4 + v_2^4v_3^2 \tag{7.14}$$
$$b^2 = \frac{4v_1^2v_3^2}{v_2^2v_1^2 + v_2^2v_3^2 + 4v_3^2v_1^2}. \tag{7.15}$$

Charged Higgs bosons

The squared mass matrix for the singly-charged scalar bosons in the original weak basis $(\phi^\pm, \Delta^\pm)$ is given by,

$$M^2_{H^\pm} = \begin{bmatrix} \kappa v_1v_3 - \frac{1}{2}\lambda_5v_3^2 & \frac{1}{2\sqrt{2}}v_2(\lambda_5v_3 - 2\kappa v_1) \\ \frac{1}{2\sqrt{2}}v_2(\lambda_5v_3 - 2\kappa v_1) & \frac{1}{4v_3}v_2^2(-\lambda_5v_3 + 2\kappa v_1) \end{bmatrix}. \tag{7.16}$$

We now define

$$\begin{pmatrix} G^\pm \\ H^\pm \end{pmatrix} = \begin{pmatrix} c_\pm & s_\pm \\ -s_\pm & c_\pm \end{pmatrix} \begin{pmatrix} \phi^\pm \\ \Delta^\pm \end{pmatrix}, \quad \text{and} \quad \mathcal{O}_\pm M^2_{H^\pm}\mathcal{O}_\pm^T = \text{diag}(0, m^2_{H^\pm}) \tag{7.17}$$

where $c_\pm$ and $s_\pm$ are given as $c_\pm = v_2/\sqrt{v_2^2 + 2v_3^2}$ and $s_\pm = \sqrt{2}v_3/\sqrt{v_2^2 + 2v_3^2}$. The massless state corresponds to the would-be Golstone bosons $G^\pm$ and the massive state $H^\pm$ is characterized by,

$$m^2_{H^\pm} = \frac{1}{4v_3}(2\kappa v_1 - \lambda_5v_3)(v_2^2 + 2v_3^2). \tag{7.18}$$

On the other hand, the doubly-charged scalars $\Delta^{\pm\pm}$ has mass

$$m^2_{\Delta^{++}} = \frac{1}{2v_3}(\kappa v_1v_2^2 - 2\lambda_4v_3^3 - \lambda_5v_2^2v_3). \tag{7.19}$$

7.2.3 Scalar boson mass sum rules

Notice that using the fact that the smallness of the neutrino mass implies that the parameters κ and v_3 are very small one can, to a good approximation, rewrite eq. (7.6) schematically in the form,

$$M_R^2 \sim \begin{pmatrix} \star & \star & 0 \\ \star & \star & 0 \\ 0 & 0 & \star \end{pmatrix} \quad \text{so that} \quad \mathcal{O}_R \sim \begin{pmatrix} c_{12} & s_{12} & 0 \\ -s_{12} & c_{12} & 0 \\ 0 & 0 & 1 \end{pmatrix}, \tag{7.20}$$

and eq. (7.11) becomes,

$$m_A^2 \sim \kappa \frac{v_2^2 v_1}{2v_3}. \tag{7.21}$$

As a result, the scalar H_3 and the pseudo-scalar A are almost degenerate,

$$m_{H_3} = (M_R^2)_{33} \approx m_A^2. \tag{7.22}$$

In the same way, by using eqs. (7.11), (7.18) and (7.19), one can derive the following mass relations,

$$m_A^2 - m_{H^+}^2 \approx \frac{\lambda_5 v_2^2}{4} \quad \text{and} \quad 2m_{H^+}^2 - m_A^2 - m_{\Delta^{++}}^2 \approx \lambda_4 v_3^2,$$

which can be rewritten in the form,

$$m_{H^+}^2 - m_{\Delta^{++}}^2 \approx m_A^2 - m_{H^+}^2 \approx \frac{\lambda_5 v_2^2}{4}. \tag{7.23}$$

This sum rule is also satisfied in the Type-II seesaw model with explicit breaking of lepton number. Imposing the perturbativity condition one finds that the squared mass difference between, say doubly and singly charged scalar bosons, cannot be too large [12]. Explicit comparison shows that λ_5 in eq. (7.4) corresponds to $\lambda'_{H\Delta}$ in Ref. [12]. Therefore when the couplings of the singlet σ in eq. (7.4) are small, λ_5 is constrained to be in the range $[-0.85, 0.85]$, so that the remaining couplings are kept small up to the Planck scale and vacuum stability is guaranteed. See Figure 4 in Ref. [12]. Likewise when one decouples the triplet one also recovers the results found in Ref. [11].

7.3 Theoretical constraints

Before analyzing the sensitivities of the searches for Higgs bosons at the LHC experiments, we first discuss the restrictions that follow from the consistency requirements of the Higgs potential. We can rewrite the dimensionless parameters $\lambda_{1,2,3}$ and $\beta_{1,2,3}$ in eq. (7.4) in terms of the mixing angles, α_{ij} and

scalar the masses $m_{H_{1,2,3}}$ by solving $\mathcal{O}_R M_R^2 \mathcal{O}_R^T = \text{diag}(m_{H_1}^2, m_{H_2}^2, m_{H_3}^2)$ and $\mathcal{O}_I M_I^2 \mathcal{O}_I^T = \text{diag}(0, 0, m_A^2)$. Hence one gets,

$$
\begin{aligned}
\lambda_1 &= \tfrac{1}{2v_2^2}\left[m_{H_1}^2 c_{13}^2 s_{12}^2 + m_{H_2}^2 \left(c_{12}c_{23} - s_{12}s_{13}s_{23}\right)^2 + m_{H_3}^2 \left(c_{12}s_{23} + s_{12}s_{13}c_{23}\right)^2\right] \\
\lambda_2 &= \tfrac{1}{2v_3^2}\left[m_{H_1}^2 s_{13}^2 + c_{13}^2\left(m_{H_2}^2 s_{23}^2 + m_{H_3}^2 c_{23}^2\right)\right] - \left(\lambda_4 + \kappa\tfrac{v_1 v_2^2}{4v_3^3}\right) \\
\lambda_3 &= \tfrac{c_{13}}{v_2 v_3}\left[m_{H_1}^2 s_{12}s_{13} + m_{H_2}^2 s_{23}\left(c_{12}c_{23} - s_{12}s_{13}s_{23}\right) - m_{H_3}^2 c_{23}\left(c_{12}s_{23} + s_{12}s_{13}c_{23}\right)\right] \\
&\quad - \left(\lambda_5 - \kappa\tfrac{v_1}{v_3}\right) \\
\beta_1 &= \tfrac{1}{2v_1^2}\left[m_{H_1}^2 c_{12}^2 c_{13}^2 + m_{H_2}^2 \left(s_{12}c_{23} + c_{12}s_{23}s_{13}\right)^2 + m_{H_3}^2 \left(s_{12}s_{23} - c_{12}c_{23}s_{13}\right)^2\right] \\
&\quad - \kappa\tfrac{v_2^2 v_3}{4v_1^3} \\
\beta_2 &= \tfrac{1}{v_1 v_2}\big[m_{H_1}^2 c_{12}s_{12}c_{13}^2 - m_{H_2}^2 (c_{23}s_{12} + c_{12}s_{13}s_{23})(c_{12}c_{23} - s_{12}s_{13}s_{23}) \\
&\quad - m_{H_3}^2 (s_{23}s_{12} - c_{12}s_{13}c_{23})(c_{12}s_{23} + s_{12}s_{13}c_{23})\big] + \kappa\tfrac{v_3}{v_1} \\
\beta_3 &= \tfrac{c_{13}}{v_1 v_3}\big[m_{H_1}^2 c_{12}s_{13} - m_{H_2}^2 s_{23}(s_{12}c_{23} + c_{12}s_{13}s_{23}) + m_{H_3}^2 c_{23}(s_{12}s_{23} - c_{12}s_{13}c_{23})\big] \\
&\quad + \kappa\tfrac{v_2^2}{2v_1 v_3}.
\end{aligned}
$$

In addition, using eqs. (7.11), (7.18) and (7.19) we can write the dimensionless parameters $\lambda_{4,5}$ and κ as functions of the vevs $v_{1,2,3}$ and the masses of the pseudo-, singly- and doubly-charged scalar bosons (i.e. m_A, $m_{H^\pm}$ and $m_{\Delta^{\pm\pm}}$, respectively) as,

$$
\begin{aligned}
\lambda_4 &= \frac{1}{v_3^2}\left(2m_{H^\pm}^2 \frac{v_2^2}{v_2^2 + 2v_3^2} - m_A^2 \frac{v_1^2 v_2^2}{v_2^2 v_3^2 + v_1^2(v_2^2 + 4v_3^2)} - m_{\Delta^{\pm\pm}}^2\right) \\
\lambda_5 &= \left(-4m_{H^\pm}^2 \frac{1}{v_2^2 + 2v_3^2} + 4m_A^2 \frac{v_1^2}{v_2^2 v_3^2 + v_1^2(v_2^2 + 4v_3^2)}\right) \\
\kappa &= 2m_A^2 \frac{v_1 v_3}{v_2^2 v_3^2 + v_1^2(v_2^2 + 4v_3^2)}.
\end{aligned}
\tag{7.24}
$$

From the theoretical side we have to ensure that the scalar potential in the model is bounded from below (BFB).

Boundedness Conditions

In order to ensure that the scalar potential in eq. (7.4) is bounded from below we have to derive the conditions on the dimensionless parameters such the quartic part of the scalar potential is positive $V^{(4)} > 0$ as the fields go to infinity. We have that the parameter $\kappa \ll 1$ (due to the smallness of the neutrino mass) and non-negative. This follows from

$$
\kappa \approx 2m_A^2 \frac{v_3}{v_1 v_2^2}. \tag{7.25}
$$

where we have used the last expression in eq. (7.24) and the fact that $v_3 \ll v_2, v_1$. Then κ is neglected with respect to the other dimensionless parameters

λ_i and β_j, i.e. $\lambda_i, \beta_j \gg \kappa$. As a result the quartic part of the potential $V^{(4)}|_{\kappa=0}$ turns to be a biquadratic form $\lambda_{ij}\varphi_i^2\varphi_j^2$ of real fields. Therefore, in this strict limit, the copositivity criteria described in [22] may be applied and the boundedness conditions for eq. (7.4) are the following,

$$\begin{aligned} &\lambda_1 > 0, \quad \beta_1 > 0, \quad \lambda_{24} > 0, \quad \hat{\lambda} \equiv \beta_2 + 2\sqrt{\beta_1\lambda_1} > 0, \\ &\tilde{\lambda} \equiv \beta_3 + 2\sqrt{\beta_1\lambda_{24}} > 0, \quad \bar{\lambda} \equiv \lambda_3 + \theta(-\lambda_5)\lambda_5 + 2\sqrt{\lambda_1\lambda_{24}} > 0, \quad \text{and} \\ &\sqrt{\beta_1\lambda_1\lambda_{24}} + [\lambda_3 + \theta(-\lambda_5)\lambda_5]\sqrt{\beta_1} + \beta_2\sqrt{\lambda_{24}} + \beta_3\sqrt{\lambda_1} + \sqrt{\hat{\lambda}\tilde{\lambda}\bar{\lambda}} > 0, \end{aligned} \tag{7.26}$$

where $\lambda_{24} \equiv \lambda_2 + \lambda_4$. In addition all the dimensionless parameters in the scalar potential are required to be less than $\sqrt{4\pi}$ in order to fulfill the perturbativity condition.

7.3.1 Astrophysical constraints

In our type-II seesaw model there are some constraints on the magnitude of $SU(2)$ triplet's vev $\langle\Delta\rangle = v_3$, that one must take into account. First of all, v_3 is constrained to be smaller than a few GeVs due to the ρ parameter ($\rho = 1.0004 \pm 0.00024$ [23]).

On the other hand, the presence of the Nambu-Goldstone boson associated to spontaneous lepton number violation and neutrino mass generation implies that there is a most stringent constraint on v_3 coming from astrophysics, due to supernova cooling. If the majoron is a strict Goldstone boson (or lighter than typical stellar temperatures) one has an upper bound for the Majoron-electron coupling

$$|g_{Jee}| \lesssim 10^{-13},$$

This is discussed, for example, in Ref. [24] and references therein. This implies

$$|g_{Jee}| = |\mathcal{O}^I_{12} m_e/v_2|.$$

Taking into account the profile of the Majoron [14] [3] one can translate this as a bound on the projection of the Majoron onto the doublet as follows [16]

$$|\langle J|\phi\rangle| = \frac{2|v_2|v_3^2}{\sqrt{v_1^2(v_2^2+4v_3^2)^2 + 4v_2^2v_3^4 + v_2^4v_3^2}} \lesssim 10^{-7}. \tag{7.27}$$

Notice that this restriction on the triplet's vev is stronger that the one stemming from the ρ parameter. The shaded region in Fig. 7.2 corresponds to the allowed region of v_3 as function of v_1.

[3] This is derived either by explicit analysis of the scalar potential or simply by symmetry, using Noether's theorem [14].

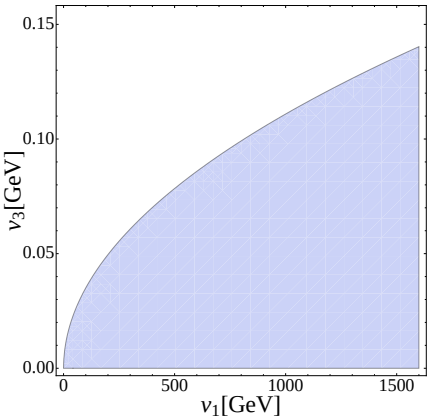

Figure 7.2: The shaded region represents the allowed region of v_3 as function of v_1.

To close this section we mention that our phenomenological analysis remains valid if the Nambu-Goldstone boson picks up a small mass from, say, quantum gravity effects.

7.4 Type-II seesaw Higgs searches at the LHC

We now turn to the study of the experimental sensitivities of the LHC experiments to the parameters characterizing the "123" type-II majoron seesaw Higgs sector, as proposed in [14]. In the following we will assume that $m_{H_1} < m_{H_2} < m_{H_3}$ where 1,2,3 refer to the mass ordering in the CP even Higgs sector. Therefore, there are two possible cases that can be considered[4]:

(i) $m_{H_1} < m_H$ and $m_{H_2} = m_H$;

(ii) $m_{H_1} = m_H$,

where m_H is the mass of the Higgs reported by the ATLAS [2] and CMS [25] collaborations, i.e. $m_H = 125.09 \pm 0.21(\text{stat.}) \pm 0.11(\text{syst.})$ GeV [26]. For case (i), we have to enforce the constraints coming from LEP-II data on the lightest CP-even scalar coupling to the SM and those coming from the LHC Run-1 on the heavier scalars. Such situation has been discussed by us in Ref. [13] in the simplest "12-type" seesaw Majoron model. In case (ii), only the constraints coming from the LHC must be taken into account.

[4]Recall that $m_{H_3} \approx m_A$, eq. (7.22), which implies that the mass of H_3 must be close to that of the doubly-charged scalar mass. Therefore, as we will see in the next section, the existing bounds on searches of the doubly-charged scalar exclude the case where m_{H_3} is lighter than the other CP-even mass eigenstates.

The neutral component of the Standard Model Higgs doublet couplings get modified as follows,

$$\phi^0 \to C_1 H_1 + C_2 H_2 + C_3 H_3 \tag{7.28}$$

where we have defined $C_i \equiv \mathcal{O}^R_{i2}$ and $\mathcal{O}^R_{ij}$ are the matrix elements of $\mathcal{O}^R$ in eq. (7.9).

7.4.1 LEP constraints on invisible Higgs decays

The constraints on H_1, when $m_{H_1} < 125\,\text{GeV}$, stem from the process $e^+e^- \to Zh \to Zb\bar{b}$ which is written as [27]

$$\begin{aligned}\sigma_{hZ\to b\bar{b}Z} =& \sigma^{SM}_{hZ} \times R_{hZ} \times BR(h \to b\bar{b}) \\ =& \sigma^{SM}_{hZ} \times C^2_{Z(h\to b\bar{b})}\,,\end{aligned} \tag{7.29}$$

where σ^{SM}_{hZ} is the SM hZ cross section, R_{hZ} is the suppression factor related to the coupling of the Higgs boson[5] to the gauge boson Z. Since $v_3 \ll v_2$, we have that the factor $R_{H_iZ} \approx C_i^2$ where $C_1 = \cos\alpha_{13}\sin\alpha_{12}$, eq. (7.28). Notice that $C_1 \approx \sin\alpha_{12}$ for the limit $\alpha_{13} \ll 1$ and then one obtains the same exclusion region depicted in Fig. 1 in Ref. [13].

7.4.2 LHC constraints on the Higgs signal strengths

In addition, we have to enforce the limits coming from the Standard Model decay channels of the Higgs boson. These are given in terms of the signal strength parameters,

$$\mu_f = \frac{\sigma^{\text{NP}}(pp \to h)}{\sigma^{\text{SM}}(pp \to h)} \frac{BR^{\text{NP}}(h \to f)}{BR^{\text{SM}}(h \to f)}, \tag{7.30}$$

where σ is the cross section for Higgs production, $BR(h \to f)$ is the branching ratio into the Standard Model final state f, the labels NP and SM stand for New Physics and Standard Model respectively. These can be compared with those given by the experimental collaborations. The most recent results of the signal strengths from a combined ATLAS and CMS analysis [28] are shown in Table 9.1.

[5] The Feynman rules for the couplings of the Higgs bosons H_i to the Z are the following: $i\frac{g^2}{2c_W^2}\left(\mathcal{O}^R_{i2}v_2 + \mathcal{O}^R_{i3}v_3\right) g_{\mu\nu}$

channel	ATLAS	CMS	ATLAS+CMS
$\mu_{\gamma\gamma}$	$1.15^{+0.27}_{-0.25}$	$1.12^{+0.25}_{-0.23}$	$1.16^{+0.20}_{-0.18}$
μ_{WW}	$1.23^{+0.23}_{-0.21}$	$0.91^{+0.24}_{-0.21}$	$1.11^{+0.18}_{-0.17}$
μ_{ZZ}	$1.51^{+0.39}_{-0.34}$	$1.05^{+0.32}_{-0.27}$	$1.31^{+0.27}_{-0.24}$
$\mu_{\tau\tau}$	$1.41^{+0.40}_{-0.35}$	$0.89^{+0.31}_{-0.28}$	$1.12^{+0.25}_{-0.23}$
μ_{bb}	$0.62^{+0.37}_{-0.36}$	$0.81^{+0.45}_{-0.42}$	$0.69^{+0.29}_{-0.27}$

Table 7.1: Current experimental results of ATLAS and CMS, Ref. [28].

One can see with ease that the LHC results indicate that $\mu_{VV} \sim 1$. In our analysis, we assume that the LHC allows deviations up to 20% as follows,

$$0.8 \leq \mu_{XX} \leq 1.2 \tag{7.31}$$

7.4.3 LHC bounds on the heavy neutral scalars

In our study we will impose the constraints on the heavy scalars from the recent LHC scalar boson searches. Therefore, we use the bounds set by the search for a heavy Higgs in the $H \to WW$ and $H \to ZZ$ decay channels in the range $[145 - 1000]$ GeV [29] and in the $h \to \tau\tau$ decay channel in the range range $[100 - 1000]$ GeV [30]. We also adopt the constraints on the process $h \to \gamma\gamma$ in the range $[65 - 600]$ GeV [31] and the range $[150, 850]$ GeV [32]. Besides, we impose the bounds in the $A \to Zh$ decay channel in the range $[220 - 1000]$ GeV [33].

7.4.4 Summary of the searches of charged scalars

The type-II seesaw model with explicit breaking of lepton number contains seven physical scalars: two CP-even neutral scalars H_1 and H_2, one CP-odd scalar A and four charged scalars $\Delta^{\pm\pm}$ and $H^{\pm}$. Such a scenario has been widely studied in the literature and turns out to be quite appealing because it could be tested at the LHC [34–44]. For instance, the existence of charged scalar bosons provides additional contributions to the one-loop decays of the Standard Model Higgs boson. Indeed, they could affect the one-loop decays $h \to \gamma\gamma$ [39, 40] and $h \to Z\gamma$ [40] in a substantial way. In this case the signal strength $\mu_{\gamma\gamma}$ can set bounds on the mass of the charged scalars, $\Delta^{\pm\pm}$ and/or $H^{\pm}$.

The doubly-charged scalar boson has the following possible decay channels: $\ell^{\pm}\ell^{\pm}$, $W^{\pm}W^{\pm}$, $W^{\pm}H^{\pm}$ and $H^{\pm}H^{\pm}$. However, it is known that for an approx-

imately degenerate triplet mass spectrum and vev $v_3 \lesssim 10^{-4}\,\text{GeV}$ the doubly charged Higgs coupling to $W^\pm$ is suppressed (because it is proportional to v_3 as can be seen from Table 7.3) and hence $\Delta^{\pm\pm}$ predominantly decays into like-sign dileptons [41, 44, 45]. In this case, CMS [46] and ATLAS [47] have currently excluded at 95% C.L., depending on the assumptions on the branching ratios into like-sign dileptons, doubly-charged masses between 200 and 460 GeV [6]. For $v_3 \gtrsim 10^{-4}\,\text{GeV}$, the Yukawa couplings of triplet to leptons are too small so that $\Delta^{\pm\pm}$ dominantly decays to like-sign dibosons, in which case the collider limits are rather weak [43, 48–50].

In the present "123" type-II seesaw model there are two additional physical scalars, a massive CP-even scalar H_3 and the massless majoron J. The latter, associated to the spontaneous breaking of lepton number, provides non-standard decay channels of other Higgs bosons as missing energy in the final state [7].

7.5 Invisible Higgs decays at the LHC

We now turn to the case of genuinely non-standard Higgs decays. We focus on investigating the LHC sensitivities on the invisible Higgs decays. In so doing we take into account how they are constrained by the available experimental data. In the previous section we mentioned that in our study the CP- even scalars obey the following mass hierarchy $m_{H_1} < m_{H_2} < m_{H_3}$. Furthermore, we will also assume that the masses m_{H_3}, m_A, m_{H^+} and $m_{\Delta^{++}}$ are nearly degenerate. As a consequence, the decay of any CP-even Higgs H_i into the pseudo-scalar A is not kinematically allowed. Therefore, the new decay channels of the CP-even scalars are just, $H_i \to JJ$ and $H_i \to 2H_j$ (when $m_{H_i} < \frac{m_{H_j}}{2}$ for $i \neq j$). The latter contributing also to the invisible decay channel of the Higgs as, $H_i \to 2H_j \to 4J$.

The Higgs-Majoron couplings are given by,

$$g_{H_a JJ} = \left(\frac{(\mathcal{O}^I_{12})^2}{v_2} \mathcal{O}^R_{a2} + \frac{(\mathcal{O}^I_{13})^2}{v_3} \mathcal{O}^R_{a3} + \frac{(\mathcal{O}^I_{11})^2}{v_1} \mathcal{O}^R_{a1} \right) m^2_{H_a}, \tag{7.32}$$

where $\mathcal{O}^I_{ij}$ are the elements of the rotation matrix in eq. (7.13) and the decay

[6] From doubly-charged scalar boson searches performed by ATLAS and CMS one can also constrain the lepton number violation processes $pp \to \Delta^{\pm\pm}\Delta^{\mp\mp} \to \ell^\pm\ell^\pm W^\mp W^\mp$ and $pp \to \Delta^{\pm\pm}H^\mp \to \ell^\pm\ell^\pm W^\mp Z$ [41]. This may also shed light on the Majorana phases of the lepton mixing matrix [34–36].

[7] These include, for example, $H_i \to JJ$ and $H^\pm \to JW^\mp$. Here we focus mainly on the first, the decays of $H^\pm$ deserve further study but it is beyond the scope of this work and will be considered elsewhere.

width is given by

$$\Gamma(H_a \to JJ) = \frac{1}{32\pi}\frac{g^2_{H_aJJ}}{m_{H_a}}\,. \tag{7.33}$$

Following our conventions we have that the trilinear coupling $H_2H_1H_1$ turns out to be,

$$\begin{aligned}\frac{g_{H_2H_1H_1}}{2} &= 3\lambda_1(\mathcal{O}^R_{12})^2\mathcal{O}^R_{22}v_2 + 3(\lambda_2+\lambda_4)(\mathcal{O}^R_{13})^2\mathcal{O}^R_{23}v_3 \\ &+\frac{(\lambda_3+\lambda_5)}{2}\left[(\mathcal{O}^R_{13})^2\mathcal{O}^R_{22}v_2 + (\mathcal{O}^R_{12})^2\mathcal{O}^R_{23}v_3 + 2\mathcal{O}^R_{12}\mathcal{O}^R_{13}(\mathcal{O}^R_{23}v_2+\mathcal{O}^R_{22}v_3)\right] \\ &+3\beta_1(\mathcal{O}^R_{11})^2\mathcal{O}^R_{21}v_1 + \frac{\beta_2}{2}\left[(\mathcal{O}^R_{12})^2\mathcal{O}^R_{21}v_1 + (\mathcal{O}^R_{11})^2\mathcal{O}^R_{22}v_2 + 2\mathcal{O}^R_{11}\mathcal{O}^R_{12}\right. \\ &\times\left.(\mathcal{O}^R_{22}v_1+\mathcal{O}^R_{21}v_2)\right] + \frac{\beta_3}{2}\left[(\mathcal{O}^R_{13})^2\mathcal{O}^R_{21}v_1 + (\mathcal{O}^R_{11})^2\mathcal{O}^R_{23}v_3 + 2\mathcal{O}^R_{11}\mathcal{O}^R_{13}\right. \\ &\times\left.(\mathcal{O}^R_{23}v_1+\mathcal{O}^R_{21}v_3))\right] + \frac{\kappa}{2}\left[-2\mathcal{O}^R_{11}\mathcal{O}^R_{13}\mathcal{O}^R_{22}v_2 - (\mathcal{O}^R_{12})^2(\mathcal{O}^R_{23}v_1+\mathcal{O}^R_{21}v_3)\right. \\ &\left.-2\mathcal{O}^R_{12}(\mathcal{O}^R_{13}(\mathcal{O}^R_{22}v_1+\mathcal{O}^R_{21}v_2)+\mathcal{O}^R_{11}(\mathcal{O}^R_{23}v_2+\mathcal{O}^R_{22}v_3))\right]. \end{aligned}\tag{7.34}$$

and hence, for example when $m_{H_1} < 2m_{H_2}$, the decay width $H_2 \to H_1H_1$ is given by

$$\Gamma\left(H_2 \to H_1H_1\right) = \frac{g^2_{H_2H_1H_1}}{32\pi m_{H_2}}\left(1-\frac{4m^2_{H_1}}{m^2_{H_2}}\right)^{1/2}. \tag{7.35}$$

As we already mentioned, a salient feature of adding an isotriplet to the Standard Model is that some *visible* decay channels of the Higgs receive further contributions from the charged scalars, namely the one-loop decays $h \to \gamma\gamma$ and $h \to Z\gamma$. That is, the scalars $H^\pm$ and $\Delta^{\pm\pm}$ contribute to the one-loop coupling of the Higgs to two-photons and to Z-photon, leading to deviations from the Standard Model expectations for these decay channels. The interactions between CP-even and charged scalars are described by the following vertices,

$$\begin{aligned} H_aH^+H^- &: ig_{H_aH^+H^-} \\ H_a\Delta^{++}\Delta^{--} &: ig_{H_a\Delta^{++}\Delta^{--}} \end{aligned}$$

where

$$\begin{aligned} g_{H_aH^+H^-} &= \frac{1}{2(v_2^2+2v_3^2)}\left[8\lambda_1\mathcal{O}^R_{a2}v_2v_3^2 + 4(\lambda_2+\lambda_4)\mathcal{O}^R_{a3}v_2^2v_3 + 2\lambda_3(\mathcal{O}^R_{a2}v_2^3 + 2\mathcal{O}^R_{a3}v_3^3)\right. \\ &+ \left.\lambda_5v_2[-2\mathcal{O}^R_{a3}v_2v_3 + \mathcal{O}^R_{a2}(v_2^2-2v_3^2)] + 4\beta_2\mathcal{O}^R_{a1}v_1v_3^2 + 2\beta_3\mathcal{O}^R_{a1}v_1v_2^2\right. \\ &+ \left.4\kappa v_2v_3(\mathcal{O}^R_{a2}v_1+\mathcal{O}^R_{a1}v_2)\right] \\ g_{H_a\Delta^{++}\Delta^{--}} &= 2\lambda_2\mathcal{O}^R_{a3}v_3 + \lambda_3\mathcal{O}^R_{a2}v_2 + \beta_3\mathcal{O}^R_{a1}v_1. \end{aligned}$$

Note that the contributions of $H^{\pm}$ and $\Delta^{\pm\pm}$ to the decays $h \to \gamma\gamma$ and $h \to Z\gamma$ are functions of the singlet's vev v_1, this is in contrast to what happens in the type-II seesaw model with explicit violation of lepton number. According to eq. (7.26) the dimensionless parameters λ_i and β_i can change the sign of the couplings of $g_{H_a H^+ H^-}$ and $g_{H_a \Delta^{++}\Delta^{--}}$, hence the contribution of the charged scalars to $h \to \gamma\gamma$ and $h \to Z\gamma$ may be either constructive or destructive.

For the computation of the decay widths $h \to \gamma\gamma$ and $h \to Z\gamma$ we use the expressions and conventions given in Ref. [51]. The decay width $\Gamma(H_a \to \gamma\gamma)$ turns out to be

$$\Gamma(H_a \to \gamma\gamma) = \frac{G_F \alpha^2 m_{H_a}^3}{128\sqrt{2}\pi^3} \left| X_F^{\gamma\gamma} + X_W^{\gamma\gamma} + X_H^{\gamma\gamma} \right|^2 \tag{7.36}$$

where G_F is the Fermi constant, α is the fine structure constant and the form factors X_i^j are given by [8],

$$\begin{aligned} X_F^{\gamma\gamma} &= -2C_a \sum_f N_c^f Q_f^2 \tau_f \left[1 + (1-\tau_f) f(\tau_f)\right], \\ X_W^{\gamma\gamma} &= C_a \left[2 + \tau_W + 3\tau_W (2 - \tau_W) f(\tau_W)\right] \\ X_H^{\gamma\gamma} &= -\frac{g_{H_a H^+ H^-} v}{2m_{H^\pm}^2} \tau_{H^\pm} \left[1 - \tau_{H^\pm} f(\tau_{H^\pm})\right] - 4 \frac{g_{H_a \Delta^{++}\Delta^{--}} v}{2m_{\Delta^{\pm\pm}}^2} \tau_{\Delta^{\pm\pm}} \\ &\times \left[1 - \tau_{\Delta^{\pm\pm}} f(\tau_{\Delta^{\pm\pm}})\right]. \end{aligned} \tag{7.37}$$

where $\tau_x = 4m_x^2/m_Z^2$. Here N_c^F and Q_F denote, respectively, the number of colors and electric charge of a given fermion. The one-loop function $f(\tau)$ is defined in appendix 7.B. The parameters C_a correspond to the Standard Model Higgs couplings in eq. (7.28).

The decay width $\Gamma(H_a \to Z\gamma)$, using the notation in Ref. [51], is expressed as follows

$$\Gamma(H_a \to Z\gamma) = \frac{G_F \alpha^2 m_{H_a}^3}{64\sqrt{2}\pi^3} \left(1 - \frac{m_Z^2}{m_{H_a}^2}\right)^3 \left| X_F^{Z\gamma} + X_W^{Z\gamma} + X_H^{Z\gamma} \right|^2 \tag{7.38}$$

[8] We have taken into account that v_3 is very small so that any contribution involving the triplet's vev is neglected. Then for instance the Feynman rule for the vertex $H_a W_\mu^+ W_\nu^-$: $i\frac{g^2}{2}(O_{a2}^R v_2 + 2O_{a3}^R v_3)\, g_{\mu\nu}$, is approximated as $\sim i\frac{g^2}{2}(O_{a2}^R v_2)\, g_{\mu\nu}$ (see Table 7.3).

where the form factors X_i^j are given by[9] ,

$$\begin{aligned}
X_F^{Z\gamma} &= -4C_a \sum_f N_c^f \frac{g_V^f Q_f m_f^2}{s_W c_W} \left\{ \frac{2m_Z^2}{(m_{H_a}^2 - m_Z^2)^2} \Delta B_0^f + \frac{1}{m_{H_a}^2 - m_Z^2} \right. \\
&\times \left. \left[(4m_f^2 - m_{H_a}^2 + m_Z^2) C_0^f + 2 \right] \right\} \\
X_W^{Z\gamma} &= \frac{C_a}{\tan\theta_W} \left\{ \frac{1}{(m_{H_a}^2 - m_Z^2)^2} \left[m_{H_a}^2 (1 - \tan^2\theta_W) - 2m_W^2 (-5 + \tan^2\theta_W) \right] m_Z^2 \Delta B_0^W \right. \\
&+ \frac{1}{(m_{H_a}^2 - m_Z^2)} \left[m_{H_a}^2 (1 - \tan^2\theta_W) - 2m_W^2 (-5 + \tan^2\theta_W) \right. \\
&+ \left. \left. 2m_W^2 \left[(-5 + \tan^2\theta_W)(m_{H_a}^2 - 2m_W^2) - 2m_Z^2 (-3 + \tan^2\theta_W) \right] C_0^W \right] \right. \\
X_H^{Z\gamma} &= -2 g_{H_a H^+ H^-} v \frac{\tan\theta_W}{(m_{H_a}^2 - m_Z^2)} \left[\frac{m_Z^2}{m_{H_a}^2 - m_Z^2} \Delta B_0^{\pm} + (2m_{H^\pm}^2 C_0^{\pm} + 1) \right] \\
&- 4 \frac{g_{H_a \Delta^{++} \Delta^{--}} v}{\tan\theta_W} \frac{(1 - \tan^2\theta_W)}{(m_{H_a}^2 - m_Z^2)} \left[\frac{m_Z^2}{m_{H_a}^2 - m_Z^2} \Delta B_0^{\pm\pm} + (2m_{\Delta^{\pm\pm}}^2 C_0^{\pm\pm} + 1) \right]
\end{aligned}$$

where C_0^b and ΔB_0^b are defined in appendix 7.B.

7.6 Type-II seesaw neutral Higgs searches at the LHC

We stated above that in our study we are assuming $m_{H_1} < m_{H_2} < m_{H_3}$ and $v_1 \gtrsim v_2$. Furthermore, because of the ρ parameter and the astrophysical constraint on the triplet's vev we also have that $v_3 \ll v_1, v_2$. We found that the smallness of v_3 and the perturbativity condition of the potential lead to a very small mixing between the mass eigenstate H_3 and the CP-even components of the fields, σ and Φ, in other words, the angles α_{13} and α_{23} must lie close to 0 or π. As a result, we obtain the following relation,

$$m_{H_3}^2 - m_A^2 \simeq 2\lambda_2 v_3^2 \Longrightarrow m_{H_3} \simeq m_A. \tag{7.39}$$

This extra mass relation is derived from eq. (7.24), by using eq. (7.25) and the fact that $\alpha_{13,23} \sim 0(\pi)$. In addition, also as a result of $\alpha_{13,23} \sim 0(\pi)$, we find that the coupling of H_3 to the Standard Model states is negligible,

$$\frac{g_{H_3 ff}}{g_{hff}^{\rm SM}} = \frac{g_{H_3 VV}}{g_{hVV}^{\rm SM}} = C_3 \sim 0. \tag{7.40}$$

In Fig. 7.12 of appendix 7.A we give a schematic illustration of the mass profile of the Higgs bosons in our model. The mass spectrum and composition are summarized in Table 7.2, and provide a useful picture in our following analyses.

[9] Here we have also assumed $v_3 \ll 1$ so as to make the following approximation, $H^+H^-Z_\mu : -ig \sin\theta_W \tan\theta_W (p_+ - p_-)_\mu$.

Analysis (i)

In this case we have taken the isotriplet vev $v_3 = 10^{-5}$ GeV, automatically safe from the constraints stemming from astrophysics and the ρ parameter. We have also considered the following mass spectrum,

$$m_{H_1} = [15, 115] \text{ GeV}, \quad m_{H_2} = 125 \text{ GeV}, \quad m_{H_3} \simeq m_A \simeq m_{H^\pm} \simeq m_{\Delta^{\pm\pm}} = 500\,\text{GeV},$$

and varied the parameters as

$$v_1 \in [100, 2500] \text{ GeV}, \quad \alpha_{12} \in [0, \pi] \quad \text{and} \quad \alpha_{13,23} = \delta_\alpha\,(\pi - \delta_\alpha) \tag{7.41}$$

where $0 \leq \delta_\alpha < 0.1$. As described in section 7.4 we must enforce the LEP constraints on the lightest CP-even Higgs H_1 and LHC constraints on the heavier scalars. The near mass degeneracy of H_3, A, $H^\pm$ and $\Delta^{\pm\pm}$ ensures that the oblique parameters are not affected. In analogy to the type-II seesaw model with explicit lepton number violation we expect that, because of $v_3 < 10^{-4}$ GeV, the doubly-charged scalar predominantly decays into same sign dileptons [41, 44, 45] and that $m_{\Delta^{\pm\pm}} = 500$ GeV is consistent with current experimental data, see subsection 7.4.4.

We show in Fig. 7.3 the mass of the lightest CP-even scalar as a function of the absolute value of its coupling to the Standard Model states, $|C_1|$ in eq. (7.28). The blue region corresponds to the LEP exclusion region and the green(red) one is the LHC allowed(exclusion) region provided by the signal strengths $0.8 < \mu_{XX} < 1.2$.

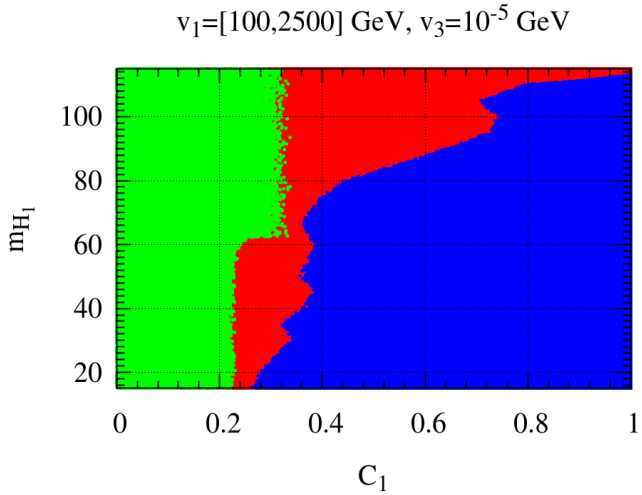

Figure 7.3: Analysis (i). The mass of the lightest CP-even scalar as a function of the absolute value of its coupling to Standard Model states. The blue region corresponds to the LEP exclusion region and the green(red) one is the LHC allowed(exclusion) region.

The presence of light charged scalars can enhance significantly the diphoton channel of the Higgs [39]. Fig. 7.4 shows the correlation between μ_{ZZ} and $\mu_{\gamma\gamma}(\mu_{Z\gamma})$ on the left(right) with $\mu_{\gamma\gamma} \lesssim 1.2$ for charged Higgs bosons of 500 GeV. The correlation between the signal strength μ_{ZZ} and the signal strengths $\mu_{\gamma\gamma}$ and $\mu_{Z\gamma}$ is shown in Fig. 7.4. Note that the former may exceed one due to the new contributions of the singly and doubly charged Higgs bosons.

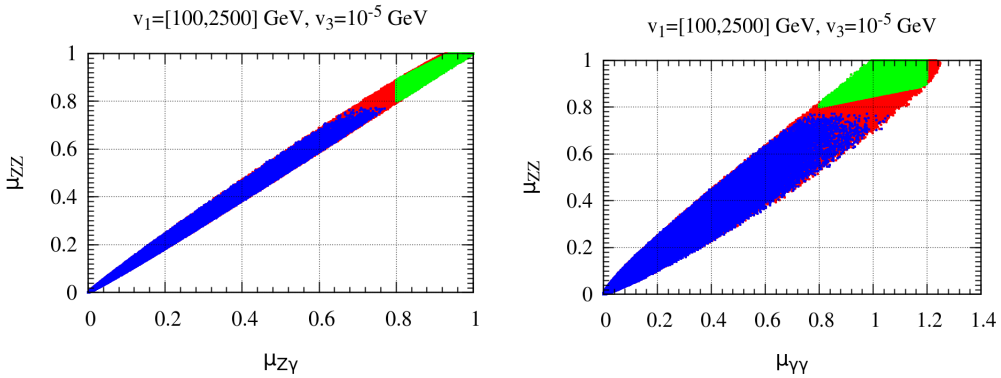

Figure 7.4: Analysis (i). On the left, we show correlation between μ_{ZZ} and $\mu_{Z\gamma}$. On the right, correlation between μ_{ZZ} and $\mu_{\gamma\gamma}$. The color code as in Fig. 7.3.

The invisible decays of the Higgs bosons, characteristic of the model, turn out to be correlated to the visible channels, represented in terms of the signal strengths, as shown in Fig. 7.5. Note that the upper bound on the invisible decays of a Higgs boson with a mass of 125 GeV has been found to be $\mathrm{BR}(H_2 \to \mathrm{Inv}) \lesssim 0.2$. This limit is stronger than those provided by the ATLAS [52] and the CMS [53] collaborations[10].

In Fig. 7.6 we depict the correlation between the invisible branching ratios of H_2 with the one of the lightest scalar boson H_1. And, as can be seen, H_1 can decay 100% into the invisible channel (majorons).

[10] The ATLAS collaboration has set an upper bound on the $\mathrm{BR}(H \to \mathrm{Inv})$ at 0.28 while the CMS collaboration reported that the observed (expected) upper limit on the invisible branching ratio is 0.58(0.44), both results at 95% C.L.

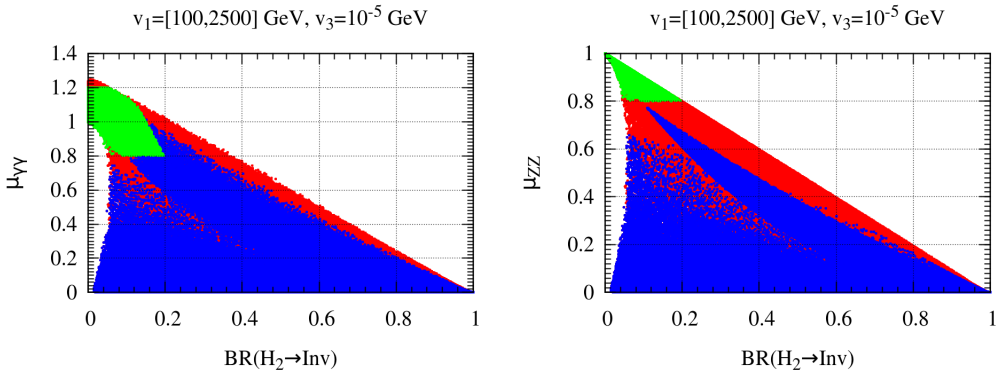

Figure 7.5: Analysis (i). On the left: the signal strength $\mu_{\gamma\gamma}$ versus BR($H_2 \to$ Inv). On the right: μ_{ZZ} versus BR($H_2 \to$ Inv). The color code as in Fig. 7.3.

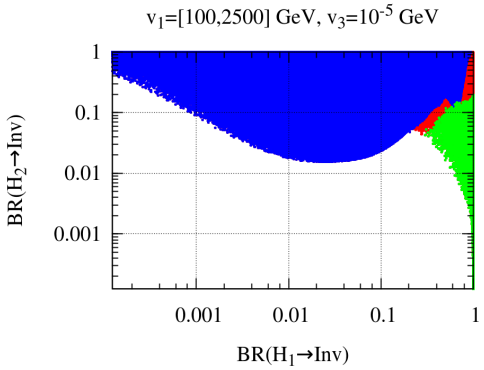

Figure 7.6: Analysis (i). Correlation between the invible branchings BR($H_2 \to$ Inv) and BR($H_1 \to$ Inv). The color code as in Fig. 7.3.

Finally, as we have mentioned we obtained that the reduced coupling of H_3 to the Standard Model states is $C_3 \sim \mathcal{O}(10^{-7})$ so that it is basically decoupled. As a result its invisible branching is essentially unconstrained, $10^{-5} \lesssim$ BR($H_3 \to$ Inv) ≤ 1. On the other hand we find that the constraint coming from the LHC on the pseudo-scalar A with a mass of 500 GeV is automatically satisfied as well, since from the LHC, $\sigma(gg \to A)$BR($A \to ZH_2$)BR($H_2 \to \tau\tau$) $\lesssim 10^{-2}$ while for $m_A = 500\,\text{GeV}$ we obtain $\sigma(gg \to A)$BR($A \to ZH_2$)BR($H_2 \to \tau\tau$) $\lesssim 10^{-15}$.

Analysis (ii)

We now turn to the other case of interest, namely

$$m_{H_1} = 125\,\text{GeV}, \quad m_{H_2} = [150, 500]\ \text{GeV}, \quad m_{H_3} \simeq m_A \simeq m_{H^\pm} \simeq m_{\Delta^{\pm\pm}} = 600\,\text{GeV},$$

with $v_3 = 10^{-5}$ GeV, as before. Now we scanned over

$$v_1 \in [100, 2500] \text{ GeV}, \quad \alpha_{12} \in [0, \pi] \text{ and } \alpha_{13,23} = \delta_\alpha \, (\pi - \delta_\alpha) \tag{7.42}$$

where $0 \leq \delta_\alpha < 0.1$. As we already mentioned in this case we only have to take into account the constraints coming from Run 1 of the LHC at 8 TeV, see Table 9.1. In practice we assume $\mu_{XX} = 1.0^{+0.2}_{-0.2}$. We show in Fig. 7.7 the correlation between μ_{ZZ} and $\mu_{\gamma\gamma}(\mu_{Z\gamma})$ on the left(right). As before, the allowed region is in green while the forbidden one is in red. We can see that $\mu_{\gamma\gamma} \lesssim 1.2$ for $m_{H^\pm} \simeq m_{\Delta^{\pm\pm}} = 600\,\text{GeV}$.

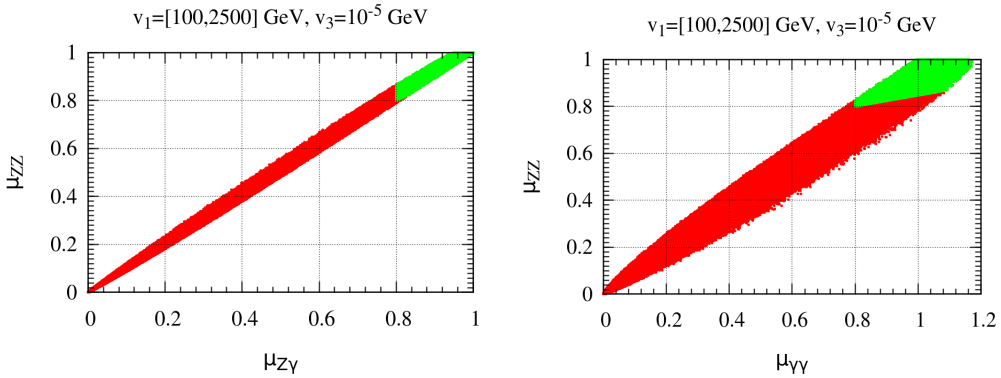

Figure 7.7: Analysis (ii). On the left, μ_{ZZ} versus $\mu_{Z\gamma}$. On the right, μ_{ZZ} versus $\mu_{\gamma\gamma}$. The allowed region (in green) is the region inside the range $\mu_{XX} = 1.0^{+0.2}_{-0.2}$ while the forbidden one (in red) is the one outside that range.

On the left(right) of Fig. 7.8 is depicted the correlation between the signal strength μ_{ZZ} ($\mu_{\gamma\gamma}$) and the branching ratio of the channel $H_1 \to JJ$. We can see in Figs. 7.8-7.10 that $\text{BR}(H_1 \to \text{Inv}) \lesssim 0.2$. One can see from Fig. 7.9 that $\text{BR}(H_1 \to \text{Inv}) \lesssim 0.1$ for $v_1 \gtrsim 2500\,\text{GeV}$.

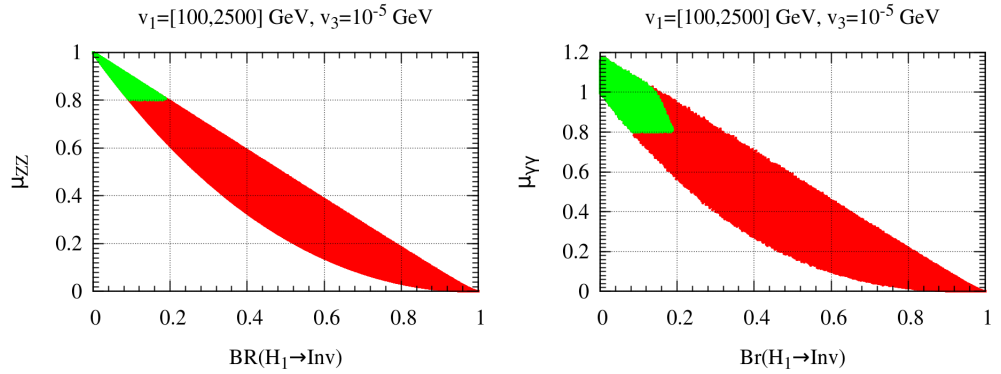

Figure 7.8: Analysis (ii). On the left: the signal strength μ_{ZZ} versus $\text{Br}(H_1 \to \text{Inv})$. On the right: $\mu_{\gamma\gamma}$ versus $\text{Br}(H_1 \to \text{Inv})$. The color code as in Fig. 7.7

In this case we find that eq. 7.32 (for $\alpha_{13,23} \sim 0(\pi)$ and $v_3 \ll v_1, v_2$) at leading order is given by,

$$g_{H_1 JJ} \sim \frac{\cos\alpha_{12}}{v_1} m^2_{H_1}, \tag{7.43}$$

where $m_{H_1} = 125\,\text{GeV}$. BR($H_1 \to$ Inv) versus the Higgs-majoron coupling $g_{H_1 JJ}$ is shown on the right of Fig. 7.9. Note also from the left panel in Fig. 7.9 that BR($H_1 \to$ Inv) is anti-correlated with v_1, as expected.

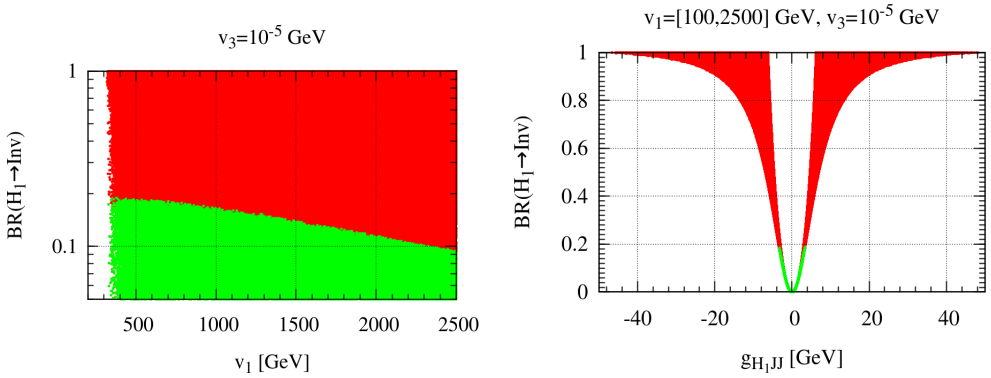

Figure 7.9: Analysis (ii). BR($H_1 \to$ Inv) versus v_1 (on the left) and BR($H_1 \to$ Inv) versus the Higgs-majoron coupling $g_{H_1 JJ}$ (on the right). The color code as in Fig. 7.7.

In Fig. 7.10 we show the correlation between the invisible branching ratio of H_2 (the Higgs with a mass in the range $150\,\text{GeV} < m_{H_2} < 500\,\text{GeV}$) and the one of H_1.

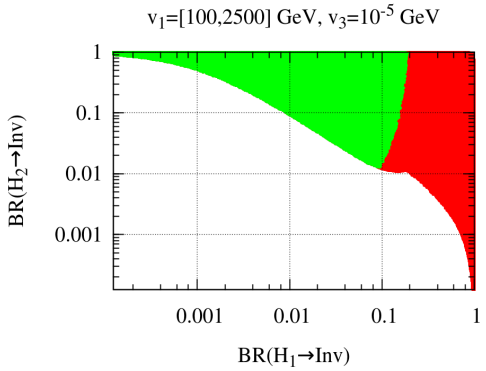

Figure 7.10: Analysis (ii). Correlation between BR($H_2 \to$ Inv) and BR($H_1 \to$ Inv). The color code as in Fig. 7.7.

We have verified that the LHC constraints on the heavy scalars (H_2, H_3 and A) are all satisfied. As an example, the reader can convince her/himself

by looking at Fig. 7.11 that H_2 easily passes the restriction stemming from $\sigma(ggH_2)\mathrm{BR}(H_2 \to \tau\tau)$ (top left) and/or $\sigma(bbH_2)\mathrm{BR}(H_2 \to \tau\tau)$ (top right). The black continuous lines on those plots represent the experimental results from Run 1 of the CMS experiment [30]. We also found that the square of the reduced coupling of H_2 to the Standard Model states is $C_2^2 \lesssim 0.1$ for $m_{H_2} = [150, 500]$ GeV. Then, one finds that the experimental upper bounds set by the search for a heavy Higgs in the $H \to WW$ and $H \to ZZ$ decay channels in [3, 29] are automatically fulfilled. However, improved sensitivities expected from Run 2 may provide a meaningful probe of the theoretically consistent region, depicted in green.

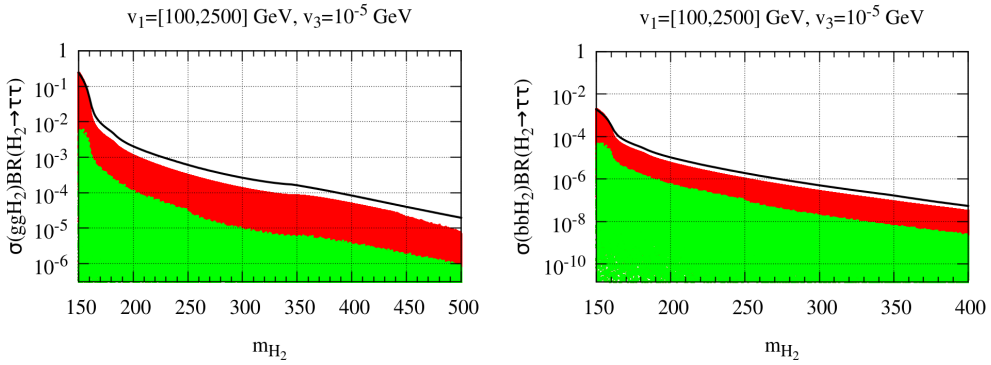

Figure 7.11: Analysis (ii). On the top right (left) $\sigma(ggH_2)\mathrm{BR}(H_2 \to \tau\tau)$ ($\sigma(bbH_2)\mathrm{BR}(H_2 \to \tau\tau)$) versus the mass of H_2.

Also in this case, H_3 is decoupled, so the restrictions on H_3 and the massive pseudoscalar A are automatically fulfilled.

7.7 Conclusions

In this paper we have presented the main features of the electroweak symmetry breaking sector of the simplest type-II seesaw model with spontaneous violation of lepton number. The Higgs sector has two characteristic features: a) the existence of a (nearly) massless Nambu-Goldstone boson and b) all neutral CP-even and CP-odd, as well as singly and doubly-charged scalar bosons coming mainly from the triplet are very close in mass, as illustrated in Fig. 7.12 of appendix 7.A. However, one extra CP-even state, namely H_2 coming from a doublet-singlet mixture can be light. After reviewing the "theoretical" and experimental restrictions which apply on the Higgs sector, we have studied the sensitivities of the searches for Higgs bosons at the ongoing ATLAS/CMS experiments, including not only the new contributions to Standard Model decay channels, but also the novel Higgs decays to majorons. For these we have

considered two cases, when the 125 GeV state found at CERN is either (i) the second-to-lightest or (ii) the lightest CP-even scalar boson. For case (i), we have enforced the constraints coming from LEP-II data on the lightest CP-even scalar coupling to the Standard Model states and those coming from the LHC Run-1 on the heavier scalars. In case (ii), only the constraints coming from the LHC must be taken into account. Such "invisible" Higgs boson decays give rise to missing momentum events. We have found that the experimental results from Run 1 on the search for a heavy Higgs in the $H \to WW$ and $H \to ZZ$ decay channels are automatically fulfilled. However, improved sensitivities expected from Run 2 may provide a meaningful probe of this scenario. In short we have discussed how the neutrino mass generation scenario not only suggests the need to reconsider the physics of electroweak symmetry breaking from a new perspective, but also provides a new theoretically consistent and experimentally viable paradigm.

Acknowledgments

Work supported by the Spanish grants FPA2014-58183-P, Multidark CSD2009-00064 and SEV-2014-0398 (MINECO), and PROMETEOII/2014/084 (Generalitat Valenciana). C. B. thanks Departamento de Física and CFTP, Instituto Superior Técnico, Universidade de Lisboa, for its hospitality while part of this work was carried out. J.C.R. is also support in part by the Portuguese Fundação para a Ciência e Tecnologia (FCT) under contracts UID/FIS/00777/2013 and CERN/FIS-NUC/0010/2015, which are partially funded through POCTI (FEDER), COMPETE, QREN and the EU.

7.A Appendix A: Higgs boson mass spectrum

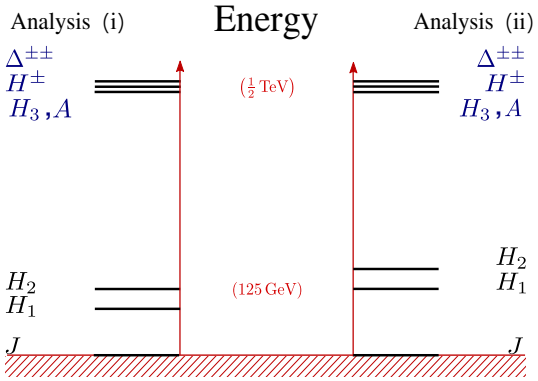

Figure 7.12: Type-II seesaw Higgs boson mass spectrum

Mass eigenstate ϕ	Mass squared m_ϕ^2	Composition
$H_i\,(i=1,2,3)$	m_i^2	$\mathcal{O}^R_{i1}R_1+\mathcal{O}^R_{i2}R_2+\mathcal{O}^R_{i3}R_3$
J	0	$\mathcal{O}^I_{11}I_1+\mathcal{O}^I_{12}I_2+\mathcal{O}^I_{13}I_3$
G^0	0	$\mathcal{O}^I_{22}I_2+\mathcal{O}^I_{23}I_3$
A	$\kappa\left(\frac{v_2^2v_1^2+v_2^2v_3^2+4v_3^2v_1^2}{2v_3v_1}\right)$	$\mathcal{O}^I_{31}I_1+\mathcal{O}^I_{32}I_2+\mathcal{O}^I_{33}I_3$
$G^\pm$	0	$c_\pm\phi^\pm+s_\pm\Delta^\pm$
$H^\pm$	$\frac{1}{4v_3}(2\kappa v_1-\lambda_5v_3)(v_2^2+2v_3^2)$	$-s_\pm\phi^\pm+c_\pm\Delta^\pm$
$\Delta^{\pm\pm}$	$\frac{1}{2v_3}(\kappa v_1v_2^2-2\lambda_4v_3^3-\lambda_5v_2^2v_3)$	$\Delta^{\pm\pm}$

Table 7.2: Scalar mass eigenstates in the model. $c_\pm = v_2/\sqrt{v_2^2+2v_3^2}$, $s_\pm = \sqrt{2}v_3/\sqrt{v_2^2+2v_3^2}$

7.B Appendix B: Loop functions

The one-loop function $f(\tau)$ used in eq. (7.37) is given by,

$$f(\tau)=\begin{cases}\arcsin^2(1/\sqrt{\tau}) & \text{if } \tau\geq 1\\ -\frac{1}{4}\left[\log\left(\frac{1+\sqrt{1-\tau}}{1-\sqrt{1-\tau}}\right)-i\pi\right]^2 & \text{if } \tau<1\end{cases} \tag{7.44}$$

The functions C_0^b and ΔB_0^b are given in terms of the Passarino-Veltman functions [54],

$$\begin{aligned} C_0^b &= C_0(m_Z^2,0,m_{H_a}^2,m_b^2,m_b^2,m_b^2)=-\frac{1}{m_b^2}I_2(\tau_b,\lambda_b),\\ \Delta B_0^b &= B_0(m_{H_a}^2,m_b^2,m_b^2)-B_0(m_Z^2,m_b^2,m_b^2)\\ &= -\frac{m_{H_a}^2-m_Z^2}{m_Z^2}-\frac{(m_{H_a}^2-m_Z^2)^2}{2m_a^2m_Z^2}I_1(\tau_b,\lambda_b)+2\frac{m_{H_a}^2-m_Z^2}{m_Z^2}I_2(\tau_b,\lambda_b) \end{aligned} \tag{7.45}$$

where $\lambda_b=4m_b^2/m_{H_a}^2$,

$$\begin{aligned} I_1(\tau,\lambda) &= \frac{\tau\lambda}{2(\tau-\lambda)}+\frac{\tau^2\lambda^2}{2(\tau-\lambda)^2}\left[f(\tau)-f(\lambda)\right]+\frac{\tau^2\lambda}{(\tau-\lambda)^2}\left[g(\tau)-g(\lambda)\right],\\ I_2(\tau,\lambda) &= -\frac{\tau\lambda}{2(\tau-\lambda)}\left[f(\tau)-f(\lambda)\right], \end{aligned} \tag{7.46}$$

and

$$g(\tau)=\begin{cases}\sqrt{\tau-1}\arcsin\sqrt{\tau} & \text{for } \tau\geq 1\\ \frac{1}{2}\sqrt{1-\tau}\left(\log\frac{1+\sqrt{1-\tau}}{1-\sqrt{1-\tau}}-i\pi\right) & \text{if } \tau<1\end{cases} \tag{7.47}$$

7.C Appendix C: Higgs boson couplings

	Vertex	Gauge Coupling
1	$H_1 W_\mu^+ W_\nu^-$	$i\frac{g^2}{2}(\mathcal{O}_{12}^R v_2 + 2\mathcal{O}_{13}^R v_3)\, g_{\mu\nu}$
2	$H_2 W_\mu^+ W_\nu^-$	$i\frac{g^2}{2}(\mathcal{O}_{22}^R v_2 + 2\mathcal{O}_{23}^R v_3)\, g_{\mu\nu}$
3	$H_3 W_\mu^+ W_\nu^-$	$i\frac{g^2}{2}(\mathcal{O}_{32}^R v_2 + 2\mathcal{O}_{33}^R v_3)\, g_{\mu\nu}$
4	$\Delta^{\pm\pm} W_\mu^\mp W_\nu^\mp$	$i2g^2\frac{v_3}{\sqrt{2}} g_{\mu\nu}$
5	$H^\pm W_\mu^\mp Z_\nu$	$i\frac{g^2}{c_W}\frac{c_\pm v_3}{\sqrt{2}} g_{\mu\nu}$
6	$G^\pm W_\mu^\mp Z_\nu$	$i\frac{g^2}{c_W}\left(\frac{v_2}{2}s_W^2 c_\pm + \frac{v_3}{\sqrt{2}}(1+s_W^2)s_\pm\right) g_{\mu\nu}$
7	$G^\pm W_\mu^\mp A_\nu$	$-iem_W g_{\mu\nu}$
8	$\Delta^{++}\Delta^{--} W_\mu^+ W_\nu^-$	$ig^2\, g_{\mu\nu}$
9	$H^+ H^- W_\mu^+ W_\nu^-$	$i\frac{g^2}{2}(1+3c_\pm^2)\, g_{\mu\nu}$
10	$G^+ G^- W_\mu^+ W_\nu^-$	$i\frac{g^2}{2}(1+3s_\pm^2)\, g_{\mu\nu}$
11	$H_1 H_1 W_\mu^+ W_\nu^-$	$i\frac{g^2}{2}(\mathcal{O}_{12}^{R\,2} + 2\mathcal{O}_{13}^{R\,2})\, g_{\mu\nu}$
12	$H_2 H_2 W_\mu^+ W_\nu^-$	$i\frac{g^2}{2}(\mathcal{O}_{22}^{R\,2} + 2\mathcal{O}_{23}^{R\,2})\, g_{\mu\nu}$
13	$H_3 H_3 W_\mu^+ W_\nu^-$	$i\frac{g^2}{2}(\mathcal{O}_{32}^{R\,2} + 2\mathcal{O}_{33}^{R\,2})\, g_{\mu\nu}$
14	$JJ W_\mu^+ W_\nu^-$	$i\frac{g^2}{2}(\mathcal{O}_{12}^{I\,2} + 2\mathcal{O}_{13}^{I\,2})\, g_{\mu\nu}$
15	$G^0 G^0 W_\mu^+ W_\nu^-$	$i\frac{g^2}{2}(\mathcal{O}_{22}^{I\,2} + 2\mathcal{O}_{23}^{I\,2})\, g_{\mu\nu}$
16	$AA W_\mu^+ W_\nu^-$	$i\frac{g^2}{2}(\mathcal{O}_{32}^{I\,2} + 2\mathcal{O}_{33}^{I\,2})\, g_{\mu\nu}$
17	$\Delta^{\pm\pm} H^\mp W_\nu^\mp$	$\mp igc_\pm\,(p_1-p_2)_\mu$
18	$\Delta^{\pm\pm} G^\mp W_\nu^\mp$	$\mp igs_\pm\,(p_1-p_2)_\mu$
19	$H_1 H^\pm W_\mu^\mp$	$\pm i\frac{g}{2}(s_\pm\mathcal{O}_{12}^R - \sqrt{2}c_\pm\mathcal{O}_{13}^R)\,(p_1-p_2)_\mu$
20	$H_2 H^\pm W_\mu^\mp$	$\pm i\frac{g}{2}(s_\pm\mathcal{O}_{22}^R - \sqrt{2}c_\pm\mathcal{O}_{23}^R)\,(p_1-p_2)_\mu$
21	$H_3 H^\pm W_\mu^\mp$	$\pm i\frac{g}{2}(s_\pm\mathcal{O}_{32}^R - \sqrt{2}c_\pm\mathcal{O}_{33}^R)\,(p_1-p_2)_\mu$
22	$H^\pm JW_\mu^\mp$	$\frac{g}{2}(s_\pm\mathcal{O}_{12}^I + \sqrt{2}c_\pm\mathcal{O}_{13}^I)\,(p_1-p_2)_\mu$
23	$G^0 H^\pm W_\mu^\mp$	$-\frac{g}{2}(s_\pm\mathcal{O}_{22}^I + \sqrt{2}c_\pm\mathcal{O}_{23}^I)\,(p_1-p_2)_\mu$
24	$AH^\pm W_\mu^\mp$	$-\frac{g}{2}(s_\pm\mathcal{O}_{32}^I + \sqrt{2}c_\pm\mathcal{O}_{33}^I)\,(p_1-p_2)_\mu$
25	$G^\pm H_1 W_\mu^\mp$	$\pm i\frac{g}{2}(c_\pm\mathcal{O}_{12}^R + \sqrt{2}s_\pm\mathcal{O}_{13}^R)\,(p_1-p_2)_\mu$
26	$G^\pm H_2 W_\mu^\mp$	$\pm i\frac{g}{2}(c_\pm\mathcal{O}_{22}^R + \sqrt{2}s_\pm\mathcal{O}_{23}^R)\,(p_1-p_2)_\mu$
27	$G^\pm H_3 W_\mu^\mp$	$\pm i\frac{g}{2}(c_\pm\mathcal{O}_{32}^R + \sqrt{2}s_\pm\mathcal{O}_{33}^R)\,(p_1-p_2)_\mu$
28	$G^\pm JW_\mu^\mp$	$-\frac{g}{2}(c_\pm\mathcal{O}_{12}^I - \sqrt{2}s_\pm\mathcal{O}_{13}^I)\,(p_1-p_2)_\mu$
29	$G^0 G^\pm W_\mu^\mp$	$\frac{g}{2}(c_\pm\mathcal{O}_{22}^I - \sqrt{2}s_\pm\mathcal{O}_{23}^I)\,(p_1-p_2)_\mu$
30	$AG^\pm W_\mu^\mp$	$\frac{g}{2}(c_\pm\mathcal{O}_{32}^I - \sqrt{2}s_\pm\mathcal{O}_{33}^I)\,(p_1-p_2)_\mu$

	Vertex	Gauge Coupling
31	$H_1 Z_\mu Z_\nu$	$i\frac{g^2}{2c_W^2}(\mathcal{O}_{12}^R v_2 + 4\mathcal{O}_{13}^R v_3)\, g_{\mu\nu}$
32	$H_2 Z_\mu Z_\nu$	$i\frac{g^2}{2c_W^2}(\mathcal{O}_{22}^R v_2 + 4\mathcal{O}_{23}^R v_3)\, g_{\mu\nu}$
33	$H_3 Z_\mu Z_\nu$	$i\frac{g^2}{2c_W^2}(\mathcal{O}_{32}^R v_2 + 4\mathcal{O}_{33}^R v_3)\, g_{\mu\nu}$
34	$\Delta^{++}\Delta^{--} Z_\mu Z_\nu$	$i\frac{2g^2}{c_W^2}(c_W^2 - s_W^2)^2\, g_{\mu\nu}$
35	$H^+ H^- Z_\mu Z_\nu$	$i\frac{g^2}{2c_W^2}(s_\pm^2(c_W^2 - s_W^2)^2 + 4s_W^4 c_\pm^2)\, g_{\mu\nu}$
36	$G^+ G^- Z_\mu Z_\nu$	$i\frac{g^2}{2c_W^2}(c_\pm^2(c_W^2 - s_W^2)^2 + 4s_W^4 s_\pm^2)\, g_{\mu\nu}$
37	$H_1 H_1 Z_\mu Z_\nu$	$i\frac{g^2}{2c_W^2}(\mathcal{O}_{12}^{R\,2} + 4\mathcal{O}_{13}^{R\,2})\, g_{\mu\nu}$
38	$H_2 H_2 Z_\mu Z_\nu$	$i\frac{g^2}{2c_W^2}(\mathcal{O}_{22}^{R\,2} + 4\mathcal{O}_{23}^{R\,2})\, g_{\mu\nu}$
39	$H_3 H_3 Z_\mu Z_\nu$	$i\frac{g^2}{2c_W^2}(\mathcal{O}_{32}^{R\,2} + 4\mathcal{O}_{33}^{R\,2})\, g_{\mu\nu}$
40	$JJ Z_\mu Z_\nu$	$i\frac{g^2}{2c_W^2}(\mathcal{O}_{12}^{I\,2} + 4\mathcal{O}_{13}^{I\,2})\, g_{\mu\nu}$
41	$G^0 G^0 Z_\mu Z_\nu$	$i\frac{g^2}{2c_W^2}(\mathcal{O}_{22}^{I\,2} + 4\mathcal{O}_{23}^{I\,2})\, g_{\mu\nu}$
42	$AA Z_\mu Z_\nu$	$i\frac{g^2}{2c_W^2}(\mathcal{O}_{32}^{I\,2} + 4\mathcal{O}_{33}^{I\,2})\, g_{\mu\nu}$
43	$\Delta^{++}\Delta^{--} Z_\mu$	$-\frac{ig}{c_W}(c_W^2 - s_W^2)\,(p_1-p_2)_\mu$
44	$H^- H^+ Z_\mu$	$\frac{ig}{2c_W}(s_\pm^2(c_W^2 - s_W^2) - 2s_W^2 c_\pm^2)\,(p_1-p_2)_\mu$
45	$G^- G^+ Z_\mu$	$\frac{ig}{2c_W}(c_\pm^2(c_W^2 - s_W^2) - 2s_W^2 s_\pm^2)\,(p_1-p_2)_\mu$
46	$H_1 J Z_\mu$	$-\frac{g}{2c_W}(\mathcal{O}_{12}^R\mathcal{O}_{12}^I - 2\mathcal{O}_{13}^R\mathcal{O}_{13}^I)\,(p_1-p_2)_\mu$
47	$G^0 H_1 Z_\mu$	$\frac{g}{2c_W}(\mathcal{O}_{12}^R\mathcal{O}_{22}^I - 2\mathcal{O}_{13}^R\mathcal{O}_{23}^I)\,(p_1-p_2)_\mu$
48	$AH_1 Z_\mu$	$\frac{g}{2c_W}(\mathcal{O}_{12}^R\mathcal{O}_{32}^I - 2\mathcal{O}_{13}^R\mathcal{O}_{33}^I)\,(p_1-p_2)_\mu$
49	$H_2 J Z_\mu$	$-\frac{g}{2c_W}(\mathcal{O}_{22}^R\mathcal{O}_{12}^I - 2\mathcal{O}_{23}^R\mathcal{O}_{13}^I)\,(p_1-p_2)_\mu$
50	$G^0 H_2 Z_\mu$	$\frac{g}{2c_W}(\mathcal{O}_{22}^R\mathcal{O}_{22}^I - 2\mathcal{O}_{23}^R\mathcal{O}_{23}^I)\,(p_1-p_2)_\mu$
51	$AH_2 Z_\mu$	$\frac{g}{2c_W}(\mathcal{O}_{22}^R\mathcal{O}_{32}^I - 2\mathcal{O}_{23}^R\mathcal{O}_{33}^I)\,(p_1-p_2)_\mu$
52	$H_3 J Z_\mu$	$-\frac{g}{2c_W}(\mathcal{O}_{32}^R\mathcal{O}_{12}^I - 2\mathcal{O}_{33}^R\mathcal{O}_{13}^I)\,(p_1-p_2)_\mu$
53	$G^0 H_3 Z_\mu$	$\frac{g}{2c_W}(\mathcal{O}_{32}^R\mathcal{O}_{22}^I - 2\mathcal{O}_{33}^R\mathcal{O}_{23}^I)\,(p_1-p_2)_\mu$
54	$AH_3 Z_\mu$	$\frac{g}{2c_W}(\mathcal{O}_{32}^R\mathcal{O}_{32}^I - 2\mathcal{O}_{33}^R\mathcal{O}_{33}^I)\,(p_1-p_2)_\mu$
55	$G^\mp H^\pm Z_\mu$	$\mp\frac{g}{2c_W}c_\pm s_\pm\,(p_1-p_2)_\mu$
56	$\Delta^{++}\Delta^{--} A_\mu A_\mu$	$8ie^2\, g_{\mu\nu}$
57	$H^- H^+ A_\mu A_\mu$	$i2e^2\, g_{\mu\nu}$
58	$G^- G^+ A_\mu A_\mu$	$i2e^2\, g_{\mu\nu}$
59	$\Delta^{++}\Delta^{--} A_\mu$	$-2ie\,(p_1-p_2)_\mu$
60	$H^+ H^- A_\mu$	$ie\,(p_1-p_2)_\mu$
61	$G^+ G^- A_\mu$	$ie\,(p_1-p_2)_\mu$
62	$\Delta^{++}\Delta^{--} A_\mu Z_\nu$	$4i\frac{eg}{c_W}(c_W^2 - s_W^2)\, g_{\mu\nu}$
63	$H^+ H^- A_\mu Z_\nu$	$i\frac{eg}{c_W}(s_\pm^2(c_W^2 - s_W^2) - 2c_\pm^2 s_W^2)\, g_{\mu\nu}$
64	$G^+ G^- A_\mu Z_\nu$	$i\frac{eg}{c_W}(c_\pm^2(c_W^2 - s_W^2) - 2s_\pm^2 s_W^2)\, g_{\mu\nu}$

Table 7.3: Feynman rules for the couplings of the Higgs bosons H_i to the gauge bosons.

BIBLIOGRAPHY

[1] G. Aad et al. (ATLAS Collaboration), *Observation of a new particle in the search for the Standard Model Higgs boson with the ATLAS detector at the LHC*, Phys.Lett. **B716** (2012) 1–29, arXiv:1207.7214 [hep-ex].

[2] G. Aad et al. (ATLAS Collaboration), *Measurements of Higgs boson production and couplings in the four-lepton channel in pp collisions at center-of-mass energies of 7 and 8 TeV with the ATLAS detector* (2014), arXiv:1408.5191 [hep-ex].

[3] V. Khachatryan et al. (CMS), *Precise determination of the mass of the Higgs boson and tests of compatibility of its couplings with the standard model predictions using proton collisions at 7 and 8 TeV*, Eur. Phys. J. **C75** (2015) 5 212, arXiv:1412.8662 [hep-ex].

[4] G. Aad et al. (ATLAS), *Measurements of the Higgs boson production and decay rates and coupling strengths using pp collision data at $\sqrt{s} = 7$ and 8 TeV in the ATLAS experiment* (2015), arXiv:1507.04548 [hep-ex].

[5] M. Baak et al., *The Electroweak Fit of the Standard Model after the Discovery of a New Boson at the LHC*, Eur. Phys. J. **C72** (2012) 2205, arXiv:1209.2716 [hep-ph].

[6] M. Baak et al. (Gfitter Group), *The global electroweak fit at NNLO and prospects for the LHC and ILC*, Eur. Phys. J. **C74** (2014) 3046, arXiv:1407.3792 [hep-ph].

[7] M. E. Peskin and T. Takeuchi, *New constraint on a strongly interacting higgs sector*, Phys. Rev. Lett. **65** (1990) 964–967, URL http://link.aps.org/doi/10.1103/PhysRevLett.65.964.

[8] G. Altarelli and R. Barbieri, *Vacuum polarization effects of new physics on electroweak processes*, Physics Letters B **253** (1991) 1 161 – 167, ISSN 0370-2693, URL http://www.sciencedirect.com/science/article/pii/0370269391913789.

[9] M. E. Peskin and T. Takeuchi, *Estimation of oblique electroweak corrections*, Phys. Rev. D **46** (1992) 381–409, URL http://link.aps.org/doi/10.1103/PhysRevD.46.381.

[10] A. Djouadi, *The Anatomy of electro-weak symmetry breaking. I: The Higgs boson in the standard model*, Phys.Rept. **457** (2008) 1–216, arXiv:hep-ph/0503172 [hep-ph].

[11] C. Bonilla, R. M. Fonseca and J. W. F. Valle, *Vacuum stability with spontaneous violation of lepton number* (2015), arXiv:1506.04031 [hep-ph].

[12] C. Bonilla, R. M. Fonseca and J. W. F. Valle, *Consistency of the triplet seesaw model revisited*, Phys. Rev. **D92** (2015) 7 075028, arXiv:1508.02323 [hep-ph].

[13] C. Bonilla, J. W. F. Valle and J. C. Romão, *Neutrino mass and invisible Higgs decays at the LHC*, Phys. Rev. **D91** (2015) 11 113015, arXiv:1502.01649 [hep-ph].

[14] J. Schechter and J. Valle, *Neutrino Decay and Spontaneous Violation of Lepton Number*, Phys.Rev. **D25** (1982) 774.

[15] A. S. Joshipura and J. Valle, *Invisible Higgs decays and neutrino physics*, Nucl.Phys. **B397** (1993) 105–122.

[16] M. A. Diaz, M. Garcia-Jareno, D. A. Restrepo and J. Valle, *Seesaw Majoron model of neutrino mass and novel signals in Higgs boson production at LEP*, Nucl.Phys. **B527** (1998) 44–60, arXiv:hep-ph/9803362 [hep-ph].

[17] Y. Chikashige, R. N. Mohapatra and R. Peccei, *Are There Real Goldstone Bosons Associated with Broken Lepton Number?*, Phys.Lett. **B98** (1981) 265.

[18] G. Gelmini and M. Roncadelli, *Left-Handed Neutrino Mass Scale and Spontaneously Broken Lepton Number*, Phys.Lett. **B99** (1981) 411.

[19] R. E. Shrock and M. Suzuki, *Invisible Decays of Higgs Bosons*, Phys. Lett. **B110** (1982) 250.

[20] S. M. Boucenna, S. Morisi and J. W. Valle, *The low-scale approach to neutrino masses*, Adv.High Energy Phys. **2014** (2014) 831598, arXiv:1404.3751 [hep-ph].

[21] J. Schechter and J. Valle, *Neutrino Masses in SU(2) x U(1) Theories*, Phys.Rev. **D22** (1980) 2227.

[22] K. Kannike, *Vacuum Stability Conditions From Copositivity Criteria*, Eur.Phys.J. **C72** (2012) 2093, arXiv:1205.3781 [hep-ph].

[23] K. A. Olive et al. (Particle Data Group), *Review of Particle Physics*, Chin. Phys. **C38** (2014) 090001.

[24] K. Choi and A. Santamaria, *Majorons and Supernova Cooling*, Phys.Rev. **D42** (1990) 293–306.

[25] V. Khachatryan et al. (CMS Collaboration), *Observation of the diphoton decay of the Higgs boson and measurement of its properties*, Eur.Phys.J. **C74** (2014) 10 3076, arXiv:1407.0558 [hep-ex].

[26] G. Aad et al. (ATLAS, CMS), *Combined Measurement of the Higgs Boson Mass in pp Collisions at $\sqrt{s} = 7$ and 8 TeV with the ATLAS and CMS Experiments*, Phys. Rev. Lett. **114** (2015) 191803, arXiv:1503.07589 [hep-ex].

[27] J. Abdallah et al. (DELPHI Collaboration), *Searches for neutral higgs bosons in extended models*, Eur.Phys.J. **C38** (2004) 1–28, arXiv:hep-ex/0410017 [hep-ex].

[28] *Measurements of the Higgs boson production and decay rates and constraints on its couplings from a combined ATLAS and CMS analysis of the LHC pp collision data at $\sqrt{s} = 7$ and 8 TeV*, Technical Report ATLAS-CONF-2015-044, CERN, Geneva (2015), URL http://cds.cern.ch/record/2052552.

[29] V. Khachatryan et al. (CMS), *Search for a Higgs Boson in the Mass Range from 145 to 1000 GeV Decaying to a Pair of W or Z Bosons* (2015), arXiv:1504.00936 [hep-ex].

[30] V. Khachatryan et al. (CMS), *Search for neutral MSSM Higgs bosons decaying to a pair of tau leptons in pp collisions*, JHEP **10** (2014) 160, arXiv:1408.3316 [hep-ex].

[31] G. Aad et al. (ATLAS), *Search for Scalar Diphoton Resonances in the Mass Range* $65-600$ *GeV with the ATLAS Detector in pp Collision Data at* $\sqrt{s} = 8\,TeV$, Phys. Rev. Lett. **113** (2014) 17 171801, arXiv:1407.6583 [hep-ex].

[32] V. Khachatryan et al. (CMS), *Search for diphoton resonances in the mass range from 150 to 850 GeV in pp collisions at* $\sqrt{s} = 8$ *TeV*, Phys. Lett. **B750** (2015) 494–519, arXiv:1506.02301 [hep-ex].

[33] G. Aad et al. (ATLAS), *Search for a CP-odd Higgs boson decaying to Zh in pp collisions at* $\sqrt{s} = 8$ *TeV with the ATLAS detector*, Phys. Lett. **B744** (2015) 163–183, arXiv:1502.04478 [hep-ex].

[34] J. Garayoa and T. Schwetz, *Neutrino mass hierarchy and Majorana CP phases within the Higgs triplet model at the LHC*, JHEP **03** (2008) 009, arXiv:0712.1453 [hep-ph].

[35] P. Fileviez Perez et al., *Testing a Neutrino Mass Generation Mechanism at the LHC*, Phys.Rev. **D78** (2008) 071301, arXiv:0803.3450 [hep-ph].

[36] P. Fileviez Perez et al., *Neutrino Masses and the CERN LHC: Testing Type II Seesaw*, Phys.Rev. **D78** (2008) 015018, arXiv:0805.3536 [hep-ph].

[37] F. del Aguila and J. A. Aguilar-Saavedra, *Distinguishing seesaw models at LHC with multi-lepton signals*, Nucl. Phys. **B813** (2009) 22–90, arXiv:0808.2468 [hep-ph].

[38] M. Aoki, S. Kanemura and K. Yagyu, *Testing the Higgs triplet model with the mass difference at the LHC*, Phys. Rev. **D85** (2012) 055007, arXiv:1110.4625 [hep-ph].

[39] A. G. Akeroyd and S. Moretti, *Enhancement of H to gamma gamma from doubly charged scalars in the Higgs Triplet Model*, Phys. Rev. **D86** (2012) 035015, arXiv:1206.0535 [hep-ph].

[40] P. S. Bhupal Dev, D. K. Ghosh, N. Okada and I. Saha, *125 GeV Higgs Boson and the Type-II Seesaw Model*, JHEP **03** (2013) 150, [Erratum: JHEP05,049(2013)], arXiv:1301.3453 [hep-ph].

[41] F. del Águila and M. Chala, *LHC bounds on Lepton Number Violation mediated by doubly and singly-charged scalars*, JHEP **03** (2014) 027, arXiv:1311.1510 [hep-ph].

[42] C.-H. Chen and T. Nomura, *Search for $\delta^{\pm\pm}$ with new decay patterns at the LHC*, Phys. Rev. **D91** (2015) 035023, arXiv:1411.6412 [hep-ph].

[43] S. Kanemura, M. Kikuchi, K. Yagyu and H. Yokoya, *Bounds on the mass of doubly-charged Higgs bosons in the same-sign diboson decay scenario*, Phys. Rev. **D90** (2014) 11 115018, arXiv:1407.6547 [hep-ph].

[44] Z.-L. Han, R. Ding and Y. Liao, *LHC Phenomenology of Type II Seesaw: Nondegenerate Case*, Phys. Rev. **D91** (2015) 093006, arXiv:1502.05242 [hep-ph].

[45] H. Sugiyama, K. Tsumura and H. Yokoya, *Discrimination of models including doubly charged scalar bosons by using tau lepton decay distributions*, Phys. Lett. **B717** (2014) 229–234, arXiv:1207.0179 [hep-ph].

[46] S. Chatrchyan et al. (CMS), *A search for a doubly-charged Higgs boson in pp collisions at $\sqrt{s} = 7$ TeV*, Eur. Phys. J. **C72** (2012) 2189, arXiv:1207.2666 [hep-ex].

[47] G. Aad et al. (ATLAS), *Search for doubly-charged Higgs bosons in like-sign dilepton final states at $\sqrt{s} = 7$ TeV with the ATLAS detector*, Eur. Phys. J. **C72** (2012) 2244, arXiv:1210.5070 [hep-ex].

[48] S. Kanemura, K. Yagyu and H. Yokoya, *First constraint on the mass of doubly-charged Higgs bosons in the same-sign diboson decay scenario at the LHC*, Phys. Lett. **B726** (2013) 316–319, arXiv:1305.2383 [hep-ph].

[49] S. Kanemura, M. Kikuchi, H. Yokoya and K. Yagyu, *LHC Run-I constraint on the mass of doubly charged Higgs bosons in the same-sign diboson decay scenario*, PTEP **2015** (2015) 051B02, arXiv:1412.7603 [hep-ph].

[50] V. Khachatryan et al. (CMS), *Study of vector boson scattering and search for new physics in events with two same-sign leptons and two jets*, Phys. Rev. Lett. **114** (2015) 5 051801, arXiv:1410.6315 [hep-ex].

[51] D. Fontes, J. C. Romão and J. P. Silva, *$h \to Z\gamma$ in the complex two Higgs doublet model*, JHEP **12** (2014) 043, arXiv:1408.2534 [hep-ph].

[52] G. Aad et al. (ATLAS), *Search for invisible decays of a Higgs boson using vector-boson fusion in pp collisions at $\sqrt{s} = 8$ TeV with the ATLAS detector* (2015), arXiv:1508.07869 [hep-ex].

[53] S. Chatrchyan et al. (CMS), *Search for invisible decays of Higgs bosons in the vector boson fusion and associated ZH production modes*, Eur. Phys. J. **C74** (2014) 2980, arXiv:1404.1344 [hep-ex].

[54] G. Passarino and M. J. G. Veltman, *One loop corrections for e^+e^- annihilation into $\mu^+\mu^-$ in the Weinberg model*, Nucl. Phys. **B160** (1979) 151–207, URL http://www.sciencedirect.com/science/article/pii/0550321379902347.

CHAPTER **8**

RELATING QUARKS AND LEPTONS WITH THE T_7 FLAVOUR GROUP

Authors: Cesar Bonilla, Stefano Morisi, Eduardo Peinado, Jose W.F. Valle.
Journal reference: Phys. Lett. B742 (2015) 99-106.

Abstract

In this letter we present a model for quarks and leptons based on T_7 as flavour symmetry, predicting a canonical mass relation between charged leptons and down-type quarks proposed earlier. Neutrino masses are generated through a Type-I seesaw mechanism, with predicted correlations between the atmospheric mixing angle and neutrino masses. Compatibility with oscillation results lead to lower bounds for the lightest neutrino mass as well as for the neutrinoless double beta decay rates, even for normal neutrino mass hierarchy.

8.1 Introduction

Ever since the discovery of the muon in the thirties particle physicists have wondered on a possible simple understanding of fermion mass and mixing patterns. The experimental confirmation of neutrino oscillations [1–4] has brought again the issue into the spotlight. Yet despite many attempts, so far the origin of neutrino mass and its detailed flavour structure remains one of the most well-kept secrets of nature. In particular the observed values of neutrino oscillation parameters [5] pose the challenge to figure out why lepton mixing angles are so different to those of quarks. Indeed the sharp differences between the flavour mixing parameters characterizing the quark and lepton sectors escalate the complexity of the flavour problem. Many extensions of the Standard Model (SM) have been proposed in order to induce nonzero neutrino masses [6] and to predict the oscillation parameters such as the neutrino mass ordering, the octant of the atmospheric mixing angle and the value of the CP-violating phase in the lepton sector.

A popular approach to tackle these issues is the use of discrete non-Abelian flavour symmetries which are known to be far more restrictive than Abelian ones [7]. In the literature there are many models based on, for instance, A_4 (the group of even permutations of a tetrahedron) whose simplest realizations predict zero reactor mixing angle and maximal atmospheric angle [8–10]. However, this nice prediction has now been experimentally ruled out [1–4] so that the corresponding models need to be revamped in order to account for observations [11].

A variety of possible predictions of flavour symmetry based models can be found, for instance [12]:

i) *neutrino mass sum rules* leading to restrictions on the effective mass parameter $|m_{ee}|$ characterizing neutrinoless double beta decay ($0\nu\beta\beta$) processes [13–16];

ii) *neutrino mixing sum rules* [17].

Here we concentrate on the alternative possibility of having *mass relations* in the charged fermion sector. For definiteness we focus on the relation in Eq.(8.1),

$$\frac{m_b}{\sqrt{m_d m_s}} \approx \frac{m_\tau}{\sqrt{m_e m_\mu}}. \tag{8.1}$$

This relation was suggested in [18–21] and can hold at the electroweak scale [1]. First we note that such a relation between down-type quark and

[1] In an early paper [22] Wilczek and Zee found, by using an $SU(2)_H$ symmetry, an extended mass relation $\frac{m_b}{\sqrt{m_d m_s}} = \frac{m_\tau}{\sqrt{m_e m_\mu}} = \frac{m_t}{\sqrt{m_u m_c}}$ which is now evidently ruled out.

charged lepton masses can be understood because of group structure, when there are three vacuum expectation values and only two invariant contractions (Yukawas) in the product, $\mathbf{3}\otimes\mathbf{3}\otimes\mathbf{3}$. For example, such relation can be obtained with other groups containing three-dimensional irreducible representations (irreps) such as, for example, $T_n \cong Z_n \rtimes Z_3$ (with $n = 7, 13, 19, 31, 43, 49$; [23]) as well as T'.

In what follows we build a flavour model for quarks and leptons based upon the smallest non-Abelian group after A_4, namely the flavour group T_7 [24–29] leading to the mass relation in Eq.(8.1). Neutrino masses are generated by implementing a Type-I seesaw [30] in contrast to the dimensional-five Weinberg operator approach used in previous Refs. [18, 19, 21]. We discuss the resulting phenomenological predictions, namely, a correlation between the lightest neutrino mass and the atmospheric angle, as well as lower bounds for the effective mass parameter $|m_{ee}|$ characterizing $0\nu\beta\beta$ decay for both neutrino mass orderings.

8.2 The model

Here we consider a model with the multiplet content in Table 8.1 where the SM electroweak gauge symmetry is crossed with a global flavour symmetry group T_7. The down-type quarks and leptons (left- and right-handed) transform as

	$\overline{L}$	ℓ_R	N_R	ν_R	$\overline{Q}$	d_R	u_{R_i}	H	φ_ν	φ_u	φ_d	ξ_ν
T_7	$\mathbf{3}$	$\mathbf{3}$	$\mathbf{3}$	$\mathbf{1}_0$	$\mathbf{3}$	$\mathbf{3}$	$\mathbf{1}_i$	$\mathbf{1}_0$	$\mathbf{3}$	$\bar{\mathbf{3}}$	$\mathbf{3}$	$\mathbf{1}_0$
$\mathbb{Z}_7$	a^3	a^3	a^5	a^2	a^3	a^3	a^2	1	a^4	a^2	a^1	a^3

Table 8.1: Matter assignments of the model where $a^7 = 1$.

triplets, RH up-type quarks transform as singlets while the SM Higgs is blind, as shown in Table 8.1. Then the Yukawa Lagrangian for the charged sector is given by,

$$\mathcal{L} = \frac{Y^\ell}{\Lambda}\overline{L}\ell_R H_d + \frac{Y^d}{\Lambda}\overline{Q}d_R H_d + \frac{Y^u}{\Lambda}\overline{Q}u_R H_u + h.c. \tag{8.2}$$

Here for simplicity we have omitted the flavour indices, and have defined $H_d \equiv H\varphi_d$, $H_u \equiv \tilde{H}\varphi_u$ and $\tilde{H} \equiv i\sigma_2 H^*$, where φ_a are T_7 flavon triplets and Λ is the scale at which these fields get their vacuum expectation values (vevs), $\langle\varphi_a\rangle$.

On the other hand, let us assume the existence of four RH-neutrinos accommodated as $\mathbf{3}\oplus\mathbf{1}_0$ under T_7 so that the Lagrangian for the neutrino sector becomes,

$$\mathcal{L}_\nu = \frac{Y_1^\nu}{\Lambda}\bar{L}N_R\tilde{H}_d + \frac{Y_2^\nu}{\Lambda}\bar{L}\nu_R H_u + \kappa_1 N_R N_R\varphi_\nu + \kappa_2\nu_R\nu_R\xi_\nu \tag{8.3}$$

where, $\tilde{H}_d \equiv \tilde{H}\overline{\varphi}_d$. Notice that the additional Abelian symmetry $\mathbb{Z}_7$ couples each T_7 flavon triplet with only one fermion sector (down-type, up-type or neutrino sector) , so that, flavons transform non-trivially under the discrete Abelian group and their charges are unrelated to each other by conjugation. Therefore, in some sense, the order of the $\mathbb{Z}_n$ symmetry is fixed by the Yukawa sector.

In what follows we will study the flavon potential for three distinct triplets under T_7. The second column of Table 8.2 shows the vacuum expectation value alignments allowed in T_7 [24, 31], with small deviations from those alignments shown in the third column.

Flavon	VEV Alignment in T_7	Model
φ_ν	$(1,1,0)$	$(1+\delta_{\nu_1}, 1, \delta_{\nu_2})$
φ_u	$(0,0,1)$	$(\delta_{u_1}, \delta_{u_2}, 1)$
φ_d	$(1,0,0)$	$(1, \delta_{d_1}, \delta_{d_2})$

Table 8.2: Vacuum expectation value alignments.

8.2.1 Flavon Potential

The Higgs scalar potential for a single T_7 flavon triplet, i.e. $\varphi \simeq \mathbf{3}$, is given by [24, 31]

$$V_s = -\mu_s^2 \sum_{i=1}^{3} \varphi_i^\dagger \varphi_i + \lambda_s \left(\sum_{i=1}^{3} \varphi_i^\dagger \varphi_i \right)^2 + \kappa_s \sum_{i=1}^{3} \varphi_i^\dagger \varphi_i \varphi_i^\dagger \varphi_i. \tag{8.4}$$

where the possible vacuum expectation value alignments are, see Appendix 8.A,

$$\begin{aligned} \langle \varphi \rangle &\sim \tfrac{1}{\sqrt{3}}(1,1,1) \quad \text{for} \quad \kappa_s > 0 \quad \text{and} \\ \langle \varphi \rangle &\sim (1,0,0), (0,1,0), (0,0,1) \quad \text{for} \quad \kappa_s < 0. \end{aligned} \tag{8.5}$$

In our case, ignoring the singlet ξ_ν, there are three triplets, φ_u, φ_d and φ_ν, with an additional $\mathbb{Z}_7$ charge so that the flavon potential is given as

$$V' = V_\nu + V_d + V_u + V_{\text{mix}}, \tag{8.6}$$

where V_α (with $\alpha = \nu, d, u$) are given by Eq.(8.29). Then, in components, V_α contain the triplet elements φ_{α_i} and the parameters μ_α^2, λ_α and κ_α. The mixing part of the potential is the following

$$\begin{aligned} V_{\text{mix}} &= \kappa_{12} \left| \sum_{i=1}^{3} \varphi_{\nu_i}^\dagger \varphi_{u_i} \right|^2 + \kappa_{13} \left| \sum_{i=1}^{3} \varphi_{\nu_i}^\dagger \varphi_{d_i} \right|^2 + \kappa_{23} \left| \sum_{i=1}^{3} \varphi_{d_i}^\dagger \varphi_{u_i} \right|^2 \\ &+ \kappa_{123} \left(\varphi_\nu \varphi_u \varphi_d + h.c. \right). \end{aligned} \tag{8.7}$$

The vev configuration written down in the second column of Table 8.2 is a minimum of the potential Eq.(8.6) when $\kappa_\nu > 0$, $\kappa_u < 0$ and $\kappa_d < 0$ and the terms κ_{13} and κ_{123}, are suppressed.[2] Notice that some vevs are orthogonal (namely, $\langle\varphi_\nu\rangle \perp \langle\varphi_u\rangle$ and $\langle\varphi_u\rangle \perp \langle\varphi_d\rangle$). This property of the vevs has been described in [31, 32]. In order to ensure a realistic model we assume small deviations from the vev canonical alignments in the middle column in Table 8.2. Such deviations can be induced by adding soft breaking terms in the flavon potential, Eq.(8.6).

8.2.2 Mass relation in down-type sector

As usual, one obtains the fermion mass matrices after electroweak symmetry breaking from the Lagrangian in Eq.(8.2). Given the T_7 multiplication rules (see Appendix 8.B), one finds that the down–type quarks and the charged lepton mass matrices turn out to have the form

$$M_f = \begin{pmatrix} 0 & e^{i\theta_f} y_1^f v_3 & y_2^f v_2 \\ y_2^f v_3 & 0 & e^{i\theta_f} y_1^f v_1 \\ e^{i\theta_f} y_1^f v_2 & y_2^f v_1 & 0 \end{pmatrix}, \tag{8.8}$$

where $f = \ell, d$ and θ_f are unremovable phases contributing to CP-violation in the lepton and quark sector. In addition, we have used the following parameterization,

$$\frac{\langle\varphi_d\rangle\langle H\rangle}{\Lambda} \approx (v_1, v_2, v_3). \tag{8.9}$$

It should be noticed that the matrices M_f in Eq.(8.8) have the same structure as those obtained with A_4 as flavour symmetry [18, 19, 21, 33]. It is useful to rewrite Eq.(8.8) in the following way,

$$M_f = \begin{pmatrix} 0 & e^{i\theta_f} a^f \alpha^f & b^f \\ b^f \alpha^f & 0 & e^{i\theta_f} a^f r^f \\ e^{i\theta_f} a^f & b^f r^f & 0 \end{pmatrix}, \tag{8.10}$$

where

$$a^f = y_1^f v_2, \quad b^f = y_2^f v_2, \quad \alpha^f = v_3/v_2 \quad \text{and} \quad r^f = v_1/v_2. \tag{8.11}$$

[2] The term proportional to κ_{13} in the potential could be suppressed by adding a term like $-\mu_{13}^2(\varphi_\nu^\dagger \varphi_d + h.c.)$ which softly breaks Z_7. The trilinear term can be forbidden by invoking an additional parity transformation over the fields.

Following the reasoning in [18, 19, 21] we consider the invariants of $M_f M_f^\dagger$ and obtain, at leading order in the limit $r^f >> \alpha^f, 1$ and $r^f >> b^f/a^f$,

$$\begin{aligned} (b^f r^f)^2 &\approx m_3^2, && (8.12)\\ b^{f\,6} r^{f\,2} \alpha^{f\,2} &\approx m_1^2 m_2^2 m_3^2, && (8.13)\\ a^{f\,2} b^{f\,2} r^{f\,4} &\approx m_2^2 m_3^2. && (8.14) \end{aligned}$$

Then, solving the last system of equations, Eqs.(8.12-8.14), one gets

$$a^f \approx \frac{m_2}{m_3}\sqrt{\frac{m_1 m_2}{\alpha^f}}, \quad b^f \approx \sqrt{\frac{m_1 m_2}{\alpha^f}}, \quad \text{and} \quad r^f \approx m_3\sqrt{\frac{\alpha^f}{m_1 m_2}}. \tag{8.15}$$

From Eq.(8.15) and the fact that the same flavon is coupled to the down-type quarks and charged leptons we are led to the mass relation in Eq.(8.1),

$$\frac{m_b}{\sqrt{m_d m_s}} \approx \frac{m_\tau}{\sqrt{m_e m_\mu}}.$$

It is worth mentioning that even when the phases θ_f appear in the invariant $\det|M_f M_f^\dagger|$ with $f = \ell, d$, that is in Eq.(8.13), the mass relation is preserved.

8.2.3 Quark mixing

From the Yukawa Lagrangian in Eq.(8.2) we have that after electroweak symmetry breaking the mass matrices for up- and down-type quarks are, respectively,

$$M_u = \begin{pmatrix} y_1^u u_1 & y_2^u u_1 & y_3^u u_1 \\ y_1^u u_2 & \omega y_2^u u_2 & \omega^2 y_3^u u_2 \\ y_1^u u_3 & \omega^2 y_2^u u_3 & \omega y_3^u u_3 \end{pmatrix} \quad \text{and} \quad M_d = \begin{pmatrix} 0 & e^{i\theta_d} a^d \alpha^d & b^d \\ b^f \alpha^d & 0 & e^{i\theta_d} a^d r^d \\ e^{i\theta_d} a^d & b^d r^d & 0 \end{pmatrix}, \tag{8.16}$$

where the parameters a^d, b^d and r^d are given by Eq.(8.15), with $\omega^3 = 1$ and the vevs u_i $(i = 1, 2, 3)$ defined through the parameterization

$$\frac{\langle \varphi_u \rangle \langle H \rangle}{\Lambda} \approx (u_1, u_2, u_3), \tag{8.17}$$

It is useful to rewrite the vevs as follows,

$$(u_1, u_2, u_3) = u_3 \left(\frac{u_1}{u_3}, \frac{u_2}{u_3}, 1\right) = u_3(\alpha_1, \alpha_2, 1), \tag{8.18}$$

in that way there are 10 free parameters in the quark sector, listed in Table 8.3. These parameters determine the six quark masses, the three CKM mixing angles and the quark CP-violating phase.

10 free parameters	a^d	b^d	r^d	y_1^u	y_2^u	y_3^u	α^d	α_1	α_2	θ_d

Table 8.3: Parameters characterizing the quark sector.

In Ref. [21] an A_4 flavour symmetry model was built leading to our mass formula in Eq. (8.1). The mass and CKM mixing parameters describing the quark sector, very similar to those in Eq.(8.16), were successfully reproduced, as seen in in Table II in [21], assuming trivial phases, namely $\theta_d = 0, \pi$ in Eq.(8.16). However, even in this trivial case there is CP-violation due to the complex phase ω. Here for simplicity we just take advantage of the results given in [21] for the quark sector of our current T_7 model. Therefore we use the following values, given in the aforementioned A_4 model,

$$\begin{aligned} r^d = 263.44\text{MeV}, \quad & y_1^u u_3 = -297393\,\text{MeV}, \\ a^d = 0.21\text{MeV}, \quad & y_2^u u_3 = -15563\,\text{MeV} \\ b^d = 10.73\text{MeV}, \quad & y_3^u u_3 = 277\,\text{MeV} \\ \alpha^d = \tfrac{v_3}{v_2} = 1.58, \quad & \alpha_1 = \tfrac{u_1}{u_3} = 2.14\lambda^4, \\ \theta_d = \pi, \quad \text{and} \quad & \alpha_2 = \tfrac{u_2}{u_3} = 1.03\lambda^2, \end{aligned} \tag{8.19}$$

and where $\lambda = 0.2$ the Cabibbo angle. The parameters r^d, a^d and b^d can be computed by carrying out a substitution of (m_1, m_2, m_3) with the actual values of the down-type quark masses (m_d, m_s, m_b) in Eq.(8.15). One can verify with ease that the predictions for the CKM mixing matrix, quark masses and CP-violation are in agreement with the experimental data [34]. Now we proceed to study the lepton sector, for which some of the parameters will be fixed by the fit in the quark sector, namely the parameters α^d and r^d.

8.2.4 Lepton mixing

As we saw above, the spontaneous breaking of the electroweak symmetry yields the following form for the charged lepton mass matrix,

$$M_\ell = \begin{pmatrix} 0 & e^{i\theta_\ell} a^\ell \alpha^\ell & b^\ell \\ b^\ell \alpha^\ell & 0 & e^{i\theta_\ell} a^\ell r^\ell \\ e^{i\theta_\ell} a^\ell & b^\ell r^\ell & 0 \end{pmatrix}, \tag{8.20}$$

where, from the T_7 multiplication rules in the appendix one finds,

$$a^\ell = y_1^\ell v_2, \quad b^\ell = y_2^\ell v_2, \quad \alpha^\ell = v_3/v_2 \quad \text{and} \quad r^\ell = v_1/v_2. \tag{8.21}$$

On the other hand, as mentioned in the introduction, here we adopt a Type-I seesaw approach for generating the neutrino masses. This is in contrast to

previous models leading to the mass formula in Eq.(8.1) from the A_4 group. In those schemes an effective dimension-five operator approach was employed. In the present case the neutrino mass matrix is given by,

$$M_\nu = -M_D M_{RR}^{-1} M_D^T \tag{8.22}$$

where,

$$M_D = \begin{pmatrix} Y_1^\nu v_2 & 0 & 0 & e^{i\theta_1} Y_2^\nu u_1 \\ 0 & Y_1^\nu v_3 & 0 & e^{i\theta_1} Y_2^\nu u_2 \\ 0 & 0 & Y_1^\nu v_1 & e^{i\theta_1} Y_2^\nu u_3 \end{pmatrix} \quad \text{and} \quad M_{RR} = \begin{pmatrix} 0 & M_3 & M_2 & 0 \\ M_3 & 0 & M_1 & 0 \\ M_2 & M_1 & 0 & 0 \\ 0 & 0 & 0 & e^{i\theta_2} M_4 \end{pmatrix}, \tag{8.23}$$

where $M_i = \kappa_1 \langle \varphi_\nu \rangle_i$ (for $i = 1, 2, 3$) and $M_4 = \kappa_2 \langle \xi_\nu \rangle$. The real matrix elements M_i satisfy $M_1 \sim M_2 \gg M_3$, Table 8.2. Notice that for complex Yukawas the mass matrices M_D and M_{RR} in Eq.(8.23) only depend on one unremovable phase.

In order to implement the vev alignments in Table 8.2 we assume that the vevs u_i and v_i in Eq.(8.23) satisfy $u_3 \gg u_{1,2}$ and $v_1 \gg v_{2,3}$. The former vev hierarchy has to do with the fit in the quark sector and the latter comes from the mass relation $r^d \gg \alpha^d, 1$. Then, the vev alignments can be rewritten as follows,

$$\begin{array}{rcrcl} u_3(\frac{u_1}{u_3}, \frac{u_2}{u_3}, 1) & = & u(\alpha_1, \alpha_2, 1) & \propto & (\delta_{u_1}, \delta_{u_2}, 1), \\ v_2(\frac{v_1}{v_2}, 1, \frac{v_3}{v_2}) & = & v(r^d, 1, \alpha^d) & \propto & (1, \delta_{d_1}, \delta_{d_2}), \\ M_3(\frac{M_1}{M_3}, \frac{M_2}{M_3}, 1) & = & M(\epsilon_1 R, R, 1) & \propto & (1 + \delta_{\nu_1}, 1, \delta_{\nu_2}) \end{array} \tag{8.24}$$

where $\alpha_1 = 2.14\lambda^4$, $\alpha_2 = 1.03\lambda^2$, $\lambda = 0.2$ and we have defined $u_3 = u$, $v_2 = v$ and $M_3 = M$.

Therefore, using Eqs. (8.23-8.24), the light neutrino mass matrix after the seesaw mechanism turns out to be

$$M_\nu = \kappa \begin{pmatrix} \epsilon_1 - 2e^{-i\theta_\nu}\alpha_1^2\epsilon_2 & -\alpha^d - 2e^{-i\theta_\nu}\alpha_1\alpha_2\epsilon_2 & -\epsilon_3 - 2e^{-i\theta_\nu}\alpha_1\epsilon_2 \\ \cdot & \frac{\alpha^d 2}{\epsilon_1} - 2e^{-i\theta_\nu}\alpha_2^2\epsilon_2 & -\frac{\alpha^d \epsilon_3}{\epsilon_1} - 2e^{-i\theta_\nu}\alpha_2\epsilon_2 \\ \cdot & \cdot & -2e^{-i\theta_\nu}\epsilon_2 + \frac{\epsilon_3^2}{\epsilon_1} \end{pmatrix}, \tag{8.25}$$

which is symmetric and $\alpha_1 = 2.14\lambda^4$, $\alpha_2 = 1.03\lambda^2$, $\lambda = 0.2$ and we have defined,

$$\begin{array}{c} \kappa \equiv \frac{(Y^\nu v)^2}{M}, \quad \epsilon_2 \equiv \frac{M(Y_2^\nu u)^2}{M_4 (Y_1^\nu v)^2}, \quad \epsilon_3 \equiv \frac{r^d}{R} \\ \text{and} \quad \theta_\nu \equiv -2\theta_1 + \theta_2. \end{array} \tag{8.26}$$

It is important to note that some parameters in the neutrino mass matrix are fixed by the fit in the quark sector. In Table 8.4 we list the parameters in

Parameters in the lepton sector	a^ℓ	b^ℓ	r^d	α^d	α_1	α_2	ϵ_1	ϵ_2	ϵ_3	θ_ℓ	θ_ν
Fixed			✓	✓	✓	✓					
Free	✓	✓					✓	✓	✓	✓	✓

Table 8.4: Parameters in the lepton sector.

the lepton sector denoting as "fixed" those determined by the fit in the quark sector. Bear in mind that down-type quarks and charged leptons couple to the same flavon φ_d and hence, $\alpha^d = \alpha^\ell$ and $r^d = r^\ell$. This is the origin of the mass relation in Eq. (8.1).

Gathering all we have in the lepton sector we can compute the lepton mixing matrix,

$$U = U_\ell^\dagger U_\nu \tag{8.27}$$

where U_ℓ and U_ν are the matrices that diagonalize the charged and neutral mass matrices, $M_\ell^2 \equiv M_\ell M_\ell^\dagger$ and $M_\nu^2 \equiv M_\nu M_\nu^\dagger$, respectively. Remind that M_ℓ is the matrix in Eq.(8.20) with one unremovable phase θ_ℓ.

8.3 Results

In our analysis, we have varied for instance ϵ_i in the range $[0, 5]$ and the phases $\theta_{\ell,\nu}$ in the range $[0, 2\pi]$. We make use of the neutrino mass matrix invariants $\mathrm{tr}M_\nu^2$, $\det M_\nu^2$ and $(\mathrm{tr}M_\nu^2)^2 - \mathrm{tr}(M_\nu^4)$ and choose to rewrite the three neutrino masses in terms of the square mass differences $\Delta m^2_{\mathrm{atm}}$ and $\Delta m^2_{\mathrm{sol}}$ and the lightest neutrino mass, m_1 for the case of normal hierarchy and m_3 for inverted hierarchy. We now sum up all our results.

The panel on the left in Fig.8.1 shows the correlation between the atmospheric angle for normal hierarchy (NH, i.e. $|m_3| > |m_2| > |m_1|$) and the sum of neutrino masses (defined as $\Sigma \equiv |m_1| + |m_2| + |m_3|$). We find that there is a lower bound for the lightest neutrino mass and that the first octant is favored by lighter neutrino masses. For reference we also display the constraint coming from the combination of cosmological CMB data from Planck and WMAP, including baryon acoustic oscillations (BAO) data from [35]. If taken at face value such stringent cosmological bound would disfavor not only heavy neutrinos but also the best fit value for the atmospheric angle lying in second octant [5].

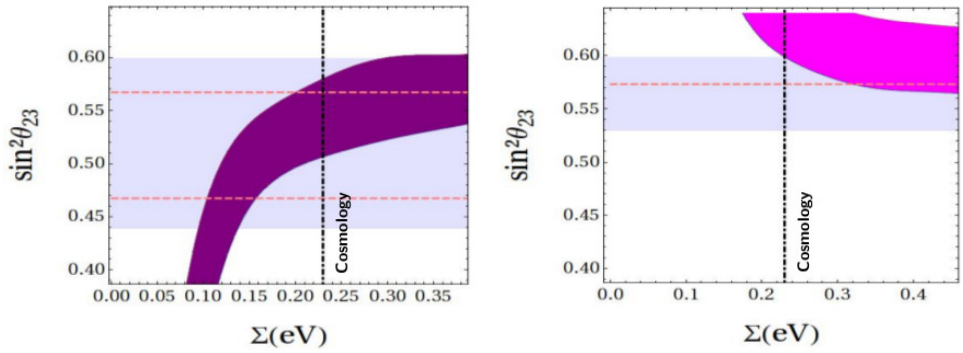

Figure 8.1: Left panel: Correlation between the atmospheric angle and the sum of neutrino masses Σ for the normal hierarchy case. Right panel: Correlation between the atmospheric angle and Σ when assuming inverted hierarchy. The horizontal dotted lines denote the best fit values for the atmospheric angle [5] while the horizontal bands are allowed at 1σ. The vertical dot-dashed line is the cosmological bound from the combination of CMB and BAO data [35]

On the other hand, a similar correlation between the atmospheric angle and the sum of neutrino masses, Σ, is also found for the inverted hierarchy case (IH, i.e. $|m_2| > |m_1| > |m_3|$). This is shown on the right panel of Fig.8.1 where the dot-dashed vertical line is the constraint coming from the same combination of cosmological data [35]. Taking the most stringent cosmological (BAO) bound into account as well as the oscillation results one sees that, at 1σ, this case would be disfavored. Indeed, if this cosmological bound is taken at face value, the second octant would be excluded for inverse hierarchy. However, as seen in Fig. 8.2, at 3σ the second octant is certainly allowed for inverted hierarchy. The resulting lower bound for the lightest neutrino mass is much tighter than the one that holds for normal hierarchy. For comparison we also display the future sensitivity of the KATRIN experiment on tritium beta decay, $\Sigma \simeq 0.6$ eV, [36].

In summary, one sees that for both hierarchies our model implies a correlation between the atmospheric angle and the lightest neutrino mass. The current neutrino oscillation experiments lead to a lower bound for m_1.

Such a lower bounds have implications for the effective mass parameter $|m_{ee}|$ specifying the neutrinoless double beta – $0\nu\beta\beta$ – decay amplitude.

Let us now turn to the implications for $0\nu\beta\beta$. In Fig. (8.2) we plot the effective parameter $|m_{ee}|$ as function of the lightest neutrino mass. The NH case corresponds to the purple/dark region, while the IH case is denoted by the magenta/light region, respectively. The vertical dot-dashed line and labeled as "Cosmology" represents the constraint coming from the combination of CMB data [35], as well as the future sensitivity of KATRIN [36] indicated by the vertical dotted line.

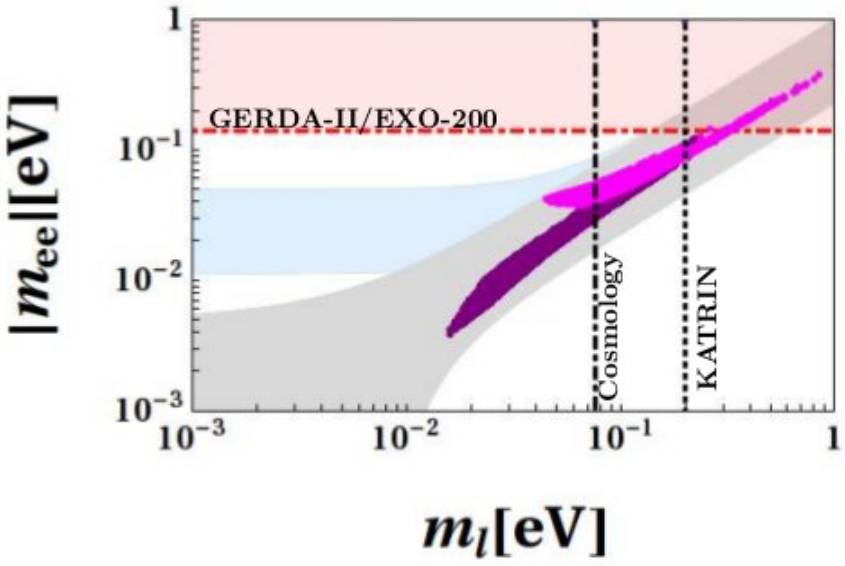

Figure 8.2: Effective neutrino mass parameter $|m_{ee}|$ versus the lightest neutrino mass for normal (purple/dark region) and inverted (magenta/light region) hierarchies. The vertical dotdashed line and labeled as "Cosmology" denotes the bound from the combination of CMB and BAO data [35]. The vertical dotted line is the future sensitivity of KATRIN, [36]. Here the oscillation constraints are taken at 3σ [5].

8.4 Conclusions

In this paper we have suggested a model based on the flavour symmetry group T_7 leading to a very successful canonical mass relation between charged leptons and down-type quarks proposed in [18, 19, 21]. Previous papers predicting this mass relation have adopted the A_4 flavour symmetry and assumed that neutrino masses were generated through higher order operators. In our T_7 model the neutrino masses are generated through the conventional Type-I seesaw mechanism.

The model leads to a correlation between the lightest neutrino mass and the atmospheric angle. This correlation implies lower bounds for the lightest neutrino mass which come from applying the neutrino oscillation constraints. These bounds on the lightest neutrino mass also translate to lower bounds on the effective amplitude parameter $|m_{ee}|$ characterizing $0\nu\beta\beta$ decay for both neutrino mass hierarchies.

Acknowledgments

Work supported by the Spanish grants FPA2011-22975 and Multidark CSD2009-00064 (MINECO), and PROMETEOII/2014/084 (Generalitat Valenciana).

8.A Appendix A: Vacuum Alignments

Let us assume that the vev of the T_7 flavon triplet is real and that the field is shifted as,

$$\varphi_i = u_i + \phi_i. \tag{8.28}$$

The flavon potential is given by [24],

$$V_s = -\mu_s^2 \sum_{i=1}^{3} \varphi_i^\dagger \varphi_i + \lambda_s \left(\sum_{i=1}^{3} \varphi_i^\dagger \varphi_i \right)^2 + \kappa_s \sum_{i=1}^{3} \varphi_i^\dagger \varphi_i \varphi_i^\dagger \varphi_i, \tag{8.29}$$

where $\lambda_s > 0$. The minimization conditions are obtained by taking,

$$\left. \frac{\partial V_s}{\partial \varphi_i} \right|_{\varphi_i \to 0} = 0, \tag{8.30}$$

which leads to the following system of equations,

$$\begin{aligned} -\mu^2 + 2(\kappa_s + \lambda_s)u_1^2 + 2\lambda_s(u_2^2 + u_3^2) &= 0 \\ -\mu^2 + 2(\kappa_s + \lambda_s)u_2^2 + 2\lambda_s(u_1^2 + u_3^2) &= 0 \\ -\mu^2 + 2(\kappa_s + \lambda_s)u_3^2 + 2\lambda_s(u_1^2 + u_2^2) &= 0. \end{aligned} \tag{8.31}$$

One set of minimization conditions is obtained by solving (8.31) for instance for μ^2, u_2 and u_3 ,

$$\begin{aligned} a) \quad & \mu^2 = 2(\kappa_s + 3\lambda_s)u_1^2, \quad u_2 = u_3 = u_1; \\ b) \quad & \mu^2 = 2(\kappa_s + \lambda_s)u_1^2, \quad u_2 = u_3 = 0; \\ c) \quad & \mu^2 = 2(\kappa_s + 2\lambda_s)u_1^2, \quad u_2 = u_1 \ \text{ and } \ u_3 = 0, \end{aligned} \tag{8.32}$$

which can be translated in the following alignments, $\langle \varphi \rangle \equiv (u_1, u_2, u_3) \sim (1,1,1)$, $\langle \varphi \rangle \sim (1,0,0)$ and $\langle \varphi \rangle \sim (1,1,0)$, respectively. In order to characterize each case in (8.32) as a local minimum we compute the Hessian matrix,

$$\mathcal{H} = \left. \frac{\partial^2 V_s}{\partial \varphi_i \partial \varphi_j} \right|_{\varphi_i \to 0}, \tag{8.33}$$

and verify its positivity, that is all its eigenvalues are positive. For case a) the Hessian matrix turns out to be,

$$\mathcal{H}_a = 8u_1^2 \begin{pmatrix} (\kappa_s + \lambda_s) & \lambda_s & \lambda_s \\ \lambda_s & (\kappa_s + \lambda_s) & \lambda_s \\ \lambda_s & \lambda_s & (\kappa_s + \lambda_s) \end{pmatrix}. \tag{8.34}$$

The eigenvalues of $\mathcal{H}_a$ are, $8u_1^2(\kappa_s, \kappa_s, \kappa_s + 3\lambda_s)$ which are positive iff $\kappa_s > 0$. For b) we have,

$$\mathcal{H}_b = 4u_1^2 \begin{pmatrix} 2(\kappa_s + \lambda_s) & 0 & 0 \\ 0 & -\kappa_s & 0 \\ 0 & 0 & -\kappa_s \end{pmatrix}, \tag{8.35}$$

which is positive definite if $-\lambda_s < \kappa_s < 0$. Finally, in the last case we have,

$$\mathcal{H}_c = 4u_1^2 \begin{pmatrix} 2(\kappa_s + \lambda_s) & 2\lambda_s & 0 \\ 2\lambda_s & 2(\kappa_s + \lambda_s) & 0 \\ 0 & 0 & -\kappa_s \end{pmatrix}. \tag{8.36}$$

The eigenvalues of $\mathcal{H}_c$ are given by, $4u_1^2(2\kappa_s, 2(\kappa_s + 2\lambda_s), -\kappa_s)$. Therefore, we have that the only possible *global* minima are,

$$\begin{aligned} a) \quad & \langle\varphi\rangle \sim (\pm 1, \pm 1, \pm 1) \ \text{ for } \ \kappa_s > 0, \\ b) \quad & \langle\varphi\rangle \sim (\pm 1, 0, 0) \ \text{ for } \ -\lambda_s < \kappa_s < 0 \end{aligned}$$

up to sign permutations in the former and permutations of the non-zero value in the latter. These other possibilities lead to degenerate vacua. In the realistic case of our model there are other terms in the potential including T_7 symmetry breaking terms needed to generate δs in Table 8.2. In general these are expected to lift the degeneracies of the above minima.

8.B Appendix B: T_7 group basics

The group T_7 is a subgroup of $SU(3)$ with 21 elements and isomorphic to $\mathbb{Z}_7 \rtimes \mathbb{Z}_3$. This group has five irreducible representations (e.i., $\mathbf{1}_0$, $\mathbf{1}_1$, $\mathbf{1}_2$, $\mathbf{3}$ and $\bar{\mathbf{3}}$) and is known as the smallest group containing a complex triplet. The multiplication rules in T_7 are the following,

$$\begin{aligned} & \mathbf{3} \otimes \mathbf{3} = \mathbf{3} \oplus \bar{\mathbf{3}} \oplus \bar{\mathbf{3}}, \quad \mathbf{3} \otimes \mathbf{3} = \bar{\mathbf{3}} \oplus \mathbf{3} \oplus \mathbf{3}, \\ & \mathbf{3} \otimes \bar{\mathbf{3}} = \sum_{\mathbf{a}=\mathbf{0}}^{\mathbf{2}} \mathbf{1_a} \oplus \mathbf{3} \oplus \bar{\mathbf{3}} \ \text{ and } \ \mathbf{3} \otimes \mathbf{1} = \mathbf{3}. \end{aligned} \tag{8.37}$$

8.B Appendix B: T_7 group basics

Let $\mathbf{X}^a = (x_1^a, x_2^a, x_3^a)^T$, $\bar{\mathbf{X}}^a = (\bar{x}_1^a, \bar{x}_2^a, \bar{x}_3^a)^T$, and $\mathbf{z}_i$ (with $i = 0, 1, 2$), be triplets, anti-triplets and singlets, respectively, under T_7 then these elements are multiplied as follows:

- $$\mathbf{X} \times \mathbf{X}' = \mathbf{X}'' + \bar{\mathbf{X}} + \bar{\mathbf{X}}', \quad \text{where} \quad \mathbf{X}'' = (x_3 x_3', x_1 x_1', x_2 x_2'),$$
$$\bar{\mathbf{X}} = (x_2 x_3', x_3 x_1', x_1 x_2') \text{and} \quad \bar{\mathbf{X}}' = (x_3 x_2', x_1 x_3', x_2 x_1'), \tag{8.38}$$
- $$\mathbf{X} \times \bar{\mathbf{X}} = \sum_{a=0}^{2} \mathbf{z}_a + \mathbf{X}' + \bar{\mathbf{X}}', \quad \text{where} \quad z_a = x_1 \bar{x}_1 + \omega^{2a} x_2 \bar{x}_2 + \omega^a x_3 \bar{x}_3,$$
$$\mathbf{X}' = (x_2 \bar{x}_1, x_3 \bar{x}_2, x_1 \bar{x}_3), \quad \text{and} \quad \bar{\mathbf{X}}' = (x_1 \bar{x}_2, x_2 \bar{x}_3, x_3 \bar{x}_1), \tag{8.39}$$
- $$\mathbf{z}_a \times \mathbf{X} = \mathbf{X}' \quad \text{where} \quad \mathbf{X}' = (z_a x_1, \omega^a z_a x_2, \omega^{2a} z_a x_3). \tag{8.40}$$

For more details about the group T_7 see for instance, Refs. [23–25].

BIBLIOGRAPHY

[1] P. Adamson et al. (MINOS Collaboration), *Improved search for muon-neutrino to electron-neutrino oscillations in MINOS*, Phys.Rev.Lett. **107** (2011) 181802, arXiv:1108.0015 [hep-ex].

[2] F. An et al. (DAYA-BAY Collaboration), *Observation of electron-antineutrino disappearance at Daya Bay*, Phys.Rev.Lett. **108** (2012) 171803, arXiv:1203.1669 [hep-ex].

[3] J. Ahn et al. (RENO collaboration), *Observation of Reactor Electron Antineutrino Disappearance in the RENO Experiment*, Phys.Rev.Lett. **108** (2012) 191802, arXiv:1204.0626 [hep-ex].

[4] K. Abe et al. (T2K Collaboration), *Indication of Electron Neutrino Appearance from an Accelerator-produced Off-axis Muon Neutrino Beam*, Phys.Rev.Lett. **107** (2011) 041801, arXiv:1106.2822 [hep-ex].

[5] D. Forero, M. Tortola and J. Valle, *Neutrino oscillations refitted* (2014), arXiv:1405.7540 [hep-ph].

[6] J. Schechter and J. Valle, *Neutrino Masses in SU(2) x U(1) Theories*, Phys.Rev. **D22** (1980) 2227.

[7] S. Morisi and J. Valle, *Neutrino masses and mixing: a flavour symmetry roadmap*, Fortsch.Phys. **61** (2013) 466–492, arXiv:1206.6678 [hep-ph].

[8] K. Babu, E. Ma and J. Valle, *Underlying A(4) symmetry for the neutrino mass matrix and the quark mixing matrix*, Phys.Lett. **B552** (2003) 207–213, arXiv:hep-ph/0206292 [hep-ph].

[9] E. Ma, *A(4) origin of the neutrino mass matrix*, Phys. Rev. **D70** (2004) 031901, hep-ph/0404199.

[10] G. Altarelli and F. Feruglio, *Tri-bimaximal neutrino mixing from discrete symmetry in extra dimensions*, Nucl. Phys. **B720** (2005) 64–88, hep-ph/0504165.

[11] S. Morisi, D. Forero, J. Romao and J. Valle, *Neutrino mixing with revamped A4 flavour symmetry*, Phys.Rev. **D88** (2013) 016003, arXiv:1305.6774 [hep-ph].

[12] S. F. King et al., *Neutrino Mass and Mixing: from Theory to Experiment*, New J.Phys. **16** (2014) 045018, arXiv:1402.4271 [hep-ph].

[13] J. Barry and W. Rodejohann, *Deviations from tribimaximal mixing due to the vacuum expectation value misalignment in A4 models*, Phys.Rev. **D81** (2010) 093002, arXiv:1003.2385 [hep-ph].

[14] J. Barry and W. Rodejohann, *Neutrino Mass Sum-rules in Flavor Symmetry Models*, Nucl.Phys. **B842** (2011) 33–50, arXiv:1007.5217 [hep-ph].

[15] L. Dorame et al., *Constraining Neutrinoless Double Beta Decay*, Nucl.Phys. **B861** (2012) 259–270, arXiv:1111.5614 [hep-ph].

[16] S. F. King, A. Merle and A. J. Stuart, *The Power of Neutrino Mass Sum Rules for Neutrinoless Double Beta Decay Experiments*, JHEP **1312** (2013) 005, arXiv:1307.2901 [hep-ph].

[17] S. King, *Predicting neutrino parameters from SO(3) family symmetry and quark-lepton unification*, JHEP **0508** (2005) 105, arXiv:hep-ph/0506297 [hep-ph].

[18] S. Morisi, E. Peinado, Y. Shimizu and J. Valle, *Relating quarks and leptons without grand-unification*, Phys.Rev. **D84** (2011) 036003, arXiv:1104.1633 [hep-ph].

[19] S. Morisi et al., *Quark-Lepton Mass Relation and CKM mixing in an A4 Extension of the Minimal Supersymmetric Standard Model*, Phys.Rev. **D88** (2013) 036001, arXiv:1303.4394 [hep-ph].

[20] F. Bazzocchi et al., *Bilinear R-parity violation with flavor symmetry*, JHEP **1301** (2013) 033, arXiv:1202.1529 [hep-ph].

[21] S. King, S. Morisi, E. Peinado and J. Valle, *Quark-Lepton Mass Relation in a Realistic A4 Extension of the Standard Model*, Phys. Lett. B **724** (2013) 68–72, arXiv:1301.7065 [hep-ph].

[22] F. Wilczek and A. Zee, *Horizontal Interaction and Weak Mixing Angles*, Phys. Rev. Lett. **42** (1979) 421.

[23] H. Ishimori et al., *Non-Abelian Discrete Symmetries in Particle Physics*, Prog.Theor.Phys.Suppl. **183** (2010) 1–163, arXiv:1003.3552 [hep-th].

[24] C. Luhn, S. Nasri and P. Ramond, *Tri-bimaximal neutrino mixing and the family symmetry semidirect product of Z(7) and Z(3)*, Phys.Lett. **B652** (2007) 27–33, arXiv:0706.2341 [hep-ph].

[25] C. Luhn, S. Nasri and P. Ramond, *Simple Finite Non-Abelian Flavor Groups*, J.Math.Phys. **48** (2007) 123519, arXiv:0709.1447 [hep-th].

[26] Q.-H. Cao, S. Khalil, E. Ma and H. Okada, *Observable T7 Lepton Flavor Symmetry at the Large Hadron Collider*, Phys.Rev.Lett. **106** (2011) 131801, arXiv:1009.5415 [hep-ph].

[27] H. Ishimori, S. Khalil and E. Ma, *CP Phases of Neutrino Mixing in a Supersymmetric B-L Gauge Model with T7 Lepton Flavor Symmetry*, Phys.Rev. **D86** (2012) 013008, arXiv:1204.2705 [hep-ph].

[28] Y. Kajiyama, H. Okada and K. Yagyu, *T7 Flavor Model in Three Loop Seesaw and Higgs Phenomenology*, JHEP **1310** (2013) 196, arXiv:1307.0480 [hep-ph].

[29] V. Vien and H. Long, *The T7 flavor symmetry in 3-3-1 model with neutral leptons*, JHEP **1404** (2014) 133, arXiv:1402.1256 [hep-ph].

[30] J. W. F. Valle, *Neutrino physics overview*, J. Phys. Conf. Ser. **53** (2006) 473–505, these review lectures were given at Corfu, 2005 and contain extensive references to the early papers on the seesaw mechanism, hep-ph/0608101.

[31] S. F. King and C. Luhn, *Neutrino Mass and Mixing with Discrete Symmetry*, Rept.Prog.Phys. **76** (2013) 056201, arXiv:1301.1340 [hep-ph].

[32] S. F. King and M. Malinsky, *A(4) family symmetry and quark-lepton unification*, Phys. Lett. **B645** (2007) 351–357, hep-ph/0610250.

[33] S. Morisi and E. Peinado, *An A4 model for lepton masses and mixings*, Phys. Rev. **D80** (2009) 113011, arXiv:0910.4389 [hep-ph].

[34] J. Beringer et al. (Particle Data Group), *Review of Particle Physics (RPP)*, Phys.Rev. **D86** (2012) 010001.

[35] P. Ade et al. (Planck Collaboration), *Planck 2013 results. XVI. Cosmological parameters* (2013), arXiv:1303.5076 [astro-ph.CO].

[36] L. Bornschein (KATRIN Collaboration), *KATRIN: Direct measurement of neutrino masses in the sub-Ev region*, eConf **C030626** (2003) FRAP14, arXiv:hep-ex/0309007 [hep-ex].

CHAPTER 9

NATURALLY LIGHT NEUTRINOS IN *DIRACON* MODEL

Authors: Cesar Bonilla, Jorge C. Romao, Jose W.F. Valle.
Journal reference: Phys. Lett. B762 (2016) 162-165.

Abstract

We propose a simple model for Dirac neutrinos where the smallness of neutrino mass follows from a parameter κ whose absence enhances the symmetry of the theory. Symmetry breaking is performed in a two–doublet Higgs sector supplemented by a gauge singlet scalar, realizing an accidental global U(1) symmetry. Its spontaneous breaking at the few TeV scale leads to a physical Nambu–Goldstone boson – the *Diracon*, denoted $\mathcal{D}$ – which is restricted by astrophysics and induces invisible Higgs decays such as $h \to \mathcal{D}\mathcal{D}$. The scheme provides a rich, yet very simple scenario for symmetry breaking studies at colliders such as the LHC.

9.1 Introduction

Establishing whether neutrinos are their own anti–particles continues to challenge experimentalists [1,2]. Likewise, the mechanism responsible for generating small neutrino masses remains as elusive as ever. It is well–known that, in gauge theories, the detection of neutrinoless double beta decay would signify that neutrinos are of Majorana type [3,4]. Although experimental confirmation of the Majorana hypothesis may come in the not too distant future [5], so far the possibility remains that neutrinos can be Dirac particles, despite the fact that the general theoretical expectation is that they are Majorana fermions [6] as given, for example, in Weinberg's dimension five operator [7]. Moreover, the most widely studied mechanism to account for the smallness of neutrino masses relative to the charged fermion masses invokes their Majorana nature, namely, the conventional high–scale type-I [6,8–11] or type-II [6,11,12] seesaw mechanism. The same happens in low–scale variants of the seesaw mechanism, see [13] for a review.

Accommodating the possibility of naturally light Dirac neutrinos constitutes a double challenge. One approach is to supplement the standard $SU(3)_C \otimes SU(2)_L \otimes U(1)_Y$ electroweak gauge structure by using extra flavor symmetries implying a conserved lepton number, so as to obtain Dirac neutrinos, as suggested in [14, 15]. Another approach would be to appeal to the existence of extra dimensions, such as in warped scenarios [16]. Alternatively, one may extend the gauge group itself, for example, by using the extended $\mathrm{SU(3)_c} \otimes \mathrm{SU(3)_L} \otimes \mathrm{U(1)_X}$ gauge structure because of its special features [17]. In this case one can obtain both the lightness as well as the Dirac nature of neutrinos as an outcome [18].

In this letter we focus on the possibility of having naturally light Dirac neutrinos with seesaw–induced masses within the framework of the simplest four-dimensional $SU(3)_C \otimes SU(2)_L \otimes U(1)_Y$gauge structure, without non-Abelian discrete flavor symmetries. To this end we impose a cyclic flavor–blind $\mathbb{Z}_5 \otimes \mathbb{Z}_3$ symmetry in a theory with enlarged symmetry breaking sector : two Higgs doublets and a singlet, see Table 9.1. We find that the resulting model has an accidental spontaneously broken U(1) symmetry that leads to the seesaw mechanism as well as the Dirac nature of neutrinos. The smallness of neutrino mass follows from the smallness of a parameter κ whose absence would increase the symmetry of the electroweak breaking sector, ensuring naturalness in 't Hooft's sense. We discuss some phenomenological features of the scheme which follow from the existence of a *Diracon* namely, the Nambu–Goldstone boson associated to the spontaneous breaking of the global accidental U(1) symmetry in the scalar sector.

9.2 The model

The lepton and scalar boson assignments of the model are summarized in Table 9.1, where a cyclic $\mathbb{Z}_5 \otimes \mathbb{Z}_3$ symmetry is assumed, so that $\omega^5 = 1$ and $\alpha^3 = 1$. The Abelian $\mathbb{Z}_5$ symmetry is used to have Dirac neutrinos in the presence of the additional doublet Φ, forbidding the terms $\overline{L}\nu_R\tilde{H}$, $\overline{L}\ell_R\tilde{\Phi}$, $\nu_R\nu_R$ and $\nu_R\nu_R\sigma$. We have used two Higgs doublets

$$H = \begin{pmatrix} h^+ \\ H^0 \end{pmatrix}, \quad \Phi = \begin{pmatrix} \Phi^0 \\ \phi^- \end{pmatrix},$$

with their conjugates defined as usual, $\tilde{H} = i\sigma_2 H^*$ and $\tilde{\Phi} = i\sigma_2\Phi^*$. On the other hand, the complementary $\mathbb{Z}_3$ symmetry [19, 20] ensures lepton number conservation also at the non-renormalizable level, ruling out possible operators of the type $\nu_R\nu_R\sigma^3$, $\nu_R\nu_R\sigma^8$, etc.

	$\overline{L}$	ℓ_R	ν_R	H	Φ	σ
$SU(2)_L$	**2**	**1**	**1**	**2**	**2**	**1**
$\mathbb{Z}_5$	ω	ω^4	ω	1	ω^3	ω
$\mathbb{Z}_3$	α^2	α	α	1	1	1

Table 9.1: Lepton and scalar boson assignments of the model, with $\omega^5 = 1$ and $\alpha^3 = 1$.

The gauge– and $\mathbb{Z}_5\otimes\mathbb{Z}_3$–invariant Yukawa Lagrangean for the lepton sector turns out to be, symbolically,

$$\mathcal{L}_Y \;=\; y^e\overline{L}e_R H + y^\nu\overline{L}\nu_R\Phi + h.c. \tag{9.1}$$

where the first term is the standard one responsible for the charged lepton masses, while the second is the one that appears in Fig. 9.1. As illustrated in the figure, the latter induces nonzero neutrino masses

$$m_\nu = \kappa y^\nu \frac{v_\sigma^2 v_H}{m_\Phi^2} \tag{9.2}$$

where we denote the three vacuum expectation values as $v_\sigma \equiv \langle\sigma\rangle$, $v_\Phi \equiv \langle\Phi\rangle$, $v_H \equiv \langle H\rangle$, and κ is a dimensionless parameter in the scalar potential. For simplicity we have omitted generation indices. Notice that the smallness of neutrino mass depends not only on the Yukawa coupling y^ν but is also related to the smallness of κ, very much like in the type-II–like seesaw mechanism.

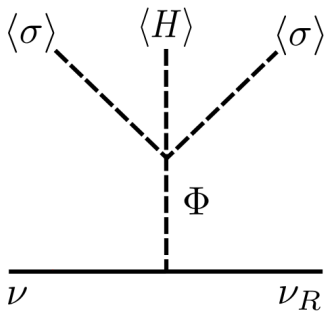

Figure 9.1: Neutrino mass generation in type-II Dirac seesaw mechanism.

9.3 Scalar Sector

The $SU(3)_C \otimes SU(2)_L \otimes U(1)_Y$invariant scalar potential consistent with the global $\mathbb{Z}_5 \otimes \mathbb{Z}_3$ symmetry is given by [1]

$$\begin{aligned} V &= -\mu_H^2 H^\dagger H - \mu_H^2 \Phi^\dagger \Phi - \mu_\sigma^2 \sigma^\dagger \sigma + \lambda_H H^\dagger H H^\dagger H + \lambda_\Phi \Phi^\dagger \Phi \Phi^\dagger \Phi + \lambda_\sigma \sigma^\dagger \sigma \sigma^\dagger \sigma \\ &+ \lambda_{H\Phi} H^\dagger H \Phi^\dagger \Phi + \lambda'_{H\Phi} H^\dagger \Phi \Phi^\dagger H + \lambda_{\sigma H} \sigma^\dagger \sigma H^\dagger H + \lambda_{\sigma\Phi} \sigma^\dagger \sigma \Phi^\dagger \Phi \\ &+ \kappa \left(\tilde{H}^\dagger \Phi \sigma^2 + h.c. \right) \end{aligned} \tag{9.3}$$

where, after acquiring vacuum expectation values (vevs) the fields are shifted as follows,

$$\begin{aligned} H^0 &= \frac{1}{\sqrt{2}} \left(v_H + R_H + i I_H \right), \quad \sigma = \frac{1}{\sqrt{2}} \left(v_\sigma + R_\sigma + i I_\sigma \right) \quad \text{and} \\ \Phi^0 &= \frac{1}{\sqrt{2}} \left(v_\Phi + R_\Phi + i I_\Phi \right), \end{aligned} \tag{9.4}$$

so the extremum conditions are,

$$\begin{aligned} \mu_H^2 &= \frac{1}{2} \left(2\lambda_H v_H^2 + \lambda_{\sigma H} v_\sigma^2 + \lambda_{H\Phi} v_\Phi^2 - \frac{\kappa v_\sigma^2 v_\Phi}{v_H} \right) \\ \mu_\Phi^2 &= \frac{1}{2} \left(\lambda_{H\Phi} v_H^2 + \lambda_{\sigma\Phi} v_\sigma^2 + 2\lambda_\Phi v_\Phi^2 - \frac{\kappa v_H v_\sigma^2}{v_\Phi} \right) \\ \mu_\sigma^2 &= \frac{1}{2} \left(\lambda_{\sigma H} v_H^2 + \lambda_{\sigma\Phi} v_\Phi^2 + 2\lambda_\sigma v_\sigma^2 - 2\kappa v_H v_\Phi \right) \end{aligned} \tag{9.5}$$

[1] This scalar potential is shared by other models with Majorana neutrinos. See for example Ref. [21].

and from these one can derive a "seesaw–type relation" amongst the vacuum expectation values given as,

$$v_\Phi \approx \kappa v_H \left(\frac{1}{\lambda_{H\Phi} \frac{v_H^2}{v_\sigma^2} + \lambda_{\sigma\Phi} - 2\frac{\mu_\Phi^2}{v_\sigma^2}} \right). \tag{9.6}$$

Notice that $v_\sigma \neq 0$ is required in order to drive $v_\Phi \neq 0$, see Fig. 9.1. Moreover one sees that the smallness of v_Φ is directly related to the smallness of κ. In other words, Φ acquires an "induced" vev v_Φ whose smallness is associated to the symmetry enhancement that results from the absence of κ. In this limit there would be a second U(1) symmetry whose associated Nambu-Golstone boson is the pseudoscalar A, see below. This means that the "induced" vev v_Φ is always very much suppressed w.r.t. the standard v_H, responsible for generating the W boson mass. In short the model has a double vev hierarchy

$$v_\sigma \gtrsim v_H \gg v_\Phi. \tag{9.7}$$

The two hierarchies are consistent with the minimization of the potential. The first is a mild hierarchy, ensuring adequate couplings for the *Diracon*, while the second one is a strong yet "natural" hierarchy, because it is related to the enhanced symmetry which would result from the absence of κ in the Lagrangean, even though, in practice, it can not be strictly realized, since we need $v_\Phi \neq 0$ for a realistic scheme.

With the information above one can immediately work our the Higgs mass spectrum. Out of the ten scalars, eight from the two–doublet structure, plus two from the extra complex singlet, we are left with seven physical ones after projecting out the three longitudinal degrees of freedom of the massive $SU(3)_C \otimes SU(2)_L \otimes U(1)_Y$gauge bosons. These correspond to three physical CP even scalars, one of which is the 125 GeV state discovered at the LHC [22–24], two physical CP odd scalars, and one electrically charged scalar. The mass squared matrices for the CP-even and CP-odd sectors, in the weak basis (H, σ, Φ) are given below,

$$M_R^2 = \begin{pmatrix} 2\lambda_H v_H^2 + \frac{\kappa v_\sigma^2 v_\Phi}{2v_H} & (\lambda_{\sigma H} v_H - \kappa v_\Phi) v_\sigma & \lambda_{H\Phi} v_H v_\Phi - \frac{\kappa v_\sigma^2}{2} \\ (\lambda_{\sigma H} v_H - \kappa v_\Phi) v_\sigma & 2\lambda_\sigma v_\sigma^2 & (\lambda_{\sigma\Phi} v_\Phi - \kappa v_H) v_\sigma \\ \lambda_{H\Phi} v_H v_\Phi - \frac{\kappa v_\sigma^2}{2} & (\lambda_{\sigma\Phi} v_\Phi - \kappa v_H) v_\sigma & 2\lambda_\Phi v_\Phi^2 + \frac{\kappa v_H v_\sigma^2}{2v_\Phi} \end{pmatrix} \tag{9.8}$$

and

$$M_I^2 = \kappa \begin{pmatrix} \frac{v_\sigma^2 v_\Phi}{2v_H} & v_\sigma v_\Phi & \frac{v_\sigma^2}{2} \\ v_\sigma v_\Phi & 2v_H v_\Phi & v_H v_\sigma \\ \frac{v_\sigma^2}{2} & v_H v_\sigma & \frac{v_H v_\sigma^2}{2v_\Phi} \end{pmatrix}, \tag{9.9}$$

where $\mathrm{diag}(m^2_{H_1}, m^2_{H_2}, m^2_{H_3}) = \mathcal{O}_R M^2_R \mathcal{O}^T_R$ and $\mathrm{diag}(0, 0, m^2_A) = \mathcal{O}_I M^2_I \mathcal{O}^T_I$.

Let us first consider the CP-odd scalars sector, its diagonalization matrix is given by,

$$\mathcal{O}_I = \begin{pmatrix} -\alpha v_H & 0 & \alpha v_\Phi \\ -2\alpha\beta v_H v_\Phi^2 & \frac{\beta v_\sigma}{\alpha} & -2\alpha\beta v_H^2 v_\Phi \\ \beta v_\sigma v_\Phi & 2\beta v_H v_\Phi & \beta v_H v_\sigma \end{pmatrix} \tag{9.10}$$

where

$$\alpha = \frac{1}{\sqrt{v_H^2 + v_\Phi^2}} \quad \text{and} \quad \beta = \frac{1}{\sqrt{v_H^2\,(v_\sigma^2 + 4v_\Phi^2) + v_\sigma^2 v_\Phi^2}}. \tag{9.11}$$

Hence one finds that the mass–eigenstate profiles are given by

$$\begin{aligned} G^0 &= \alpha(-v_H I_H + v_\Phi I_\Phi) \\ \mathcal{D} &= \alpha\beta(-2v_H v_\Phi^2 I_H + \frac{v_\sigma}{\alpha^2} I_\sigma - 2v_H^2 v_\Phi I_\Phi) \\ A &= \beta\,(v_\sigma v_\Phi I_H + 2v_H v_\Phi I_\sigma + v_H v_\sigma I_\Phi)\,. \end{aligned} \tag{9.12}$$

One sees that the projective nature of Eq. (9.9) (two–dimensional null space) clearly implies two massless states whose profiles follow just from symmetry reasons. Due to the smallness of v_Φ, the main components of G^0, $\mathcal{D}$ and A are the imaginary parts of the $SU(2)_L$ Higgs doublet H, the singlet σ and the doublet Φ, respectively. Indeed the first massless CP–odd eigenvector G^0 pointing mainly along H corresponds to the unphysical longitudinal mode of the Z boson. The second massless state $\mathcal{D}$ is mainly singlet and we call it the *Diracon*, i.e. the physical Nambu-Golstone boson associated to the accidental U(1) symmetry. It is the analogue of the Majoron present in the "123" type-II seesaw scheme of [11], and is associated with the type-II Dirac neutrino seesaw mechanism illustrated in Fig. 9.1. On the other hand the massive pseudoscalar state A pointing mainly along the weak isodoublet direction has mass

$$m_A^2 = \frac{\kappa\,(v_H^2\,(v_\sigma^2 + 4v_\Phi^2) + v_\sigma^2 v_\Phi^2)}{2v_H v_\Phi}, \tag{9.13}$$

which would vanish in the (unphysical) limit $\kappa = v_\sigma = v_\Phi = 0$.

Turning now to the charged sector we have, in the basis $(h^\pm, \phi^\pm)$, the following mass squared matrix,

$$M^2_{H^\pm} = \begin{pmatrix} \left(\lambda'_{H\Phi} v_\Phi + \frac{\kappa v_\sigma^2}{v_H}\right) v_\Phi & -\lambda'_{H\Phi} v_H v_\Phi - \kappa v_\sigma^2 \\ -\lambda'_{H\Phi} v_H v_\Phi - \kappa v_\sigma^2 & \left(\lambda'_{H\Phi} v_H + \frac{\kappa v_\sigma^2}{v_\Phi}\right) v_H \end{pmatrix} \tag{9.14}$$

whose eigenstates are the longitudinal W–boson and a physical state $H^{\pm}$ of (squared) mass

$$m^2_{H^{\pm}} = \left(v_H^2 + v_\Phi^2\right)\left(\lambda'_{H\Phi} + \frac{\kappa v_\sigma^2}{v_H v_\Phi}\right). \tag{9.15}$$

Notice that, taking into account the smallness of the neutrino mass, i.e. $\kappa \ll 1$, and using Eq. 9.6 one finds that the Higgs mass spectrum further simplifies to,

$$M_R^2 \approx \begin{pmatrix} 2\lambda_H v_H^2 & \lambda_{\sigma H} v_H v_\sigma & 0 \\ \lambda_{\sigma H} v_H v_\sigma & 2\lambda_\sigma v_\sigma^2 & 0 \\ 0 & 0 & \frac{\lambda_{H\Phi} v_H^2 + \lambda_{\sigma\Phi} v_\sigma^2}{2} \end{pmatrix} \tag{9.16}$$

$$m_A^2 \approx \frac{\lambda_{H\Phi} v_H^2 + \lambda_{\sigma\Phi} v_\sigma^2}{2} \tag{9.17}$$

$$m^2_{H^{\pm}} \approx \lambda_{\sigma\Phi}\frac{v_\sigma^2}{2} + \left(\lambda_{H\Phi} + \lambda'_{H\Phi}\right)\frac{v_H^2}{2} \tag{9.18}$$

Comparing the CP–even and CP–odd sectors it follows that $m_{H_3} \approx m_A$. Hence by using Eq. (9.18) and Eq. (9.17) we find that the following mass relation holds,

$$m^2_{H^{\pm}} - m_A^2 \approx \lambda'_{H\Phi}\frac{v_H^2}{2}.$$

9.4 Phenomenological considerations

The above model of electroweak breaking is rather similar to the inert doublet model [25], implying the absence of tree–level flavor-changing neutral currents. There are, however, important new features. A noticeable difference of this model when compared with various variants of two–Higgs doublet models is the existence of the accidental U(1) symmetry. This global symmetry is spontaneously broken by the vev of σ implying the existence of a corresponding Nambu-Goldstone boson given in Eq. (9.12). Its couplings to neutrinos can be easily obtained from Noether's theorem. Likewise one can determine its coupling to charged leptons, for instance electrons. The latter would lead to excessive stellar cooling through the Compton–like process $\gamma + e \to e + \mathcal{D}$ [26], unless

$$|g_{ee\mathcal{D}}| = \left|(\mathcal{O}_I)_{21}\frac{m_e}{v_H}\right| \lesssim 10^{-13} \tag{9.19}$$

hence, using Eq. (9.10), one finds

$$2\alpha\beta v_\Phi^2 \lesssim \frac{10^{-13}}{m_e} \tag{9.20}$$

where α and β are given in Eq. (9.11). Taking into account that $v_H = \sqrt{v_{SM}^2 - v_\Phi^2}$ (where $v_{SM} = 246$ GeV), one writes Eq. (9.20) only in terms of v_σ and v_Φ. The allowed region of these vevs is delimited by the bound on $g_{ee\mathcal{D}}$ as illustrated in Fig. 9.2. The shaded area is the region allowed by stellar energy loss limits.

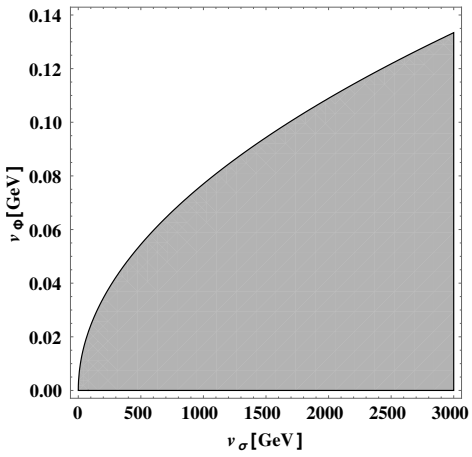

Figure 9.2: The shaded region is allowed by stellar energy loss limits.

Let us now comment on boundedness conditions and vacuum stability. Taking $\kappa \ll 1$, one can see that the copositivity criterium applies so one can easily obey the relevant conditions [27]. Concerning stability and perturbativity, we finds extented regions of consistency as a result of the presence of the extra scalar boson states [28, 29]. Moreover, in the limit $m_{H_3} \sim m_A \sim m_{H^\pm}$, it is well–known that the oblique S,T,U parameters are well under control, so that these precision observables does not pose great problems either [30, 31].

Concerning collider phenomenology, notice that the physical Nambu – Goldstone boson induces invisible Higgs boson decays $h \to \mathcal{D}\mathcal{D}$. These decays are rather analogous to the invisible CP–even Higgs decays into *Majorons* which are present in Majorana neutrino schemes, such as the "123" seesaw [11] with spontaneous lepton number violation [32]. Likewise, one has the new pseudoscalar decays $A \to h\mathcal{D}$ and $A \to \mathcal{D}\mathcal{D}\mathcal{D}$ in addition to the Standard Model decay modes. For charged scalars, there are also new decay channels into leptons, i.e. $H^\pm \to \ell^\pm \nu_R$, which should be taken into account in search analyses [33]. Future experimental searches at the LHC should probe the theory in a rather significant way within a relatively wide region of parameters.

9.5 Summary and conclusions

We presented a very simple model where neutrinos are Dirac fermions and their mass can naturally arise from TeV–scale physics, associated to a small parameter κ whose absence would enhance the symmetry of the theory. This is realized in an enlarged scalar sector consisting of two doublets and a singlet Higgs carrying an accidentally conserved global U(1) charge. Its spontaneous violation leads to the existence of a physical Nambu–Goldstone boson which is restricted by astrophysics. Let us mention that the presence of gravity could induce masses for neutrinos [34] and/or the Diracon [35] breaking the Abelian discrete symmetries. This breaking may, however, be avoided if the latter are part of a gauge discrete symmetry [36]. We have discussed the symmetry structure of the model, the connection to neutrino mass generation, and indicated how it provides new collider signatures induced by invisible Higgs boson decays. In summary, the model provides an interesting scheme for neutrino mass generation. Its scalar sector constitutes an interesting alternative for electroweak symmetry breaking studies, both theoretically and experimentally. Its simplicity, its close connection to neutrino masses and the presence of an accidental global U(1) symmetry give it unique features. Details as well as additional phenomenological features will be discussed elsewhere.

Acknowledgments

We thank Thomas Neder and Eduardo Peinado for useful comments. This work is supported by the Spanish grants FPA2011-2297, FPA2014-58183-P, Multidark CSD2009-00064, SEV-2014-0398 (MINECO) and PROMETEOII / 2014/ 084 (GVA).

BIBLIOGRAPHY

[1] A. S. Barabash, *Double Beta Decay: Historical Review of 75 Years of Research*, Phys. Atom. Nucl. **74** (2011) 603–613, arXiv:1104.2714 [nucl-ex].

[2] F. T. Avignone, S. R. Elliott and J. Engel, *Double Beta Decay, Majorana Neutrinos, and Neutrino Mass*, Rev. Mod. Phys. **80** (2008) 481–516, arXiv:0708.1033 [nucl-ex].

[3] J. Schechter and J. Valle, *Neutrinoless Double beta Decay in SU(2) x U(1) Theories*, Phys.Rev. **D25** (1982) 2951.

[4] M. Duerr, M. Lindner and A. Merle, *On the Quantitative Impact of the Schechter-Valle Theorem*, JHEP **1106** (2011) 091, arXiv:1105.0901 [hep-ph].

[5] A. Gando et al. (KamLAND-Zen), *Search for Majorana Neutrinos near the Inverted Mass Hierarchy Region with KamLAND-Zen*, Phys. Rev. Lett. **117** (2016) 8 082503, [Addendum: Phys. Rev. Lett.117,no.10,109903(2016)], arXiv:1605.02889 [hep-ex].

[6] J. Schechter and J. Valle, *Neutrino Masses in SU(2) x U(1) Theories*, Phys.Rev. **D22** (1980) 2227.

[7] S. Weinberg, *Varieties of Baryon and Lepton Nonconservation*, Phys. Rev. **D22** (1980) 1694.

[8] M. Gell-Mann, P. Ramond and R. Slansky, *Complex spinors and unified theories* (1979), print-80-0576 (CERN).

[9] T. Yanagida, *Kek lectures* (KEK lectures, 1979), ed. O. Sawada and A. Sugamoto (KEK, 1979).

[10] R. N. Mohapatra and G. Senjanovic, *Neutrino mass and spontaneous parity nonconservation*, Phys. Rev. Lett. **44** (1980) 91.

[11] J. Schechter and J. Valle, *Neutrino Decay and Spontaneous Violation of Lepton Number*, Phys.Rev. **D25** (1982) 774.

[12] G. Lazarides, Q. Shafi and C. Wetterich, *Proton Lifetime and Fermion Masses in an SO(10) Model*, Nucl.Phys. **B181** (1981) 287–300.

[13] S. M. Boucenna, S. Morisi and J. W. F. Valle, *The low-scale approach to neutrino masses*, Adv. High Energy Phys. **2014** (2014) 831598, arXiv:1404.3751 [hep-ph].

[14] A. Aranda et al., *Dirac neutrinos from flavor symmetry*, Phys. Rev. **D89** (2014) 3 033001, arXiv:1307.3553 [hep-ph].

[15] S. Kanemura, K. Sakurai and H. Sugiyama, *Probing Models of Dirac Neutrino Masses via the Flavor Structure of the Mass Matrix*, Phys. Lett. **B758** (2016) 465, arXiv:1603.08679 [hep-ph].

[16] P. Chen et al., *Warped flavor symmetry predictions for neutrino physics*, JHEP **01** (2016) 007, arXiv:1509.06683 [hep-ph].

[17] M. Singer, J. Valle and J. Schechter, *Canonical Neutral Current Predictions From the Weak Electromagnetic Gauge Group SU(3) X u(1)*, Phys.Rev. **D22** (1980) 738.

[18] J. W. F. Valle and C. A. Vaquera-Araujo, *Dynamical seesaw mechanism for Dirac neutrinos*, Phys. Lett. **B755** (2016) 363–366, arXiv:1601.05237 [hep-ph].

[19] E. Ma and R. Srivastava, *Dirac or inverse seesaw neutrino masses with $B-L$ gauge symmetry and S_3 flavor symmetry*, Phys. Lett. **B741** (2015) 217–222, arXiv:1411.5042 [hep-ph].

[20] E. Ma, N. Pollard, R. Srivastava and M. Zakeri, *Gauge $B-L$ Model with Residual Z_3 Symmetry*, Phys. Lett. **B750** (2015) 135–138, arXiv:1507.03943 [hep-ph].

[21] W. Wang and Z.-L. Han, *Global $U(1)_L$ Breaking in Neutrinophilic 2HDM: From LHC Signatures to X-Ray Line* (2016), arXiv:1605.00239 [hep-ph].

[22] G. Aad et al. (ATLAS Collaboration), *Observation of a new particle in the search for the Standard Model Higgs boson with the ATLAS detector at the LHC*, Phys.Lett. **B716** (2012) 1–29, arXiv:1207.7214 [hep-ex].

[23] S. Chatrchyan et al. (CMS Collaboration), *Observation of a new boson at a mass of 125 GeV with the CMS experiment at the LHC*, Phys.Lett. **B716** (2012) 30–61, arXiv:1207.7235 [hep-ex].

[24] G. Aad et al. (ATLAS, CMS), *Combined Measurement of the Higgs Boson Mass in pp Collisions at $\sqrt{s} = 7$ and 8 TeV with the ATLAS and CMS Experiments*, Phys. Rev. Lett. **114** (2015) 191803, arXiv:1503.07589 [hep-ex].

[25] G. C. Branco et al., *Theory and phenomenology of two-higgs-doublet models*, Phys. Reports **516** (2012) 1 1–102.

[26] N. Viaux et al., *Neutrino and axion bounds from the globular cluster M5 (NGC 5904)*, Phys. Rev. Lett. **111** (2013) 231301, arXiv:1311.1669 [astro-ph.SR].

[27] K. Kannike, *Vacuum Stability Conditions From Copositivity Criteria*, Eur.Phys.J. **C72** (2012) 2093, arXiv:1205.3781 [hep-ph].

[28] C. Bonilla, R. M. Fonseca and J. W. F. Valle, *Vacuum stability with spontaneous violation of lepton number*, Phys. Lett. **B756** (2016) 345–349, arXiv:1506.04031 [hep-ph].

[29] C. Bonilla, R. M. Fonseca and J. W. F. Valle, *Consistency of the triplet seesaw model revisited*, Phys. Rev. **D92** (2015) 7 075028, arXiv:1508.02323 [hep-ph].

[30] W. Grimus, L. Lavoura, O. Ogreid and P. Osland, *A Precision constraint on multi-Higgs-doublet models*, J.Phys. **G35** (2008) 075001, arXiv:0711.4022 [hep-ph].

[31] W. Grimus, L. Lavoura, O. Ogreid and P. Osland, *The Oblique parameters in multi-Higgs-doublet models*, Nucl.Phys. **B801** (2008) 81–96, arXiv:0802.4353 [hep-ph].

[32] M. A. Diaz, M. A. Garcia-Jareno, D. A. Restrepo and J. W. F. Valle, *Neutrino mass and missing momentum Higgs boson signals*, Phys. Rev. **D58** (1998) 057702, arXiv:hep-ph/9712487 [hep-ph].

[33] G. Aad et al. (ATLAS), *Search for charged Higgs bosons in the $H^{\pm} \to tb$ decay channel in pp collisions at $\sqrt{s} = 8$ TeV using the ATLAS detector*, JHEP **03** (2016) 127, arXiv:1512.03704 [hep-ex].

[34] G. Dvali and L. Funcke, *Small neutrino masses from gravitational θ-term*, Phys. Rev. **D93** (2016) 11 113002, arXiv:1602.03191 [hep-ph].

[35] S. R. Coleman, *Why There Is Nothing Rather Than Something: A Theory of the Cosmological Constant*, Nucl. Phys. **B310** (1988) 643.

[36] L. M. Krauss and F. Wilczek, *Discrete gauge symmetry in continuum theories*, Phys. Rev. Lett. **62** (1989) 1221.

CHAPTER 10

TWO-LOOP DIRAC NEUTRINO MASS AND WIMP DARK MATTER

Authors: Cesar Bonilla, Ernest Ma, Eduardo Peinado, Jose W.F. Valle.
Journal reference: Phys. Lett. B762 (2016) 214-218.

Abstract

We propose a "scotogenic" mechanism relating small neutrino mass and cosmological dark matter. Neutrinos are Dirac fermions with masses arising only in two–loop order through the sector responsible for dark matter. Two triality symmetries ensure both dark matter stability and strict lepton number conservation at higher orders. A global spontaneously broken U(1) symmetry leads to a physical *Diracon* that induces invisible Higgs decays which add up to the Higgs to dark matter mode. This enhances sensitivities to spin–independent WIMP dark matter search below $m_h/2$.

10.1 Introduction

Two of the main observational shortcomings of the Standard Model is that it lacks neutrino masses [1] as well as a viable candidate for cosmological dark matter [2]. Even though light neutrinos themselves can account only for a very small fraction of the dark matter, they may hold the key to the basic understanding of what causes the dark matter to exist in the first place. Indeed, the existence of neutrino masses and of cosmological dark matter may be closely interconnected in several ways [3]. For example, the mechanism of neutrino mass generation itself can involve the exchange of particles which make up the bulk of the observed dark matter. This is the main idea of scotogenic models [4,5]. The prototype model is based on the assumption that the dark sector, odd under a parity symmetry, is connected with the neutrino sector through the generation of the light neutrino masses. The dark matter particle plays the role of messenger of radiative neutrino mass generation [6,7]. In the simplest conventional scenario [4], the dark matter is made up of a weakly interacting massive particle (WIMP), for example, the lightest scalar component of an inert Higgs doublet.

In this letter we explore the possibility of generating scotogenic Dirac neutrino masses radiatively, by forbidding lepton number violation through the cyclic Z_3 symmetry. This ensures strict lepton number conservation and the Diracness of neutrinos at higher orders. Another discrete Z_3 symmetry is responsible for dark matter stability. Neutrino masses are generated only at the two–loop level, through the same sector responsible for cosmological dark matter. This new realization combines the idea of two–loop scotogenic neutrino masses suggested in [8] with the idea of having a conserved lepton number leading to the Dirac nature of neutrinos. In our model there is a global U(1) symmetry which forbids the usual Dirac mass term of the neutrinos with the standard Higgs [9, 10] [1]. This symmetry breaks spontaneously leading to a physical Goldstone boson – a gauge singlet *Diracon* [12] – which induces invisible Higgs decays. These are analogous to the invisible Higgs decays by Majoron emission in models with Majorana neutrinos [13]. The extra invisible channel adds up to the Higgs boson decays to pairs of dark matter particles at collider experiments, providing tighter limits on WIMP dark matter below $m_h/2$.

[1] In contrast to Refs. [9, 10], neutrinos here are Dirac fermions, as opposed to Quasi-Dirac [11].

10.2 The model

We will consider a simple extension of the standard $SU(3)_C \otimes SU(2)_L \otimes U(1)_Y$model with the symmetries and field content indicated in Table 10.1, where ω and α are cube roots of unity, i.e. $\omega^3 = 1 = \alpha^3$. There are two complex $SU(2)_L$ doublets, H and η and three complex singlets, σ, χ and ξ.

	$\bar{L}$	ν^c	H	η	N	S	σ	ξ	χ
$SU(2)_L$	2	1	2	2	1	1	1	1	1
$U(1)_D$	-1	3	0	0	-1	1	2	-2	0
Z_3^{DM}	1	1	1	α	α	α	1	α^2	α
Z_3	ω	ω^2	1	1	ω	ω^2	1	1	1

Table 10.1: Relevant particle content and quantum numbers of the model.

The invariant Yukawa Lagrangian is given by

$$\mathcal{L} = y^{\nu} \bar{L} \tilde{\eta} S + y^{R} \nu^{c} N \xi + \lambda N S \chi. \tag{10.1}$$

The scalar potential can be separated as follows

$$\mathcal{V} = V + V(H, \eta) + V(\xi, \sigma, \chi, H, \eta), \tag{10.2}$$

where the first term V in the scalar potential contains the relevant terms for the generation of the neutrino masses, namely,

$$V = \lambda_1^{\chi} H^{\dagger} \eta \chi^{*} + \lambda_2^{\chi} \chi \sigma \xi + \lambda_3^{\chi} \chi^3 + h.c. \tag{10.3}$$

while the second term $V(H, \eta)$ is the Higgs potential associated to the η doublet

$$\begin{aligned} V(H,\eta) &= \mu_1^2 H^{\dagger} H + \mu_2^2 \eta^{\dagger} \eta + \lambda_1 |H|^4 + \lambda_2 |\eta|^4 + \lambda_3 |H|^2 |\eta|^2 \\ &+ \lambda_4 |H^{\dagger} \eta|^2 + \lambda_5 \left[(H^{\dagger} \eta)^2 + h.c. \right]. \end{aligned} \tag{10.4}$$

The last term $V(\xi, \sigma, \chi, H, \eta)$, is given by

$$\begin{aligned} V(\xi,\sigma,\chi,H,\eta) &= \mu_{\xi}^2 \xi \xi^{*} + \mu_{\sigma}^2 \sigma \sigma^{*} + \mu_{\chi}^2 \chi \chi^{*} + \lambda_{\xi} (\xi \xi^{*})^2 + \lambda_{\sigma} (\sigma \sigma^{*})^2 \\ &+ \lambda_{\chi} (\chi \chi^{*})^2 + \lambda_{\sigma\xi} \sigma \sigma^{*} \xi \xi^{*} + \lambda_{\chi\xi} \chi \chi^{*} \xi \xi^{*} + \lambda_{\chi\sigma} \chi \chi^{*} \sigma \sigma^{*} \\ &+ \lambda_{\chi H} \chi \chi^{*} H^{\dagger} H + \lambda_{\chi\eta} \chi \chi^{*} \eta^{\dagger} \eta + \lambda_{\xi H} \xi \xi^{*} H^{\dagger} H \\ &+ \lambda_{\xi\eta} \xi \xi^{*} \eta^{\dagger} \eta + \lambda_{\sigma H} \sigma \sigma^{*} H^{\dagger} H + \lambda_{\sigma\eta} \sigma \sigma^{*} \eta^{\dagger} \eta. \end{aligned} \tag{10.5}$$

After spontaneous symmetry breaking the fields are shifted as follows,

$$H = \begin{pmatrix} H^+ \\ \frac{1}{\sqrt{2}}(v_h + h^0 + iA^0) \end{pmatrix}, \qquad \eta = \begin{pmatrix} \eta^+ \\ \frac{1}{\sqrt{2}}(\eta_R + i\eta_I) \end{pmatrix},$$
$$\sigma = \frac{1}{\sqrt{2}}(v_\sigma + \sigma_R + i\sigma_I), \qquad \chi = \frac{1}{\sqrt{2}}(\chi_R + i\chi_I), \qquad \xi = \frac{1}{\sqrt{2}}(\xi_R + i\xi_I). \tag{10.6}$$

Notice that there are no vacuum expectation values (vevs) for scalars η, χ, ξ which are charged under Z_3^{DM}.

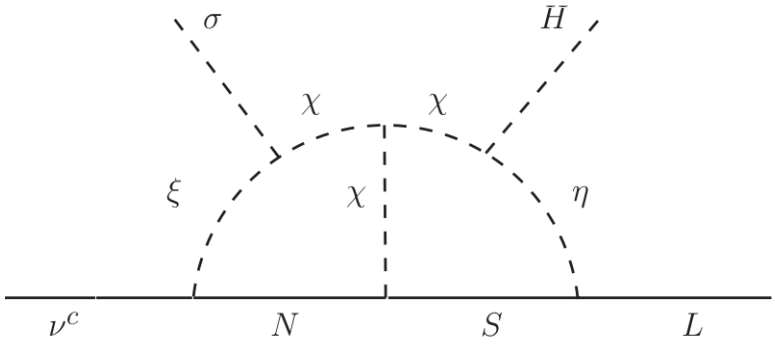

Figure 10.1: Two–loop generation of Dirac neutrino mass.

The fermions N and S will form heavy Dirac neutrinos by pairing with their corresponding partners $\bar{N}$ and $\bar{S}$. The light neutrinos acquire their masses via the loop in Fig. 10.1. From the minimization of the scalar potential, the scalar fields charged under the Z_3^{DM} do not acquire vacuum expectation values (vevs), while for the Higgs and the σ fields, there are two relevant tadpole equations:

$$\begin{aligned} \mu_1^2 &= \lambda_1 v_h^2 + \tfrac{1}{2}\lambda_{\sigma H} v_\sigma^2, \\ \mu_\sigma^2 &= \lambda_2 v_\sigma^2 + \tfrac{1}{2}\lambda_{\sigma H} v_h^2. \end{aligned} \tag{10.7}$$

The corresponding mass matrix for the CP-even "active" scalars is

$$M_R^2 = \begin{pmatrix} 2\lambda_1 v_h^2 & \lambda_{\sigma H} v_h v_\sigma \\ \lambda_{\sigma H} v_h v_\sigma & 2\lambda_\sigma v_\sigma^2 \end{pmatrix}. \tag{10.8}$$

The pseudoscalars include the unphysical Goldstone boson G^0 and a physical one, $\mathcal{D}$, namely the *Diracon*. In contrast to that of Ref. [12] the *Diracon* here is a pure singlet under weak SU(2) and hence is not subject to the strong astrophysical bound coming from stellar cooling considerations [14].

The mass matrices for the scalar and pseudoscalar "dark" sector (charged under Z_3^{DM}) in the basis η, χ, ξ are given as

$$\mathcal{M}_R^2 = \begin{pmatrix} \frac{1}{2}\left(\lambda_{345}^+ v_h^2 + \lambda_{\sigma\eta} v_\sigma^2 - 2\mu_\eta^2\right) & \frac{\lambda_1^\chi v_h}{2\sqrt{2}} & 0 \\ \frac{\lambda_1^\chi v_h}{2\sqrt{2}} & \frac{1}{2}\left(\lambda_{\chi H} v_h^2 + \lambda_{\xi\sigma} v_\sigma^2\right) & \frac{\lambda_2^\chi v_\sigma}{\sqrt{2}} \\ 0 & \frac{\lambda_2^\chi v_\sigma}{\sqrt{2}} & \frac{1}{2}\left(\lambda_{\xi H} v_h^2 + \lambda_{\sigma\xi} v_\sigma^2\right) \end{pmatrix}, \tag{10.9}$$

and

$$\mathcal{M}_I^2 = \begin{pmatrix} \frac{1}{2}\left(\lambda_{345}^- v_h^2 + \lambda_{\sigma\eta} v_\sigma^2 - 2\mu_\eta^2\right) & -\frac{\lambda_1^\chi v_h}{2\sqrt{2}} & 0 \\ -\frac{\lambda_1^\chi v_h}{2\sqrt{2}} & \frac{1}{2}\left(\lambda_{\chi H} v_h^2 + \lambda_{\xi\sigma} v_\sigma^2\right) & -\frac{\lambda_2^\chi v_\sigma}{\sqrt{2}} \\ 0 & -\frac{\lambda_2^\chi v_\sigma}{\sqrt{2}} & \frac{1}{2}\left(\lambda_{\xi H} v_h^2 + \lambda_{\sigma\xi} v_\sigma^2\right) \end{pmatrix}, \tag{10.10}$$

where the parameter $\lambda_{345}^\pm$ is given by

$$\lambda_{345}^\pm \equiv \lambda_3 + \lambda_4 \pm \lambda_5. \tag{10.11}$$

Finally, the mass for the "inert" electrically charged scalar is given by

$$\mathcal{M}_{\eta^+}^2 = \frac{1}{2}\left(-2\mu_\eta^2 + \lambda_3 v_h^2 + \lambda_{\sigma\eta} v_\sigma^2\right). \tag{10.12}$$

10.3 Dark matter annihilation

As usual in scotogenic models [4] [6, 7] dark matter in our model can be either scalar or fermionic. Here we focus on the first case, where the dark matter candidate is the lightest scalar eigenstate of $\mathcal{M}_{R,I}^2$ in Eqs. (10.9) and (10.10), which can be a general mixture of Z_3^{DM}–charged doublet and singlet scalars η, χ and ξ. An important requirement for the dark matter interpretation of such candidate is that its relic abundance matches the value observed by the Planck collaboration. There are in principle three possibilities [2]:

- mainly doublet dark matter
- generic doublet–singlet dark matter combination
- mainly singlet dark matter

[2] In order to generate nonzero neutrino mass through Fig. 10.1 none of the λ_i^χ couplings can vanish exactly. Hence the dark matter candidate is necessarily a combination of the triality–carrying scalars.

The first case can be arranged if the coupling λ_1^χ is suppressed and/or the vev of σ is large. In this case one looses the signature corresponding to invisible Higgs decay to the *Diracon*, Eq. (10.13). The dark matter candidate is well studied in other similar scenarios such as the scotogenic model [4] and the Inert Doublet Model [15–17]. In this context, the sign of the dimensionless coupling λ_5, determines whether the dark matter has a either CP-odd or CP-even nature, and the correct relic abundance constrains the parameter $\lambda_{345}^{\pm}$ in Eq. (10.11) [17].

In the second and most general case the situation is analogous to that of sneutrino dark matter in the inverse seesaw model described in Ref. [18, 19]. The dark matter candidate is made up of a singlet-doublet combination with potentially "comparable" components, and can lead both to an adequate relic density as well as to a detectable signal in nuclear recoil.

Finally, the last and simplest of the three cases, corresponds to that in which the dark matter candidate is mainly singlet and is detected primarily by the Higgs portal interaction. In the present model, the dark matter singlet would be given mainly by a combination of the fields χ and ξ. Without loss of generality we will denote as X the lightest combination of these singlets [3].

However, thanks to the Z_3^{DM} nature of our dark matter candidate and to the presence of the *Diracon*, there are other distinctive features in our case. Indeed, due to the cubic terms in the scalar potential, one finds that, besides annihilations, semi-annihilation processes play an important role in determining the dark matter relic density, as explained carefully in Ref. [20]. In contrast to the case of Z_2 dark matter, the dark matter spin–independent direct detection cross section is no longer directly related to the annihilation cross section.

In the case of interest, the limit in which the dark matter candidate X is stabilized by the Z_3^{DM} symmetry has been studied in detail in Ref. [20, 21]. In this case the dimensionful term λ_χ^3 contributes to the semi-annihilation processes like, for instance, $XX \to X^* h$ that can dominate in the determination of the relic density. As a result the λ_{XH} coupling no longer links the annihilation rate to the spin independent nuclear recoil detection cross section, in contrast to the more familiar case in which dark matter is stabilized by the Z_2 symmetry [22].

Over and above this observation, our model has further distinctively novel features associated to the presence of the *Diracon*. This leads to genuinely new interactions absent in previous dark matter models, including the simplest benchmark model studied in [22] as well as the possibilities analyzed in Refs. [20, 21]. Indeed, concerning dark matter annihilation, there are new

[3] We assume that the doublet-singlet mixing is negligible. Then, we define $X \equiv c_\alpha \chi - s_\alpha \xi$ and $\bar{X} \equiv s_\alpha \chi + c_\alpha \xi$.

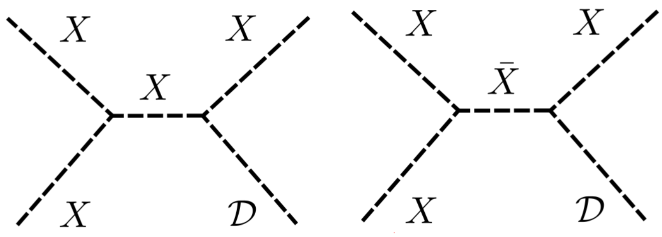

Figure 10.2: Dark matter semi-annihilation channels involving the *Diracon*.

semi-annihilation channels involving the *Diracons*, as illustrated in Fig. 10.2 [4]. These which should allow one to suppress the X relic density with respect to the cases considered in these references. In addition, the *Diracon* plays a role in detection, see next.

10.4 Dark matter detection

Encouraged by the above arguments concerning dark matter annihilation and semi-annihilation processes and in view of the positive results of Ref. [21], here we take for granted that an adequate relic abundance of the dark matter candidate particle can be ensured. We focus, instead, on another most salient feature of our model, namely, the presence of the invisible Higgs boson decays into *Diracons*, i.e.

$$h \to \mathcal{D}\mathcal{D}, \tag{10.13}$$

and its impact upon the dark matter detection prospects. Such decays through *Diracon* emission are the exact analogue of the invisible Higgs decays by Majoron emission in models with Majorana neutrinos [13]. As long as the $h \to \mathcal{D}\mathcal{D}$ coupling is non–zero, this Higgs decay mode also contributes in the range $m_X < m_h/2$, that is, when the Higgs decay into dark matter is kinematically allowed. The current bound on the invisible Higgs decays is given by $\mathcal{BR}_{\rm Inv} \equiv \frac{\Gamma_{\rm Inv}}{\Gamma_{\rm Inv}+\Gamma_{\rm Vis}} < 17\%$ [23]. In this scenario, the invisible Higgs decay width, $\Gamma_{\rm Inv}$, "always" has a contribution coming from its decay into *Diracons*, $\Gamma^{\mathcal{D}}_{\rm Inv} \equiv \Gamma(h \to \mathcal{D}\mathcal{D})$. As a result, for $m_X < m_h/2$, where m_X is the dark matter mass, the invisible decays have two sources, the $h \to \mathcal{D}\mathcal{D}$ and $h \to XX$, i.e. $\Gamma_{\rm Inv} = \Gamma^X_{\rm Inv} + \Gamma^{\mathcal{D}}_{\rm Inv}$. The Standard Model Higgs is in general a combination of the doublet H and the singlet σ, if we assume that the mixing between them is small, then $\Gamma_{\rm Vis}$=$\Gamma^{SM}_{\rm Total}$ = 4.434 MeV, so that the bound on the invisible width is $\Gamma_{\rm Inv}$¡0.908169 MeV. In this region there is a stronger constraint for the quartic coupling of the Higgs with the dark matter, as seen in Fig. 10.3. In this figure we display the constraints on λ_{HX} from the invisible decays of the

[4] A detailed determination of the relic density lies outside the scope of this paper.

Higgs (red region) as well as from the LUX [24] and PandaX [25] direct detection spin–independent cross section (purple and blue region, respectively).

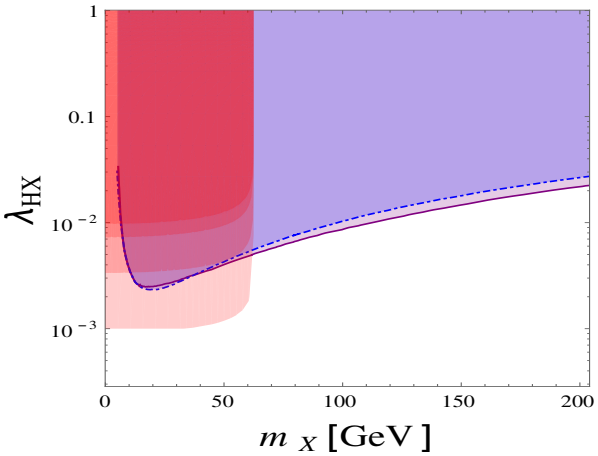

Figure 10.3: Exclusion regions in the (m_X,λ_{HX})-plane. The constraint from invisible Higgs decays is indicated in red. The continuous purple line correspond to the recent limit reported by LUX [24] from dark matter searches while the dot-dashed blue one indicates the current bound given by PandaX [25]. The different shades in red for the invisible decays define different contributions of $\Gamma^{\mathcal{D}}_{\rm Inv}$ to $\mathcal{BR}_{\rm Inv}$ (see text).

The different shades in red in Fig. 10.3 correspond to different contributions of decays of Higgs into *Diracons*, $\Gamma^{\mathcal{D}}_{\rm Inv}$, the smaller the contribution of $\Gamma^{\mathcal{D}}_{\rm Inv}$, the darker the region. For instance, the darkest red corresponds to the "standard" case with $\Gamma^{\mathcal{D}}_{\rm Inv} = 0$, while the lightest one is for $\Gamma^{\mathcal{D}}_{\rm Inv} = 0.9$ MeV. As a result the region excluded by the invisible Higgs decays in the (m_X,λ_{HX})–plane can be broader than the exclusion region set by the LUX data for the mass range $m_X < m_h/2$. In other words, the presence of the extra invisible decay channel into *Diracons* effectively increases the sensitivities to spin–independent WIMP dark matter searches below $m_h/2$.

10.5 Summary

In this letter we have proposed a low–scale mechanism for naturally small Dirac neutrino masses generated only at the two–loop level. The sector responsible for cosmological dark matter acts as messenger of neutrino mass generation. Both dark matter stabilitity and strict lepton number conservation are "symmetry protected". The presence of a global spontaneously broken U(1) symmetry leads to a physical Goldstone boson, dubbed *Diracon*, that

induces new invisible Higgs decays detectable at LHC and other collider experiments. The coexistence of such decays with the Higgs to dark matter channel, if kinematically allowed, leads to stronger sensitivities which we have quantified using current constraints from the LHC. Detailed analysis of the primordial WIMP dark matter density lies outside the scope of the present letter and will be presented elsewhere.

Acknowledgments

This work is supported by the Spanish grants FPA2011-2297, FPA2014-58183-P, Multidark CSD2009-00064, SEV-2014-0398 (MINECO) and PROMETEOII / 2014/084 (GVA). EP is supported in part by PAPIIT IA101516 and PAPIIT IN111115. EP would like to thank the IFIC CSIC/UV for the hospitality. We thank Roberto Lineros for discussions.

BIBLIOGRAPHY

[1] J. W. Valle and J. C. Romao, *Neutrinos in high energy and astroparticle physics*, Wiley-VCH, Berlin, 1st edition edition (2015).

[2] G. Bertone, D. Hooper and J. Silk, *Particle dark matter: Evidence, candidates and constraints*, Phys.Rept. **405** (2005) 279–390, arXiv:hep-ph/0404175 [hep-ph].

[3] J. W. F. Valle, *Neutrinos and dark matter*, J. Phys. Conf. Ser. **384** (2012) 012022.

[4] E. Ma, *Verifiable radiative seesaw mechanism of neutrino mass and dark matter*, Phys. Rev. **D73** (2006) 077301, arXiv:hep-ph/0601225 [hep-ph].

[5] J. Kubo, E. Ma and D. Suematsu, *Cold Dark Matter, Radiative Neutrino Mass, $\mu \to e\gamma$, and Neutrinoless Double Beta Decay*, Phys.Lett. **B642** (2006) 18–23, arXiv:hep-ph/0604114 [hep-ph].

[6] M. Hirsch et al., *WIMP dark matter as radiative neutrino mass messenger*, JHEP **1310** (2013) 149, arXiv:1307.8134 [hep-ph].

[7] A. Merle et al., *Consistency of WIMP Dark Matter as radiative neutrino mass messenger*, JHEP **07** (2016) 013, arXiv:1603.05685 [hep-ph].

[8] E. Ma, *Z(3) Dark Matter and Two-Loop Neutrino Mass*, Phys. Lett. **B662** (2008) 49–52, arXiv:0708.3371 [hep-ph].

[9] L. Bento and J. W. F. Valle, *The Simplest model for the 17-KeV neutrino and the MSW effect*, Phys. Lett. **B264** (1991) 373–380.

[10] J. T. Peltoniemi, D. Tommasini and J. W. F. Valle, *Reconciling dark matter and solar neutrinos*, Phys. Lett. **B298** (1993) 383–390.

[11] J. Valle, *Neutrinoless Double Beta Decay With Quasi Dirac Neutrinos*, Phys.Rev. **D27** (1983) 1672–1674.

[12] C. Bonilla and J. W. F. Valle, *Naturally light neutrinos in Diracon model* (2016), arXiv:1605.08362 [hep-ph].

[13] A. S. Joshipura and J. Valle, *Invisible Higgs decays and neutrino physics*, Nucl.Phys. **B397** (1993) 105–122.

[14] G. G. Raffelt, *Stars as laboratories for fundamental physics: The astrophysics of neutrinos, axions, and other weakly interacting particles*, University of Chicago press (1996).

[15] N. G. Deshpande and E. Ma, *Pattern of Symmetry Breaking with Two Higgs Doublets*, Phys.Rev. **D18** (1978) 2574.

[16] Q.-H. Cao, E. Ma and G. Rajasekaran, *Observing the Dark Scalar Doublet and its Impact on the Standard-Model Higgs Boson at Colliders*, Phys. Rev. **D76** (2007) 095011, arXiv:0708.2939 [hep-ph].

[17] A. Ilnicka, M. Krawczyk and T. Robens, *Inert Doublet Model in light of LHC Run I and astrophysical data*, Phys. Rev. **D93** (2016) 5 055026, arXiv:1508.01671 [hep-ph].

[18] C. Arina et al., *Minimal supergravity sneutrino dark matter and inverse seesaw neutrino masses*, Phys. Rev. Lett. **101** (2008) 161802, arXiv:0806.3225 [hep-ph].

[19] H. An, P. S. B. Dev, Y. Cai and R. N. Mohapatra, *Sneutrino Dark Matter in Gauged Inverse Seesaw Models for Neutrinos*, Phys. Rev. Lett. **108** (2012) 081806, arXiv:1110.1366 [hep-ph].

[20] G. Bélanger, K. Kannike, A. Pukhov and M. Raidal, *Minimal semi-annihilating $\mathbb{Z}_N$ scalar dark matter*, JCAP **1406** (2014) 021, arXiv:1403.4960 [hep-ph].

[21] G. Belanger, K. Kannike, A. Pukhov and M. Raidal, *Z_3 Scalar Singlet Dark Matter*, JCAP **1301** (2013) 022, arXiv:1211.1014 [hep-ph].

[22] L. Feng, S. Profumo and L. Ubaldi, *Closing in on singlet scalar dark matter: LUX, invisible Higgs decays and gamma-ray lines*, JHEP **03** (2015) 045, arXiv:1412.1105 [hep-ph].

[23] P. Bechtle et al., *Probing the Standard Model with Higgs signal rates from the Tevatron, the LHC and a future ILC*, JHEP **11** (2014) 039, arXiv:1403.1582 [hep-ph].

[24] D. S. Akerib et al. (LUX), *Results from a search for dark matter in the complete LUX exposure*, Phys. Rev. Lett. **118** (2017) 2 021303, arXiv:1608.07648 [astro-ph.CO].

[25] A. Tan et al. (PandaX-II), *Dark Matter Results from First 98.7 Days of Data from the PandaX-II Experiment*, Phys. Rev. Lett. **117** (2016) 12 121303, arXiv:1607.07400 [hep-ex].